

# AM

1

# Perspectives

Editors

Philipp L. Rosendahl

Bruno Figueiredo

Michela Turrin

Ulrich Knaack

Paulo J. S. Cruz





# AM

1

# Perspectives

**Editors**

**Philipp L. Rosendahl**

**Bruno Figueiredo**

**Michela Turrin**

**Ulrich Knaack**

**Paulo J. S. Cruz**



***Research in additive  
manufacturing  
for architecture  
and construction***

**Laboratory of Landscapes,  
Heritage and territory**

**Institute of Structural  
Mechanics and Design**

**SOAP | Stichting  
OpenAccess Platforms**

**AM Perspectives**  
**Research in additive manufacturing**  
**for architecture and construction**

AM Perspectives results from a collaboration between the Landscapes, Heritage and Territory Laboratory, University of Minho (Lab2PT); Architecture, Construction and Technology Hub, University of Minho (ACTech Hub); Institute of Structural Mechanics + Design, TU Darmstadt (ISM+D); the Generative Design Lab, TU Darmstadt (GDL); Faculty of Architecture and the Built Environment, TU Delft; Stichting OpenAccess Platforms (SOAP).

**Editors**

Philipp L. Rosendahl  
Bruno Figueiredo  
Michela Turrin  
Ulrich Knaack  
Paulo J. S. Cruz

**Design and layout**

Joana Lourencinho Carneiro

**Publishers**

Lab2PT – Landscapes, Heritage and Territory Laboratory,  
University of Minho, Guimarães.  
ISM+D – Institute of Structural Mechanics + Design,  
TU Darmstadt, Darmstadt.  
SOAP – Stichting OpenAccess Platforms, Rotterdam.

© 2024, by Editors, authors and Lab2PT, ISM+D and SOAP.

**AM Perspectives is published under a CC-BY-4.0 licence.**

**You are free to:**

Share – copy and redistribute the material in any medium or format for any purpose, even commercially. Adapt – remix, transform, and build upon the material for any purpose, even commercially. The licensor cannot revoke these freedoms as long as you follow the license terms.

**Under the following terms:**

Attribution – You must give appropriate credit, provide a link to the license, and indicate if changes were made. You may do so in any reasonable manner, but not in any way that suggests the licensor endorses you or your use.  
No additional restrictions – You may not apply legal terms or technological measures that legally restrict others from doing anything the license permits.

For general questions, please contact SOAP | Stichting OpenAccess directly at [admin@openaccess.ac](mailto:admin@openaccess.ac) or visit [www.openaccess.ac](http://www.openaccess.ac) for further information.

**ISBN/EAN** 978-90-833861-8-8

**e-ISBN** 978-989-8963-91-8

**DOI** 10.47982/a82n7r50

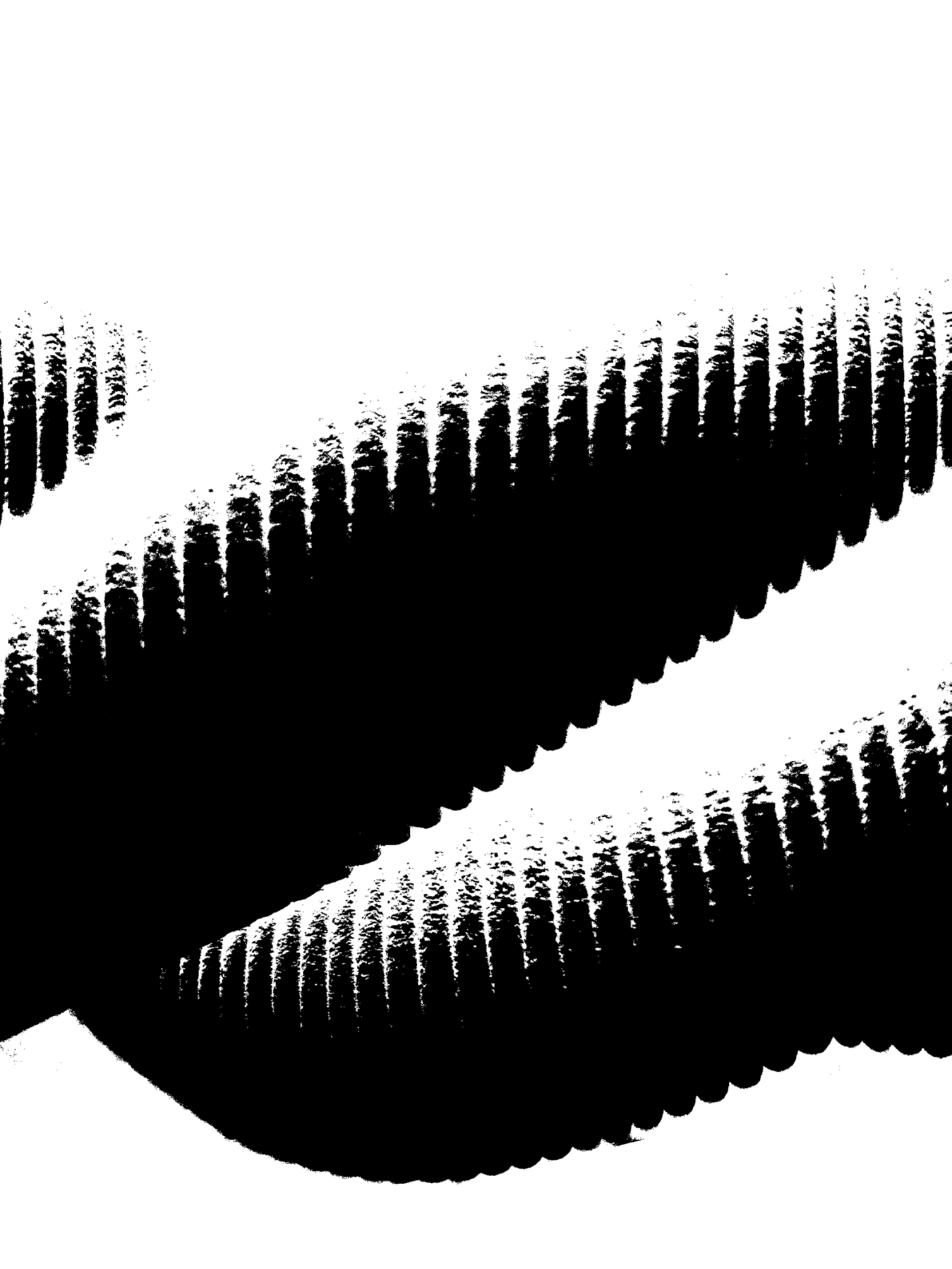
**Financial support**

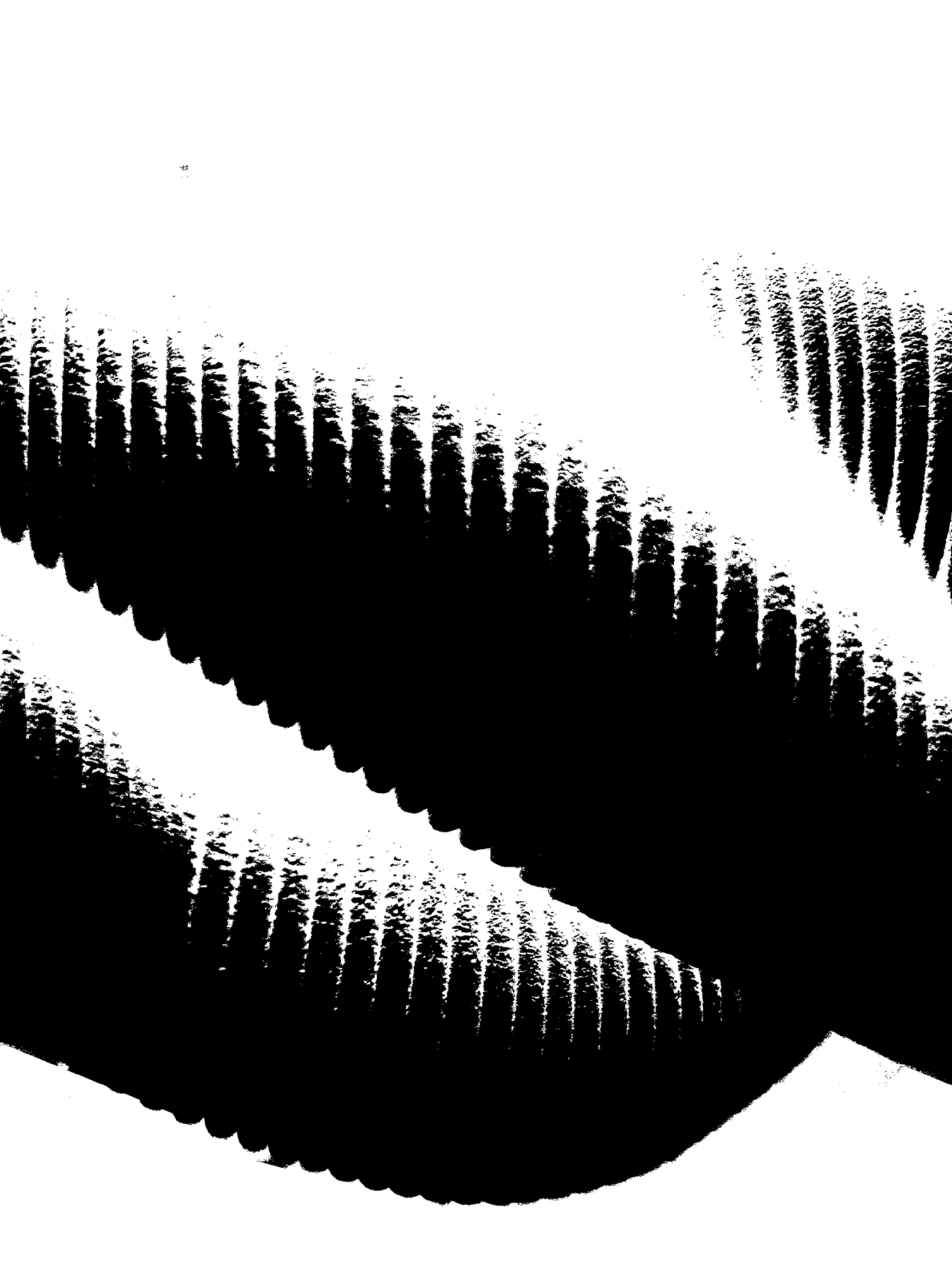
AM Perspectives has been made possible by financial support of the Multiannual Funding of the Landscape, Heritage and Territory Laboratory (Lab2PT), Ref. UID/04509/2020, financed by national funds (PIDDAC) through the FCT/MCTES.



SOAP | Stichting OpenAccess Platforms









# 1. *Full complexity realm*

- 17 BUILDING KNOWLEDGE THROUGH PRINTING: REDISCOVERING THE ARCHITECTURAL PROJECT IN THE AGE OF DATA

Georg Vrachliotis

- 19 BIOPRINTED BUILDINGS: NATURE'S MATERIALS & STRATEGIES IN ADDITIVELY MANUFACTURED ARCHITECTURES

Katia Zolotovskiy  
Laia Mogas-Soldevila

- 27 PRINT LOCAL!

Oliver Tessmann  
Nadja Gaudillière-Jami  
Max Benjamin Eschenbach

# 2. *Integral realm*

- 39 MATERIAL BALANCE DESIGN: DIGITAL TOOLS AND CIRCULAR INNOVATIONS FOR A NEW TECHNOLOGICAL CULTURE IN ARCHITECTURE

Ingrid Paoletti  
Olga Beatrice Carcassi  
Maria Anishchenko

- 47 LINES OF CODE AND CODED CLAY; A PLEA FOR THE INACCURACY

Erno Langenberg

- 53 DESIGNING MATERIAL ARCHITECTURES

David Correa

- 61 MULTI-MATERIAL FACADE COMPONENTS BY ADDITIVE MANUFACTURING WITH REACTIVE POLYMERS

Adam Pajonk

- 69 DOME LIGHT: MEDITATING DIRECTIONAL ILLUMINATION USING SECTIONAL VARIABILITY IN 3D CLAY PRINTING

James Clarke-Hicks  
Isabel Ochoa

- 77 BIOMATERIALS: ADVANTAGES AND DISADVANTAGES OF THE USE OF CHITOSAN IN AM

Tatiana Campos  
Paulo Cruz  
Bruno Figueiredo

# 3. *Fundamental realm*

- 89 CARBON-DRIVEN DESIGN OF 3D CONCRETE PRINTED HORIZONTAL STRUCTURES

Roberto Naboni  
Luca Bresceghello

- 97 THE JOURNEY TO ACHIEVE SUSTAINABILITY AND CIRCULARITY IN ADDITIVE MANUFACTURING OF CONSTRUCTION MATERIALS

Sandra S. Lucas

- 101 ADDITIVE MANUFACTURING OF GLASS: TEST SETUPS TO DETERMINE THE COMPONENT STRENGTH WITH PHOTOELASTIC IN-SITU MEASUREMENTS

Philipp Amir Chhadeh  
Kerstin Thiele  
Maren Dietrich  
Christin Lippold  
Ulrich Knaack  
Jens Schneider  
Matthias Martin Seel

- 119 SOLAR-SINTERING WITH IN-SITU MATERIAL

Marvin Kehl  
Tom Finger

- 131 OPTIMIZATION OF 3D PRINTED PAPER PASTE AND ITS PERFORMANCE ACCORDING TO SHRINKAGE FOR THE BUILD ENVIRONMENT

Dunia A. Abdullah Agha  
Ulrich Knaack

- 139 3D PRINTING WOOD FOR CUSTOM-DESIGN WINDOW FRAMES**  
Christopher Bierach  
Serdar Aşut  
Alexsander Alberts Coelho  
Michela Turrin  
Ulrich Knaack
- 149 ADDITIVE MANUFACTURING WITH BAMBOO: MECHANICALLY INFORMED INFILL WALL MADE WITH BAMBOO DUST AND FIBERS**  
Jasmine Wong  
Serdar Aşut  
Stijn Brancart
- 157 GEOMETRY ACQUISITION WITH COMPUTER VISION APPLIED TO WAAM**  
Juan Ojeda  
Ulrich Knaack  
Philipp L. Rosendahl
- 167 CONCRETE AM: STATUS OF THE DEVELOPMENT OF A ROBOTIC ARM-BASED EXTRUSION SETUP**  
João Ribeiro  
Bruno Figueiredo  
Paulo J. S. Cruz, Aires Camões
- 183 THE FLUSH INTEGRATION OF ADDITIVELY MANUFACTURED CERAMIC COMPONENTS IN BUILDINGS**  
Alexander Wolf
- 191 ADDITIVE MANUFACTURING EARTH-BASED COMPOSITE: DEFINING OPTIMUM COMPUTATIONAL METHODOLOGY FOR BUILDING SHELL GEOMETRY**  
Mohamad Fouad Hanifa  
Bruno Figueiredo  
Paulo Mendonça
- 209 CERAMIC AM FUNCTIONAL STRUCTURES**  
João Carvalho  
Bruno Figueiredo  
Paulo J.S. Cruz
- 215 DESIGN OF WAAM-STEEL NODES FOR RELIABLE CONSTRUCTION**  
Maren Erven  
Jörg Lange
- 223 WIRE ARC ADDITIVE MANUFACTURING OF STEEL COLUMNS**  
Benedikt Waldschmitt  
Jörg Lange  
Christopher Borg Costanzi
- 237 AM STRUCTURAL NODES FOR FREEFORM STEEL & GLASS FACADES**  
Lia Tramontini  
Sebastian Thieme  
Manuel Mueller  
Radenko Zoric  
Laurent Giampellegrini  
Matthias Oppe
- 245 CONTRIBUTORS**
- 247 EDITORS**

As technology continues to evolve, it has made a significant impact on the field of architecture and construction. The introduction of additive manufacturing, also known as 3D printing, has transformed the way architects and construction professionals approach design and engineering. With the ability to print structures layer by layer, this technology offers a level of precision and complexity that was previously impossible. The current state of research on additive manufacturing for architecture and construction is rapidly expanding, and this book aims to provide an overview of the latest developments in this exciting field at the Technical University of Darmstadt, Delft University of Technology, and the University of Minho.

The book covers the materials and processes used in additive manufacturing for construction, the challenges and opportunities of scaling up 3D printing for large-scale projects, and case studies of innovative 3D-printed structures. We explore the potential implications of additive manufacturing for sustainability, affordability, and accessibility in the construction industry.

Looking to the future, we offer ideas and insights into the possibilities of 3D printing as an ecosystem. As technology continues to improve and costs decrease, additive manufacturing could become a widespread and accessible method of construction, with implications for everything from disaster relief housing to space colonization. The potential for customization and personalization in 3D printing also offers exciting possibilities for individual homeowners and small-scale projects.

We aim at providing a comprehensive overview of the current state of research on additive manufacturing for architecture and construction, while also exploring the exciting potential for this technology in the years to come. We hope this book will inspire architects, engineers, and researchers to explore the possibilities of 3D printing and to embrace the opportunities for innovation and creativity that it presents.

Philipp L. Rosendahl  
Bruno Figueiredo  
Michela Turrin  
Ulrich Knaack  
Paulo J. S. Cruz



**1.  
Full  
complexity  
realm**

Additive Manufacturing (AM) has become widely accepted as a fast, cost-effective, and sustainable way to produce customised functional prototypes and products. It enables developing complex shapes and structures that were previously impossible or expensive to produce using traditional construction methods [1, 2]. Besides the so called “complexity for free”, well known advantages compared to other manufacturing processes include multi-material processes, high precision and accuracy, increased automation, decreased need of assembling, among others - applied in rapid-prototyping, manufacturing, and remanufacturing of products [3].

The research on AM is an extremely fertile and fast developing field [4]. The newest generations of AM machinery are overcoming many of the perceived limitations of their predecessors. Furthermore, the range of materials available for AM systems continues to expand and improvements to software and postprocessing technologies are further streamlining the end-to-end journey from concept to finished component [5, 6].

**AM+ efficiency.** AM innovation, once related to formal freedom, is now driven to efficiency. Understanding the possibility of designing customised elements lead to the development of high-performance components, with embedded functions attuned to specific requirements. Examples include potentially decreasing the energy usage, or energy gain, for the operation of buildings in different climate contexts [7, 8]. At the same time, the development of AM is widely considered to meet current challenges in our quest for a sustainable built environment, from the point of view of overall energy consumption, but also embodied carbon, and efficient use of natural resources. Increasing attention is devoted to AM for an optimised use of materials and emerging avenues for new sustainable materials (e.g. fully biobased).

Hybrid processes are also key, not only within AM but also with other manufacturing processes, to leverage their best potentials and overcome limitations with complementarity. Herzog and Tille highlight advantages in combining moulding and AM [9]. Traditionally, hybrid manufacturing includes combinations of additive and subtractive manufacturing. The term “AM+” refers instead to the combination of a wider range of processes that mix metal AM with processes ‘X’, that act before, during, or after the AM process, to address matters such as residual stresses, surface quality, anisotropy, and mechanical properties. Those processes ‘X’ include ultrasound for stress relief annealing, laser shot peening, rolling, or hammering for controlling the microstructure and residual stresses, as well as hybrid combinations of AM with other unit manufacturing processes, such as forming or machining [10].

**Smart AM.** Moreover, the AM precision achieved through the seamless integration of automation and robotics systems, coupled with the application of Artificial Intelligence (AI) and Machine Learning (ML), further enhances the optimisation of design and manufacturing processes within this complex realm [11, 12, 13].

Traditionally, AM systems follow pre-programmed procedures that may not be optimal for every situation. Specific environmental conditions and printing parameters - temperatures, cooling rates, or extrusion rates - must be carefully analysed to identify areas for improvement and optimisation. By feeding this information into ML tools, AM systems can learn from experience and make intelligent decisions based on real-time data. New knowledge and predictive models can be an outcome [14]. By intelligently pursuing objectives based on real-time data, AM systems can optimise their processes, by adapting them to changing conditions and by determining the best course of action to reduce errors. This is expected to have significant implications for construction industries as it can lead to a more solid understanding of 3D printed materials, a faster and more efficient production of high-quality products, reducing costs and improving overall project timelines. Tuvayanond and Prasittisopin explored how AI can automate the design and optimisation of AM processes in construction [15], while ML could be used to analyse data and predict defects, reduce waste and to foster more sustainable buildings [16].

**Biomimicry.** In addition to its integration with material science, AI, and robotics, AM has also been explored in the field of biomimicry, which is an emerging new frontier greatly relevant for the architectural, engineering and construction sector. Pawlyn discussed the application of biomimicry in architecture, where nature-inspired designs could lead to more sustainable and efficient buildings [17]. The author suggested that AM could be used to fabricate complex geometries inspired by natural forms, leading to increased structural efficiency and reduced environmental impact. The emergent practices of bio-design have the potential to significantly impact this scenario. Among others, biomimicry empowers materials chemistry at the level of molecular-scale bio-inspired design; and synthetic biology is opening new ways of integrating technology with nature, blurring the boundaries of technology and nature by designing living beings as artefacts and physically and/or chemically defining conditions that can produce living structures [18].

Inspiration by nature has driven the development of material manufacturing methods able produce soft materials, deforming as soft organisms, examples of which can be found among 3D printed shape-programmable materials [19]. Some fields already integrate inputs from multiple approaches. For example, the emergent field of soft robotics

grounds into biomimetic chemistry for the development of soft and plastic materials, into synthetic biology for the design of living entities as computational machines, and roots into the idea of decentralised intelligence in contrast to a central control [18].

**Smart Materials.** AM is marked by continual advancements and innovations, particularly in the development of techniques but also in new and highly adaptable and efficient materials. These materials stand to benefit from the integration of computational-driven design, AI techniques and the creation of virtual replicas of both products and manufacturing processes. Also, a close link with material science is key for AM future developments, from process design to structural applications and circularity [20, 21, 22].

AM can be a key driver in the development of responsive materials, self-healing polymers, thermally activated polymers, smart nanocomposites, piezoelectric materials, shape memory alloys, and shape memory polymers applicable in the construction industry by enabling the creation of structures that are adaptive, durable, and sustainable. Multi-Material Additive Manufacturing (MMAM) is an emerging manufacturing approach that is gaining interest in architecture and construction as an expansion of AM, leading towards components with heterogeneous material composition and a high degree of adaption towards structural, environmental, and design criteria [23]. Unlike traditional construction methods, which rely largely on the assembly of single materials or elements, MMAM enables the creation of objects with different material properties without the need for subsequent assembly. Ultimately, this change can address inefficiencies in manufacturing and construction by reducing the number of production steps required while providing solutions to problems that are associated with connecting individual materials or elements [24, 25].

**Bioprinting.** The possibility to produce living structures is increasingly developed and projects a new avenue also for architecture. 3D Bioprinting refers to AM processes incorporating bio-inks with cells and/or biocompatible materials [26]. While its applications used to target nearly exclusively 3D tissue engineering, cutting-edge applications for the construction industry are rapidly emerging, including living building materials. Envisioning the future of AM in construction, we can see a world where buildings are constructed using a combination of grown, composed, and living materials. Composed materials involve combining different materials to create new materials with specific properties.

Engineered living materials is a growing field where AM can have a substantial impact for the building sector, including for biomineralized solutions [27], mycelium-based solutions [28], hierarchical composites with organic components toward autonomous growth, and other recently surveyed avenues [29]. For example, mycelium, one of the grown materials, is the vegetative part of a fungus that can be grown into specific shapes to create building components like bricks or insulation. Another example is bacterial cellulose, which can be grown into sheets and used for applications like acoustic insulation or as a building material in its own right. Living materials are a particularly exciting area of biodesign with potential applications in the construction industry. By using living cells or tissues, we can create building materials that can sense and respond to changes in the environment, self-repair damage, or even grow and adapt over time. For example, researchers have developed bacteria that can detect cracks in concrete and heal them using calcium carbonate.

At a time when AM is on the verge of overcoming challenges such as controlling the behaviour of materials and optimisation processes, its integration with AI, ML, robotics and biomimetics offers promising ways to overcome some of these limitations, but above all to drive advances in sustainable construction and reshape the built environment for a more efficient and reactive future. A shift from the need to control nature to being part of an unpredictable, dynamic and fundamentally interconnected complex system [30, 31] impacts the built environment. AM full complex realm puts design and construction in the perspective of a holistic and participatory conception of nature that is expected to incorporate dimensions of cognitive biology, consciousness and ecosystem models, quantum physics and chaos theory studies, among others.

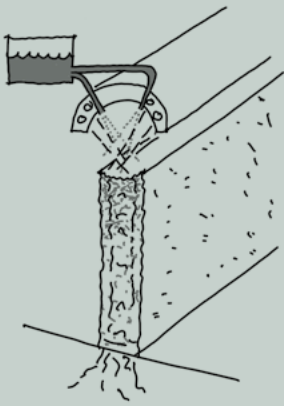
[1] Huang, Y., Leu, M. C., Mazumder, J., & Donmez, A. (2015). Additive manufacturing: current state, future potential, gaps and needs, and recommendations. *Journal of Manufacturing Science and Engineering*, 137(1), 014001. <https://doi.org/10.1115/1.4028725>

[2] Mehrpouya, M., Dehghanghadikolaei, A., Fotovvati, B., Vosooghnia, A., Emamian, S. S., & Gisario, A. (2019). The potential of additive manufacturing in the smart factory industrial 4.0: A review. *Applied Sciences*, 9(18), 3865. <https://doi.org/10.3390/app9183865>

[3] Kanishka, K., & Acherjee, B. (2023). Revolutionizing manufacturing: A comprehensive overview of additive manufacturing processes, materials, developments, and challenges. *Journal of Manufacturing Processes*, 107, 574-619. <https://doi.org/10.1016/j.jmapro.2023.10.024>

- [4] Parvanda, R., & Kala, P. (2023). Trends, opportunities, and challenges in the integration of the additive manufacturing with Industry 4.0. *Progress in Additive Manufacturing*, 8(3), 587-614. <https://doi.org/10.1007/s40964-022-00351-1>
- [5] Singh, N., Siddiqui, H., Koyalada, B. S. R., Mandal, A., Chauhan, V., Natarajan, S., ... & Kumar, S. (2023). Recent advancements in additive manufacturing (AM) techniques: a forward-looking review. *Metals and Materials International*, 29(8), 2119-2136. <https://doi.org/10.1007/s12540-022-01380-9>
- [6] Bromberger, J., Ilg, J. and Miranda, A.M. (2022), The mainstreaming of additive manufacturing, *Operations Practice*, McKinsey & Company. <https://www.mckinsey.com/capabilities/operations/our-insights/the-mainstreaming-of-additive-manufacturing>
- [7] Christen, H., van Zijl, G., & de Villiers, W. (2023). Improving building thermal comfort through passive design—An experimental analysis of phase change material 3D printed concrete. *Journal of Cleaner Production*, 392, 136247. <https://doi.org/10.1016/j.jclepro.2023.136247>
- [8] Piccioni, V., Leschok, M., Lydon, G., Cheibas, I., Hischer, I., Dillenburger, B., ... & Schlueter, A. (2023, June). Printing thermal performance: an experimental exploration of 3DP polymers for facade applications. In *IOP Conference Series: Earth and Environmental Science* (Vol. 1196, No. 1, p. 012063). IOP Publishing. <https://doi.org/10.1088/1755-1315/1196/1/012063>
- [9] Herzog, T., & Tille, C. (2021). Review and new aspects in combining multipoint moulding and additive manufacturing. *Applied Sciences*, 11(3), 1201. <https://doi.org/10.3390/app11031201>
- [10] Bambach, M., Beese, A.M., Lin, F and Tekkaya, A.E. (2021), Editorial, *J. Mater. Process. Technol.*, 294, 117103. <https://doi.org/10.1016/j.jmatprotec.2021.117103>
- [11] Wang, C., Tan, X. P., Tor, S. B., & Lim, C. S. (2020). Machine learning in additive manufacturing: State-of-the-art and perspectives. *Additive Manufacturing*, 36, 101538. <https://doi.org/10.1016/j.addma.2020.101538>
- [12] Qin, J., Hu, F., Liu, Y., Witherell, P., Wang, C. C., Rosen, D. W., ... & Tang, Q. (2022). Research and application of machine learning for additive manufacturing. *Additive Manufacturing*, 52, 102691. <https://doi.org/10.1016/j.addma.2022.102691>
- [13] Parsazadeh, M., Sharma, S., & Dahotre, N. (2023). Towards the next generation of machine learning models in additive manufacturing: A review of process dependent material evolution. *Progress in Materials Science*, 135, 101102. <https://doi.org/10.1016/j.pmatsci.2023.101102>
- [14] Rossi, G., Chiuidea, R. S., Hohegger, L., Lharchi, A., Harding, J., Nicholas, P., ... & Thomsen, M. R. (2022). Statistically modelling the curing of cellulose-based 3d printed components: Methods for material dataset composition, augmentation and encoding. In *Design Modelling Symposium Berlin* (pp. 487-500). Cham: Springer International Publishing. [https://doi.org/10.1007/978-3-031-13249-0\\_39](https://doi.org/10.1007/978-3-031-13249-0_39)
- [15] Tuvayanond, W., & Prasittisopin, L. (2023). Design for manufacture and assembly of digital fabrication and additive manufacturing in construction: a review. *Buildings*, 13(2), 429. <https://doi.org/10.3390/buildings13020429>
- [16] Živković, M., Žujović, M., & Milošević, J. (2023). Architectural 3D-Printed Structures Created Using Artificial Intelligence: A Review of Techniques and Applications. *Applied Sciences*, 13(19), 10671. <https://doi.org/10.3390/app131910671>
- [17] Pawlyn, M. (2019). *Biomimicry in Architecture*. RIBA Publishing. <https://doi.org/10.4324/9780429346774>
- [18] Bensaude-Vincent, B., 2019. Bio-informed emerging technologies and their relation to the sustainability aims of biomimicry. *Environmental Values*, 28(5), pp.551-571. <https://doi.org/10.3197/096327119X15579936382392>
- [19] Qi, S., Guo, H., Fu, J., Xie, Y., Zhu, M. and Yu, M., 2020. 3D printed shape-programmable magneto-active soft matter for biomimetic applications. *Composites Science and Technology*, 188, p.107973. <https://doi.org/10.1016/j.compscitech.2019.107973>
- [20] Bourell, D., Kruth, J. P., Leu, M., Levy, G., Rosen, D., Beese, A. M., & Clare, A. (2017). *Materials for additive manufacturing*. CIRP annals, 66(2), 659-681. <http://dx.doi.org/10.1016/j.cirp.2017.05.009>
- [21] Colorado, H. A., Velásquez, E. I. G., & Monteiro, S. N. (2020). Sustainability of additive manufacturing: the circular economy of materials and environmental perspectives. *Journal of Materials Research and Technology*, 9(4), 8221-8234. <https://doi.org/10.1016/j.jmrt.2020.04.062>
- [22] Liu, G., Zhang, X., Chen, X., He, Y., Cheng, L., Huo, M., ... & Lu, J. (2021). Additive manufacturing of structural materials. *Materials Science and Engineering: R: Reports*, 145, 100596. <https://doi.org/10.1016/j.mser.2020.100596>
- [23] Pajonk, A., Prieto, A., Blum, U. and Knaack, U. (2022), Multi-material additive manufacturing in architecture and construction: a review, *J. Build. Eng.*, 45 (2022), Article 103603. <https://doi.org/10.1016/j.jobe.2021.103603>
- [24] Excell, J. (2013), *The Rise of Multi-Material 3D Printing*, *The Engineer*. Available at: <https://www.theengineer.co.uk/the-rise-of-multi-material-3d-printing/>, Accessed 24th March 2024 <https://www.theengineer.co.uk/content/in-depth/the-rise-of-multi-material-3d-printing/>
- [25] Keating, S. (2014), *Beyond 3D Printing: the new Dimensions of additive fabrication*. J. Follett (Ed.), *Designing for Emerging Technologies: UX for Genomics, Robotics, and the Internet of Things*, O'Reilly Media. pp379-405 <http://hdl.handle.net/1721.1/95739>
- [26] Crook, J. M. (2020). *3D Bioprinting*. *Methods in Molecular Biology; Humana*: New York, NY, USA, 2140.
- [27] Reinhardt, O., Ihmann, S., Ahlhelm, M., & Gelinsky, M. (2023). 3D bioprinting of mineralizing cyanobacteria as novel approach for the fabrication of living building materials. *Frontiers in Bioengineering and Biotechnology*, 11, 443. <https://doi.org/10.3389/fbioe.2023.1145177>
- [28] Bitting, S., Derme, T., Lee, J., Van Mele, T., Dillenburger, B., & Block, P. (2022). Challenges and opportunities in scaling up architectural applications of mycelium-based materials with digital fabrication. *Biomimetics*, 7(2), 44. <https://doi.org/10.3390/biomimetics7020044>
- [29] Jones, R. J., Delesky, E. A., Cook, S. M., Cameron, J. C., Hubler, M. H., & Srubar III, W. V. (2022). Engineered living materials for construction. In *Engineered Living Materials* (pp. 187-216). Cham: Springer International Publishing. [https://doi.org/10.1007/978-3-030-92949-7\\_7](https://doi.org/10.1007/978-3-030-92949-7_7)
- [30] Iouguina, A., Dawson, J.W., Hallgrímsson, B. and Smart, G., (2014). Biologically informed disciplines: A comparative analysis of bionics, biomimetics, biomimicry, and bio-inspiration among others. *International Journal of Design & Nature and Ecodynamics*, 9(3), pp.197-205. <https://doi.org/10.2495/DNE-V9-N3-197-205>
- [31] Wahl, D.C., (2006). Bionics vs. biomimicry: from control of nature to sustainable participation in nature. *Design and nature III: comparing design in nature with science and engineering*, 87, pp.289-298. <https://doi.org/10.2495/DN060281>





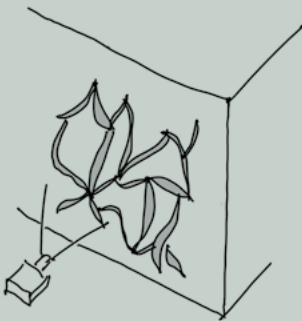
**AUTOMATED WALL GROWER**  
 Ok, we can extrude concrete and clay - but why not extrude biobased materials like fungi and have them grow in as a structural/architectural shape? Investigation about the amount of light, the speed of the process and possible geometries and qualities promises good opportunities!



**ENERGY GUIDES SELF-ASSEMBLY**  
 Positioning of components is a problem. We have tried to solve it with robots. But what if we find an energy-based assembly method that allows the structures to self-erect?



**CLIMATE-ADAPTATIVE BUILDINGS**  
 Considering that a building material can be adjusted in its geometry, we would create a climate-responsive building. And here additive manufacturing comes into play: mechanical or pneumatic systems have been thought up but have not been successful - if we now transfer the same physical concepts to simpler manufacturing technologies, they could work not only on a small experimental scale but also as a customised mass product.



**LIGHT-DIRECTED SELF-ASSEMBLY**  
 Another external impulse to organise the geometries to be built. Using self-growing materials, being directed by defined light impulses.

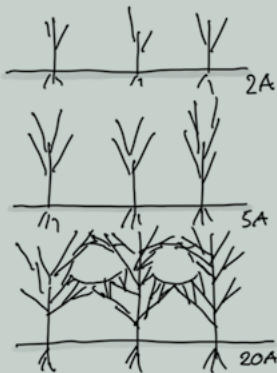


**LOAD-ADAPTIVE BUILDINGS**  
 Considering a building material that, under load, becomes structurally activated and therefore allows geometries to reinforce areas of a structure under tension or pressure - this would create fast-reacting structures and therefore reduce the mass of material required for their performance.



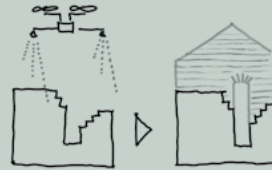
### PRINTED SEED BOMBS

Imagine a bio-based printed unit with incorporated plant seeds, to be placed as greening bombs in artificial environments. As well as promoting biodiversity, it could, for instance, enable the development of root systems to improve structural integrity.



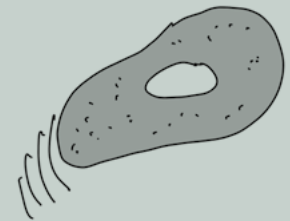
### SELF-GROWING BUILDINGS

An idea that we already introduced, but imagine the possibility of defining the natural growth mechanism as additive printing. Consider the growth of rings of a tree, the potential of training trees to grow and create volumes and structures - it may take time, but it's a carbon-negative process!



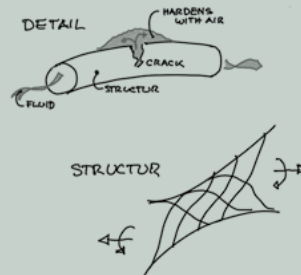
### REGROWING

The regeneration of buildings by bioactivated materials, through processes similar to the growth of shrubs and ivy that occupy voids in ruined spaces. Now imagine that we can control the geometry, volume and performance of this self-growing building. To be developed!



### SELF-PROPAGATING NANO BUILDER

A concept we find in medicine and biology - but not in construction - bio-robot controlled light and magnetic impulse. So, envision, that we can programme these individual builders. Open questions: technology, energy resources, construction material and control interaction - to be developed!



### SELF-REINFORCING STRUCTURES

Imagine a complex structure, being filled with fluid, hardening on contact with air - in the event of damage, this fluid would fill the crack self-healing the structure, keeping or improving its performance: to be developed!

# BUILDING KNOWLEDGE THROUGH PRINTING: REDISCOVERING THE ARCHITECTURAL PROJECT IN THE AGE OF DATA

Georg Vrachliotis

“At the theoretical level, calculative thinking has penetrated ever deeper into phenomena. It has analyzed them, as a result of which phenomena have increasingly taken on the structure of calculative thinking. Not only in physics do they break down into particles, but in biology, for example, into genes, in neurophysiology into point-like stimuli, in linguistics into phonemes, in ethnology into cultural terms or in psychology into actomes. There is no longer any talk of the original “extended thing”, but of swarms of particles structured according to fields. (...) The world has thus taken on the structure of the numerical universe, which poses confusing problems of knowledge when computers have shown that calculative thinking can not only decompose (analyze) the world into particles, but also reassemble (synthesize) them.”<sup>1</sup>

Vilém Flusser’s sharp insights, published in 1991 in the book “The Aesthetics of Electronic Media,” cut to the heart of a major technological and social shift that we are still navigating today. Flusser, one of the most innovative public intellectuals in the realm of digital culture of the last century, recognized early on how technology would shake up society, and specifically, the fields of architecture and design. The roots of today’s data-driven world were set down in the 1990s, after the initial excitement over post-war cybernetics<sup>2</sup> and the personal computer boom of the 1980s. Since then, we’ve seen a data explosion in everything from peo-

ple’s habits to energy use, changing how we understand our buildings and cities. The full impact of designing in a data society became apparent just after the turn of the millennium. Since then, additive manufacturing and 3D printing, has deeply penetrated the foundation of architectural research and design practice. Now, architects have a digital toolbox – with everything from blueprints to stats – unlike anything before. This digital deep-dive doesn’t just change how we see buildings; it questions the old ways of making them. It challenges architects: How do we adapt to this transition and meet today’s environmental and social demands? In other words: We need to find a way to make design culture click with the data pulse of our era. Additive manufacturing technologies could be a key. It’s more than a building tool; it’s a game-changer in how we think about and interact with

<sup>1</sup> V. Flusser: “Digitaler Schein”, in: *Digitaler Schein. Ästhetik der elektronischen Medien*, F. Rötzer Ed. Suhrkamp, 1991, p. 152.

<sup>2</sup> G. Vrachliotis: *The New Technological Condition. Architecture and Design in the Age of Cybernetics*, Basel: Birkhauser, 2022.

spaces. And it's become clear, perhaps even to the staunchest skeptics and most ardent doubters, that the very nature of architecture – the craft of building and the art of design – hasn't just survived the digital revolution; it has flourished.

## THE PRODUCTIVITY OF DIGITAL UNREST

Vilém Flusser was ahead of his time, understanding how digital tech could shake things up in our world. He saw that it could change almost everything - from aesthetics to culture to politics. Flusser dug into how digital media changes the way we handle things from objects to open spaces, sparking new ways for people to interact and create together. He showed us how data technology breaks down the world into bits and then puts it back together, starting a crucial discussion about our digital age. Now, as artificial intelligence becomes part of everyday life, his ideas are even more relevant. Flusser tells us we have got to keep questioning and shaping how we use technology in architecture, making sure it works for us and not the other way around. The evolution of design has been a constant in architecture, tied together by a continuous thread of technological innovation: from the dawn of computer-aided design to the expansive digital networks and complex machine learning models of today, one thing hasn't changed: our growing obsession with data. This isn't just about numbers; it's about how we have always interacted with the world, through the cultural techniques of reading, writing, and even printing.

## RECODING OF (THE) BUILDING

As buildings evolve into interactive and responsive data hubs, pressing issues concerning privacy and security come to the fore. The ethical responsibility of architects and developers is magnified as they must safeguard the integrity and protection of personal data collected. Architecture is no longer an isolated art form or a purely functional structure; it has become a vibrant ecosystem that harmonizes technology, humanity, data, and environment into a coherent whole. This was not always the case. There was a time when architectural focus was split between expansive urban mappings and detailed microscopic material studies.

Now, we are witnessing a resurgence of building scale in architecture – the rediscovery of the building, but under entirely new technological conditions. Contemporary concepts like smart design systems, sensor environments, material passports, digital twins, and open data are gaining traction. Our buildings and bodies have transformed into living data repositories, offering real-time insights into our

interactions with and perceptions of the built environment. Buildings have transcended their role as mere static symbols; they have become dynamic entities where symbols beget more symbols, positioning buildings as promising data repositories. It's as if we're flipping the script on the network society, triggering a profound reassessment and recalibration of fundamental architectural principles—from protection, comfort, and climate to privacy, security, and even our human interactions within these spaces.

## THE ARCHITECTURAL (DATA) PROJECT

This rediscovery of the building in architecture reflects a growing interest in weaving data technology into the physical realm of design and engineering. Smart façade systems that respond to climate variations, and energy-generating materials are just a few examples of how data technology is being seamlessly integrated into our built environments. Also, the adoption of material passports for complete traceability of materials used in a structure signals a paradigm shift toward sustainability and a circular economy. The list of innovations is extensive and ever-growing. Amidst all this innovation, additive manufacturing technologies enter the scene with the poise of a patient team player. And that is perhaps its most intriguing attribute for the current discourse. By moving from the production of small components to the scale of buildings, 3D printing contributes another critical element to the journey of rediscovering the architectural project in the age of data. In this dynamic landscape, 3D printing stands not merely as a technological feat but as a cultural reinvention, echoing Flusser's vision of creating worlds within the numerical universe. This isn't just about constructing buildings; This isn't just about constructing buildings; it's about creating a new architectural language that speaks to our interconnected approach to design as storytelling. It's where every printed structure reflects the intelligence and intent of our time, materializing Flusser's abstract "numerical universe" into tangible forms. By redefining the very atoms of architectural creation, it allows us to build not just structures, but narratives about architecture and the built environment: curated data, design, and human experience, all converging to architectural space on the building scale. Flusser's contemplations remind us that the fabric of our buildings is interwoven with the threads of our society's most pressing stories. We are tasked with more than design; we are encoding our values and visions into the very fabric of our habitats. Thus, the architectural project today is a testament to our ability to harness technology not only for innovation but for expression—building spaces that are informed by data yet guided by the timeless design principles of architecture.

# BIOPRINTED BUILDINGS: NATURE'S MATERIALS & STRATEGIES IN ADDITIVELY MANUFACTURED ARCHITECTURES

Katia Zolotovskiy  
Laia Mogas-Soldevila

## ADDITIVE MANUFACTURING WITH NATURE'S MATERIALS

Printing of bio-based architectures has recently gained interest. This is because new tools have been developed that can operate with water-based mixtures, and new blends have been tested from abundant natural materials, waste streams, or translated from fields such as food industry or biomedical research. At the part, object, or sample scale researchers have printed vessels from sawdust (Rael and Fratello 2018), biopolymer leathers from shrimp shells and silk protein (Mogas-Soldevila et al. 2021), or latticed proto-bricks from eggshell and plant fiber (Tovar 2023). Structural large-

scale 3d-printed material applications have been developed as demonstrators of a bio-based future for the construction industry. They range from grown and bio-bound panels from mycelium (Modanloo et al. 2021), concrete formwork from sawdust (Dayyem Khan et al. 2023), ultra thin sand composite arch and dome systems (Lasting et al. 2022), modular walls from recycled newspaper (Rech et al. 2022), shrimp-based tower skins ((L. Mogas-Soldevila et al. 2015; Duro-Royo et al. 2018)), free-form cellulose pillars (Sanandiya et al. 2018), or soil pods and shells for housing (Moretti 2023; Fratello 2021) (Figure 1). However, as discussed later, limitations arise when looking at whole bio-based additively manufactured assemblies or when including living materials within designs.



Figure 1: Top - Mycelium panels (Modanloo et al. 2021), sawdust formwork (Dayyem Khan et al. 2023), ultra thin earth arch (Lasting et al. 2022), recycled cellulose modular wall (Rech et al. 2022). Bottom - Shrimp bioplastic skins (Duro-Royo et al. 2018), cellulose-chitin pillar (Sanandiya et al. 2018), and earth pods (Fratello 2021).

## Materials Catalog in Biomaterial Architectures

Materials involved in this new wave of natural and bio-based additive manufacturing solutions naturally decay without toxicity, can be derived from abundant local resources, and display promising mechanical performance. For instance, pervasive biopolymers like chitin and cellulose, or extracts from waste like bone glue (Christ, Koss, and Ottosen 2019; Sanandiyana et al. 2018) are used as mixture binders. Similarly living fungal hyphae can digest and bond to the surface of organic substrates and form entangled networks that enhance the mechanical strength of mycelium-based structures (Saez et al. 2022). Natural gums like guar, xanthan, locust bean, gellan, or sodium alginate help increase viscosity and cohesion in composites. Minerals from eggshells like calcium carbonate, kaolinite clays, or silica sand provide compression strength and aggregate bulk in ceramic like materials augmented by binders that help bypass firing (Harrison 2022). Plant and tree derived fillers from sawdust, lignin, coco coir, bamboo, flax, sisal, or hemp contribute to tensile strength and can be printed in blends as short directional particles or sprayed as bending-improving networks (Mohan Kumar et al. 2023; Syngellakis 2015a). Plasticizers like sorbitol or glycerol contribute to processability and to durability by flexibilizing biopolymers and resulting constructs (Vieira et al. 2011). Direct printing of hydrogels with living cells like microalgae proposes bio-receptive facades able to produce oxygen via photosynthesis, current via algal biophotovoltaics, as well as aliments or fuel when positioned in building skins if encapsulation to preserve humidity is ensured (Malik et al. 2020). Using waste materials within printable blends can reduce the ecological footprint of transportation and harvest and alleviate landfill pressures. Some examples are cellulose from insulation and recycled newspaper, cotton fibers from clothing, agricultural byproducts like bagasse and corn husks.

## Fabrication and Formats in Biomaterial Architectures

Manufacturing platforms are composed of motion systems such as 3-axis computer numerical control (CNC) platforms, or 6-axis robotic arms. Their extrusion or direct printing end-effectors are powered by auger screws, stepper motor pushed plungers, or pneumatic syringes, and they all operate at room temperature and ambient conditions relying on water content evaporation as curing process (Mogas-Soldevila et al. 2014; Rech et al. 2022; Moretti 2023; Dayyem Khan et al. 2023). Results are promising and define 2.5-dimensional and 3-dimensional printed structures at multiple scales with functional targets in buildings such as; upholstery, construction formwork, facade panels, divider walls, columns, arches, or entire shells. However, complex

building systems made of bio-based materials are yet to be devised as challenges arise at the interfaces which have yet to be well studied.

## MANUFACTURING STRATEGIES FROM NATURE'S ADDITIVE GROWTH

Material organization strategies in nature can inform additive manufacturing with biobased materials. In nature, organisms harness various materials from their environment to build their structures, grow, and repair themselves. The material components of growth processes, such as brittle biological ceramics and compliant polymers, have poor mechanical properties. Organisms assemble these materials into structural biomineralized composites that have order-of-magnitudes better mechanical properties using the spatial articulation of soft and hard phases (Ortiz and Boyce 2008; Meyers, McKittrick, and Chen 2013; Yang et al. 2018). In addition, a vast variety of material architectures with adaptive properties from the same constituent materials can be assembled even within the same organism and result in the structure of the composite material being well adapted to its function (Yang et al. 2018). A good example is how abalone assembles its shell - first, the organism's cells organize into tissue patterns. Then, the cells secrete organic molecules that guide the process of deposition of calcium carbonate crystals - a process called biomineralization. In this guided assembly, the shell shifts between different crystalline structures, from an inner layer of flat, plate-like crystals to the outer layer, which is made up of vertical crystals to create an exceptionally strong surface (Frølich et al. 2017). By controlling this process, the abalone assembles a single material with properties of a composite material and creates a structure with significant strength with little expenditure of energy.

Biomineralized structural materials are usually composites of rigid mineral building blocks (calcium carbonate, calcium phosphate, silica) and organic macromolecules (proteins and polymers). Although many of the superior properties of these material systems come from nano and microscale interactions, some principles and processes of adaptive assembly in structural biomineralized materials can be relevant to additive manufacturing for architectural construction. Here we summarize recent developments in material science mimicking spatial organization of structural materials in nature with multi-material 3D printing. These include rigid-flexible layered structures, graded interfaces between materials and components, and actuated composites of interlocking rigid components embedded in flexible surfaces.

### **Layered structures (nacre)**

Nacre is the inner layer of many mollusc shells that consists of a complex arrangement of stacked parallel layers of aragonite (a form of calcium carbonate) separated by thin layers of organic matrix (Figure 2) (Jia, Deng, and Li 2022). Laminated composites mimicking this unique brick-and-mortar structure of nacre using multi material 3d printing were fabricated on macroscale (Dimas et al. 2013; Tran et al. 2017; Gu, Takaffoli, and Buehler 2017; Frölich et al. 2017). These composites demonstrate a combination of strength, toughness, and iridescence, that exceeds far beyond the mechanical properties of a solid block of rigid material and allows complex geometries to be fabricated. Bridges between the rigid layers in the laminated structure allow for efficient energy dissipation (L. Li and Ortiz 2015). The ply structure can be parametrically tuned for the performance and geometry needed (Gu et al. 2017).

### **Sutured joints and graded interfaces (ammonoid shells, skull, beak)**

Suture joints, often observed in the skulls of vertebrates, are interlocking, jagged connections between bones, providing both strength and flexibility (Figure 3). These interfaces are often combined with a gradual change in material properties that reduce stress concentrations in connections between different materials (Lin et al. 2014; Lin et al. 2014). Suture joints with tunable geometries and hierarchical orders were fabricated using Objet Connex 500 from rigid and flexible polymers (Lin et al. 2014; Lin et al. 2014). Graduate transition of material properties between rigid and soft has been demonstrated in materials and objects (Araya et al. 2013; Smith et al. 2020).

### **Actuated composites (fish, chitin)**

Flexible natural exoskeletons such as fish and chitin armors allow tunable flexibility, ranges of motion, as well as structural rigidity and protection from impact. These protective and flexible surfaces consist of topologically interlocking rigid components / plates connected to the body and to themselves by weak organic fibers. Parametric design of 3D printed actuated composites based on fish exoskeleton and chiton armor were designed and fabricated (Duro-Royo et al. 2015; Zolotovskiy et al. 2021) (Figure 4). The parametric modeling allows tunability of components' size, geometry, and joint configuration. The three dimensional shape of components and their interlocking can also adapt to ranges of motion and create tunable actuation. Other 3D printed actuated composites were designed by embedding overlapping rigid plates in flexible substrate (Rudykh and Boyce

2014; Browning, Ortiz, and Boyce 2013). The lamination angle and the degree of overlap can be tuned to achieve varying degrees of curvature, reduce weight, and increase toughness – properties relevant for architectural applications (Ghosh et al. 2016; Browning et al. 2013).

## **OUTLOOK INTO BIOMATERIALS MANUFACTURING EMBRACING NATURE'S STRATEGIES**

In contrast to human-made assemblies, structural systems in nature are complex systems that do not rely on transport and parts. Instead, soft and hard materials are spatially articulated from the environment molecule-by-molecule and layer-by-layer. Initial prototypes of additively manufactured biobased-building assemblies comprise clay pillar supports, cellulose latticed partitions, and timber slabs wound with flax fiber (ANCB 2022). These and other attempts, are typically mechanically connected by non-biomaterial fasteners in lack of graded, plated, or sutured joinery negotiating stiff to flexible constructs as observed in nature's grown materials. Using 3D printing for spatial articulation of soft and hard materials at material interfaces can improve structural performance and enable environmental interaction such as humidity and light -triggered actuation.

Another opportunity for harnessing living-like design features for additive manufacturing in architecture are living building materials (Nguyen et al. 2018; Chen et al. 2022). Incorporating and sustaining living cells on non-living scaffolds can support environmental cue sensing, information processing, material synthesis, growth, movement, self-repair, energy production, and waste management. For 3D printing living cells can be integrated into paste-like substrates. To make it compatible with 3D printing, material has to flow smoothly out of the nozzle at a specific rate without clogging, maintain its shape after extrusion, and allow layers to bond. A 3D printing process of hydrogels was developed in which suspended bacterial spores can be engineered to respond to stimuli or produce chemicals on demand and spontaneously germinate in cracks to allow self-healing (González et al 2020). Other examples include; hydrophilic bacteria printed on textiles to activate flapping interfaces within structures as they respond to humidity in their immediate surroundings (Wang et al. 2017); hard mycelium blocks bio-welded with sheets of soft living mycelium films allowing for flexible hinges that are strongly biologically bound and able to stay flexible during assembly (McBee et al. 2022); or functionally graded material prints ((Y. Li et al. 2020; Bader et al. 2016; Ren et al. 2022) that can help transition between hard areas in structures and propose interfaces with less friction and higher fracture resistance. Living cells in structures can undergo continuous self-assembly and adapta-



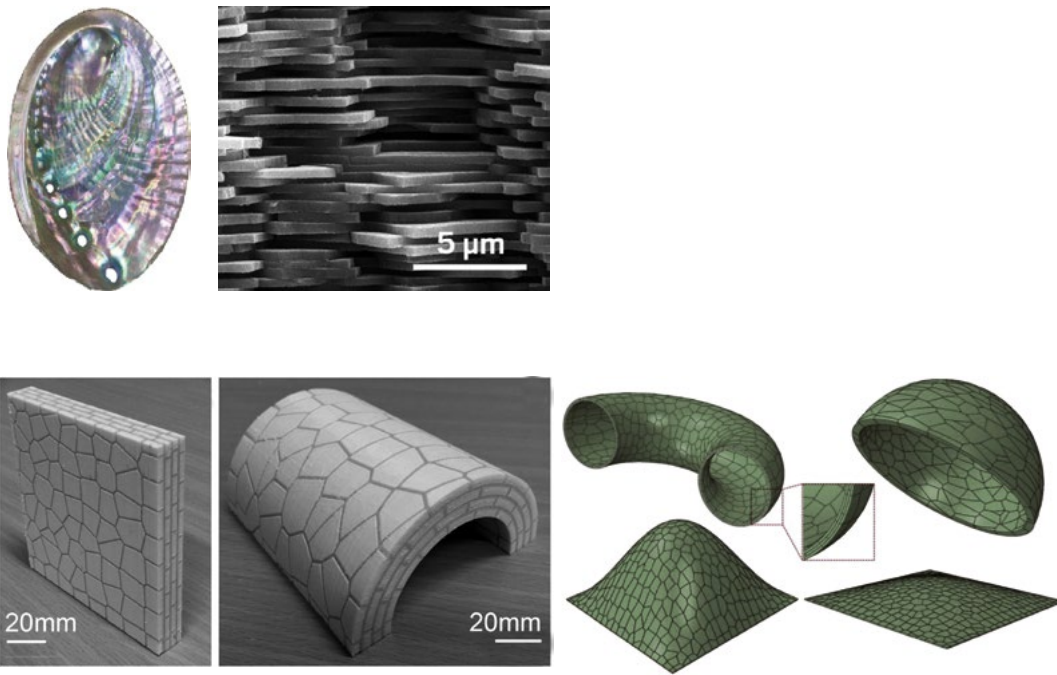


Figure 2: Top - Abalone shell and its nacre brick-and-mortar structure, bottom: 3D printed prototypes with nacreous Voronoi pattern from ABS/PLA materials allows them to accommodate complex geometries and achieve toughness, flexibility, and reduce weight (Tran et al. 2017).

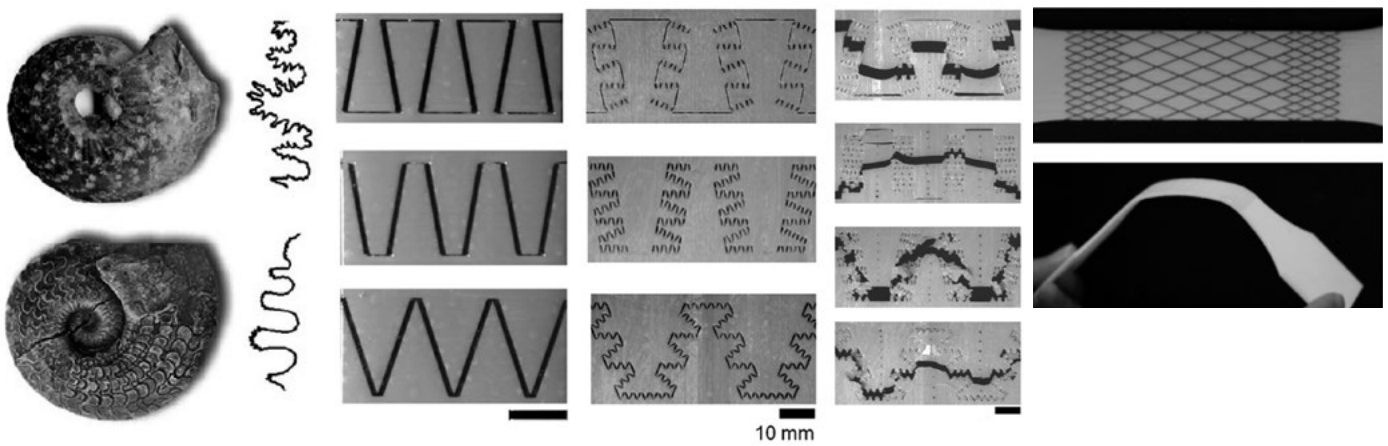


Figure 3: Hierarchical suture lines of connection in ammonoid shells (Lin et al. 2014); 3D printed suture joints using Objet Connex 500 (Lin et al. 2014).

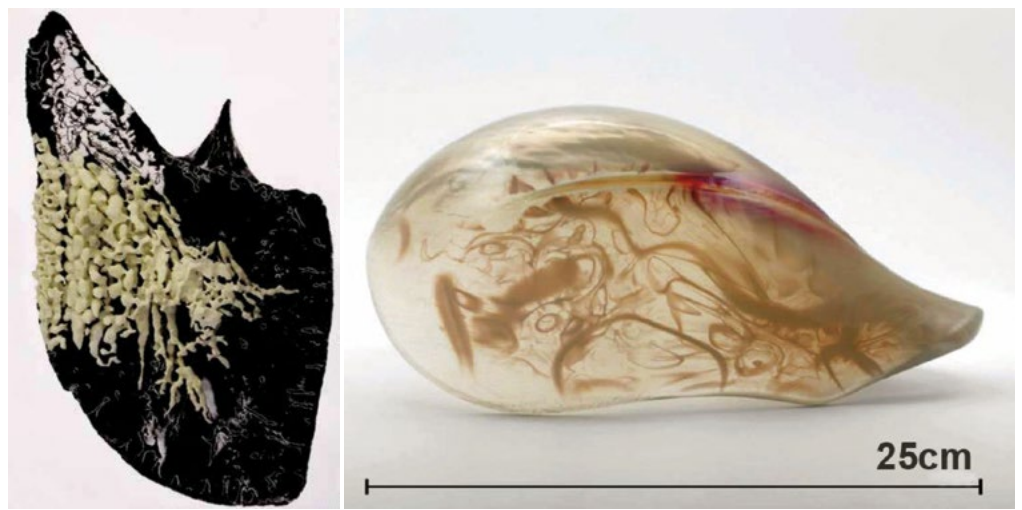


Figure 3 (part 2): Graded material interfaces 3D printed using Objet Connex 500 using Vero (rigid) and Tango (flexible) materials in 2.5D (Araya et al. 2013) and 3D objects (Smith et al. 2020).

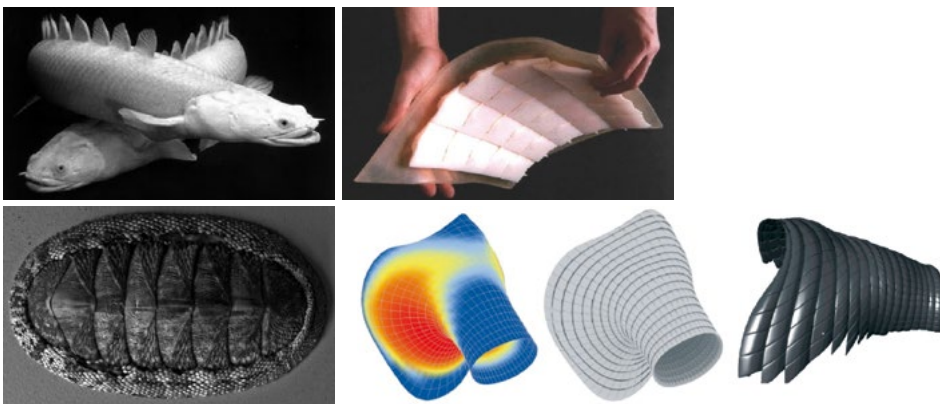


Figure 4: Strong and flexible armors (top left: *Polypterus senegalus* fish armor, bottom left: chiton armor outer ridge); right top and bottom: Parametric design of flexible 3D printed armor with Objet Connex 500 using Vero (rigid) and Tango (flexible) materials based on fish (Duro-Royo et al. 2015).

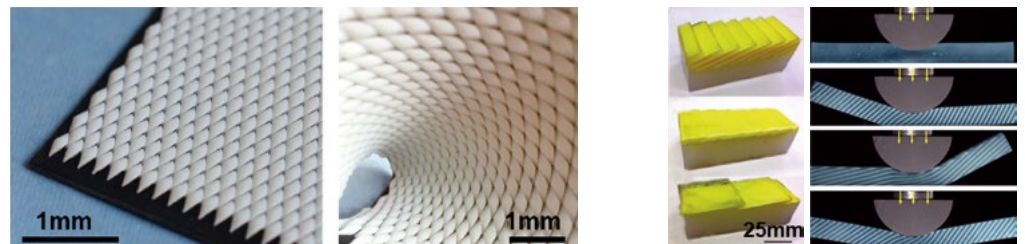


Figure 4 (part 2): Tunable rigid-flexible chiton-inspired surface (Connors et al. 2019); Overlapping plates design embedded in flexible substrate (Rudykh and Boyce 2014) with tunable mechanical behavior (Browning, Ortiz, and Boyce 2013).

tion of material configuration over time and even trigger self repair in the presence of building pathologies (Jonkers 2007), bio-mineralizing enzymes within printed materials are able to selectively harden soft constructs as they can metabolically secrete calcium carbonate on demand (Chen et al. 2022).

In conclusion, there is enormous potential for future bioprinted buildings to not only integrate nature's building methods but also living self-assembly and environmental responsiveness. This chapter proposes the first step towards this vision in adopting natural material spatial articulation strategies into additive bioprinting methods.

## REFERENCES

ANCB. 2022. "Living Prototypes: Digital Fabrication With Biomaterials Exhibition." Berlin, Germany: The Aedes Metropolitan Laboratory.

Araya, Sergio, Ekaterina Zolotovskiy, Felipe Veliz, Juha Song, Steffen Reichert, Mary Boyce, and Christine Ortiz. 2013. "Bio-inspired Performative Composite Structures."

Bader, Christoph, William G. Patrick, Dominik Kolb, Stephanie G. Hays, Steven Keating, Sunanda Sharma, Daniel Dikovskiy, et al. 2016. "Grown, Printed, and Biologically Augmented: An Additively Manufactured Microfluidic Wearable, Functionally Templated for Synthetic Microbes." *3D Printing and Additive Manufacturing* 3 (2): 79–89. <https://doi.org/10.1089/3dp.2016.0027>.

Browning, Ashley, Christine Ortiz, and Mary C. Boyce. 2013. "Mechanics of Composite Elasmoid Fish Scale Assemblies and Their Bioinspired Analogues." *Journal of the Mechanical Behavior of Biomedical Materials*, Science and Engineering of Natural Materials: Merging Structure and Materials, 19 (March): 75–86. <https://doi.org/10.1016/j.jmbbm.2012.11.003>.

Chen, Guangda, Xiangyu Liang, Pei Zhang, Shaoting Lin, Chengcheng Cai, Ziyi Yu, and Ji Liu. 2022. "Bioinspired 3D Printing of Functional Materials by Harnessing Enzyme-Induced Biomineralization." *Advanced Functional Materials* 32 (34): 2113262. <https://doi.org/10.1002/adfm.202113262>.

Christ, J, H Koss, and L M Ottosen. 2019. "A Concrete Composite from Biologically Based Binders and Mineral Aggregates for Constructional 3D-Printing."

Connors, Matthew, Ting Yang, Ahmed Hosny, Zhifei Deng, Fatemeh Yazdandoost, Hajar Massaadi, Douglas Eernisse, et al. 2019. "Bioinspired Design of Flexible Armor Based on Chiton Scales." *Nature Communications* 10 (1): 5413. <https://doi.org/10.1038/s41467-019-13215-0>.

Dayyem Khan, Muhammad, Tharanesh Varadharajan, Zachary Keller, and Mania Aghaei Meibodi. 2023. "BioMatters: The Robotic 3D-Printed Biodegradable Wood-Based Formwork for Cast-in-Place Concrete Structures." In *ACADIA Habits of the Anthropocene*. (upcoming).

Dimas, Leon S., Graham H. Bratzel, Ido Eylon, and Markus J. Buehler. 2013. "Tough Composites Inspired by Mineralized Natural Materials: Computation, 3D Printing, and Testing." *Advanced Functional Materials* 23 (36): 4629–38. <https://doi.org/10.1002/adfm.201300215>.

Duro-Royo, Jorge, Josh Van Zak, Andrea Ling, Yen-Ju Tai, Nicolas Hogan, Barrak Darweesh, and Neri Oxman. 2018. "Designing a Tree: Fabrication Informed Digital Design and Fabrica-

tion of Hierarchical Structures." *Proceedings of IASS Annual Symposia* 2018 (13): 1–7.

Duro-Royo, Jorge, Katia Zolotovskiy, Laia Mogas-Soldevila, Swati Varshney, Neri Oxman, Mary C. Boyce, and Christine Ortiz. 2015. "MetaMesh: A Hierarchical Computational Model for Design and Fabrication of Biomimetic Armored Surfaces." *Computer-Aided Design* 60: 14–27.

Fratello, Virginia San. 2021. "Emerging Objects." In *Digital Fabrication in Interior Design*. Routledge.

Frølich, Simon, James C. Weaver, Mason N. Dean, and Henrik Birkedal. 2017. "Uncovering Nature's Design Strategies through Parametric Modeling, Multi-Material 3D Printing, and Mechanical Testing." *Advanced Engineering Materials* 19 (6): e201600848. <https://doi.org/10.1002/adem.201600848>.

Ghosh, Ranajay, Hamid Ebrahimi, and Ashkan Vaziri. 2016. "Frictional Effects in Biomimetic Scales Engagement." *Europhysics Letters* 113 (3): 34003. <https://doi.org/10.1209/0295-5075/113/34003>.

González, Lina M., Nikita Mukhitov, and Christopher A. Voigt. 2020. "Resilient Living Materials Built by Printing Bacterial Spores." *Nature Chemical Biology* 16 (2): 126–33. <https://doi.org/10.1038/s41589-019-0412-5>.

Gu, Grace X., Mahdi Takaffoli, and Markus J. Buehler. 2017. "Hierarchically Enhanced Impact Resistance of Bioinspired Composites." *Advanced Materials* 29 (28): 1700060. <https://doi.org/10.1002/adma.201700060>.

Harrison, Robert. 2022. *Sustainable Ceramics: A Practical Approach*. 1st ed. Bloomsbury Publishing. <https://www.bloomsbury.com/in/sustainable-ceramics-9781789941227/>.

Jia, Zian, Zhifei Deng, and Ling Li. 2022. "Biomaterialized Materials as Model Systems for Structural Composites: 3D Architecture." *Advanced Materials* 34 (20): 2106259. <https://doi.org/10.1002/adma.202106259>.

Jonkers, Henk M. 2007. "Self Healing Concrete: A Biological Approach." In *Self Healing Materials: An Alternative Approach to 20 Centuries of Materials Science*, edited by Sybrand van der Zwaag, 195–204. Springer Series in Materials Science. Dordrecht: Springer Netherlands. [https://doi.org/10.1007/978-1-4020-6250-6\\_9](https://doi.org/10.1007/978-1-4020-6250-6_9).

Lasting, Liam N., I. Lee, L. Mogas-Soldevila, and M. Akbarzadeh. 2022. "Terrene 1.0: Innovative, Earth-Based Material for the Construction of Compression-Dominant Shell Structures." In . <https://www.semanticscholar.org/paper/Terrene-1.0-%3A-Innovative%2C-Earth-Based-Material-for-Lasting-Lee/46e87ec49ab4d3a489d52eeb2dcccdf84293bfa95>.

Li, Ling, and Christine Ortiz. 2015. "A Natural 3D Interconnected Laminated Composite with Enhanced Damage Resistance." *Advanced Functional Materials* 25 (23): 3463–71. <https://doi.org/10.1002/adfm.201500380>.

Li, Yan, Zuying Feng, Liang Hao, Lijing Huang, Chenxing Xin, Yushen Wang, Emiliano Bilotti, et al. 2020. "A Review on Functionally Graded Materials and Structures via Additive Manufacturing: From Multi-Scale Design to Versatile Functional Properties." *Advanced Materials Technologies* 5 (6): 1900981. <https://doi.org/10.1002/admt.201900981>.

Lin, Erica, Yanning Li, Christine Ortiz, and Mary C. Boyce. 2014. "3D Printed, Bio-Inspired Prototypes and Analytical Models for Structured Suture Interfaces with Geometrically-Tuned Deformation and Failure Behavior." *Journal of the Mechanics and Physics of Solids* 73 (December): 166–82. <https://doi.org/10.1016/j.jmps.2014.08.011>.

Lin, Erica, Yanning Li, James C. Weaver, Christine Ortiz, and Mary C. Boyce. 2014. "Tunability and Enhancement of Mechanical Behavior with Additively Manufactured Bio-Inspired Hier-

- archical Suture Interfaces." *Journal of Materials Research* 29 (17): 1867-75. <https://doi.org/10.1557/jmr.2014.175>.
- Malik, Shneel, Julie Hagopian, Sanika Mohite, Cao Lintong, Laura Stoffels, Sofoklis Giannakopoulos, Richard Beckett, et al. 2020. "Robotic Extrusion of Algae-Laden Hydrogels for Large-Scale Applications." *Global Challenges* 4 (1): 1900064. <https://doi.org/10.1002/gch2.201900064>.
- McBee, Ross M., Matt Lucht, Nikita Mukhitov, Miles Richardson, Tarun Srinivasan, Dechuan Meng, Haorong Chen, et al. 2022. "Engineering Living and Regenerative Fungal-Bacterial Biocomposite Structures." *Nature Materials* 21 (4): 471-78. <https://doi.org/10.1038/s41563-021-01123-y>.
- Meyers, Marc André, Joanna McKittrick, and Po-Yu Chen. 2013. "Structural Biological Materials: Critical Mechanics-Materials Connections." *Science* 339 (6121): 773-79. <https://doi.org/10.1126/science.1220854>.
- Modanloo, Behzad, Ali Ghazvinian, Mohammadreza Matini, and Elham Andaroodi. 2021. "Tilted Arch; Implementation of Additive Manufacturing and Bio-Welding of Mycelium-Based Composites." *Biomimetics* 6 (4): 68. <https://doi.org/10.3390/biomimetics6040068>.
- Mogas-Soldevila, L., Jorge Duro-Royo, Daniel Lizardo, Markus Kayser, Sunanda Sharma, Steven J. Keating, John Klein, Chikara Inamura, and N. Oxman. 2015. "DESIGNING THE OCEAN PAVILION: Biomaterial Templating of Structural, Manufacturing, and Environmental Performance." In . <https://www.semanticscholar.org/paper/DESIGNING-THE-OCEAN-PAVILION%3A-Biomaterial-of-and-Mogas-Soldevila-Duro-Royo/34637602502a8215bd5828709326c092844b416c>.
- Mogas-Soldevila, L., G. Matzeu, M. Lo Presti, and F. G. Omenetto. 2021. "Additively Manufactured Leather-like Silk Protein Materials." *Materials & Design* 203 (May): 109631. <https://doi.org/10.1016/j.matdes.2021.109631>.
- Mogas-Soldevila, Laia, Jorge Duro-Royo, and Neri Oxman. 2014. "Water-Based Robotic Fabrication: Large-Scale Additive Manufacturing of Functionally Graded Hydrogel Composites via Multichamber Extrusion." *3D Printing and Additive Manufacturing* 1 (3): 141-51. <https://doi.org/10.1089/3dp.2014.0014>.
- Mohan Kumar, K., Venkatesh Naik, Vijayanand Kaup, Sunil Waddar, N. Santhosh, and H. V. Harish. 2023. "Nontraditional Natural Filler-Based Biocomposites for Sustainable Structures." *Advances in Polymer Technology* 2023 (May): e8838766. <https://doi.org/10.1155/2023/8838766>.
- Moretti, Massimo. 2023. "WASP in the Edge of 3D Printing." In *3D Printing for Construction with Alternative Materials*, edited by Bárbara Rangel, Ana Sofia Guimarães, Jorge Lino, and Leonardo Santana, 57-65. Digital Innovations in Architecture, Engineering and Construction. Cham: Springer International Publishing. [https://doi.org/10.1007/978-3-031-09319-7\\_3](https://doi.org/10.1007/978-3-031-09319-7_3).
- Nguyen, Peter Q., Noémie-Manuelle Dorval Courchesne, Anna Duraj-Thatte, Pichet Praveschotinunt, and Neel S. Joshi. 2018. "Engineered Living Materials: Prospects and Challenges for Using Biological Systems to Direct the Assembly of Smart Materials." *Advanced Materials* 30 (19): 1704847. <https://doi.org/10.1002/adma.201704847>.
- Ortiz, Christine, and Mary C. Boyce. 2008. "Bioinspired Structural Materials." *Science* 319 (5866): 1053-54. <https://doi.org/10.1126/science.1154295>.
- Rael, Ronald, and Virginia San Fratello. 2018. *Printing Architecture: Innovative Recipes for 3D Printing*. Chronicle Books.
- Rech, Arianna, Ruxandra Chiujea, Claudia Colmo, Gabriella Rossi, Paul Nicholas, Martin Tamke, Mette Ramsgaard Thomsen, and Anders E. Daugaard. 2022. "Waste-Based Biopolymer Slurry for 3D Printing Targeting Construction Elements." *Materials Today Communications* 33 (December): 104963. <https://doi.org/10.1016/j.mtcomm.2022.104963>.
- Ren, Lei, Zhenguo Wang, Luquan Ren, Zhiwu Han, Qingping Liu, and Zhengyi Song. 2022. "Graded Biological Materials and Additive Manufacturing Technologies for Producing Bioinspired Graded Materials: An Overview." *Composites Part B: Engineering* 242 (August): 110086. <https://doi.org/10.1016/j.compositesb.2022.110086>.
- Rudykh, Stephan, and Mary C. Boyce. 2014. "Transforming Small Localized Loading into Large Rotational Motion in Soft Anisotropically Structured Materials." *Advanced Engineering Materials* 16 (11): 1311-17. <https://doi.org/10.1002/adem.201400162>.
- Saez, Dana, Denis Grizmann, Martin Trautz, and Anett Werner. 2022. "Exploring the Binding Capacity of Mycelium and Wood-Based Composites for Use in Construction." *Biomimetics* 7 (2): 78. <https://doi.org/10.3390/biomimetics7020078>.
- Sanandiyá, Naresh D., Yadunund Vijay, Marina Dimopoulou, Stylianos Dritsas, and Javier G. Fernandez. 2018. "Large-Scale Additive Manufacturing with Bioinspired Cellulosic Materials." *Scientific Reports* 8 (1): 8642. <https://doi.org/10.1038/s41598-018-26985-2>.
- Smith, Rachel Soo Hoo, Christoph Bader, Sunanda Sharma, Dominik Kolb, Tzu-Chieh Tang, Ahmed Hosny, Felix Moser, James C. Weaver, Christopher A. Voigt, and Neri Oxman. 2020. "Hybrid Living Materials: Digital Design and Fabrication of 3D Multimaterial Structures with Programmable Biohybrid Surfaces." *Advanced Functional Materials* 30 (7): 1907401. <https://doi.org/10.1002/adfm.201907401>.
- Syngellakis, S. 2015a. *Natural Filler and Fibre Composites*. WIT Transactions on State-of-the-Art in Science and Engineering. Wessex Institute of Technology Press. <https://www.witpress.com/books/978-1-78466-147-2>.
- Tovar, Enrique. 2023. "Digital Fabrication and Biomaterials in Architecture: Fusing Identity and Technology," 2023.
- Tran, Phuong, Tuan D. Ngo, Abdallah Ghazlan, and David Hui. 2017. "Bimaterial 3D Printing and Numerical Analysis of Bio-Inspired Composite Structures under in-Plane and Transverse Loadings." *Composites Part B: Engineering* 108 (January): 210-23. <https://doi.org/10.1016/j.compositesb.2016.09.083>.
- Vieira, Melissa Gurgel Adeodato, Mariana Altenhofen da Silva, Lucielen Oliveira dos Santos, and Marisa Masumi Beppu. 2011. "Natural-Based Plasticizers and Biopolymer Films: A Review." *European Polymer Journal* 47 (3): 254-63. <https://doi.org/10.1016/j.eurpolymj.2010.12.011>.
- Wang, Wen, Lining Yao, Chin-Yi Cheng, Teng Zhang, Hiroshi Atsumi, Luda Wang, Guanyun Wang, et al. 2017. "Harnessing the Hygroscopic and Biofluorescent Behaviors of Genetically Tractable Microbial Cells to Design Biohybrid Wearables." *Science Advances* 3 (5): e1601984. <https://doi.org/10.1126/sciadv.1601984>.
- Yang, Yang, Xuan Song, Xiangjia Li, Zeyu Chen, Chi Zhou, Qifa Zhou, and Yong Chen. 2018. "Recent Progress in Biomimetic Additive Manufacturing Technology: From Materials to Functional Structures." *Advanced Materials* 30 (36): 1706539. <https://doi.org/10.1002/adma.201706539>.
- Zolotovskiy, Katia, Swati Varshney, Steffen Reichert, Eric M. Arndt, Ming Dao, Mary C. Boyce, and Christine Ortiz. 2021. "Fish-Inspired Flexible Protective Material Systems with Anisotropic Bending Stiffness." *Communications Materials* 2 (1): 1-10.

# PRINT LOCAL!

Oliver Tessmann

Nadja Gaudillière-Jami

Max Benjamin Eschenbach

## INTRODUCTION

Additive manufacturing in architecture matured at a breathtaking pace. The journey from the first lab tests to printed multi-family houses took only a couple of years. Parallel and coalescing innovations in computational design, robotics and material science paved the way to a fast transfer from research to practice, after a longer period in which brilliant but singular ideas could not prevail alone. The multiple pieces of the puzzle must fall together to turn concepts into technologies. Interdisciplinarity has played a crucial role in the development of 3D-printing technologies for the built environment, involving engineers, architects, roboticists,

material and computer scientists all together in the creation of adequate systems and materials. It is again interdisciplinarity that has allowed for bridges to be created between academia and practice, fostering the transfer of these systems and materials to the construction industry. While great achievements have been made within the last years and with 3D-printing and AM on its way of becoming state of the art in first practice contexts, it is the research and development that needs to set a new focus: How can AM contribute to an urgently needed new way of construction that addresses the climate crisis, material scarcity and affordable housing? While these problems are well-known for quite a while, their consequences are now becoming globally tangible.

For the research in 3D-printing and AM we therefore identified a series of tightly intertwined topics and challenges. In order to significantly lower Global Warming Potential (GWP) of construction we need to build with different materials than steel and concrete. However, biomaterials, ceramics and raw earth require different engineering approaches as the isotropic materials of XX<sup>th</sup> century constructions. Besides questions of printability, mastering anisotropic material properties and behavior that changes over time requires different tools for design, analysis and simulation. How do we model and simulate these anisotropic, weak and rapidly decaying materials? An architecture based on natural materials has a different expression and different tectonics. For structural behavior geometry becomes more important than material capacity. Erosion, decay and shorter element lifespans call for reversible and modular constructions to respond to more tightly keyed maintenance/refurbishment cycles. Local materials require adaptable, local, robust and decentralized AM technologies. How do we nevertheless achieve an architectural scale without being forced to build machines larger than the building we want to 3D-print? How can we use AM to improve, refurbish and extend valuable existing structures?

Printing locally enables a drastic reduction of the environmental footprint. But it goes hand in hand with tackling these challenges within the development of AM processes and uses in architecture. Through a series of research projects led by the Digital Design Unit (DDU), we demonstrate how computational tools can be leveraged for resource locality, novel design aesthetics and technical decentralization.

## **LOCAL MATERIALS - MATTER AS MET**

Research in 3D-printing biomaterials, ceramics and raw earth printing methods has provided us with a number of alternatives to concrete and its high environmental costs (Munch-Petersen & Beim 2022). As is the case in vernacular construction, raw earth can be harvested on site directly on the ground and used as 3D-printing material for the building parts. The extreme locality of such a process ensures, at material level, a much more sustainable approach to construction. The diversity in geological landscapes however requires a systematic adaptation of the material recipe, and 3D-printing systems robust enough to account for such variations. Furthermore, the choice of additives for the material recipe and of means to render the 3D-printing system robust must be approached with care. Resorting to chemical additives can indeed lead to a reduction in the CO<sub>2</sub> footprint of the project, but to an increase of other impacts, such as human or eco-toxicity (Kuzmenko et al. 2020). The familiar

quality assurance measures developed for industrial and standardized materials are no longer effective here. Fast and reliable material analysis is required, combined with computational recipe generation that is capable of predicting material behavior based on analysis data of grain size, bulk cones and other parameters. Our Printsugi research project demonstrates the concept of linking computational design with local material performance (Eschenbach et al. 2023). Printsugi binds together raw materials as found on site, such as rocks or logs, by connectors 3D-printed from the local soil. The printing process is one link in a larger digital process chain that requires 3D-scanning, computational analysis of local materials and recipe design (Figure 1).

However, limits to the use of these new materials in 3D-printing processes exist. They generally have much lower structural performances than the materials we are used to resorting to, as has been shown in material evaluation studies (Fabbri et al. 2022). Therefore form-active systems and compression-only structures gain novel importance as structural means in architecture. Besides different forms, organic materials create a different aesthetic, as they often are raw and irregular, with very organic aspects - unlike what 3D-printing has strived to achieve when creating custom concrete recipes. We regard Scan-Print-Assemble as digital process chain and Printsugi as strategy for local material use as conceptual building blocks for a digital and contemporary strategy to engage with existing material, structures and buildings.

## **MATERIAL - DRIVEN AESTHETICS**

Research in ceramics 3D-printing at DDU aims at investigating new aesthetics that we can mobilize together with new materials to foster change, contributing not only to new technical options, but also to new narratives. Through such change, we could gain new habits of construction, and through them tackle the different performances of the materials we now strive towards.

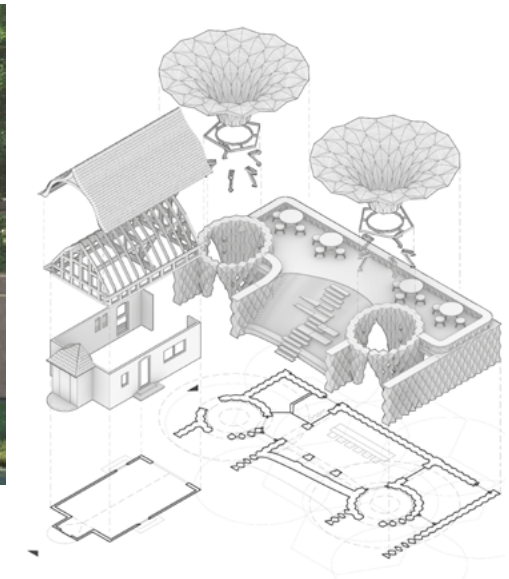
As part of the 2023 PRINT!Architecture DDU design studio, in which students designed an extension of a small Art Deco Building in Frankfurt (Fig. 2), the participants investigated aesthetic aspects of the ceramic 3D-printing process, crafting a number of refined details in exploring layer orientations and their interconnections beyond the mere horizontal stacking, playing with lines, borders, deformations, textures and patterns (Figure 3). Not only are these material details specific to the fabrication process of ceramic 3D-printing, they are also the trace of the computational means that allow for such achievements. Part of the work of DDU on ceramic 3D-printing is the development of a bespoke slicer enabling the creation of custom paths (Figure 4).



Figure 1: The Digital Rubble Arc and the Printsugi Rock Tower, both relying on the Scan-Print-Assemble process (Image: DDU).



Figure 2: Extension project for a small Art Deco building in Frankfurt, as part of the 2023 PRINT!Architecture DDU design studio (Design and Image: Joshua Schäfer).



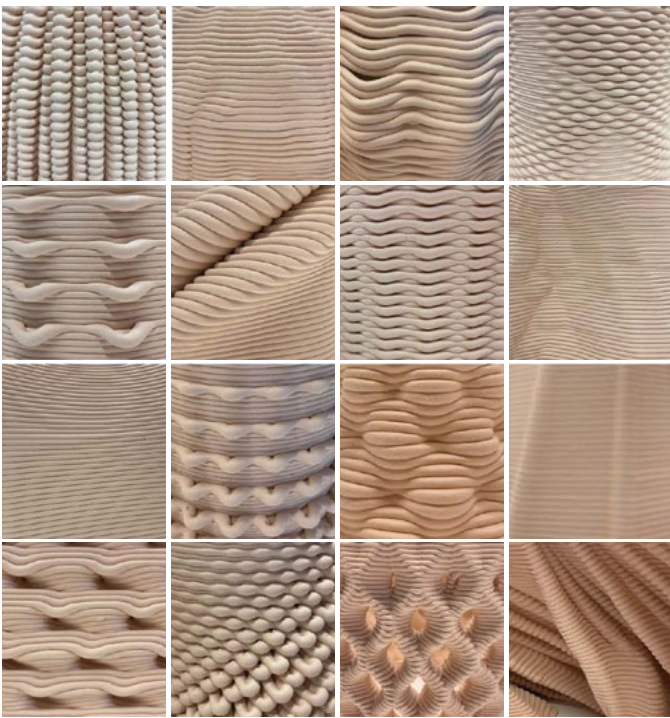


Figure 3: Textures and border effects resulting from the exploration of the 3D-printing ceramic process (Image: DDU)

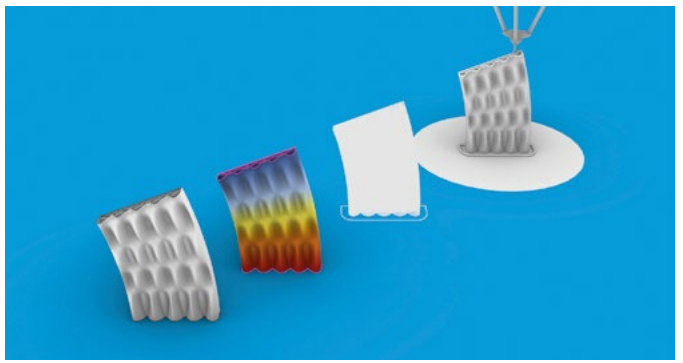


Figure 4: Slicer (Image: DDU)



Figure 5: Spiraling paths prints (Image: DDU).

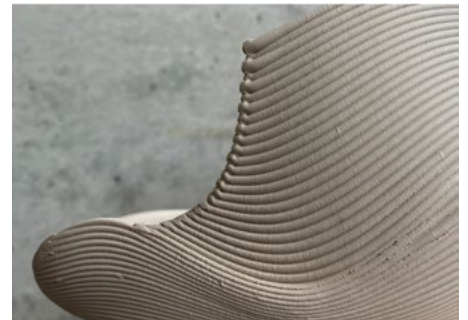


Figure 6: Non-planar 3D-printing (Design: Kaan Aydogan, Image: DDU).



Figure 7: Material contrast created by the combination of 3D-printed ceramics with a wooden structure (Design: Jasmin Imkeller, Image: DDU).



On Figure 5, are examples of spiraling print paths, avoiding the traces left in the print when the extruder steps from one layer to the other and creating a continuity across all the print. The slicer also allows for the plane in which the layer is placed to change its orientation (Figure 6), allowing for more stability during printing overhanging structures. This also allows for the orientation of the layers perpendicularly to the load paths. The viscosity and rheology of ceramics allow for printing cantilering layers which set after printing, creating a vivid surface structure that reveals material properties and the play at hand when varying the water amount in the recipe (Figure 3). These textures can also reflect the material's origin, as all grounds have different clay compositions, which can induce changes in the behavior and create bespoke ornamental textures reacting to the locality of the material.

Ceramics being brittle and rather weak materials, they require large interfaces between load-transferring parts. Figure 7 shows printed elements almost embracing a wooden member. To an extent, the material contrasts achieved through such placing processes can also foster new aesthetics, an aspect explored both in the Printsugi project, confronting clay and stone, and in the PRINT!Architecture studio, confronting wood and clay. The frailty and refinement of details investigated here, contrasted with the rawness of materials chosen, can become a carrier for the new materials stories needed (Rigobello & Ayres 2021). The design details act as a means of value creation, highlighting a role for architects and designers that cannot be held by others.

## CIRCULAR MATERIALS

Yet challenges remain in this design pursuit as well. From the regularity of layers seen here in ceramics prints to the irregularities often seen in biomaterials prints, layers and texture details would take on very different aspects. Furthermore, the faster degradation can not only damage those details, but also bring forward material aspects we are unused to seeing in buildings. Could this be an element to play with in designing 3D-printed details, revealing new details or patterns as the material ages? Or should new repair and recycling tactics be put in place to maintain those new materials? This points to another crucial aspect in facing the renewed challenges of sustainable 3D-printing: the temporality of an architectural project. Temporality at a material level, with decay, but also temporality at component level, with the question of assembly.

If value creation is an intrinsic part of circular economy, and if the material choice and details design can enable us to create value in the new components, then they must be allowed to remain as long as possible in the system. It is

then reuse, rather than repair or recycling, that is mobilized, through design for disassembly.

DDU tackles this across a range of projects blending the 3D-printing of all or part of the components together with digital assembly strategies. Printsugi takes advantage of the uneven geometries of the rocks to develop placing strategies that create interlocking effects between the rocks and the ceramic connectors. The Rubble Arch designed with the Scan-Print-Assemble process leverages the center of gravity of the rocks to equilibrate them within the arch, requiring a minimum of matter to 3D-print connectors maintaining them in place (Wibranek & Tessmann 2019). DDU furthermore explores micro-modular constructions in which small-scale, interlocking elements are reversibly assembled through autonomous robots. The fabrication-agnostic approach combines elements from different manufacturing origins and a range of materials that perform in different ways (load-bearing, climate regulating, light directing etc.). More importantly, however, is the aim to make constructions reversible and to automatize costly assembly processes through the use of robots. This research seeks to make tightly keyed maintenance and refurbishment cycles economically feasible so that the change to more natural materials in architecture is encouraged.

Not only is design for disassembly crucial to reuse strategies in the built environment. It is also a way into new strategies for building 3D-printing and the issue of scaling up that it poses. By remaining at a small component scale and developing approaches to accumulate these components together rather than printing big, more sustainable methods will be enforced. By avoiding very large 3D-printing systems, we might also avoid the potentially high environmental costs that are associated with them in other indicators than greenhouse gasses, such as metallic resources depletion (Kuzmenko et al. 2020). Giving up on going big and aiming at smaller assembled components also enable us to more easily replace them, allowing us to handle the faster decay of biomaterials as we could replace components.

## CONCLUSION

Matter as met: using materials directly available on site to print only what is necessary to make use of the existing, thus shifting towards a very local additive manufacturing. Material-driven aesthetics: using the technological potential of AM and of computational tools to foster an appreciation of the very local. Circular materials: creating assembly cascades, both at the material and at the component level, to keep the created architectures as long as possible in the loop.

These new approaches go with new logistics on the construction site, as it is not anymore about allowing very large printers to be put on site or near, but to bring large

sets of smaller components or of pre-assembled sections on site. But the potential replacement of components also points to different logistics after construction, during the life of the building. Sustainable 3D-printing then becomes an issue of maintenance, which implies not only technical issues, but also a social dimension. Care for a building can help foster links within a community, rendering it more resilient (Rigobello & Ayres 2021). The limited existence in time of a project's component is then another frailty that we can build upon to create new narratives and habits, creating a collective experience of the built environment as part of which to develop care.

## REFERENCES

- Eschenbach, M.B., Gaudillière-Jami, N., & Tessmann, O. (2023). *Printsugi. Matter as met, matter as printed. Leveraging computational design tools for a more virtuous material extraction and end-of-life.* In Sustainable Development Goals Series, Mette Ramsgaard Thomsen et al. (Eds): *Design for Rethinking Resources.*
- Fabbri, A., Morel, J.C., Aubert, J.E., Bui, Q.B., Gallipoli, D., & Reddy, B.V.V. (2022). *Testing and Characterisation of Earth-based Building Materials and Elements, State-of-the-Art Report of the RILEM TC 274-TCE,* Springer.
- Kuzmenko, K., Gaudillière, N., Feraille, A., Dirrenberger, J., & Baverel, O. (2020). *Assessing the environmental viability of 3D concrete printing technology.* In *Impact: Design With All Senses: Proceedings of the Design Modelling Symposium, Berlin 2019* (pp. 517-528). Springer International Publishing.
- Munch-Petersen, P., & Beim, A. (2022). *The Construction Material Pyramid: 'Upfront impacts' as a methodical change in architectural design.* In *Structures and Architecture A Viable Urban Perspective?* (pp. 371-378). CRC Press.
- Rigobello, A., & Ayres, P. (2021). *Fragile computation: rethinking information technologies to foster situated ecologies.* In *Proceedings of the Deep City Conference 2021.*
- Wibranek, B., & Tessmann, O. (2019). *Digital rubble compression-only structures with irregular rock and 3D printed connectors.* In *Proceedings of IASS Annual Symposia (Vol. 2019, No. 6, pp. 1-8).* International Association for Shell and Spatial Structures (IASS).

# 2. Integral realm

AM opens access to new formal, material, and production explorations, offering architects, engineers, and builders a new design and construction paradigm that leverages a range of benefits. These include reducing waste, increasing efficiency, and improving sustainability of the built environment. It is in our interest to explore this integrative vision, a realm of AM for architecture, building, and construction, that we propose to address through: Function, Tectonics and, Sustainability and Circularity.

**Function.** The concept of functionality in architecture is related with the performance of the built environment. Additive manufacturing (AM) is transforming the architecture and construction industry by providing innovative solutions to design challenges, and by enabling the development of high-performance building components [1]. AM eases the integration of hierarchical, grading, and multiscale structures design, functional texture, and adaptive and kinetic components, which are key elements to improve building component properties and the functionality of buildings.

The use of AM technology allows the production of structures that can perform multiple functions, reducing the need for separate components, and improving overall efficiency. For instance, the use of a hierarchical approach to structure design, incorporating multiscale structures, and grading structures can result in custom structures that are lightweight, yet durable, and that can withstand a range of loads and stresses [2, 3]. This is particularly useful in the design of both structural and facade parts. By tailoring the composition of the building component to its specific function, it can achieve better performance and with the least amount of resources needed.

Another way of achieving custom performance for architectural configurations is by the intersection of functional textures with AM. By combining material properties, AM processes, and architectural geometry composition, designers can create custom textures that provide specific functional performance for light, heat, and sound, creating comfortable and efficient living spaces. Additionally, they allow the improvement of the materials performance, for instance, by increasing the absorption properties of surfaces, enhancing the acoustic properties of walls [4, 5].

Additive manufacturing plays a crucial role in the development of custom adaptive structures, such as kinetic structures, that respond to specific environmental or use conditions. These structures can be achieved by controlling the material behaviour, including its physical reaction to the environment or other external inputs such as temperature, pressure, or humidity variation, or even electrical stimulus by incorporating alloy materials [6].

Simulation models are key tools for the design team to preview the building performance. In multicriteria models

several aspects of building performance, such as structural, thermal, light, acoustics, MEP, etc., can be balanced simultaneously, ensuring they meet the specific needs of the building. This approach can be further enhanced through the use of AI, which can analyse and optimize the design for better performance [7].

In order to extend the control of a building's performance throughout its life cycle, but also in the construction, or assembly stages, the use of digital twins is an useful tool to monitor the performance of the building in real-time, allowing for predictive maintenance and optimization. AM can have a main role on this by automatically integrating sensors and sensorial materials in the building components, allowing for real-time monitoring and control of key parameters, such as temperature, humidity, and air quality [8].

The integration of function into AM produced building components is a key topic towards an integral realm in the use of AM technology for sustainable built environments [9]. The integration of hierarchical structures, multiscale compositions, functional textures, adaptive structures, functional simulation models, and digital twin models are all important tools that can be used to achieve this goal. By leveraging these tools and integrating function into building components, architects and engineers can design more sustainable and high-performance buildings that respond to the specific needs of the built environment [10].

**Tectonics.** Tectonics in architecture and construction refers to the way in which structures and building components are assembled and constructed. Visual, haptic, and meaningful experiences are important considerations when designing and constructing buildings. AM technology offers unique opportunities for exploring tectonics, namely circular tectonics, with the ability to create buildings that not only follow compositional principles but also propose sustainable and circular methods [11].

The concept of "form follows production" suggests that the design of a building should be influenced by the production methods used to construct it. Additive manufacturing processes can enable architects to design buildings with production in mind, rather than retrofitting design to fit traditional construction techniques [12]. This can result in buildings that are optimized for their manufacturing processes, and therefore more sustainable, efficient, and economical. For example, AM can produce building components that are lightweight, energy-efficient, and require fewer materials than traditional construction methods.

Circular tectonics indicates the way in which structures are assembled and constructed with the aim of reducing waste and increasing efficiency. The use of modular and prefabricated components that can be easily assembled and disassembled is an important principle in achieving

circularity in building and construction, prioritizing circular economy principles, such as resource efficiency, waste reduction, and reuse. A key aspect is the ability of AM to produce customised fittings connections, with reversible behaviour, providing the assembly and disassembly of parts, but also multiple configurations and combinatorial possibilities. Considering several degrees of reversibility and categories of connections that can be addressed. Circular tectonics also involves designing buildings as systems that can adapt and evolve over time, rather than as static objects [13, 14].

**Visual Expression and Tactual Experience.** Visual expression and tactual experience are essential components of architectural design. The first refers to the aesthetic and symbolic qualities of a building, while tactual experience refers to the physical and sensory qualities of a space or a building. Additive manufacturing processes can enhance both visual expression and haptic experience by enabling the creation of intricate and customisable geometries, textures, and patterns that are not achievable using traditional construction methods, providing tactile and immersive experiences for the inhabitants [15].

Meaningful experience is often achieved through the integration of cultural, social, and historical references into building design. Additive manufacturing processes can facilitate emotional and psychological impact of the built environment on its occupants by enabling the production of customized and personalized building components that reflect the specific needs and preferences of the building's occupants. For example, 3D printing can be used to create personalized facades that incorporate cultural or historical motifs, thereby creating a sense of place and identity for the building and its occupants.

Simultaneously, additive manufacturing involves the successive overlapping of layers. A compositional process, where each layer can be customised either to achieve a specific expression or meet specific performance goals, incorporating both emotional and sustainable behaviours.

**Sustainability and Circularity.** In addition to addressing the functional and tectonic aspects, the integration of sustainability and circularity principles into the design and construction process is essential to achieve a more sustainable built environment. Additive manufacturing technology can contribute to this goal by enabling the use of biogenic materials, reducing waste, and facilitating the design for assembly and disassembly.

AM enables the integration of materials engineered from waste, further promoting circularity. The use of recycled

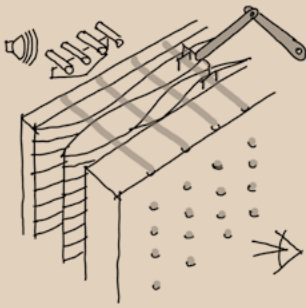
and biogenic materials can reduce the environmental impact of construction and help to create a circular economy. Materials such as wood and other plant-based materials have a low carbon footprint, as they store carbon during their growth, and their use in construction can replace materials with a high carbon footprint such as concrete and steel [16, 17]. AM allows for precise and efficient use of these materials, minimizing waste and increasing their structural performance. Moreover, the use of biogenic materials can also provide a more tactile and natural experience for the occupants, contributing to the AM tectonic properties.

Design for Assembly and Disassembly is a key principle to enhance circularity of building components in the construction industry. As mentioned, AM can contribute to this approach in the production of custom fittings and connection systems, facilitating material recovery and building components reuse. This approach reduces the amount of waste generated during the construction process and the need for new materials, minimizing the environmental impact of the construction industry [18].

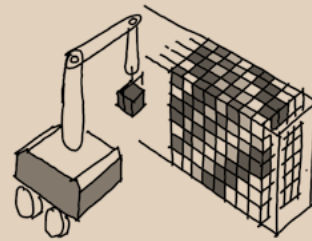
Additive Manufacturing is essential to shift from the traditional linear economy to a circular economy that minimizes waste, maximizes the use of available resources, and promotes sustainable practices. Additive Manufacturing is a tool that can facilitate this transition by producing optimised, custom-designed parts and using recycled materials and waste to create new building components.

In conclusion, the Integral Realm of AM in the architecture, building, and construction sector encompasses function, tectonics, and sustainability and circularity. These topics are interdependent and should not be understood in isolation from each other to revolutionize the way we design, build, and experience the built environment. By enhancing multiscale structures, circular tectonics, and the ability to use recycled and biogenic materials in AM reinforces the reuse of waste, decarbonisation, CO<sub>2</sub> capture, energy saving and energy self-sufficiency, promoting novel possibilities to create buildings that are not only aesthetically defined but also functional, sustainable, and circular.

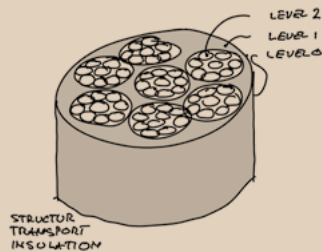
- [1] Lim, S., & Buswell, R. A. (2012). Developments in construction-scale additive manufacturing processes. *Automation in Construction*, 21, 262-268. <https://doi.org/10.1016/j.autcon.2011.06.010>
- [2] Boschmann, E., & Krieg, O. D. (2020). Architectural Additive Manufacturing: Opportunities and Challenges for Structural Design. *Frontiers in Built Environment*, 6, 205. <https://doi.org/10.3389/fbuil.2020.00005>
- [3] Gosselin, C., & Duballet, R. (2018). Additive construction methods using lightweight 3D-printed formwork: A review. *Automation in Construction*, 91, 332-344. <https://doi.org/10.1016/j.autcon.2018.03.009>
- [4] Pajonk, A., Prieto, A., Blum, U., & Knaack, U. (2022). Multi-material additive manufacturing in architecture and construction: A review. *Journal of Building Engineering*, 45, 103603. <https://doi.org/10.1016/j.jobbe.2021.103603>
- [5] Pessoa, S., Guimarães, A. S., Lucas, S. S., & Simões, N. (2021). 3D printing in the construction industry - A systematic review of the thermal performance in buildings. *Renewable and Sustainable Energy Reviews*, 141, 110794. <https://doi.org/10.1016/j.rser.2021.110794>
- [6] Correa, D. (2022). 4D printed hygroscopic programmable material architectures. Stuttgart: Institute for Computational Design and Construction, University of Stuttgart. <https://dx.doi.org/10.18419/opus-12374>
- [7] Ashour, Y., & Kolarevic, B. (2015). Heuristic Optimization in Design. In *ACADIA 2105: Computational Ecologies: Design in the Anthropocene* (pp. 357-369). Cincinnati. ISBN 978-0-692-53726-8.
- [8] Xin, Y., Feng, Y., & Zhong, B. (2020). Digital twin-driven building energy performance evaluation: A review. *Building and Environment*, 177, 106824. <https://doi.org/10.1016/j.buildenv.2020.106824>
- [9] Sanjuan-Delmás, D., Alcalá, J., & García-Segura, T. (2020). Additive manufacturing for the construction industry: A review. *Construction and Building Materials*, 231, 117171. <https://doi.org/10.1016/j.conbuildmat.2019.117171>
- [10] Kwon, H., Eichenhofer, M., Kyttas, T., & Dillenburger, B. (2019). Digital Composites: Robotic 3D Printing of Continuous Carbon Fiber-Reinforced Plastics for Functionally-Graded Building Components. In J. Willmann, P. Block, M. Hutter, K. Byrne, & T. Schork (Eds.), *Robotic Fabrication in Architecture, Art and Design 2018* (pp. 363-372). Cham: Springer. [https://doi.org/10.1007/978-3-319-92294-2\\_28](https://doi.org/10.1007/978-3-319-92294-2_28)
- [11] Oxman, R. (2012). Informed tectonics in material-based design. *Design Studies*, 33(5), 427-455. <https://doi.org/10.1016/j.destud.2012.05.005>
- [12] Woensel, R.V., Oirschot, T.V., Burgmans, M.J., Mohammadi, M., & Hermans, K. (2018). Printing Architecture: an overview of existing and promising additive manufacturing methods and their application in the building industry. *The international journal of the constructed environment*, 9, 57-81. <https://doi.org/10.18848/2154-8587/CGP/v09i01/57-81>
- [13] Bedarf, P., Szabo, A., Zanini, M., & Dillenburger, B. (2023). Robotic 3D Printing of Geopolymer Foam for Lightweight and Insulating Building Elements. *3D Printing and Additive Manufacturing*. <https://doi.org/10.1089/3dp.2023.0183>
- [14] Labonnote, N., Rønnquist, A., Manum, B., & Rütther, P. (2016). Additive construction: State-of-the-art, challenges and opportunities. *Automation in Construction*, 72(Part 3), 347-366. <https://doi.org/10.1016/j.autcon.2016.08.026>
- [15] Tibbitts, S. (2017). An Introduction to Active Matter. In S. Tibbitts (Ed.), *Active Matter* (pp. 11-17). Cambridge, MA: MIT Press. <https://doi.org/10.7551/mitpress/11236.003.0003>
- [16] Das, A. K., Agar, D. A., Rudolfsson, M., & Larsson, S. H. (2021). A review of wood powders in 3D printing: Processes, properties and potential applications. *Journal of Materials Research and Technology*. <https://doi.org/10.1016/j.jmrt.2021.07.110>
- [17] Le Duigou, A., & Correa, D. (2022). 4D printing of natural fiber composite. In *Smart Materials in Additive Manufacturing, Volume 1: 4D Printing Principles and Fabrication* (pp. 297-333). Elsevier. <https://doi.org/10.1016/B978-0-12-824082-3.00028-3>
- [18] Roxas, C.L., Bautista, C.R., Dela Cruz, O.G., Dela Cruz, R.L., de Pedro, J.P., Dungca, J., Lejano, B.A., & Ongpeng, J.M. (2023). Design for Manufacturing and Assembly (DfMA) and Design for Deconstruction (DfD) in the Construction Industry: Challenges, Trends and Developments. *Buildings*. <https://doi.org/10.3390/buildings13051164>



**ACOUSTIC AND LIGHT**  
 Imagine the opportunity to create a wall that allows you to achieve specific light/transparency combined with acoustic performance that meets defined needs in a single production process. Automated addition of acoustic absorbers and glass fibres – for transparency – to a printed concrete wall.



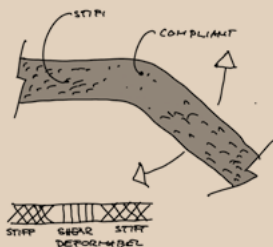
**CELLULAR PRINTED WALL**  
 Yes, we have already discussed whether a brick wall is in fact one of the earliest forms of additive manufacturing, and to a certain extent the following can be argued: the combination of automated assembly with the concept of an open grid structure to be filled with functionalised building blocks (cells) will make it possible to obtain a wall that meets specific performance needs.



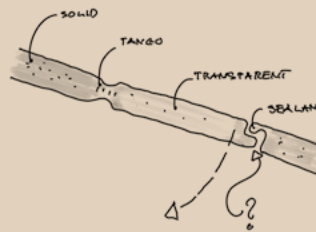
**HIERARCHICAL MATERIAL**  
 Inspired by the structures of bio-organisms, such as the structure of grass, it is proposed to design multifunctional construction components by combining a set of layers, in accordance with specific hierarchical functions, that can be produced in a single process by additive manufacturing.



**LIGHT COLUMN**  
 Additive manufactured sponge-like structure with integrated lenses to reflect and guide light according requested design and functionality.

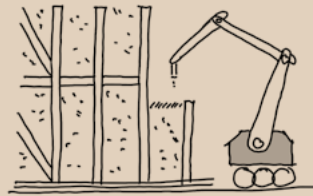


**METAMATERIAL HINGE**  
 Hinges not made from mechanical parts, but printed all at once with different materials or with different internal geometries, providing customised rigidity and deformation capacity to these components.



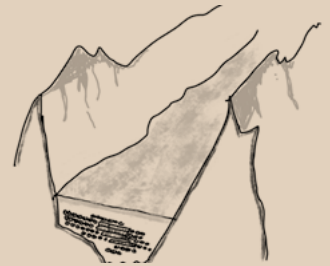
**MONOLITHIC WINDOW**  
 Imagine a window made up of just glass-based material, a monolithic window, which by additive manufacturing methods could have solid and opaque parts contiguous to flexible sections – like the tango material – or even to transparent parts.

# SUSTAINABILITY + CIRCULARITY



## AUTOMATED STICK BUILDING

When we think of circularity, building with wood seems like an obvious choice. The integration of automation processes could speed up the manufacture of structural wooden grids, which are labour-intensive. These systems could be even more sustainable if they were combined with AM of materials such as clay and natural fibres for the infill.



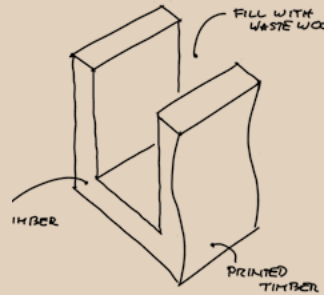
## CO2 GRAVEYARD

If we aim to store CO2 and elevate this to a higher level, building with wood would be just one part of the solution. Picture filling a valley with both deceased and living trees, carefully placed in trenches or stowed away, under a sufficiently thick layer of soil that prevents their decomposition. This method hinders the return of the CO2 they captured to the atmosphere, effectively creating a carbon sink.



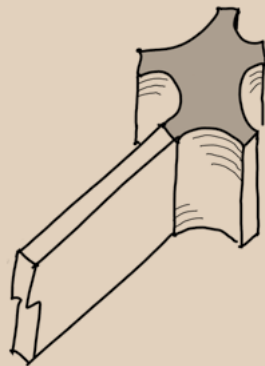
## LOW ENERGY PRINTING

AM technologies are becoming more reliable and prevalent in the construction industry. Should we consider increasing the use of polymers, which melt at lower temperatures, instead of printing in steel or glass that require high temperatures and energy consumption? Yes, this needs to be evaluated in terms of the component's intended usage over time!



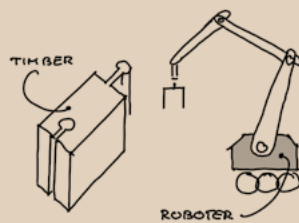
## MAX WOOD!

Considering the successful development of AM wood, we can envisage wood-print-mould systems capable of being filled with wood waste. This approach maximises wood storage and increases CO2 sequestration.



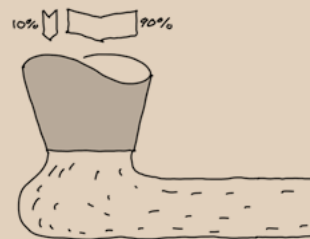
## SIMPLE TIMBER

There are limitations in using timber to construct complex free-form structures, usually restricted to flat parts manufactured by linear cuts. To enhance their use in more complex design solutions, the AM of customised knots defined to connect linear timber elements can be a smart strategy to consider. Incorporating features that facilitate easy assembly and disassembly makes these systems even more relevant and sustainable.



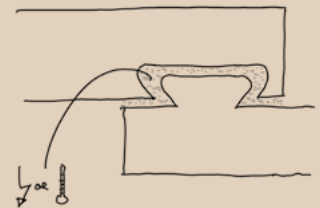
## WOOD BRICKS

Picture the next level of building blocks technology resting in pre-milled wood bricks, a step beyond traditional tree-based methods. Automation for manufacturing and assembly is coupled with precise positioning, where the interlocking of these bricks is facilitated by variations in humidity.



## WOOD CREATE

Although the use of wood fibres as reinforcement in a concrete matrix to enhance stress resistance is a known process, consider the use of extrusion system, similar to 3D-printed concrete, to extrude a material composite that optimises the wood usage in a ratio of 90% fibre and 10% matrix.



## THE INTERLOCKER

We have learned that interlocking systems are effective for deconstruction. They could be even more efficient if we could secure them for the intended lifespan. A solution could be a mortar or adhesive material with hardening or softening properties that can be activated or deactivated by temperature, humidity, or electricity. This innovation would significantly enhance their efficiency and durability.



# MATERIAL BALANCE DESIGN: DIGITAL TOOLS AND CIRCULAR INNOVATIONS FOR A NEW TECHNOLOGICAL CULTURE IN ARCHITECTURE

Ingrid Paoletti

Olga Beatrice Carcassi

Maria Anishchenko

The work on Material Balance Design implies to incorporate environmental issues both in production efficiency models and in pro-active eco-efficiency research methods, while involving technical design and building processes. In this paper, three case studies are showcased as examples of the Material Balance Design approach, namely MAT. RES, Desert tectonics and Senseknit pavilions. These projects developed by Material Balance Research group (Politecnico di Milano, 2019) intend to promote a homeostatic relationship with the environment that preserves resources and at the same time reduces waste through new responsible materials on an environmental, architectural, and technological scale

## INTRODUCTION

This study proposes a framework to develop new approaches to calibrate design, material productivity and eco-efficiency. From the Material Balance principle (Paoletti and Nastri, 2021) according to the relations of equilibrium that account for streams by which energy is produced, exchanged, transformed and consumed (i.e. with the application of the "law of conservation of mass" based on the to the relationship of equilibrium between the energy that is produced, exchanged, transformed and consumed (i.e. with the application of the "law of conservation of mass"), it is possible to appreciate how the in architectural practices,

all inputs used in the production processes are resulting in accumulation or waste, as it is possible to see in equation 1:

(1)

$$\text{INPUT} + \text{GENERATION} = \text{OUTPUT} + \text{CONSUMPTION} + \text{ACCUMULATION}$$

With an innovative Material Balance Design approach, the equation 1 its interpreted by looking at i) the inputs we put in the world through design, ii) what we do generate with the materials used in architecture and its meaning, and iii) by questioning which purpose have the systems we build and how can we can re-balance our impact on the earth. On

this basis, the work on Material Balance Design implies the objectives to incorporate environmental issues both in production efficiency models and in pro-active eco-efficiency research methods, involving the incorporation into technical design and building processes. This approach considers the development of technical elaboration of the environmental reality and the anticipation of the environmental outcomes. Moreover, it focuses on the functional, productive and material optimization with the support of new forms of calibration and material densities, sizes and structural performances (with less material and wasted energy), with the use of “digital/virtual design” procedures, “productive/constructive customization” technics and “executive design” methods. Observes therefore how the production, consumption and distribution activities have a direct relation with nature, which provides raw material to the economy for its production and consumption activities with a more circular approach. Here, the materials are fast progressing in terms of micro, meta and macro systems, they are no more the only refuge of creativity and influenced by digital means. With enabling tools such as advanced manufacturing technologies, which is a manufacturing process developed in an industrial context where precision and direct production is requested, and computational design, which refers to a procedure which interprets mathematical data informing the design in order to give directional results materials can be customized up to their molecular structure to have a functionally graded material systems, as Nature does. Some of the outcomes of the Material Balance Design are presented in the paragraphs below. They concern the development of these new responsible materials on an environmental, architectural, and technological scale. Through the definition of a new design paradigm, these projects intend to promote a homeostatic relationship with the environment that preserves resources and at the same time reduces waste.

## **MAT.RES (MATERIAL RESILIENCE). FROM A MICROSCOPE TO A PROTOTYPE FOR A RESILIENT ARCHITECTURE**

MAT.RES project was born as a “matereoteca” – a library of innovative sustainable architectural materials to be presented during the Venice Biennale 2020 for the Italian pavilion. In researching the best way to represent a series of various materials from the partners, we have chosen to work with a metaphor of resilience through an installation that evokes the trunk of a tree. With their fibrous and robust structure, tree trunks show us some of the strategies nature has developed to positively respond to difficulties and trauma to survive efficiently and competitively (Figure 1).

MAT.RES tells the resilient behavior of tree trunks with their complex system of the longitudinal and transverse vessels, the central pith, and the bark. It is done out of innovative materials from the culture of architecture, interior spaces, and fashion, becoming a living laboratory of resiliency, with a biological, organic, sustainable, recycled origin, which grow and transform over time. From natural composite materials like mycelium, coffee waste, cellulose, to 4D printing, from plants that produce energy to fabrics with optical, acoustic, or thermosensitive properties to natural or recycled fibers (Figure 2).

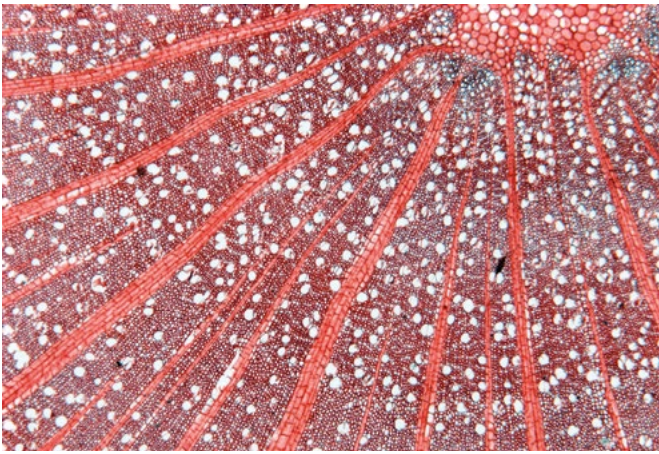
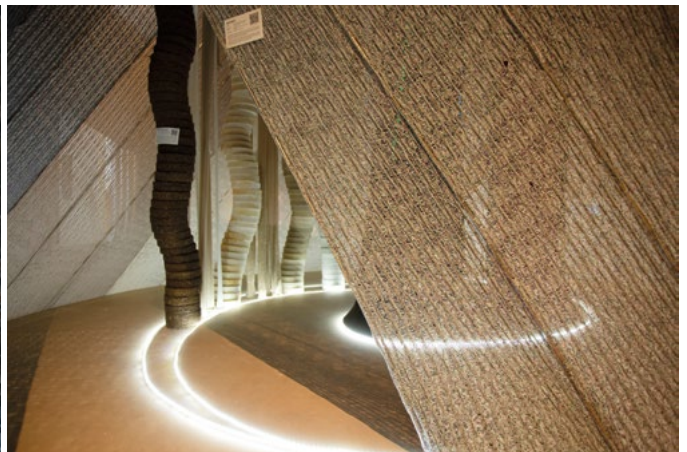


Figure 1: A tree trunk section under a microscope (©Material Balance Research).



Figure 2: On the left: the overall look of the MAT.RES pavilion. On the right: the internal columns with the highlighted path (©Material Balance Research).



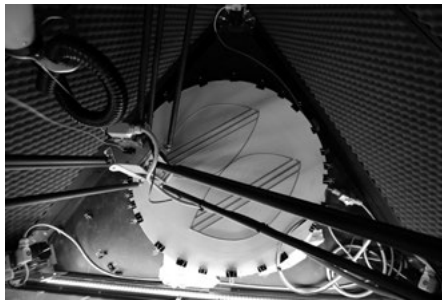


Figure 3: From left to right: linen tubes imitating the vessels; the overall look of the pavilion from the inside; The 4d-printed column; the moss installation; mycelium growth (©Material Balance Research).

The external layer of textiles represents a tree's bark with function as a barrier that protects the internal vessels and defines the borders. This shell is made of knitted fabrics of organic cotton, a lightweight, completely biodegradable material that has characterized the overall shape of the installation while being breathing and translucent to give a hint to the visitors on what they can expect to find inside. The internal vessels are composed of materials of various origins. The main path is framed by rigid and semi-rigid columns. The space between them is filled with fabric tubes that imitate the trunk vessels, the components of a trunk that have a crucial function of bringing water and minerals from roots to leaves and vice versa. For these hanged elements, another traditional organic material was chosen – linen. Linen has a high resistance to traction and elongation, is extraordinarily bright and silky, and has high hygroscopic properties. Linen does not require much water to grow and is biodegradable. The installation's core comprises a series of rigid columns and hung elements of various origins. The presented materials were either provided by partners, who have chosen their innovative and avant-garde products, or were developed in the SAPER.lab as a result of scientific research. Below are some of the materials produced at the SAPER.lab for the MAT.RES installation (Figure 3).

4D textiles emulate the dynamism of nature. 4d-textiles are produced by 3d-printing on pre-stretched elastic fabrics. The combination of additive manufacturing and tension-active mechanisms cause planar distortion, and therefore, shape-shifting. Morphing textiles generate complex large-scale three-dimensional shapes starting from simple two-dimensional patterns. One of the semi-rigid columns was composed of dense spacer fabrics. Thanks to a significant thickness and porous structure, this material is an excellent noise absorber that can be used to improve the acoustic of spaces. Produced with the technology of computational knitting, they can take various forms to fit the best in the space.

Nature is also embedded as vertical moss in the resilience manufacture. Scientific literature proves that vertical greening systems may provide many environmental advantages. In indoor spaces, they save energy for cooling and heating, improve air quality, and provide acoustic insulation. In outdoor spaces, they absorb CO<sup>2</sup> and release oxygen, create habitat for biodiversity, provide social and psychological comfort, and improve urban water management, contributing at mitigating the urban heat island effect.

Mycelium-based composites are used as acoustics and thermal insulation. Grown in form and combined with rattan, mycelium is reinforced like concrete is supported by steel in a novel application. Coffee bricks were developed in a search for the application of coffee waste. Mixed with bamboo fibers and natural coccoina glue, they can be used as insulation, a sustainable alternative to the existing solutions.

Among the materials presented by the partners were the G+ graphene nanoplatelets-based thermal circuit printed on polyamide fabric, bricks of recycled cotton cellulose for insulation, fabrics photoluminescent and low-melt yarns, and wool cylinders for electromagnetic protection.



Figure 4: Façade view of the final project (©Material Balance Research).



Figure 5: 3D printing process of one façade element (©Material Balance Research).

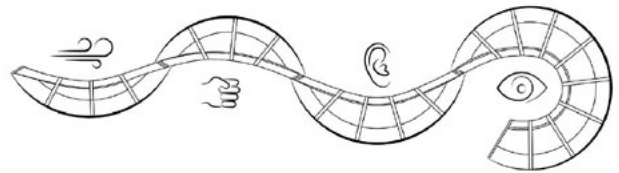


Figure 6: The schematic plan of the pavilion (©Material Balance Research).



Figure 7: The overall look of the Senseknit pavilion exposed during the Design week in Milan in 2019 (©Material Balance Research).

## **DESERT TECTONICS. USE OF SAND WASTE FROM CONSTRUCTION SITE AS NEW MATERIAL DESIGN**

The research hereby proposed illustrates the project of a 3D printed facade shading system for a service pavilion at Expo 2020 in Dubai, the design is easy replicable and can be feasible also for other overlay spaces. Hence, the design for this facade had to fulfill the typical features of temporary architecture for Expo (Figure 4): lightweight (ease of transport and on-site Construction), modularity (easy assembly and designed for production), flexibility (ability to cover many functions and to adapt to different constraints), identity (reflection of the identity of the hosting country).

The concept, is inspired by the local environment and architecture: the pattern is created by the winds drifting through the dune sand related to the tradition of filtering light and creating privacy through ornamental screens. Algorithms modulate landscapes of curves, which are materialized into three-dimensional geometries displaying gradients of porosity, curvature, and thickness (Figure 5).

Hence it is possible to physically “slide” these parameters on the Grasshopper definition that assess the design. Through computational design the facade concept has been optimized for additive manufacturing. Many tests have been conducted on polymeric printable materials, through a climatic chamber in Politecnico di Milano (Laboratorio Prove Materiali), to ensure material performances and durability at high temperatures. Then a campaign of digital fabrication tests has been started to optimize, simultaneously, the shape of the facade and the printing settings (such as retraction value, layer height, speed). The results can be deepen in the research proposed by Grassi et al (Grassi et al., 2019).

## **SENSEKNIT PAVILION. RE-INVENTING RECYCLED TEXTILES WITH COMPUTATIONAL KNITTING**

Senseknit is a pavilion that was born to explore the potentiality of knitted fabrics for the architectural applications. This installation, produced in a collaboration between Material Balance Research Group, SAPERLab, and TextilesHUB from the Department of Architecture, Built environment and Construction engineering, and the Laboratory of Knitting from the Department of Design of Polkitecnico di Milano, was presented at MADE EXPO 2019, Design Week 2019, and Tensinet Symposium 2019 in Milan. The pavilion demonstrated a way to combine tradition, innovation, and digital culture - vital elements to transform design and Construction fields. Textile environments have a potentiality to be a sustainable

alternative to conventional construction materials if that they can satisfy the safety and architectural comfort aspects. Both can be controlled on fiber composition level and by the way of fabric production. In the ‘Senseknit’ pavilion the engineered fibers and the advanced technology of digital knitting were used to investigate the way how textiles can influence the architectural comfort. The pavilion is parametrically designed as a curved wall that bending and curving forms 4 partly closed areas which are used to demonstrate the different architectural qualities of the textiles (Figure 6).

The base structure is wood cut with the computer-numerical-control machine (CNC) and assembled of 22 blocks. The wooden structure is covered from both sides with 90m<sup>2</sup> of knitted textiles, optimized with digital knitting technology. This technology permits seamless non-uniform fabrics to be created in a fast and waste-free manner. Linking it with performance-driven optimization programs that help to achieve higher-performance textiles minimizing the material usage (Anishchenko, 2020) (Figure 7).

The pavilion ‘SenseKnit’ offers four thematic areas of sensorial comfort, characterized by different types of fabrics produced on demand to maximize the acoustic and climatic comfort, obtain visual effects, and structural force. Acoustic comfort is essential for different contexts, particularly for public spaces. The noise absorbing characteristics grow with the increase of the overall material surface and the porosity level. To achieve that the fabrics were produced out of the special noise-absorbing fiber and formed in a 3D pattern. The aim of the structural part was to identify the areas exposed to the major stress and reinforce them by manipulating the fabric density. This creates a lighter structure, keeping the reinforcement where needed only. From the climatic point of view, knitted textiles are used for the control of air movement to obtain distributed flow. Fabrics with differentiated density distribution help to block or free the airflow to obtain the desired effect. From the optical point of view, the level of openness of the knitted textiles helps to control the level of light and to create desired visual effects, filtering the light in different modes and intensities. The proposed scenarios display the potential of digital knitting and technical fibers as advanced technologies and materials that can revolutionize how we design and inhabit spaces. This intuitive environmental performance of the knitted textiles, with performative purposes, transforms the ancient tradition of the past into a future perspective.

## ACKNOWLEDGEMENTS

The authors would like to acknowledge:

- x The Material Balance Research Group, in particular Arch. Saverio Pasquale Spadafora, Giulia Grassi, Danilo Casto, Al-Azri, Valeria Marsaglia and Andrea Giglio, and Anna Barbara (PoliMI, Dip. Design), Federico Leoni (Università di Verona, Dip. Scienze Umane) and Stefano Gomarasca (Università degli Studi di Milano, Environmental Science and Policy Dep.) for the realization of MAT.RES. Some elements of the exposition were realized with the support of Luigi De Nardo from the Chemistry Department of Politecnico di Milano and companies Directa-Plus, Lanificio dell'Olivo, Artemaglia, Sesia, Shima Seiki Italia spa, Aquafil spa, lafil spa, Sinterama spa, AlessandroSimoni, Milleforma.
- x Renaud Denhaive (PhD Candidate, MIT), Sonia Lupica Spagnolo (Associate professor, Politecnico di Milano), Lapo Naldoni (R&D Department, WASP) for their dedicated contributions during the Desert tectonics project development.
- x Prof. Alessandra Zanelli and Arch. Elpiza from the Laboratory TextilesHUB and Prof. Giovanni Maria Conti, Ph.D. Martina Motta, Dott. Carlotta Bellissimo from the Laboratory of knitting for their precious contribution in the design and fabrication of the Sense-Knit pavilion.

## REFERENCES

- Anishchenko, M., 2020. Bespoke knitted textiles for large-scale architectural projects, in: SpringerBriefs in Applied Sciences and Technology. pp. 75–82. [https://doi.org/10.1007/978-3-030-54081-4\\_7](https://doi.org/10.1007/978-3-030-54081-4_7)
- Grassi, G., Lupica Spagnolo, S., Paoletti, I., 2019. Fabrication and durability testing of a 3D printed façade for desert climates. *Addit. Manuf.* 28, 439–444. <https://doi.org/10.1016/j.addma.2019.05.023>
- Paoletti, I., Nastri, M., 2021. The Material Balance Manifesto. Scientific Approach and Methodologies, in: Paoletti, I., Nastri, M. (Eds.), *Material Balance: A Design Equation*. Springer International Publishing, Cham, pp. 1–23. [https://doi.org/10.1007/978-3-030-54081-4\\_1](https://doi.org/10.1007/978-3-030-54081-4_1)
- Politecnico di Milano, 2019. Material Balance Research [WWW Document]. URL <https://www.materialbalance.polimi.it/> (accessed 9.30.22).



# LINES OF CODE AND CODED CLAY; A PLEA FOR THE INACCURACY

Erno Langenberg

How do we design for the additive manufacturing of clay, to be used for architectural applications? How does thinking from the digital production process (design to fabrication) change the way of designing and the perception of form? How do we bring together the necessary, inherently, multidisciplinary knowledge to work in the field of additive manufacturing of clay?

These were the questions that have arisen during an extended period of formal experimentation with 3D printing clay and I wanted to address in my talk at W.AMCA – Workshop on Additive Manufacturing and Construction Automation – held at the University of Minho on May 24<sup>th</sup>, 2022; as food for thought in the discussion during this workshop. In this text, I want to focus on the first two aspects; the digital tool and its influence on architectural design.

How do we design for the additive manufacturing of clay, to be used for architectural applications? How does thinking from the digital production process (design to fabrication) change the way of designing and the perception of form? How do we bring together the necessary, inherently, multidisciplinary knowledge to work in the field of additive manufacturing of clay?

These were the questions that have arisen during an extended period of formal experimentation with 3D printing clay and I wanted to address in my talk at W.AMCA – Workshop on Additive Manufacturing and Construction Automation – held at the University of Minho on May 24<sup>th</sup>, 2022; as food for thought in the discussion during this workshop. In

this text, I want to focus on the first two aspects; the digital tool and its influence on architectural design.

3D printing with clay occupies a special place in the field of Additive Manufacturing (AM) for architectural applications. Due to the need for the clay to be fired after 3D printing to become a weatherproof ceramic element to be used for a long-lasting architectural application, the scale of the printed object will always be limited in size. Therefore the process is significantly different from 3D printing with concrete, where potentially a whole building could be printed as one single object. 3D-printed ceramic architectural objects will therefore almost inevitably be part of a series of similar objects. This brings the thinking about 3D printing

ceramic objects in the realm of industrial product design or even craft and therefore closely related to the manufacturing tool and the making process, closer than in most modern architectural practices. It is this close relation to the tool and making in the design process which I would like to address as an important key to advancing this technology. The quote below, from the exhibition “Flashback Carrilho da Graça” on display at the Casa da Arquitetura, Matosinhos, in 2022, visited during the workshop, strengthens my belief in the importance of knowing the tool of choice and learning from its working.

Carrilho da Graça believes that all disciplines work on the same kind of concerns and that from each discipline, and from its tools, it is possible to reach similar conclusions and discoveries. (Marta Sequeira curator of the exhibition Flashback Carrilho da Graça, Casa da Arquitectura, Matosinhos, 2022)

## DIGITAL CLAY COILING

In essence, 3D printing with clay is a process of building up an object layer by layer by coiling plastic clay with a computer controlled machine. This coiling itself is a traditional way of constructing with clay where objects are made by constructing walls by stacking hand-rolled or extruded coils. The main difference between 3D printing and this old craft is the potential of digitally controlling the shape, size, and placement of the coils.

Then, to ‘print’ any object, an ‘idea’ of the object has to be digitised after which it needs to be translated into code for the printer to execute. In general, this takes place via specialised software (slicers) which are designed in such a way that there is little or no prior knowledge needed of the used printing technology. Commonly, users input a preconceived idea (design) of an object in this software after which the code for the fabrication process is generated without paying too much attention to the making process. For most AM processes, this is sufficient for a good result. However, in the case of 3D printing with clay, this method leads to unsatisfying results. This is, amongst other causes, because the commonly available software doesn’t take into account the (unpredictable) material behaviour of clay.

## LEARNING FROM OTHER DISCIPLINES

To improve the 3D printing process from design to fabrication, knowledge from a wide variety of disciplines and work fields need to be involved. One can think for example of academics specialised in chemistry or fluid dynamics to

study the influence of the chemical composition of the clay on the flow and hardening of the clay during and after the extrusion. However, also, important lessons can be learned from various craftspeople, who often have a lifelong hands-on experience with the material and production processes, and know typical solutions for common problems.

To be useful for future users this knowledge of the material and the fabrication process then needs to be included in the future design and manufacturing explorations; either through the designer’s or collaborating experts’ experience with the tool and or material or in the software itself. The first requires a long learning trajectory of the user or collaboration with experts. For the latter, the software needs to be greatly improved by including the knowledge mentioned above. If this software package is supplemented with computational design capabilities, a powerful system can be created which makes the design process truly informed and ultimately allows for an intuitive play between the digital and the physical.

## NEXT STEPS

To build this digital design system we need to ask what aspects of the fabrication tools we have to look into, what knowledge to incorporate, and also importantly ask what the aim is of this software; what is a logical place in the production of architecture, where 3D printing ceramics makes sense? In general, there are five key benefits that AM has over traditional manufacturing: cost, speed, quality, innovation/transformation, and impact. That being said, AM will not replace existing conventional production methods. However, it is expected to revolutionise many niche areas.[1] At the moment, cost, speed, and quality are not the characteristics of this relatively new technology, although this might change in the future with the advancement of the tools. Innovation and transformation and impact, however, seem to me the most interesting benefit to explore first to find the right niche area.

Working on these topics, I took a design-by-doing approach; a hands-on exploration into new ways of producing ceramics. I believe that a free exploration of the possibilities the technology offers can take an essential role in further developing the field of 3D printing ceramics; by posing novel questions, searching for answers in uncommon ways and places, and by exploring lucky mistakes.

Below I mention two aspects that came forward during my explorations which can be interesting avenues to explore further: the use of the mark of the tool and its glitches, and secondly how to scale up the production process. Both, in a way, have a great deal to do with (the lack of) accuracy, working with an unruly material like clay.

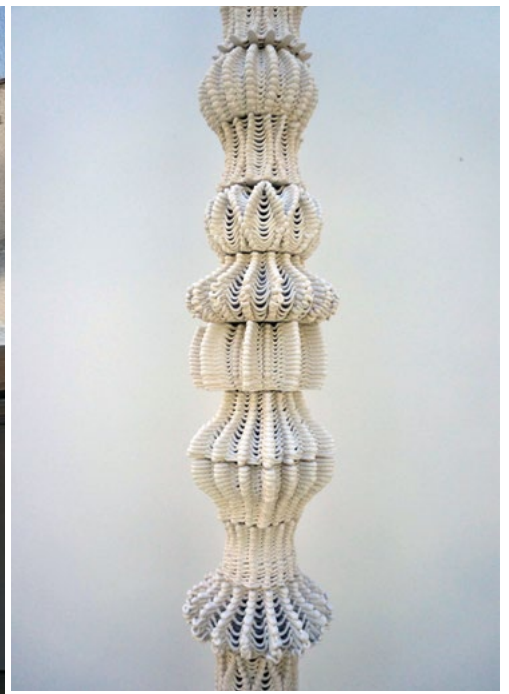
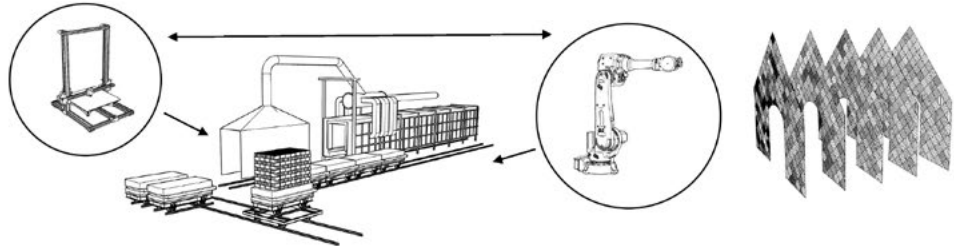
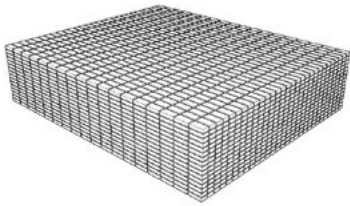


Figure 1: Column 11001111001010011000101000, built out of 26 bespoke 3D printed stacked elements, ELstudio, 2016.

Fired bricks - ceramics



Small - local



Medium/Large - Regional/National

Figure 2: Two manufacturing systems for fired bricks considering scale and production context

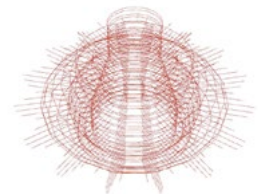
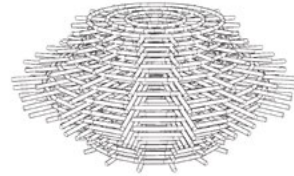
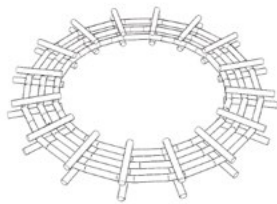
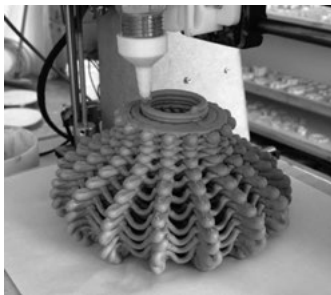


Figure 3: Column stave 3D printing process, its 3D model and printing, Cove Park Craft Residency, ELstudio, 2016.

## TOOL EXPRESSION AND EXPLORING GLITCHES

When a designer or maker is familiar with the tool, or this knowledge is incorporated into the software in the future, they can take advantage of or explore the specific marks of the process or tools involved.

Like the marks of the gouge in woodwork or brush strokes in a painting, a designer can use these aspects for aesthetic expression. One example is the Column 11001111001010011000101000, produced in 2016, which utilises the thread-like quality of the extruded clay. By controlling the tool via the toolpath which was designed through computational design – Rhino and Grasshopper – the material got a soft, organic, almost woven, feel to it. Similarly, unavoidable aspects of the process like mistakes and glitches can be used. Designer Hella Jongerius, for example, utilised, previously unwanted, marks of the production process in her B-Series ceramic tableware to produce unique pieces industrially; a comment on the impersonal feel of industrially produced products, compared to hand-produced ones.

Moreover, these marks or glitches can be explored for new performative aspects. To improve structural performance and stability during printing [2] or layer adhesion [3] for example. It is these later explorations that are, in my opinion, interesting to research, especially when combined with the digital aspect of the process. By using computational design methods, it is possible to generate endless variations. Linked with data from the physical experiments it becomes possible to explore these artefacts fast and cheaply for unknown performance, novel ways of (architectural) assemblies, or connections between elements.

## SCALING UP

For a project in Nijmegen in the Netherlands, I was asked to design and produce the cladding for a façade of a building, to be produced locally by 3D printing local clay with limited means. One of the first questions was how to produce at the architectural scale with the given means; a desktop-size 3D printer, medium-sized kiln, shovel, and mixer.

Considering the tools available, the project can be feasible within the given time frame. Though, only with the increase in printing capacity and a great amount of human labour attending the printers. This approach is suitable for a project of this size in an experimental context. However, for bigger commercial projects, this process needs to be looked at critically; the system needs to scale up in several ways, which touches both the technological as well as design aspects of the system.

The most obvious aspect to improve is the technology itself: the printing speed needs to go up and human involvement needs to be minimised to reduce time and cost. This means the printers should not only be faster but also more reliable, to avoid human attendance at the printer and assure a predictable result. Predictability and repeatability at the moment are rather poor when printing with clay, which leads to a great amount of waste and time loss. The repeatability is poor because of the unpredictable clay (especially local clay) and fluctuation in environmental conditions like the humidity, temperature, and draft to name a few. These are solvable technological problems, however, time and investments are needed.

Finally, to improve the process, one can look at the question of lack of predictability and repeatability as a design problem. An avenue to explore is to let go of the accuracy altogether and devise a design that allows for variation between the 3D prints, similar to the way old stone houses are built. In these houses, no single stone is the same, but still, a straight functional wall is produced. The shape of the stones themselves is never repeated, nor is there any connecting part. It is the system as a whole that makes it work. When using local clay and local machines, maybe this is the only way forward; a design system that combines production with high-tech machines, with a low-tech formal approach.

A positive side effect of this approach can also be that it leads to a more sustainable way of producing. With the option to produce less accurately, there is no need to go to great lengths to produce identical precise items and therefore the production process has fewer rejects, which results in less waste and is, therefore, more sustainable.

## REFERENCES

- [1] Attaran, M. (2017) "The rise of 3-D printing: The advantages of additive manufacturing over traditional manufacturing", *Business Horizons*, 60(5), pp. 677-688.
- [2] Mohite, A. & Kotnik, T. (2019) Speed of Deposition: Vehicle for structural and aesthetic expression in CAM. *Architecture in the Age of the 4th Industrial Revolution: Proceedings of the 37th eCAADe and 23rd SIGraDi Conference*. Sousa, J.P., Xavier, J.P. & Castro Henriques, G. (eds.). Porto, Portugal: eCAADe, Vol. 1. pp. 729-738.
- [3] Farahbakhsh, Mehdi & Kalantar, Negar & Rybkowski, Zofia. (2021). Impact of Robotic 3D Printing Process Parameters on Bond Strength: A Systematic Analysis Using Clay-Based Materials.



Figure 4: Column built of 3D printed clay staves, Cove Park Craft Residency, ELstudio, 2016.



Figure 4: Print & Burn project that examines innovative applications of 3D printing of clay by the control of the printing path and material variations, European Ceramic Work Centre, ELstudio, 2016.

# DESIGNING MATERIAL ARCHITECTURES

David Correa

Design extends beyond shape and form; it integrates multiple scales of material assemblies and processes of making. However, this sentiment is easily challenged by disciplinary boundaries, contractual structures of project delivery, or practical manufacturing logistics. Considering design as something that happens in the studio and not on the shop floor or at the manufacturing plant presents limitations to the design process itself. Developing a material intuition, rooted in materialization processes, offers designers access to a multi-scalar approach to architectural design thinking. This essay discusses the design logic behind four design projects that have been produced as part of a body of work focused on multi-scalar design in architecture. Each project considers the role of architectural thinking as a method for the logical organisation of materials in space that are in service of functional performance. These functional goals include both mechanical behaviour across hierarchical scales but also human inhabitation and experiential delight. Each project explores a different material and set of techniques, including 1) 4D printing with hygroscopic polymers, 2) 3D printed clay masonry, 3) Doubly curved wood structure using a stressedskin system, and 4) Elastic bending and weaving of bamboo reeds in a canopy structure. It is the hope of the author that this discussion will reinforce the reader's interest in engaging design as an integrative process of functional material articulation across multiple interdependent scales.

## INTRODUCTION

Biological organisms are almost entirely made of hierarchical materials (Elices, 2000; Dunlop and Fratzl, 2013; Fratzl and Weinkamer, 2007). Small units of microscopic cells are organised into meso-scale tissue structures that are themselves further arranged one level up into specialised organs (Dunlop and Fratzl, 2013). As of this writing, the use of biological growth processes remains largely at arms length for designers. Harvested tissue, such as wood, leather, mycelium, or bone are common building blocks of industrialised processes of manufacturing at the macro-scale – through the milling, moulding or refining of bulk materials. However, directly harnessing the genetic instructions of growth processes to tailor micro and meso-scale architectures in an integrated

design-to-production workflow remain elusive. Performance through form is a well understood principle in the engineering of large artefacts (like ships, planes or buildings), but it is at the microscopic level that the role of form and geometry play its greatest role. From crystalline structures in minerals, protein chains in animals, to cellulose fibres in plants, it appears that the smaller the building block the more potential it has for functional specialisation (Fratzl and Weinkamer, 2007).

In architecture, the stone, followed shortly by the brick, have been one of the fundamental design units across geographic regions. While not as suitable for mass production, more interesting vernacular structures harnessed fibre composites in the form of bundled reeds, straw and wood as their fundamental construction unit to design high performance buildings in every continent (Oliver, 2007; Julian Lienhard, 2014).

It could be assumed that the level of precision in which each material could be organised can be loosely correlated to the level of functional performance that could be achieved; a technical development that could be further tracked across generations, and in tandem with other contemporary innovations. In general, the organisation of material in space requires the highest level of design intelligence to produce the best performance. One example would be the precise organisation of brick to form a barrel vault, or the interconnectivity of stamped steel components to form the monocoque structure of a car. In both instances, the bulk properties of steel and terracotta as well as the macro-scale form of the vault or the car are intrinsic to the type of functional performance each can have.

Starting with small units that can be precisely organised to support the functional goals of the macro-scale shape of the artefact seems like a good plan. The smaller the unit and the higher the precision of organisation the higher the potential for technical improvement and localised specialisation. One technology that excels at this is 3D printing. In essence, 3D printing is an additive process that can precisely position units of material that will bond to each other to form progressively larger and larger structures until the total part is completed. How this bonding of units occurs, and how the units of material are deposited, will dictate the given name of the technology and the design space of each approach. Some of the most common 3DP technologies include: Fused Filament Fabrication (FFF), Selective Laser Sintering (SLS), binder jetting, stereolithography, multi jet fusion, among many others (Chen et al. 2019; Wolf et al., 2022; Ngo et al., 2018). Fused Filament Fabrication (FDM or FFF) or Liquid Deposition Modelling (LDM) rely on the continuous extrusion of a filament of material that will be subsequently fused to itself on a subsequent layer (Ahn et al., 2002; Das et al., 2021).

The extrusion process affects the microstructure of the filament itself, the shape of the filament and the adhesion properties between extruded filaments (Ziemian et al., 2012; Sood et al., 2010). As the material builds a pattern within a layer, these extrusion related properties give the resulting material direction dependent properties that are further developed across multiple layers. At the microscopic scale the extrusion process tends to orient the smaller units within the flow of material - like polymer chains (Cole et al., 2016) or fillers (Le Duigou and Correa, 2022). At the meso-scale, each layer forms a pattern of interconnected, fused units of filament, which determine mechanical properties. As layers accumulate, the relation between each of those intermediate meso-scale structures compound to form a fibrous composite material with direction dependent (anisotropic) properties. Fibrous composites are very efficient and widely used by both biological organisms (Elices, 2000), and industrial production processes (Le Duigou et al., 2020). In nature, wood is the most abundant fibrous composite, as long chains of cellulose are used to form micro fibrils, then fibril bundles, then all the way into forming the wood grain of the trunk of a tree (Dinwoodie, 2000; Ajdary et al. 2020). The mechanical

efficiency of wood as well as its propensity to warping during drying are both directly linked to its physical properties as a fibrous composite. As an example of an industrial process, the same tree trunk is carefully cut into thin sheets of veneer that are subsequently cross laminated to form plywood - a more dimensionally stable laminate fibrous composite.

#### 4D printing with hygroscopic polymers

A 3D printed part, made via FFF, has very similar properties to plywood; both are fibrous laminate composites, and its fracturing patterns can be predicted based on the raster patterns that compose each layer (Ziemian et al. 2012). The valuable difference here is that the design process for 3D printing allows for the design of each layer, or even further, it allows for the localised design of differentiated regions within each layer (Correa 2022; Poppinga et al. 2020). Figure 1 shows a 3D printed part with only two layers where each layer has a pattern of concentric circles. This component, however, is not designed for dimensional stability. Instead, each filament has oriented hydrogel particles that swells with water. The particles have been aligned during the extrusion, which directs the swelling to occur predominantly tangential to the direction of extrusion. In other words, the filaments swell more to the side than towards the length - therefore pushing on each other. The compounded effect of this small expansion results in conical protrusions that only appear after submersion in water. In this case the design of the final shape starts with the design of the microscopic properties of the material and carries across the intricate spatial and formal architecture of the layered material. The designer is then both responsible for the design of the global shape, the one with the protrusions, but also the design of all the material architectures that make said shape-change deformation possible. These are many intermediate, meso-scale interactions between the filaments that are embedded in the material during the design of the printing tool path. The design of these multiple meso-scale interaction is of great interest for designers. 4D printing is fundamentally an integrative design process and it offers a great example of a design process that encompasses both material architecture, form, function and kinematic transformation.

#### 3D printed clay masonry

3D printing with clay is called Liquid Deposition Modelling as the clay is not melted, as is the case in FFF, but instead it is deposited as a highly viscous liquid (Clarke-Hicks et al., 2022; Ngo et al., 2018). The material remains malleable throughout the printing process, and it only partially achieves a certain level of hardness after drying. As a ceramic material, the clay printed part only achieves its full mechanical properties after firing. It is during the kiln firing that the minerals and particles within the clay body fuse to form a rather durable, crystalline material (Bechthold and Weaver, 2017). Similar to the FFF, the process of extrusion affects the properties of the clay.



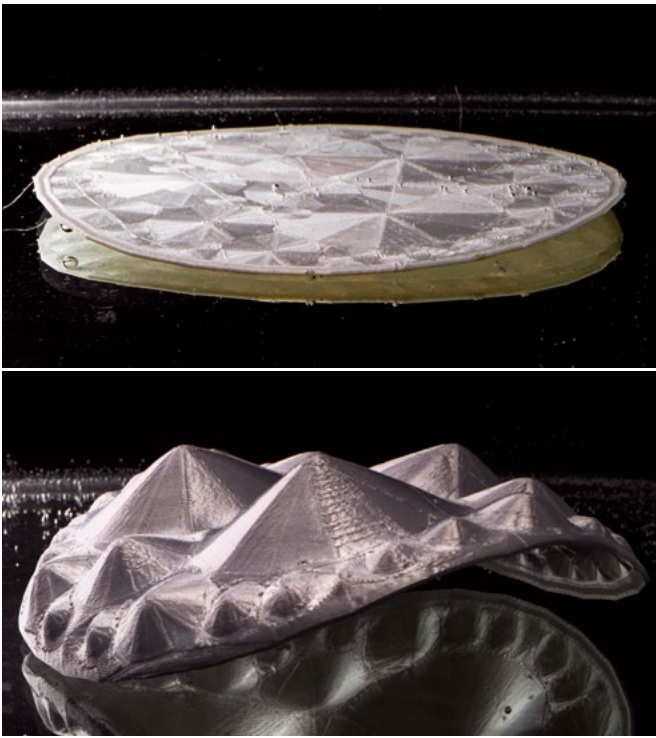


Figure 1: 4D printed disk that was printed using a hydrogel composite polymer. Two kinematic states, before (top) and after shape-change transformation in response to water submersion (bottom). (Research and image by David Correa).

Potters and other craftsman describe clay as having a memory, which refers to the orientation of particles within the clay body (Anderson, 2019). There is not much literature regarding the microscopic effects of 3DP extrusion in the clay body, but the empirical observation of clay printing pieces appears to indicate similar direction dependent properties that correlate to the direction of printing; this will include shrinkage and stress concentrations that often results in visible and invisible fractures during firing. At the visible meso-scale the same laminate properties of FFF are clearly seen. The prints can easily delaminate and fracture at the seams between layers. Unlike FFF, most clay prints tend to be hollow. This means that the printed components rely heavily on the cross section of the wall architecture, also referred to as the shell in FFF printing. This design space can be used to reinforce the structural stability of the print (Seibold et al., 2018; Shi et al., 2019), add texture (Wu et al., 2022), affect porosity (Dutto et al., 2022), add detail ornamentation through unsupported overhangs (Shi et al. 2019; Gürsoy, 2018; Rael and San Fratello, 2018) and most recently it can also be used as a functional feature to diffuse light. The latter has been particularly successful at changing the way light bounces through the ceramic's architecture in the shade of a lamp or through subsurface scattering in porcelain (Clarke-Hicks, 2021; Ochoa, 2021; Clarke-Hicks et al., 2022).

The HIVE project in Figure 2 uses the architecture of this layering process as a tool to design a tactile ornamentation feature. One scale up, the system also uses the tool path design to integrate multiple sections of the print, by crossing the path over itself in the apertures, to optimise structural stability. In this project, this intermediate design space reduced the number of components from 700 individual units to 175. Connecting back to the micro-scale structure, the stoneware clay body used in the print was selected for its mechanical properties and colour but also because of its porosity. Since some of the masonry units virtually hang from the edges of the wall, the mortar needs the masonry units to be porous to ensure proper bonding. This adhesion relied on both the formulation of the mortar, the porosity of the clay body and the resulting 3DP texture of the printed part. This is again another example of a multi-scalar approach to design using a rather simple material system such as clay.

#### **Doubly curved wood structure using a stressed-skin system**

The highest performance is generally achieved when every scale of the material structure is engaged during the design process. However, this is not always practical when working with tight deadlines or when the scale is so large that it is simply not cost effective to do so. In these instances, the best course of action is to investigate what the inherent bulk properties of the given material are and develop a design strategy that makes the most use of those properties. In other words, to use the material not as a receptacle of form but as an active

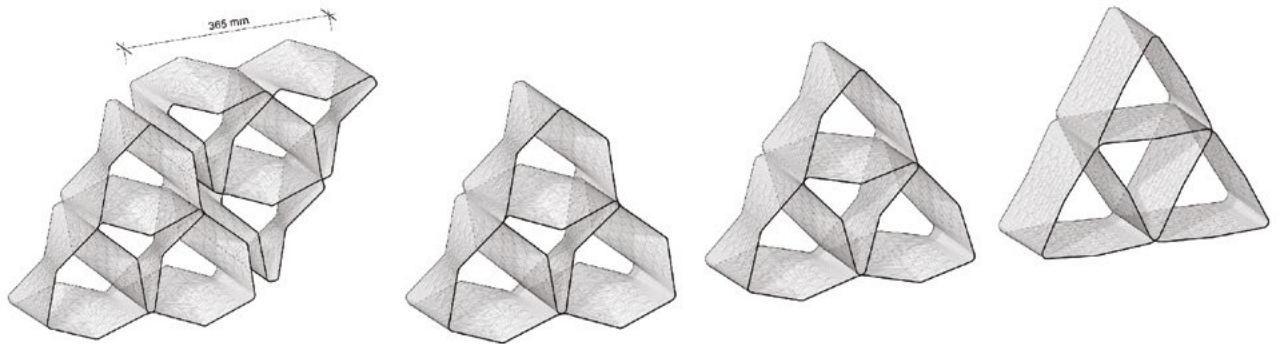


Figure 2: Hive is a clay printed masonry wall composed of 175 unique units. Project located in Toronto, Canada. The project was developed by Ye Sul E. Cho, Ji Shi, Meghan Taylor, James Clarke-Hicks, Isabel Ochoa and David Correa. (Images by David Correa).

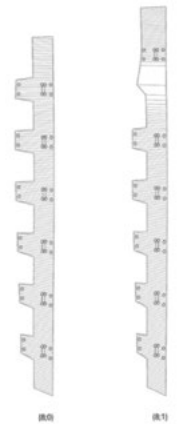
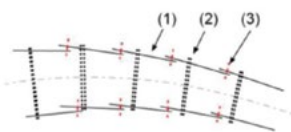
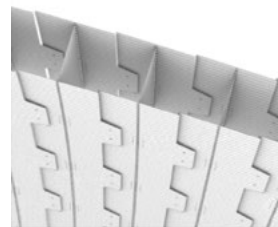
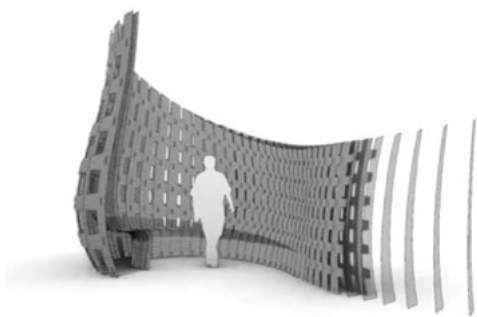


Figure 3: Example 3, layered materials for layered macro-scale structures Wonder Wood Pavilion constructed as part of the 2018 Robot Made Workshop at UBC, Vancouver. (Meyboom et al. 2019) (image by David Correa and Annalisa Meyboom)

participant in the architecture of the larger functional system.

In the case of plywood, previously established as an industrially produced laminate fibrous composite, the cross laminated meso-scale architecture of the wood veneer layers gives it unique elastic bending properties. For the Wander Wood pavilion (Figure 3), these properties were strategically used to create the doubly curved skin of the structure. The plywood skin defines the geometry of the pavilion but it also acts as its primary structure by acting as the flanges withing a stressed-skin structural system (Meyboom et al., 2019). Thicker plywood is used for the internal webs connecting the two outer skin layers. Plywood thickness is correlated with an increased number of layers and a resulting higher bending stiffness. This is a very intuitive consideration to make at this scale, as the difference in stiffness can be easily experienced when manipulating plywood sheets. Lastly, six axis robotic milling is used to cut each skin section while embedding helpful assembly information, such as wood on wood connections for the webs and pre-drilled perforations for rivets.

Accounting for the elastic bending radius of the plywood skin, each segment of the skin has tabs that allow each segment to bend in two directions. The rivet perforations in the tabs define its exact connection point between each section in an overlapping sequence. The complex double curved pavilion was fabricated and assembled in only three days as part of a five-day workshop on advanced wood fabrication. Four other pavilions have been built investigating similar integrative design strategies (Meyboom and Correa, 2022; Correa et al., 2019).

### **Elastic bending and weaving of bamboo reeds in a canopy structure**

Similar to nature, local design challenges require a strategic use of local materials and local resources. The last project presented here is a canopy pavilion designed to protect visitors from the rain in their trajectory from the bus to a performance space (Figure 4). Located in Guilin, China, the site is subjected to seasonal flooding (up to 4m high - just under the canopy) and it is surrounded by a lush bamboo field. Composed of long fibrous bundles arranged in a honeycomb-like matrix, bamboo is also a fibrous composite material (Gibson et al. 1995).

However, unlike woody trees (like the maple or cedar), the bamboo plant is a grass. With unique anatomical features, such as a hollow stem, bamboo can withstand significant elastic deformation without breaking - normally generated by wind. Using the local bamboo, as the architectural building block, offered local material availability and extensive local craftsmanship expertise. To harness these two advantages, a lightweight space frame steel structure is used to withstand the seasonal flooding while the architectural and formal expression of the project is defined by the bamboo cladding. Each piece of bamboo is selected for its mechanical properties from various bamboo species and graded based on its

thickness and length. The elastic properties of the material, combined with extensive local craftsmanship, allows each strip to be weaved into the assembly while forming a seamless surface that requires no additional fasteners to hold its shape. While the bamboo does not play a role in the primary structural system, acting only as cladding, its material properties are celebrated in its assembly and visual expression.

Beyond a multi-scalar approach to the material itself, the integrative design process for this project achieves a positive engagement with the local socio-cultural context and its ecological implications.

## **CONCLUSION**

Four projects were presented, each using a very different material (hygroscopic polymers, clay, wood and bamboo) but with a common approach to design. In each instance, formal, spatial, functional and structural logics are applied across multiple material scales. Much like it is found in biological organisms, this hierarchical integration has allowed each material architecture to provide resiliency, multi-functionality, and local adaptation to both internal and external requirements.

Internal requirements comprised system interactions to address load conditions at the component level, assembly logic or overall mechanical stability. External requirements involved the ability of the system to accommodate different spatial needs such as formal, structural or aesthetic changes across the structure.

The 4D printed disk highlights the close interaction between the internal material articulation of the designed material architecture and the resulting differentiated shape-change transformation, which occurs in response to water submersion. In the clay project this localized adaptation can be seen in the change of aperture openings to modulate privacy between the two sides of the wall, and in the tailored surface ornamentation of each masonry component. In the Wander Wood pavilion, the stressed skin changes curvatures several times across the length of the pavilion from synclastic to anticlastic curvature. The system is also pushed to its formal limits in the internal space to accommodate a bench like protrusion for seating. Correspondingly, the bamboo project celebrates these external adaptation challenges by demonstrating the ability of the bamboo cladding to seamlessly transition from wall to ceiling in multiple ways while providing great visual delight.

In summary, architectural design thinking offers a very valuable set of tools for the logical articulation of formal and functional relations. Using this integrative design approach to the multiple scales of material production and assembly has demonstrated potential at many levels. It is the hope of the author that this discussion, and corresponding demonstrator projects, will reinforce the reader's interest in engaging design as an integrative process of functional material articulation across multiple interdependent scales.

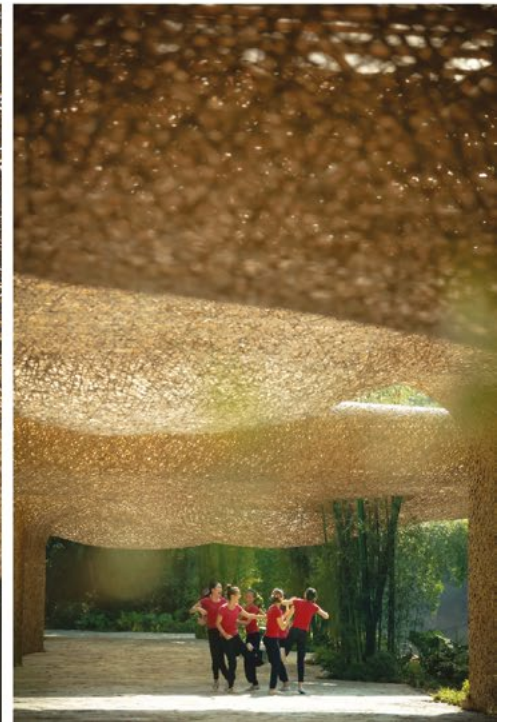


Figure 4: Bamboo Bamboo, Canopy and Pavilions in Guilin, China. Designed by LLLab, 2020.

## REFERENCES

- M. Elices, Ed., *Structural biological materials. Design and structure-property relationships*, 1st ed., Pergamon materials series, v. 4, Amsterdam, s.l., New York, 2000.
- J. W.C. Dunlop and P. Fratzl, "Multilevel architectures in natural materials," *Scripta Materialia*, vol. 68, no. 1, pp. 8-12, 2013.
- P. Fratzl and R. Weinkamer, "Nature's hierarchical materials," *Progress in Materials Science*, vol. 52, no. 8, pp. 1263-1334, 2007.
- P. Oliver, *Encyclopedia of vernacular architecture of the world*. Abingdon: Routledge, 2007.
- J. Lienhard, "Bending-Active Structures. Form-finding strategies using elastic deformation in static and kinematic systems and the structural potential therein," Doctoral dissertation, University of Stuttgart, Stuttgart. Institute of Building Structures and Structural Design, 2014.
- Z. Chen, Z. Li, J. Li, C. Liu, C. Lao, Y. Fu, et al., "3D printing of ceramics: A review," *Journal of the European Ceramic Society*, vol. 39, no. 4, pp. 661-687, 2019.
- A. Wolf, P. L. Rosendahl, and U. Knaack, "Additive manufacturing of clay and ceramic building components," *Automation in Construction*, vol. 133, p. 103956, 2022.
- T. D. Ngo, A. Kashani, G. Imbalzano, K. T.Q. Nguyen, and D. Hui, "Additive manufacturing (3D printing): A review of materials, methods, applications and challenges," *Composites Part B: Engineering*, vol. 143, pp. 172-196, 2018.
- S.-H. Ahn, M. Montero, D. Odell, S. Roundy, and P. K. Wright, "Anisotropic material properties of fused deposition modelling ABS," *Rapid Prototyping Journal*, vol. 8, no. 4, pp. 248-257, 2002.
- A. K. Das, D. A. Agar, M. Rudolfsson, and S. H. Larsson, "A review on wood powders in 3D printing: Processes, properties and potential applications," *Journal of Materials Research and Technology*, 2021.
- C. Ziemian, M. Sharma, and S. Ziemian, "Anisotropic mechanical properties of ABS parts fabricated by fused deposition modelling," in *Mechanical engineering*, InTech, 2012.
- A. K. Sood, R. K. Ohdar, and S. S. Mahapatra, "Parametric appraisal of mechanical property of fused deposition modelling processed parts," *Materials & Design*, vol. 31, no. 1, pp. 287-295, 2010.
- D. P. Cole, J. C. Riddick, H. M. Iftexhar Jaim, K. E. Strawhecker, and N. E. Zander, "Interfacial mechanical behavior of 3D printed ABS," *J. Appl. Polym. Sci.*, vol. 133, no. 30, p. 913, 2016.
- A. Le Duigou, D. Correa, "4D printing of natural fiber composite," in *Smart Materials in Additive Manufacturing*, Volume 1: 4D Printing Principles and Fabrication, Elsevier, pp. 297-333, 2022.
- A. Le Duigou, D. Correa, M. Ueda, R. Matsuzaki, and M. Castro, "A review of 3D and 4D printing of natural fibre biocomposites," *Materials & Design*, p. 108911, 2020.
- J. M. Dinwoodie, "Timber, its nature and behaviour," 2nd ed. London, New York, England: E & FN Spon; BRE with the support of the Centre for Timber Technology and Construction at BRE, 2000.
- R. Ajdary, B. L. Tardy, B. D. Mattos, L. Bai, and O. J. Rojas, "Plant Nanomaterials and Inspiration from Nature: Water Interactions and Hierarchically Structured Hydrogels," *Advanced Materials*, e2001085, 2020.
- D. Correa, "4D printed hygroscopic programmable material architectures," Stuttgart: Institute for Computational Design and Construction, University of Stuttgart, Research reports / Institute for Computational Design and Construction, 9, 2022.
- S. Poppinga, D. Correa, B. Bruchmann, A. Menges, and T. Speck, "Plant movements as concept generators for the development of biomimetic compliant mechanisms," *Integrative and Comparative Biology*, vol. 60, no. 4, pp. 886-895, 2020.
- J. Clarke-Hicks, I. Ochoa, and D. Correa, "Harnessing plastic deformation in porous 3D printed ceramic light screens," *Archit. Struct. Constr.*, vol. 8, p. 483, 2022.
- M. Bechthold and J. C. Weaver, "Materials science and architecture," *Nature Reviews Materials*, vol. 2, p. 17082, 2017.
- T. Anderson, "Techno File: Clay Memory," *Ceramics Monthly*, Available online at URL, <https://ceramicartsnetwork.org/ceramics-monthly/ceramics-monthly-article/Techno-File-Clay-Memory> checked on 2/23/2023.
- Z. Seibold, K. Hinz, J. López, N. Alonso, S. Mhatre, and M. Bechthold, "Ceramic Morphologies: Precision and Control in Paste-Based Additive Manufacturing," *Proceedings of the 38th Annual Conference of the Association for Computer Aided Design in Architecture (ACADIA)*, 2018.
- J. Shi, Y. Cho, M. Taylor, and D. Correa, "Guiding Instability A craft-based approach for modular 3D clay printed masonry screen units," in *Blucher Design Proceedings*, 37 Education and Research in Computer Aided Architectural Design in Europe and XXIII Iberoamerican Society of Digital Graphics. Joint Conference (N. 1). Porto, Portugal, September 10-12. São Paulo: Editora Blucher, pp. 477-484, 2019.
- Y. M. Wu, A. Kenny, I. Kim, and D. Correa, "Embedding ornament: Custom nozzle design in 3-D clay printing," in *Structures and Architecture A Viable Urban Perspective?*, 1st ed., CRC Press, pp. 1077-1086, 2022.
- A. Dutto, M. Zanini, E. Jeoffroy, E. Tervoort, S. A. Mhatre, Z. B. Seibold, et al., "3D Printing of Hierarchical Porous Ceramics for Thermal Insulation and Evaporative Cooling," *Adv. Mater. Technol.*, p. 2201109, 2022.
- B. Gürsoy, "From Control to Uncertainty in 3D Printing with Clay," in *Proceedings of the 36th eCAADe Conference - Volume 2*, vol. 2, Lodz, Poland, September 19-21, 2018. Lodz: Lodz University of Technology, pp. 21-29. Available online at URL, 2018.
- R. Rael and V. San Fratello, *Printing architecture. Materials and methods for 3D printing*, First edition, Hudson New York: Princeton Architectural Press, 2018.
- J. Clarke-Hicks, "Grading Light: Utilizing plastic deformation to functionally grade ceramic light screens," Master of Architecture, UWSpace, Waterloo, Ontario, 2021.
- I. Ochoa, "Grading Light: Utilizing plastic deformation to functionally grade ceramic light screens," Master of Architecture, UWSpace, Waterloo, Ontario. School of Architecture, 2021.
- A. Meyboom and D. Correa, "The path to future wood: Component based structural assembly systems," in *Structures and Architecture A Viable Urban Perspective?*, 1st ed., CRC Press, pp. 303-310, 2022.
- D. Correa, O. D. Krieg, and A. Meyboom, "Beyond Form Definition: Material Informed Digital Fabrication in Timber Construction," in *Digital Wood Design. Innovative Techniques of Representation in Architectural Design*, vol. 2, F. Bianconi and M. Filippucci, Eds., 1st ed. Springer International Publishing (essentials, 24), pp. 61-92, 2019.
- A. Meyboom, D. Correa, and O. D. Krieg, "Stressed Skin Wood Surface Structure," in *ACADIA 2019: Ubiquity and Autonomy*, ACADIA (ACADIA proceedings), pp. 470-477, 2019.
- L. J. Gibson, M. F. Ashby, G. N. Karam, U. Wegst, and H. R. Shercliff, "The Mechanical Properties of Natural Materials. II. Microstructures for Mechanical Efficiency," *Proceedings: Mathematical and Physical Sciences*, vol. 450, no. 1938, pp. 141-162, 1995.

# MULTI-MATERIAL FACADE COMPONENTS BY ADDITIVE MANUFACTURING WITH REACTIVE POLYMERS

Adam Pajonk

The use of additive manufacturing with multiple materials has the potential to introduce a fundamental shift in the manufacturing of objects. Recent studies demonstrate that this approach can introduce added benefits such as custom-tailored material properties, added functionalities, and reduced assembly processes. However, the use of multiple materials in additive manufacturing is vastly limited to small-scale applications, while at the same time, mono-material additive manufacturing has made a substantive impact in architecture and construction. To that end, it is necessary to develop and adopt new techniques and methodologies for multi-material additive manufacturing, in order to expand its application in architecture and construction similar to mono-material additive manufacturing.

In this article, we provide an overview of our research progress in multi-material additive manufacturing, including our developed process that utilises reactive polymers and our current focus to integrate multi-material additive manufacturing into construction processes. Specifically, we focus on a parametric-design-to-in-situ-manufacturing workflow for multi-material façade components.

## INTRODUCTION

Additive manufacturing undoubtedly holds enormous potential for the field of architecture and construction. For instance, in 2020 the Germany-based construction company PERI Group in collaboration with the architectural office Mense Korte Architekten erected an additive manufactured residential building by 3d concrete printing [1]. Particularly the ability to produce finished parts directly from digital designs is making this technology a promising alternative to traditional manufacturing and construction techniques. As research and development in this field continues, we can expect to see more innovative applications of additive manufacturing in the built environment.

Multi-material additive manufacturing, can be seen as a particularly interesting field of development with a high potential to change our current ways of how we manufacture objects. Instead of assembling individual parts made out of different materials, the use of multi-material additive manufacturing enables to bypass this process by combining different materials in a single process [2]. This allows for a fundamental shift in the way we think about the design and construction of objects. Away from the production of homogeneous parts that are only after the manufacturing assembled to larger components, towards components that can already be produced out of multiple materials in a functional state [3]. In addition to all advantages of additive manufacturing, the ability to vary different materials across

the volume of the printed part adds a new dimension of design freedom which otherwise is difficult to achieve.

When it comes to the production of large-scale components, however, additive manufacturing remains predominantly limited to processing only one material. Particularly for architecture and construction, the use of multiple materials holds great potential, as many building components require the assembly of multiple materials which can often hinder the efficiency of the construction process. The building façade in particular presents a high potential to benefit from this approach, since the façade and its components are generally required to fulfill several functions at the same time and has to coordinate different environmental and user related conditions, typically resulting in constructions that are composed of different materials [4].

The aim of this research is to investigate the potential of multi-material additive manufacturing, which involves developing a method for producing large-scale components with varying materials using additive manufacturing and exploring the integration of this process for façade construction. The following sections present our current work and the future outlook of this research, with a focus on a novel approach that applies multi-material additive manufacturing in façade construction by directly manufacturing façade components on-site.

## **CHALLENGES IN IMPLEMENTING MULTI-MATERIALITY IN ADDITIVE MANUFACTURING FOR CONSTRUCTION**

Additive manufacturing, more commonly known as 3d-printing is a process where a digital three-dimensional model, initially generated by computer-aided design (CAD) is converted into a physical object by successively depositing and joining a material, typically in a layer by layer fashion [5,6]. Additive manufacturing comes in a variety of different processing techniques and with different materials. Scaling up these processes for application in architecture and construction, however, involves several key factors that need to be considered.

First, the size of the build volume. The build volume of an additive manufacturing process is defined as the usable volume available for the manufacturing machine to build parts. The volume is typically restricted by the build platform, on top of which parts are produced or the build chamber which represents the enclosure where parts are manufactured [7]. In large-scale additive manufacturing several solutions exist to manufacture large objects. First, through the use of available machines with the largest possible size to produce parts that are subsequently transported and installed on the construction site and combined to larger assemblies [8]. Second, through the use of large manipulators that can be used for additive manufacturing, such as gantry

systems or six-axis robotic arms that can be implemented either in a factory environment or directly on the construction site [1, 9]. Finally, through the use of autonomous robots that are able to move and operate in a construction environment [10]. However, development in this area is still less evolved compared to other approaches.

Another factor to consider in scaling up additive manufacturing is the printing speed. It is essential to ensure that the printing process can be completed within a reasonable timeframe. However, increasing the speed of the manufacturing process can have a negative impact on the quality of the finished parts. This can result in larger layer heights and widths of the extrusion, which in turn can limit the ability to integrate fine details. Furthermore, through the use of large layer heights, the layer structure could become more visible which is often the case in concrete 3D printing of entire building structures [1, 9].

The third factor to consider when scaling up additive manufacturing is material selection. The choice of material plays a key role and has to consider process-related materials requirements and requirement imposed by the intended application. For instance, Lim et al. discussed the requirements for materials that are used in extrusion-based processes for concrete 3d printing and identified four key characteristics: pumpability, printability, buildability, and open time [11]. However, when using a different additive manufacturing process, the required material properties may vary significantly.

Finally, when manufacturing large-scale parts, logistics and transportation need to be considered carefully. When the parts are produced in a factory environment, individual components must be stored, transported and coordinated for installation at the construction site. Alternatively, to avoid transportation and logistics issues, components can be printed directly on-site, as is often the case with concrete 3d printing of entire building structures. However, this approach is mainly limited to concrete 3d printing.

Although there are different solutions available to address the challenges of using additive manufacturing in architecture and construction, the implementation of multi-material additive manufacturing remains mostly limited to the manufacturing of small-scale parts [12, 13, 14, 15] and applications that are limited to using concrete for solid wall constructions [16, 17, 18, 19, 20, 21] and therewith only provide a solution to a limited range of functions for a building façade. Furthermore, recent research in other fields beyond the building façade industry has proposed a new approach for large-scale additive manufacturing of structures made of biopolymers [22], however, these findings are applicable only to the proposed bio-based materials, which are still of limited relevance for building facades.

As a result, current research has not found a solution for large-scale, non-solid wall façade components by being either limited in terms of size and location of the additive



manufacturing process, or in terms of material that has been used [23]. In order to address this gap a novel multi-material additive manufacturing process was developed that can be used in large-scale additive manufacturing and allows to change the material properties of the extruded material in a single 3d print.

### **MULTI-MATERIALITY THROUGH ON THE FLY COMPOSING OF REACTIVE POLYMERS MIXTURES**

Recent advances in additive manufacturing has enabled the use of reactive polymer systems through extrusion-based processes [24, 25]. These processes utilise two-component reactive polymers such as epoxy resins, acrylate, silicone, polyurethane and polyester for a three-dimensional buildup of physical objects in a layer by layer fashion. In these systems, a chemical reaction is achieved by mixing two pre-condensed components that contain all necessary components for the reaction [26]. Therefore, the two-components are processed simultaneously by a dosing unit and mixed right before extrusion. Rapid curing time and increased viscosity of the uncured polymer components prevent the extruded mixture from collapsing and ensure quick curing for the application of additional layers.

The setup for additive manufacturing with reactive polymers used in this research consists of a mixing and extrusion head which is responsible for metering and mixing the two-components of the polymer system. Attached to a six-axis robot arm, and synchronised with its movements, the mixing and extrusion head also controls the deposition of the material along a specified given path. Material cartridges hold the individual components of the polymer system. Pressurised air is used to transport the components to the material inlets of the mixing and extrusion head.

Furthermore, extrusion-based processes with thermosetting polymers do not rely on a specific build platform or a build chamber. This makes the process adaptable for the large-scale manufacturing of objects using a gantry system or a six-axis robotic arm. Therefore, this process can be regarded as a promising platform for additive manufacturing in architecture and construction applications [Fig.1].

The material properties of reactive polymers can be tailored to a wide range of requirements [27, 28]. Our approach takes inspiration from this potential and implements the ability to customise the material properties of the extruded material by altering the individual components of the two-component mixture. To implement this into the additive manufacturing process, we extended the mixing and extrusion head with additional material inlets, allowing the components of the two-component mixture to be altered by switching between different component inlets.

To gain new insights into multi-material additive manufacturing with reactive polymers, initial tests and exploratory experiments were conducted. The experiments utilised a polyurethane system, which enables the creation of polyurethane with varying mechanical properties by switching the individual components. By doing so, a flexible-cured and a hard-cured polyurethane can be achieved that can be incorporated into a 3d print. The results of these experiments first show different modes for implementing material transitions through the process of additive manufacturing [Fig.2, Fig.3], and second, generated insights on implementing mechanisms and anisotropic material behaviour through combining the hard-cured and the flexible-cured polyurethane across specific geometries [Fig.4]. Ultimately these experiments demonstrate that this approach allows to incorporate material transitions across different axes of the additively manufactured object and enables to deliberately manufacture mechanisms and anisotropic material behaviour through the combination of different materials.

Another characteristic of thermosetting polymers is the ability to create a strong adhesive bonding between two materials [28]. This characteristic can be utilised in additive manufacturing by directly printing onto a second object as a permanent build platform. To test this, cylinders with a diameter of 50mm and a height of 5 mm were printed on a concrete plate casted with C25/30 grade concrete, a multi-purpose concrete used for high-strength construction projects [Fig.5]. A primer for polyurethane materials was applied beforehand to the concrete plate to increase the bonding strength of the printed cylinders. After printing and curing, the samples were tested for adhesive bonding strength by applying a pulling force on the printed cylinders perpendicular to the plate. The average adhesive bond strength of 3204.4N was achieved for the cylinders, resulting in an adhesive bond strength of 1.63 N/mm<sup>2</sup> for the 3d printed material. This test demonstrates the potential of additive manufacturing with reactive polymers for permanently applying 3d prints on a second surface which simultaneously serves as a build platform.

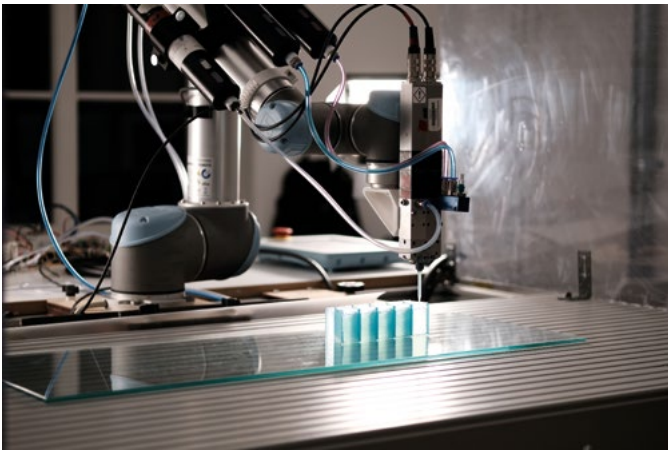


Figure 1: Image of the setup for additive manufacturing with reactive polymers, including the added multiple material inlets at the mixing and extrusion head, mounted on a six-axis robotic arm.

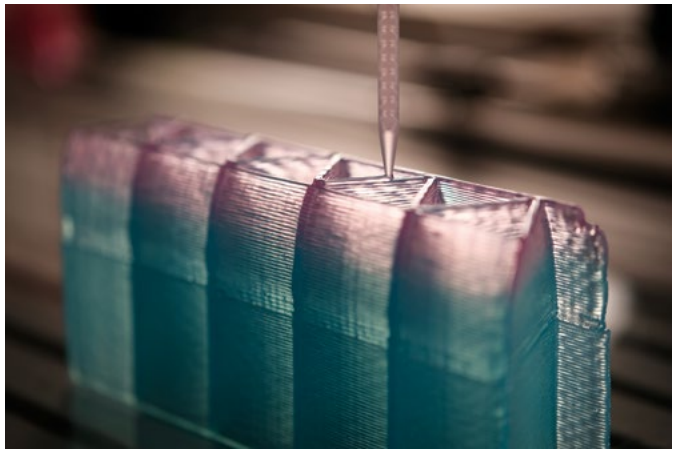


Figure 2: Image of a printed structure with two different materials sections implemented across different layers, a hard-cured polyurethane section (blue) and a flexible-cured polyurethane section (pink).

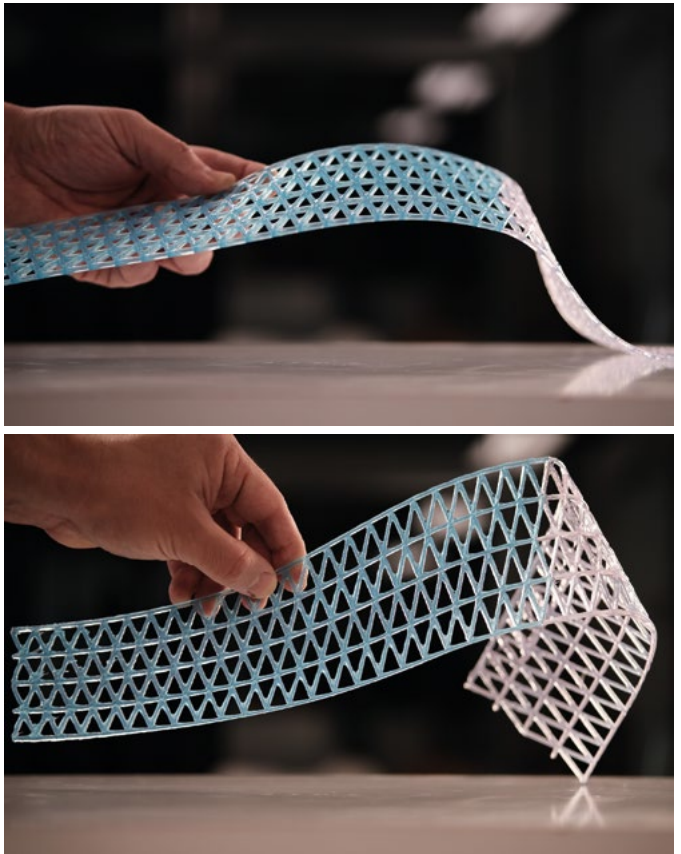


Figure 3: Image of a printed structure with two different materials sections implemented within a single layer, a hard-cured polyurethane section (blue) and a flexible-cured polyurethane section (pink).

## IMPLEMENTING MULTI-MATERIAL ADDITIVE MANUFACTURING INTO CONSTRUCTION PROCESSES

When it comes to the construction of buildings, the labour-intensive nature of the construction process often leads to errors due to poor communication between planning and execution [29, 30, 31, 32], high construction tolerances, and the associated effort required to align components accordingly [32, 33, 34] which ultimately, can lead to a higher construction inefficiency [31]. To address these issues, additional methods are needed to handle spatial uncertainties [32] or the construction process must wait for preceding trades to correct their errors [31]. On top of this, there is an increasing shortage of skilled workers and high risks for occupational diseases and accidents during construction, placing additional stress on the construction activities [35, 36]. In addition, on-site logistics of already manufactured components often require extensive handling and storage, resulting in longer lead times, repeated movement, and increased risk of damage from other workers [31, 32, 34].

Our current and future work aims to address the challenges of construction processes by proposing a parametric-design-to-in-situ-manufacturing workflow for multi-material facade components based on as build conditions. By utilising already erected components as the build platform for the manufacturing process, we can minimise the need for extensive on-site logistics, reduce the risk of errors due to poor communication between planning and execution, and optimise construction tolerances. The use of multi-materials also allows addressing specific requirements of the facade components, such as the handling of movements of the components from changes in temperature or other impacts.

The first step of the proposed workflow involves collecting input data from the building site and the planned location, including a digitised model, the orientation and positioning of the to be printed facade component, and information on additional components, such as glass units, that are to be installed into the facade component.

Following this, the digitised location can be used to generate a customised digital model of the facade component. For each digital model that is generated, a custom data set is generated as well, containing the layer and material information of the model.

Next, a robot program is created that controls the movement of the robot arm and extrusion commands for the multi-material mixing and extrusion head.

Finally, the manufacturing process of the component takes place directly on-site and in the permanent location of the facade component. The printed component then mediates between the high accuracy requirements of the glass unit and the potential deviations and tolerances of the building structure, becoming an integral part of the construction process.

Initial tests have been conducted on a L-shaped segment of a wooden frame, testing the proposed workflow and identifying critical points that need to be addressed in future research. First, the frame segment and its position in relation to the robotic arm was digitised by reading in the corner points of the frame segment, and remodelling the frame in a computer-aided design environment (Rhino 3D). On the basis of this model, a simple geometry that consists of a single line that runs parallel to the frame segment was generated and sliced into multiple layers that resemble the original geometry.

In order to 3D print this geometry, however, the ability to adjust the orientation of the extruder outlet in relation to the frame segment needs to be considered. Therefore, a specific module was developed in the programming environment of the computer aided design software, that allows to adjust the orientation of the extruder head to a variable build platform. This allows for applying a 3d print to a surface that has multiple faces oriented in different directions (multi-planar surface). In our test, the multi-planar surface is represented by the frame segment.

Finally, the geometry was applied directly on the frame segment, using the proposed manufacturing method. The constant aligning of the print head along the frame segment enabled the application of the polyurethane material also on vertical surfaces. Ultimately, this demonstrates the production of components on a second, multi-planar surface, eliminating the need for dedicated manufacturing environments and subsequent transportation of components to their final location.

Our future work will continue focusing on implementing the multi-material additive manufacturing process for facade components into a given location. To this end, we will test the parametric design-to-in-situ manufacturing workflow using a window-frame as a use-case. Multiple materials will be used to address specific requirements of the window-frame through the design of the frame component.

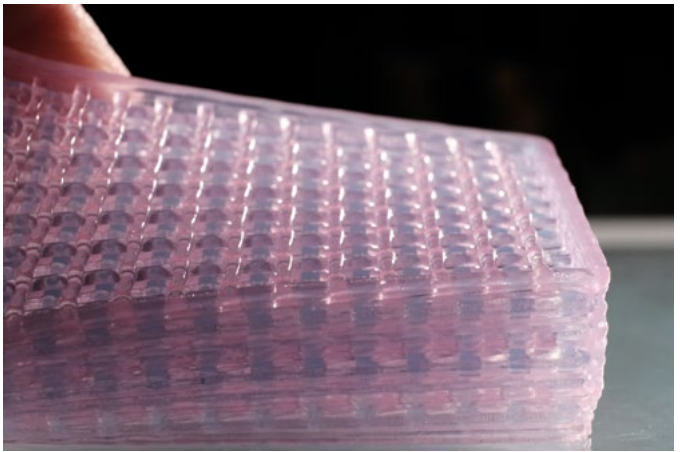


Figure 4: Image of a printed structure that exhibit anisotropic material behavior through the combination of a hard-cured polyurethane (blue) and a flexible-cured polyurethane (pink).



Figure 5: Image of 3d printed cylinders pulled perpendicular from a concrete plate during an adhesive bond strength test.

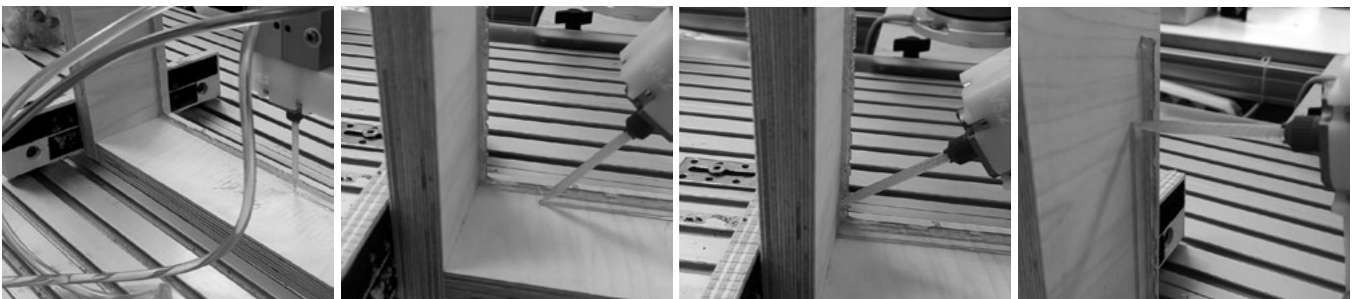


Figure 6: Image sequence of the 3d printing process onto a wooden frame segment with two different surface orientations

## CONCLUSION

An overview of our research progress in multi-material additive manufacturing for architecture and construction was provided.

This includes our developed process that utilises reactive polymers for additive manufacturing large-scale components with varying material properties. An overview of insights gained through the explorative experimentation with the manufacturing process was presented.

Furthermore, our current focus on integrating the multi-material additive manufacturing process into a workflow for parametric-design-to-in-situ-manufacturing of façade components was also presented alongside initially conducted tests.

## REFERENCES

- [1] P. Hanaphy, "PERI Constructing Germany's First "Market-Ready," Available from: <https://3dprintingindustry.com/news/peri-constructing-germanys-first-market-ready-3d-printed-residential-building-176638/> [Accessed: 20.02.2023].
- [2] S. Keating, "Beyond 3D Printing: The New Dimensions of Additive Fabrication" in *Designing for Emerging Technologies: UX for Genomics, Robotics, and the Internet of Things*, J. Follett (Ed.), O'Reilly Media, pp. 379-405.
- [3] T. Wiscombe, "Beyond Assemblies: System Convergence and Multi-Materiality" in *Bioinspiration Biomimetics*, 2012 Mar; 7(1).
- [4] U. Knaack, T. Klein, M. Bilow, and T. Auer, *Facade Principles of Construction*. Basel: Birkhäuser Verlag, 2007.
- [5] A. Gebhardt, J. Kessler, and L. Thurn, *3D Printing: Understanding Additive Manufacturing*. Munich: Carl Hanser Verlag, 2019.
- [6] I. Gibson, D. Rosen, and B. Stucker, *Additive Manufacturing Technologies*. New York, NY: Springer, 2015.
- [7] ISO/ASTM 52900:2021, *Additive Manufacturing - General Principles - Terminology*. Geneva, Switzerland: International Organization for Standardization, 2021.
- [8] M. A. Meibodi, A. Jipa, R. Giesecke, D. Shammam, M. Bernhard, M. Leschok, K. Graser, B. Dillenburger, „Smart Slab: Computational Design and Digital Fabrication of a Lightweight Concrete Slab" in *ACADIA 2018: Re/Calibration: On Imprecision and Infidelity*, A. J. A. Phillip, D. S. Marcella (Ed.), Mexico City, Mexico: Association for Computer-Aided Design in Architecture, 2018.
- [9] WASP S.r.l., "TECLA," Available from: <https://www.3dwasp.com/en/3d-printed-house-tecla/> [Accessed: 20.02.2023].
- [10] Institute for advanced architecture of Catalonia, "Minibuilders," Available from: <https://iaac.net/project/minibuilders/> [Accessed: 20.02.2023].
- [11] S. Lim, R. Buswell, T. Le, R. Wackrow, S. Austin, A. Gibb, and T. Thorpe, "Development of a Viable Concrete Printing Process," Proceedings of the 28th ISARC, Seoul, Korea, pp. 665-670, 2011.
- [12] M. Rafiee, R. Farahani, and D. Therriault, "Multi-Material 3D and 4D Printing: A Survey," *Advanced Science*, 7(12), 2020.
- [13] M. Vaezi, S. Chianrabutra, B. Mellor, and S. Yang, "Multiple material additive manufacturing - Part 1: a review," *Virtual and Physical Prototyping*, 8(1), pp. 19-50, 2013.
- [14] J. E. M. Teoh, C. K. Chua, Y. Liu, and J. An, "4D printing of customised smart sunshade: A conceptual study," In *Challenges for Technology Innovation: An Agenda for the Future*. C. Rijo, S. Gracio, and S. Antunes (Ed.), pp. 105-113, 2017.
- [15] D. Correa, A. Papadopoulos, C. Guberan, N. Jhaveri, S. Reichert, A. Menges, and S. Tibbits, "3D-Printed Wood: Programming Hygroscopic Material Transformations," *3D Printing and Additive Manufacturing*, 2(3), pp. 106-116, 2015.
- [16] Y. W. D. Tay, J. H. Lim, M. Li, and M. J. Tan, "Creating functionally graded concrete materials with varying 3D printing parameters," *Virtual and Physical Prototyping*, 17(3), pp. 662-681, 2022.
- [17] G. Dielemans, D. Briels, F. Jaugstetter, K. Henke, and K. Dörfler, "Additive Manufacturing of Thermally Enhanced Lightweight Concrete Wall Elements with Closed Cellular Structures," *Journal of Façade Design and Engineering*, 9(1), pp. 59-72, 2021.
- [18] Z. F. Ahmed, F. P. Bos, M. C. A. J. van Brunschot, and T. A. M. Salet, "On-demand additive manufacturing of functionally graded concrete," *Virtual and Physical Prototyping*, 15(2), pp. 194-210, 2020.
- [19] F. Craveiro, S. Nazarian, H. Bartolo, P. Bartolo, and J. Duarte, "An automated system for 3D printing functionally graded concrete-based materials," *Additive Manufacturing*, 33, 2020.
- [20] R. Duballet, C. Gosselin, and R. Roux, "Additive Manufacturing and Multi-Objective Optimization of Graded Polystyrene Aggregate Concrete Structures," In *Modelling Behaviour*, M. Thomsen, M. Tamke, C. Gengnagel, B. Faircloth, and F. Scheurer (Ed.), *Modelling Behaviour*. Cham: Springer, pp. 225-235, 2015.
- [21] N. Oxman, S. Keating, and E. Tsai, "Functionally Graded Rapid Prototyping," *Proceedings of VRAP: Advanced Research in Virtual and Rapid Prototyping*, pp. 483-489, 2011.
- [22] J. Duro-Royo, J. Van Zak, Y. Tai, A. Ling, N. Hogan, B. Darweesh, L. Mogas-Soldevilla, D. Lizardo, C. Bader, J. Costa, S. Sharma, J. Weaver, and N. Oxman, "Programmable Water-Based Biocomposites For Digital Design And Fabrication Across Scales", Available from: <https://www.media.mit.edu/projects/aguahoja/overview/> [Accessed: 21.02.2023].
- [23] A. Pajonk, A. Prieto, U. Blum, and U. Knaack, "Multi-material additive manufacturing in architecture and construction: A review," *Journal of Building Engineering*, 45, 2022.
- [24] O. Uitz, P. Koirala, M. Tehrani, and C. C. Seepersad, "Fast, low-energy additive manufacturing of isotropic parts via reactive extrusion," *Additive Manufacturing*, 41, 2021.
- [25] C. Saalbach, and L. Wietfeld, "Verarbeitung von Polyurethanen mit Hilfe der Additiven Fertigung: Das Liquid Additive Manufacturing (LAM) macht es erstmals möglich." *PUMagazin*, 04, pp. 246-248, 2017.
- [26] C. Defonseka, *Two-Component Polyurethane Systems*, Berlin Boston: Walter de Gruyter GmbH, 2019.
- [27] M. F. Sonnenschein, *Polyurethanes Science, Technology, Markets, and Trends*, Hoboken NJ, USA: John Wiley & Sons, Inc, 2021.
- [28] K. Uhlig, *Polyurethan Taschenbuch*, Munich Vienna: Carl Hanser Verlag, 2006.
- [29] A. R. Atkinson, "The pathology of building defects; a human error approach," *Engineering Construction and Architectural Management*, Vol.9, No. 1, pp. 53-61, 2002.
- [30] A. R. Atkinson, "The role of human error in construction defects," *Structural Survey*, Vol. 17, No. 4, pp. 231-236, 1999.
- [31] B. G. Hwang, X. Zhao, and T. H. V. Do, "Influence of Trade-Level Coordination Problems on Project Productivity," *Project Management Journal*, Vol. 45, No. 5, pp. 5-14, 2014.

- [32] S. Forsman, N. Björngrim, A. Bystedt, L. Laitila, P. Bomark, and M. Öhman, "Need for Innovation in Supplying Engineer-To-Order Joinery Products to Construction: A Case Study in Sweden," *Construction Innovation*, Vol. 12, No. 4, pp. 464-491. 2012.
- [33] T. C. Pavitt, and A. G. F. Gibb, "Interface Management within Construction: In Particular, Building Façade," *Journal of Construction Engineering and Management*, Vol. 129, No. 1, 2003.
- [34] J. Eom, and Y. Kang, "Curtain Wall Construction: Issues and Different Perspectives among Project Stakeholders," *Journal of Management in Engineering*, Vol. 38, No. 5, 2022.
- [35] V. Arndt, D. Rothenbacher, U. Daniel, B. Zschenderlein, S. Schubert, and H. Brenner, "Construction work and risk of occupational disability: a ten year follow up of 14474 male workers," *Occup Environ Med*, 62(8), pp. 559-566, 2005.
- [36] e.V. Hauptverband der Deutschen Bauindustrie, „Bauwirtschaft im Zahlenbild 2020“ Available from: <https://www.bauindustrie.de/zahlen-fakten/bauwirtschaft-im-zahlenbild> [Accessed: 21.02.2023].

# DOME LIGHT: MEDITATING DIRECTIONAL ILLUMINATION USING SECTIONAL VARIABILITY IN 3D CLAY PRINTING

James Clarke-Hicks  
Isabel Ochoa

Dome Light considers a fabrication method for generating ceramic light screens using Liquid Deposition Modelling (LDM) with clay, allowing for variable sectional conditions that regulate illumination. Functionally Graded Additive Manufacturing (FGAM) is implemented to generate custom tool paths prioritising sectional performance over a global geometry. It implements customised methods for altering light scattering behaviour rooted in both fired ceramic traits and the working properties of clay. The sectional profile of the Dome Light is defined by compounded deformation that forms multilayered apertures, directing light downwards and eliminating glare. The tool path isolates and controls deformation, creating a non-linear relationship between illumination and porosity that remains structurally stable during wet-processing and facilitates the mediation of light.

## MEDIATING LIGHT WITH FUNCTIONALLY GRADED SECTIONAL CONDITIONS

Formative manufacturing techniques aim to produce sectional consistency in contemporary architectural ceramics [1]. These techniques, such as extrusion and slip casting, regulate the viscoelastic properties of clay during wet-processing. Their use of formwork ensures units have uniform sectional qualities well-suited to producing aggregate ceramic systems with identical components as discussed by Bechthold et al. (2018) [2]. Formal consistency is therefore utilised at the expense of variable sectional geometries

within individual ceramic elements. This research proposes an alternative fabrication methodology using Liquid Deposition Modelling (LDM) with clay that yields variable sectional conditions in ceramic screens. The resulting research prototypes utilise porous, multi-layered sectional conditions that can hardly be produced using other ceramic fabrication methods [3]. The research prototype presented here is a ceramic screen that mediates light using variable sectional geometries.

The plasticity, tensile strength and viscid properties of clay allow it to take on complex geometries that can result in significant degrees of plastic deformation during LDM. A digital workflow is developed to study the behav-

jour of clay across physical prototypes using Functionally Graded Additive Manufacturing (FGAM) [4] or Functionally Graded Rapid Prototyping (FGRP) [5]. FGAM is a 3D printing process that organises material deposition based on performance requirements and material properties. This research utilises FGAM to investigate how clay's plastic deformation during LDM can mediate sectional conditions in ceramic components [6].

### **Regulating deformation with tool path design**

FGAM workflows and LDM can harness clays' unique material behaviours to create novel design languages. The tool mark can impact the surface of a 3D-printed part from the meso scale of the individual print layer to the macro scale of the artefact global geometry. This research proposes that the striations left by the extruder can regulate sectional performance rather than be treated as a byproduct of the manufacturing process. When surveying the field of LDM printing with clay, three applications of the tool path are prevalent: the tool path as a byproduct of form definition, the tool path as an expression of ornament, and the tool path as a function of performance [6]. The third application of the tool path is utilised in this research to harness the sagging behaviour of clay when 3D-printing porous geometries. This process is characterised by the high degree of physical deviation between the 3D-printed tool path and the digital print trajectory.

Other researchers are also stepping away from conventional deposition methodologies that utilise the tool path as a byproduct of form definition. 'Spatial Print Trajectory', a research from AlOthman et al. (2019) [7] uses the tool path to mediate density and structural rigidity in 3D-printed clay components. Clay coils are unconventionally 'folded' over the z-axis using non-planar extrusion to form self-supporting porous structures. Other research projects, such as 'Informed Ceramics' [8] and 'Free Form Clay Deposition in Custom Generated Mold' [9] utilise the viscoelastic properties of clay to allow the material to adapt to freeform moulds during LDM.

The prototypes created in this research seek to design tool paths rather than global geometries. The 'oversized' clay print coil is prone to plastic deformation during LDM. This behaviour cannot be addressed by universal slicer software parameters that prioritise the reduction of print time and material use [10]. Slicer software was, therefore, an ineffective tool for processing complex geometries with significant intended deviations from digital print trajectories to physical outputs. Custom design of the toolpath through computational modelling in Grasshopper facilitates a digital-to-physical workflow that enables the controlled deformation of the clay to grade light across ceramic components.

### **Working properties and fired ceramic traits**

The performance attributes of clay can be divided into two types: working properties and fired ceramic traits. Dome Light project is part of a larger ongoing research body entitled 'Grading Light' that is preoccupied with both types of performance attributes (Figure 1). Isabel Ochoa and James Clarke-Hicks initiated Grading Light at the University of Waterloo, School of Architecture, in 2019. The fabrication methodologies developed in Grading Light are designed to allow material performance to drive formal qualities. Dome Light presents a ceramic light screen that embodies this research agenda.

Dome Light utilises highly customised methods for altering light scattering behaviour rooted in both fired ceramic traits and working properties (Figure 2). This prototype focuses on harnessing the direction of incident light through porous, multilayered component sections [1]. Various clay bodies were rigorously tested to identify material behaviours that generated consistent light scattering behaviours while still allowing for a high degree of flexibility within a digital-to-physical workflow.

Generally, clay bodies that fire to neutral white tones tend to have high proportions of Kaolin, Nepheline Syenite and plasticizers, making them highly viscid and challenging to process through syringe extruder systems. Comparatively less viscid clay bodies, such as terracotta, are easier to process through digital-to-physical workflows. However, the same components in the clay that make it less viscid tend to make it a darker colour in its fired ceramic state, diminishing light scattering effects. PSH-516, a commercially available cone 6 clay, was selected to produce the Dome Light. PSH-516 fires to a vitreous white ceramic, making it ideal for facilitating the analysis of light scattering effects and directional diffusion. PSH-516 is also relatively easy to process with enough viscosity to promote layer-to-layer adhesion with minimal applied pressure.





Figure 1: 'Grading Light' exhibition at the Canadian Clay and Glass Gallery, 2022.



Figure 2: Dome Light final prototype. Clarke-Hicks J (2021) Grading Light: Utilising plastic deformation to functionally grade ceramic light screens. Dissertation, University of Waterloo





Figure 3: 12 illuminated aperture iterations applied to a cylindrical base geometry. Clarke-Hicks J (2021) Grading Light: Utilising plastic deformation to functionally grade ceramic light screens. Dissertation, University of Waterloo.

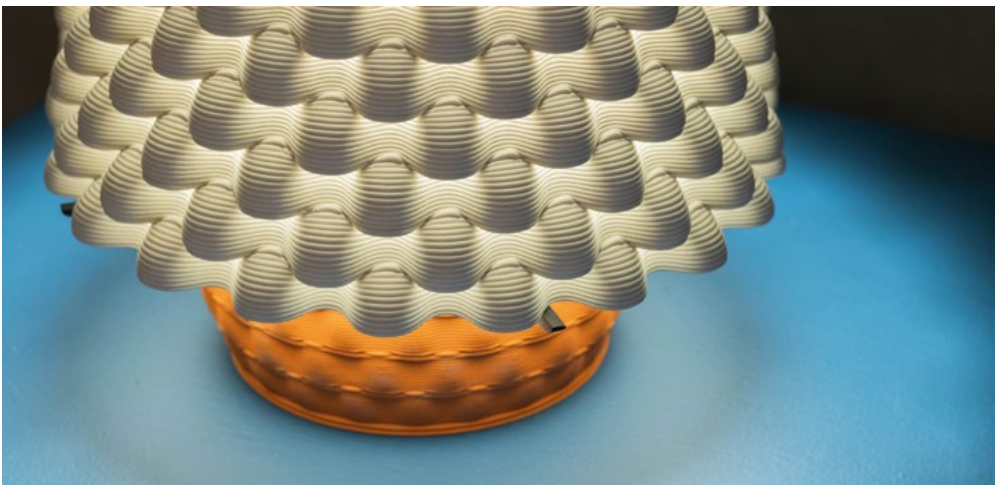


Figure 4: Dome Light illuminated detail on display at the Canadian Clay and Glass Gallery, 2022.

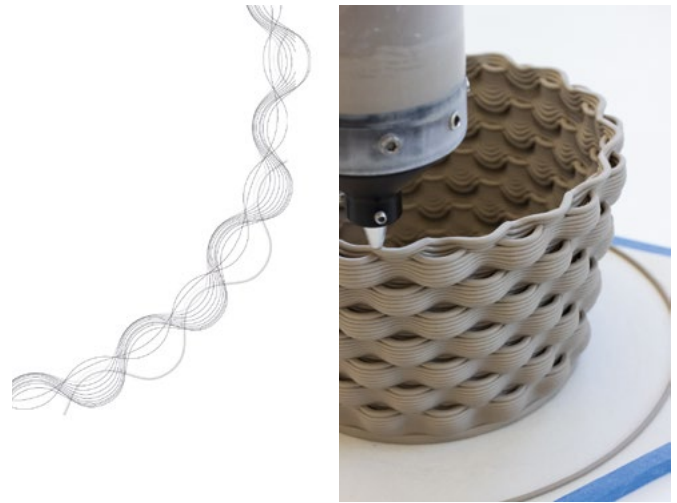


Figure 5: Tool path plan and print in progress. Clarke-Hicks J (2021) Grading Light: Utilising plastic deformation to functionally grade ceramic light screens. Dissertation, University of Waterloo.

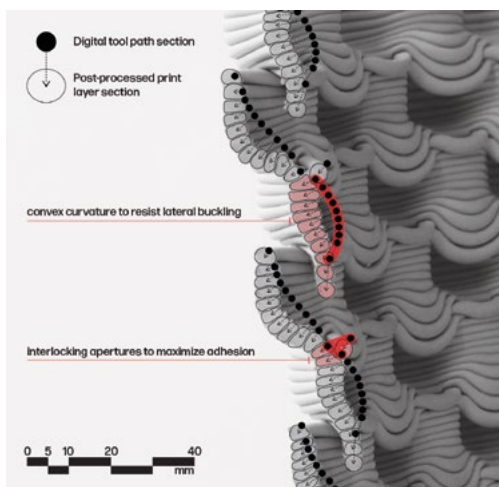


Figure 6: Physical section and digital tool path overlay of the Dome Light. Clarke-Hicks J (2021) Grading Light: Utilising plastic deformation to functionally grade ceramic light screens. Dissertation, University of Waterloo.

## MULTILAYERED SECTIONAL CONDITIONS AS A PRODUCT OF CONTROLLED DEFORMATION

The tool paths are designed to deviate substantially from layer to layer, creating significant gaps in the wall section. In the broader body of 'Grading Light,' these gaps are called 'apertures.' Apertures are created by unsupported overhangs and compounded deformation over several vertically repeating print layers. The discontinuity and porosity created by apertures in the wall section must be regulated and isolated. To prevent structural collapse or a print from 'unravelling,' print layers must realign with the digital tool path and isolate plastic deformation within a limited area [1]. The tool path is designed using an iterative physical-to-digital workflow that allows for understanding the relationship between aperture size and placement relative to the stability of the global geometry (Figure 3). Apertures in the Dome Light are confined within horizontal rows or 'bands' along the surface of the printed part. If the plastic deformation of print layers causes the material to be displaced away from a single row, aperture size becomes inconsistent and structural collapse becomes more probable.

### Dome Light overview

The sectional profile of the Dome Light is defined by compounded deformation that forms multilayered apertures. These multilayered apertures create directional illumination downwards and eliminate direct glare (Figure 4). The Dome Light is printed with a Potterbot SLX-1 at 40mm/s, a step height of 1.9mm, and a constant extrusion multiplier of 12. Apertures follow an eleven-layer cycle forming light channels through semi-domes expressed on the screen's outer surface. The depth of the semi-domes determines brightness levels. As the apertures expand, more light can filter through the wall section. However, this relationship between illumination and depth is non-linear. The formation of the semi-dome apertures displace material outwards and must be compensated by increasingly dramatic overhangs (Figure 5).

The span between unsupported overhangs can reach up to 30mm. At this point, indirect illumination starts to diminish as the elastic properties of the clay reach their maximum elastic capacity, and the overhang print coil collapses into the aperture below. This multilayered light channel relies upon very little direct adhesion between rows of apertures as the bulk of the material is directed toward forming the semi-dome shape. The resulting sectional profile of the Dome Light has a tendency for lateral buckling in the wall section, leading to total structural collapse. Two strategies are implemented in the Dome Light to maximise the gradient of controlled light diffusion while mitigating the tendency for buckling [3]. Both Strategies utilise controlled deformation to preserve structural integrity (Figure 6).

The first strategy is maximising adhesion between stacked rows of apertures. The tool path is designed to interlock print layers between apertures. The penultimate print layer in a sequence is the first layer of the subsequent aperture formation. All apertures' first and last layers are interlocked to create a larger lamination area.

The second strategy for tackling lateral buckling while maximising illumination involves printing the internal wall of apertures with a convex curvature. Altering the tool path to create a convex curvature shifts the centre of mass within the wall section by offsetting the outward deformation occurring in the semi-dome aperture. During LDM, the convex inner surface deforms into a flat plane. This plane creates a stable surface for the adhesion of successive print layers.

## CONCLUSION

Dome Light project implements a digital-to-physical workflow that utilises custom tool path generation to control the plastic deformation of clay in LDM. This workflow is used to create light screens with a multilayered wall section that filters illumination. Dome Light represents a single implementation of an evolving working methodology that defines custom tool paths rooted in studies of material behaviour. By isolating and confining deformation to individual apertures, the fabrication methodologies developed in this research can be applied to a wide range of global geometries, such as light fixtures and aggregate masonry systems. This research methodology is founded on cycles of rapid physical prototyping with LDM, reinforcing that material behaviour can catalyse novel fabrication methods and new design languages.

## ACKNOWLEDGEMENTS

Dome Light builds on research initiated at the University of Waterloo School of Architecture by Adjunct Professors Isabel Ochoa and James Clarke-Hicks as part of their Master's thesis, supervised by Associate Professor David Correa. Dome Light is part of Isabel Ochoa and James Clarke-Hicks' larger ongoing body of work entitled 'Grading Light.' 'Grading Light' explores how designing custom digital tool paths, not otherwise possible through slicer software, can capitalise on the way that print layers deform to create porous geometries that alter light-scattering behaviour.

## REFERENCES

- [1] I. Ochoa, *Grading Light: Utilizing plastic deformation to functionally grade ceramic light screens*, Dissertation, University of Waterloo, 2021.
- [2] M. Bechthold, A. Kane, and N. King, *Ceramic Material Systems in Architecture and Interior Design*, Basel, Birkhauser, 2015.
- [3] J. Clarke-Hicks, I. Ochoa, and D. Correa, "Harnessing plastic deformation in porous 3D printed ceramic light screens," in *Architecture, Structures and Construction*, 3, pp. 193-204, Dec. 2022. DOI:10.1007/s44150-022-00079-0.
- [4] N. Oxman, S. Keating, and E. Tsai, "Functionally Graded Rapid Prototyping," in *Innovative Developments in Virtual and Physical Prototyping*, P. J. da Silva Bartolo, Ed. Taylor & Francis Group, London, 2011, pp. 483-489. DOI: 10.1201/b11341-78.
- [5] R. Mahamood and E. Akinlabi, "Introduction," in *Functionally Graded Materials*, C. Bergmann, Ed. Springer, Cham, 2017, pp. 1-8. DOI: 10.1007/978-3-319-53756-6.
- [6] J. Clarke-Hicks, *Grading Light: Utilizing plastic deformation to functionally grade ceramic light screens*, Dissertation, University of Waterloo, 2021.
- [7] S. AlOthman, H. Im, F. Jung, and M. Bechthold, "Spatial Print Trajectory: Controlling Material Behaviour with Print Speed, Feed Rate, and Complex Print Path," in *ROBARCH 2018*, J. Wilmann et al., Eds. Springer, Cham, 2018. DOI: 10.1007/978-3-319-92294-2\_13.
- [8] M. Ko, D. Shin, H. Ahn, and H. Park, "Informed Ceramics: Multi-Axis Clay 3D Printing on Freeform Molds," in *ROBARCH 2018*, J. Wilmann et al., Eds. Springer, Cham, 2018. DOI: 10.1007/978-3-319-92294-2\_23.
- [9] K. Dunn, D. W. O'Connor, M. Niemela, and G. Ulacco, "Free Form Clay Deposition in Custom Generated Molds: Producing Sustainable Fabrication Processes," in *ROBARCH 2016*, D. Reinhardt et al., Eds. Springer, Cham, 2016. DOI: 10.1007/978-3-319-26378-6\_25.
- [10] D. Gourdoukis, "Digital Craftsmanship: From the Arts and Crafts to Digital Fabrication," in *ISSN 2309-0103*, vol. 2, no. 4, pp. 43-54, 2015.

# BIOMATERIALS: ADVANTAGES AND DISADVANTAGES OF THE USE OF CHITOSAN IN AM

Tatiana Campos

Paulo Cruz

Bruno Figueiredo

This work presents a study that proposes the use of materials of natural origin, such as seafood waste, in the Additive Manufacturing (AM) of architectural components. The study is motivated by the problem associated with the excessive use of non-renewable resources, the cause of significant climate change on our planet and the exponential reduction of biodiversity. It is necessary to seek responsible solutions that indirectly take advantage of abundant natural resources, such as cellulose and chitosan - materials originating from plants and food waste - defining more sustainable manufacturing processes.

In this way, the research aims to demonstrate the possibility of producing new materials from seafood waste, as well as its advantages and limitations for its use in architectural applications.

## CONTEXT

The use of materials of natural origin for the definition of architectural and construction systems can be found not only in vernacular architecture but also in contemporary architecture.[1] Architect Shigeru Ban has succeeded in giving a new life to the architectural and structural use of cardboard tubes, in programmes on a wide range of scales, from small emergency shelters to cathedrals or concert halls.[2] Kengo Kuma, tested the integration of cellulose for application in structural components, offering new uses and exploring the potential of conventional solutions, such as the traditional Shoji - wood and cellulose sliding panels

or doors.[3] Within of the MIT Media Lab's Mediated matter group, coordinated by Neri Oxman (until 2021), Duro-Royo et al. (2018) [4] present a research on the use of shellfish waste to produce decorative architectural elements, such as the Aquahoja pavilion - a steel structure, coated with cellulose and chitosan-based bioplastics. The Shellworks research group, as the name suggests, has also taken advantage of shellfish waste, developing a set of specialised equipment for the extraction of chitin and chitosan, creating a set of highly sustainable and biodegradable materials.

The high pollution problems are associated with the excessive use of non-renewable materials, for example, in the construction sector - one of the biggest pollut-

ers worldwide – is provoking a more responsible attitude among many professionals and researchers in the search for more sustainable solutions.[5] Polysaccharides, proteins and lipids are degradable, sustainable and biocompatible, and environmentally friendly polymers, such as cellulose, starch, chitosan, seaweed, can be used as raw material for other composite materials due to their low cost and excellent performance. Authors such as Lesna et al. (2020) [6] motivated by the problem of plastic waste, explored new and more sustainable architectural applications in the project Bio-degradable shelter, developing an integral system of architectural elements based on materials of natural origin – a mixture with fungal chitosan, seaweed derivatives agar-agar sodium alginate, water, and others. At the University of Singapore [7], a 1m high column was designed using materials of natural origin – cellulose and chitosan. The authors Campos et al. (2022) [8-10] have researched and developed projects that focus on adopting more sustainable practices in architecture and construction through the exploitation of biodegradable materials in additive manufacturing.

## MATERIAL PREPARATION AND COMPOSITION

The research focuses (1) on the development of natural-based composite materials, namely based on shellfish waste, and (2) biodesign, by studying the composition and behaviour of the material, and (2) the AM of architectural applications. The integration of these resources aims to maximise their use, using local natural materials and minimise the environmental impact associated with the production of non-renewable materials such as cement.

Shellfish waste, such as seafood shells, fish scales, squid skins and fungal cells, are rich in chitin – the second most abundant natural biopolymer on the planet. Chitin is a monomer structurally similar to cellulose (the most abundant polymer on the planet) and is obtained by a set of chemical processes – demineralisation, deproteinization – from shellfish waste.[11] In addition, when transformed, it originates a new natural polymer, the chitosan. Chitosan is the main material of this study, being tested in combination with other natural materials, such as acetic acid, cellulose, starch and additives like glycerine.

### Preparation

The material preparation consists of a combination of 80%-90% water (v/v), 4%-8% chitosan (w/v), 4%-8% starch (w/v), 4% glycerine (v/v) and according to the final properties required, 0%-12% cellulose (w/v) is added. After homogenisation of the components, the mixture is heated until it forms

a viscous pulp. Then, as the temperature decreases, 2%-4% acetic acid (v/v) is added to the material.

Once the base mixture was developed [9-10], the study of the material was divided into three working groups, comparing the proportions of chitosan and starch added. In group A the properties of the mixture were studied, the percentage of chitosan was the same as starch. In group B, the percentage of chitosan was higher than the percentage of starch. In group C the percentage of chitosan was lower than that of starch. This comparison was fundamental to determine which proportion presented the best results for subsequent use in AM.

### Composition

Changing the proportions of the different constituents in the mixtures, results in a set of different behaviours and properties in the obtained samples. These samples vary in terms of mechanical and physical properties, such as elasticity, rigidity, strength, flexibility, shape recovery, transparency, density and colour. Figure 1 (left side) shows a set of different mixtures and Figure 1 (right side) the difference between a sample produced without glycerine (stiffer) and with glycerine (flexible).

When added to the mixture, cellulose is intended to intensify the rigidity and mechanical strength of the object produced. The greater its proportion, the greater the rigidity of the material. The chitosan, on the other hand, when added and depending on the proportion added, is intended to confer greater strength, transparency, density and colour to the material obtained. It is responsible for the final appearance of the mixture. Chitosan introduces the colour and, in turn, the acetic acid besides increasing the fluidity of the mixture also controls the final transparency. Finally, glycerine gives flexibility to the material. The higher the proportion of added glycerine, the greater the flexibility of the material and consequently the lower the stiffness.

## ADDITIVE MANUFACTURING

The primary objective of this research is to create a framework, composed of a set of mixtures easily adjusted and adapted to the desired functionalities. This framework, as it is possible to observe in Figure 2, it is composed of three groups; the first 'Biopolymers' combines the materials and develops a set of mixtures based on natural materials; the second 'Characteristics' studies different properties and behaviours of each mixture produced; finally, the third 'Technology' applies the material in the AM, digital modelling and g-code generation, AM and drying of objects.

During the study of the materials and the performance of a set of previous tests, it was found that they pre-





Figure 1: Different material finishes (left side).  
Behaviour of the material with glycerine (right side).

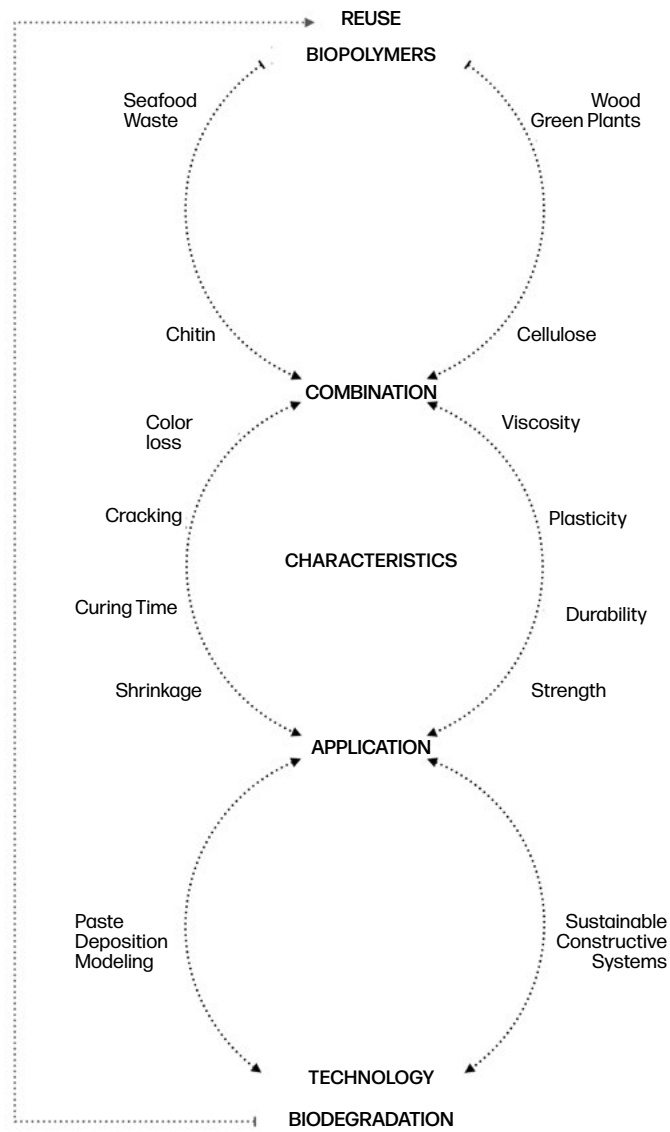


Figure 2: Framework diagram, the use of natural materials and the creations of mixtures, the studied characteristics and the technology used.

sented some limitations in terms of their ability to build in layers.[9-10] As a way of getting around this factor, a number of applications were analysed, such as meshes, patterns and coatings. In each test the mixtures were manipulated to optimise their behaviour when used in AM. The PEM (Paste Extrusion Modelling) technique was used to manufacture the objects, taking advantage of the laboratory equipment, such as the Lutum 2.0 Mini<sup>®</sup>, a three axes printer with a build area of 435x460x450mm (X, Y and Z).

### Two-dimensional or planar geometries

Given the limitations of the material behaviour in terms of constructability, a set of two-dimensional meshes were developed. The possibility of adapting the mixtures to the object to be produced resulted in a set of geometries with different physical and mechanical behaviours, creating intelligent and sustainable materials. Taking into account the properties of the equipment and the material properties – high fluidity – with the aid of Rhinoceros<sup>®</sup> and Grasshopper set of meshes with continuous printing paths were designed in order to avoid possible interruptions during manufacturing.

Each geometry consists of only one print layer (Figure 3, left side). Throughout the initial tests the proportions of chitosan, acetic acid and glycerine added were varied, strongly influencing the behaviour of the meshes produced (Figure 3, right side).

### Shape memory

As already stated previously, colour and transparency are strongly influenced by the proportion of chitosan introduced in the mixture. These tests also allowed to verify that the bending or deformation capacity is delimited by the ratio of glycerine.

In a second phase, a set of new study parameters were defined: (1) the possibility of adding cellulose fibres, to reduce fluidity and increase the resistance of the material; (2) the possibility of increasing the material's buildability; and (3) the possibility to create geometries with shape memories, acquiring the mould configuration without losing it.

In order to increase the material's buildability, we first designed a new geometry, with a variable design and four print layers, then we added a proportion of virgin cellulose fibres to the developed mixture, and, finally, a comparison was made between two objects, with different manufacturing parameters.

Comparing the above parameters, we find that aesthetically both responded equally, as it can be seen in Figure 4, assuming the mould geometry, however the physical and mechanical behaviour is distinct. Object A (Figure 4, left side) is more susceptible to shape loss than object B (Figure 4, right side), due to the lack of cellulose fibres in

the mixture. The introduction of cellulose fibres makes it possible to manufacture more resistant objects and with overlapping layers, but this parameter is still very limited (Figure 4, right side).

### Two-dimensional geometry on a substrate

Observing the behaviour of the previously objects (Figure 4), it was concluded that the mixtures present potentialities: (1) the introduction of cellulose fibres provides greater resistance to the object – makes it rigid; and (2) the lack of cellulose fibres turns the material into a flexible and resistant bioplastic. In this way, and taking into account the parameters observed, a new study test was developed with the aim of creating a highly customisable bioplastic by adding an internal structure that gives it resistance.

The creation of the bioplastic (Figure 5, left side), consists of the previous deposition of a mixture with a high degree of fluidity - mixture composed by chitosan and glycerine and the printing of a geometry with a degree of rigidity on the previously deposited layer - mixture composed by chitosan, cellulose and glycerine.

The union of the different mixtures, produced a material: (1) highly resistant, due to cellulose fibres; (2) flexible, due to the presence of glycerine; (3) customisable, in colour, transparency and internal geometry; and (4) recyclable. The internal geometry was printed on the substrate and as the water evaporated from the material during drying, the mesh became embedded.

### Wall covering system

Taking advantage of the constructive properties and the limitations of the previously studied material, A curtain wall made of tiles – BioTILES – was proposed to test it as an architectural system. A prototype of the wall composed of 35 tiles was manufactured and assembled in a vertical exhibitor. This exhibitor results from a reinterpretation of the old 'soletos' used in Portuguese historic buildings and aim to develop new decorative wall coverings. The 'soletos' have a fishscale-like shape, are tiles of small dimensions, manufactured from slate rocks, with thin thicknesses, overlapping each other, and fixed on a wooden lath.[10]

It was our intention to test the effect of transparency, textures and shadows originated in the superposition of the BioTILES along the curtain wall. Like the 'soletos', the BioTILES were designed taking into account the shape and fixing system. For each module a different pattern was developed, inspired in the silhouette of the leaf veins, as it can be seen in Figure 6. The pattern presented in Figure 6, is variable and has the function of giving resistance to the module.

For the production of the different modules, the same method as the previous AM method was used (Figure 7), first a mixture was placed inside the mould, with a

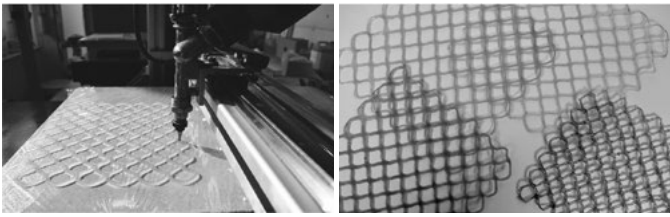


Figure 3. Printed with a natural shellfish waste mix (left side). Multiple meshes printed with different mixtures (right side).

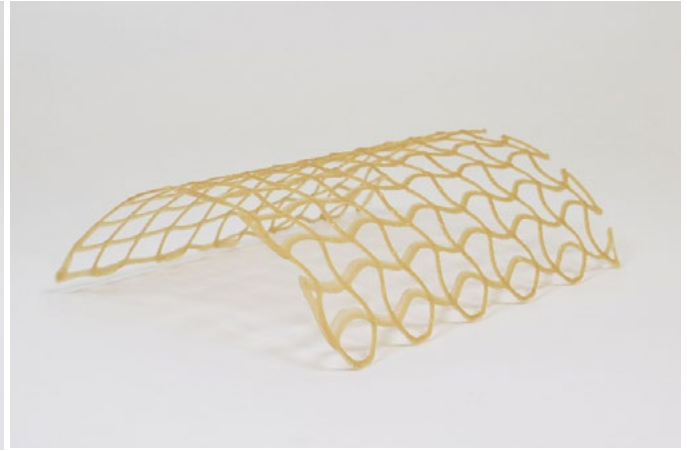


Figure 4. Object A (left side) produced with a mixture of chitosan and glycerine. Object B (right side) produced with a mixture of chitosan, cellulose and glycerine.

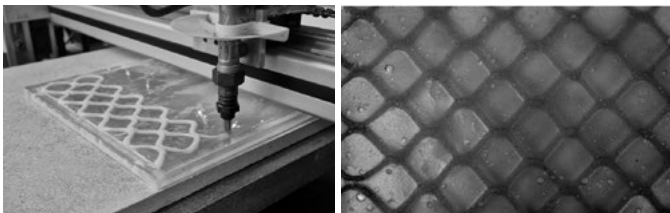


Figure 5. Printing the geometry on the substrate (left side). Substrate - Mixture with chitosan, glycerine. Geometry - Mixture with chitosan, cellulose and glycerine (right side).

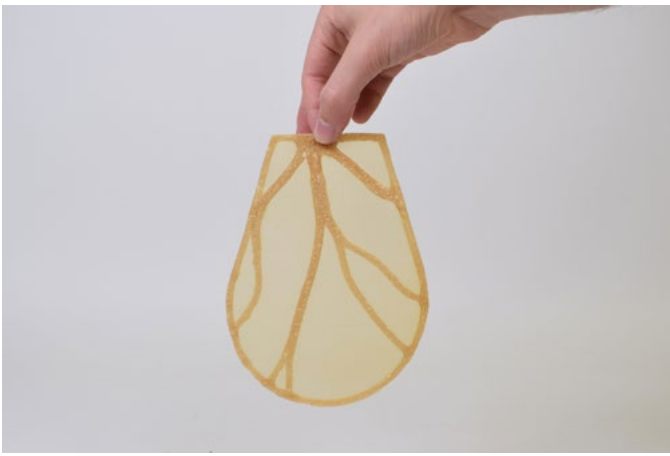


Figure 6. Presentation of a final module.

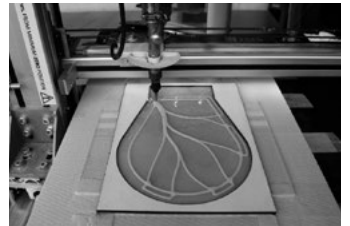
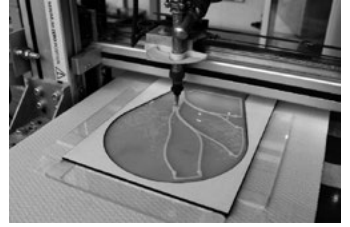


Figure 7. Printing a module using the PEM technique (Paste Extrusion Modelling).



Figure 8. Presentation of the exhibitor.

high degree of flexibility, then the developed and different geometry was printed on the previous substrate.

After drying we can see that the different components are able to maintain the desired initial shape, due to the presence of the rigid internal structure. Under normal conditions 22°C and 36% humidity, approximately, the modules would dry out in 5 days. In Figure 8, we can see the assembled exhibitor, with the 35 overlapping tiles. Each module is composed of different patterns.

## CONCLUSION

Motivated by the need to find a new strategy to reduce the continuous accumulation of seafood waste in the fishing industry, we have developed a set of natural, non-toxic, low-cost, renewable, sustainable and biodegradable mixtures. With the use of natural biopolymers, we have developed new architectural applications - meshes, patterns and coatings - fully customisable. In the different applications we were able to observe the limitations associated with the use of the material in AM. The alteration of the proportions of the different mixtures produced, confer different mechanical, physical and aesthetic behaviours, such as:

- × The proportion of chitosan strongly influences the shade of the material;
- × Cellulose considerably decreases the transparency;
- × Glycerine provides flexibility and resistance to possible breaks.

In addition, the fluidity of the material strongly restricts printing on the Z axis. The architectural applications developed are printed on a flat surface and then moulded as desired. Chitosan is a biodegradable and sustainable material; however, however it has a short durability period, unlike other research performed at ACL (Advanced Ceramics R&D Lab) with cellulose.

## ACKNOWLEDGEMENTS

This work was financed by the Project Lab2PT - Landscapes, Heritage and Territory laboratory - UIDB/04509/2020 through FCT - Foundation for Science and Technology and the FCT Doctoral Grant with the reference SFRH/BD/144794/2019. We thank to RAIZ - Institute Research of Forest and Paper, for their support and partnership in this re-search, namely through the supply of cellulose. We are grateful to the Institute of Design of Guimarães for hosting and supporting the Advanced Ceramics R&D Lab on the use of their facilities and equipment.

## REFERENCES

- [1] S. Solanki, *Why materials Matter: Responsible Design for a better world*. Volume 1. (1st ed.). New York: Prestel Publishing, 2018.
- [2] R. Miyaki, I. Luna, L.A. Gould, Shigeru Ban: *Paper in Architecture*. Volume 1. Rizzoli, 2009.
- [3] K. Frampton, K. Kuma, Kengo Kuma: *Complete works*. Volume 2. Thames and Hudson Ltd, 2018.
- [4] J. Duro-Royo, J. Van Zak, A. Ling, Y. Tay, N. Hogan, B. Darweesh, N. Oxman, "Designing a tree: Fabrication informed digital design and fabrication of hierarchical structures," in Annual IASS symposium, Proceedings of the IASS Symposium (International Association for Shell and Spatial Structures): Creativity in structural design, Boston, USA, July 16-20, 2018. Vol.1, pp.1-8.
- [5] K. Treggiden, *Wasted: When Trash Becomes Treasure*. Volume 1. (1st ed.). Ludion Publishers, 2020.
- [6] J.M. Lesna, P. Nicholas, "De Gardus," in CAADRIA 2020 RE: Antropocene Design in the age of humans: Proceedings of the 25th International Conference of the Association for Computer-Aided Architectural Design Research in Asia, Hong Kong, China. Vol. 2, pp. 383-392.
- [7] S. Dritsas, Y. Vijay, S. Halim, R. Teo, N. Sanandhya, J.G. Fernandez, "Cellulosic Bio-composites for Sustainable Manufacturing," in *Fabricate 2020: Proceedings of the Fabricate 2020*, London, England, April, 2020. Vol 1, pp. 74-81.
- [8] T. Campos, P.J.S Cruz and B. Figueiredo, "The use of natural materials in additive manufacturing of buildings components: Towards a more sustainable architecture," in *Towards new, configurable architecture: Proceedings of the 39th International Hybrid Conference on Education and Research in Computer Aided Architectural Design in Europe*, Novid Sad, Serbia, September 8-10, 2021. Vol 1, pp. 355-364.
- [9] T. Campos, P.J.S. Cruz and B. Figueiredo, "Experimentation of natural materials: The use of chitin in additive manufacturing," in *Structures and Architecture A viable Urban perspective: Proceedings of the Fifth International Conference on Structures and Architecture*, Aalborg, Denmark, July 8-8, 2022. Vol 2, pp. 7-8.
- [10] T. Campos, P.J.S. Cruz and B. Figueiredo, "BioTILES: A sustainable interior wall panels," in *BE-AM Symposium and Exhibition: Proceedings of the of BE-AM 2022 - Symposium for Additive Manufacturing in the Built Environment*, Frankfurt, Germany, November 15-18, 2022. Vol 1, pp. 25-32.
- [11] V. Azevedo, S. Chaves, D. Bezerra, M. Lia Fook, A. Costa, "Quitina e Quitosano: aplicações como biomateriais," in *Revista eletrónica de materiais e processos*. Vol. 2-3, pp. 27-34.

# 3. Fundamental mental realm

Effectively implementing additive solutions for construction requires knowledge and components from three fundamental domains: materials, the process itself, and the geometry of printed goods.

**Materials.** Research on materials covers the preparation of existing construction materials for additive processes, and the development of both sustainable and highly performant materials. The former may involve altering the material properties or adjusting the composition to improve compatibility with the additive manufacturing process [1]. The latter may include bio-based or recycled materials that have a lower environmental impact than traditional construction materials. For instance, additive manufacturing cement must have tailored flow properties to enable its extrusion, while still maintaining the required strength and durability [2]. Newly developed materials can be biodegradable polymer composites made from renewable resources while again meeting certain mechanical requirements. New performance materials enable lighter constructions and have the potential to reduce embodied carbon through increased strength, durability, or insulation, and, hence, reduction of material needed [3].

Combining different materials enables the creation of new composite materials with enhanced properties. For instance, combining concrete with reinforcing fibres can produce a material with improved strength and durability [4]. Other material combinations can be used to produce materials with unique properties, such as flexibility or conductivity. Flexible electronics, for instance, combine conductive and non-conductive materials to produce structures that can be bent and twisted—properties needed for the application in additive process chains.

Crucial to all construction materials is knowledge of their mechanical properties. In order to ensure that the final product meets the required specifications, the elastic properties, strength, fracture toughness, fatigue limit, and other material properties must be characterised. This involves testing the material under various loading conditions and environments to ensure that it performs as expected. While materials testing is an established and well-documented field, 3D printed materials pose new challenges. In particular process-induced hygrothermal shrinkage and notches originating from the layerwise assembly are challenges that research needs to address [5].

Unique to additive manufacturing is its possibility to produce meta and hierarchical materials. Meta materials are a class of materials that have properties not found in natural materials [6]. They feature a specifically engineered microstructure to produce properties, such as negative refractive index, tunable stiffness, or acoustic properties that allow them to bend sound waves around an object [7].

Hierarchical materials have a microstructure with multiple levels of organisation, each level characterised by a different length scale. In other words, hierarchical materials have a complex, multi-scale structure that provides unique mechanical and physical properties [8]. While not all hierarchical materials are meta materials, many meta materials can be created through a hierarchical approach, by designing the structure of the material at multiple length scales. This way, additive manufacturing allows for the creation of materials with unique and customizable properties that can be tailored to specific applications, including in the building and construction sector.

The form or shape raw materials are supplied for additive manufacturing is an important consideration. They must be supplied in a form that is suitable for the specific additive manufacturing process. This may involve grinding the material into a powder, extruding it into a filament, or applying a binder to a powder [9]. The form of raw materials has the potential to significantly reduce storage, enable on-site production, and, hence, reduce transportation and the carbon footprint of production. This has implications for the logistics of additive manufacturing and bridges research on materials and the printing process.

**Additive Manufacturing Process.** Crucial to the generation of objects from filaments, pastes, powders, or liquids is the additive process itself. Controlling it requires the identification of stable process windows for the entirety of process parameters involved, such as power input, flow rate, scan speed, temperature, pressure, among others [10].

The process window refers to the domain where process parameters that lead to a satisfactory product overlap. Its identification may involve empirical testing of different parameters sets and monitoring the resulting product to identify the optimal conditions, but also the theoretical development of nondimensional scaling laws between input parameters and generated output. Running the process within a well-defined process window ensures consistent and repeatable results but requires monitoring. This may involve using sensors, cameras, computer vision, and adjusting the process parameters in real-time to maintain the desired conditions.

By generating finished goods without intermediate steps, AM allows building components to be produced on-site. Both on-site and off-site production each have their own advantages and disadvantages, and the choice will depend on the specific requirements of the project. On-site production can reduce transportation costs and enable the production of customised products, while off-site production can reduce production time and improve quality control [11]. A continuation of this line of thought leads to fully automated and finally autonomous production. By automating

the production process, it is possible to improve efficiency and reduce the risk of errors. This may involve using robots or other automated equipment to perform the printing process, as well as automated quality control systems to ensure that the final product meets the required specifications [12]. Full autonomy of production refers to the ability of the system to operate without human intervention. This can be achieved through the use of artificial intelligence and machine learning algorithms that can monitor and control the production process in real-time [13].

In terms of cost efficiency, processing speed is one of the biggest inhibitors of large-scale deployment of the technology [14]. Although with automation, 3D printing can enable faster production by operating longer and more continuously than humans, today this is still a promise that needs to be fulfilled [15]. Optimising for process speed may involve using multiple print heads or optimising the print path to minimise the print time. This goes in line with energy-aware process planning. While 3D printing pledges to reduce energy consumption and embodied carbon by saving material, the production process itself must be performed energy-conscious to fulfil this promise and reduce the environmental impact of our technology [16].

Finally, many of the above points can be enabled through process simulation. By simulating logistics, printing process, and final part, it is possible to identify potential issues and optimise production planning, process parameters, and product geometry before printing. This can, of course, help to reduce waste and improve performance [17].

**Geometry.** More than with traditional means of fabrication, the geometric freedom of additive manufacturing puts an emphasis on the geometry of printed objects. Computational design tools can be used to generate complex geometries that are difficult or impossible to achieve using traditional manufacturing techniques, leading to new possibilities in terms of design and functionality [18].

Most obviously, by optimising the geometry of the object, it is possible to minimise the amount of material used, reducing costs and environmental impact. This can be achieved through techniques such as lattice structures, where the object is printed with a complex internal structure that provides strength while minimising material usage, or interlocking structures with high strength-to-weight ratios. Exploring new geometries that are inaccessible with traditional means of manufacturing allows for the creation of structures that are more efficient, more lightweight, and more sustainable than their traditionally-manufactured counterparts [19].

Although additive manufacturing provides unprecedented design freedom, it introduces geometric peculiarities into printed structures. Mitigating the influence of

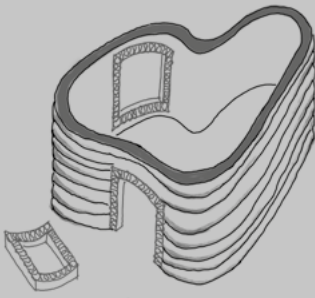
notches introduced by layer-by-layer printing is a concern. Notches can introduce stress concentrations weakening the overall structure. Developing techniques to minimise their impact is subject to today's research. This may involve using algorithms to optimise the orientation of the printed layers or using post-processing techniques to smooth out the surface. Since they can often not be avoided entirely, computational tools for their structural assessment are required [20].

The development of metamaterials is a concern of materials research but also pure geometric exploration. By designing the geometry of the object at a very small scale, it is possible to control the behaviour of electromagnetic and acoustic waves, leading to the creation of materials with unique properties. This can have a wide range of applications in areas such as communication, sensing, and energy harvesting.

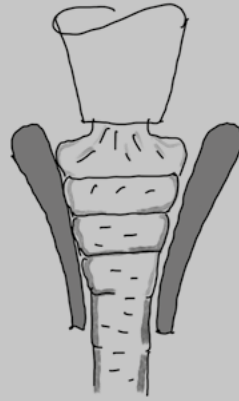
In summary, the geometry of 3D printed objects is a critical factor when designing for additive manufacturing. Reproducing structures that can be fabricated using traditional manufacturing techniques cannot harness the full potential of additive technologies and, hence will not yield competitive products for the building and construction market. By using computational design tools, optimising the geometry of the object, and taking advantage of the unique properties of 3D printed objects, however, it is possible to create new materials and structures with unique properties and applications with the potential to disrupt the industry [21].



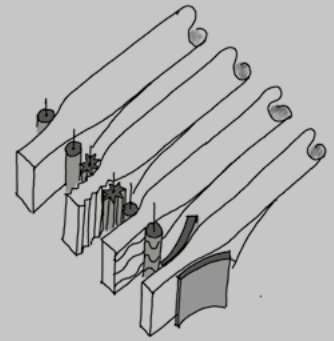
- [1] Buchanan, C., & Gardner, L. (2019). Metal 3D printing in construction: A review of methods, research, applications, opportunities and challenges. *Engineering Structures*, 180, 332-348. <https://doi.org/10.1016/j.engstruct.2018.11.045>
- [2] Lim, S., Buswell, R. A., Le, T. T., Austin, S. A., Gibb, A. G., & Thorpe, T. (2012). Developments in construction-scale additive manufacturing processes. *Automation in Construction*, 21, 262-268. <https://doi.org/10.1016/j.autcon.2011.06.010>
- [3] Bos, F., Wolfs, R., Ahmed, Z., & Salet, T. (2016). Additive manufacturing of concrete in construction: Potentials and challenges of 3D concrete printing. *Virtual and Physical Prototyping*, 11(3), 209-225. <https://doi.org/10.1080/17452759.2016.1209867>
- [4] Shakor, P., Nejadi, S., Paul, G., & Malek, S. (2019). Review of emerging additive manufacturing technologies in 3D printing of cementitious materials in the construction industry. *Frontiers in Built Environment*, 4, 85. <https://doi.org/10.3389/fbuil.2018.00085>
- [5] Pacillo, G. A., Ranocchiani, G., Loccarini, F., & Fagone, M. (2021). Additive manufacturing in construction: A review on technologies, processes, materials, and their applications of 3D and 4D printing. *Material Design & Processing Communications*, 3(5), e253. <https://doi.org/10.1002/mdp2.253>
- [6] Surjadi, J. U., Gao, L., Du, H., Li, X., Xiong, X., Fang, N. X., & Lu, Y. (2019). Mechanical metamaterials and their engineering applications. *Advanced Engineering Materials*, 21(3), 1800864. <https://doi.org/10.1002/adem.201800864>
- [7] Valipour, A., Kargozarfard, M. H., Rakhshi, M., Yaghootian, A., & Sedighi, H. M. (2022). Metamaterials and their applications: An overview. *Proceedings of the Institution of Mechanical Engineers, Part L: Journal of Materials: Design and Applications*, 236(11), 2171-2210. <https://doi.org/10.1177/1464420721995858>
- [8] Fratzl, P., & Weinkamer, R. (2007). Nature's hierarchical materials. *Progress in Materials Science*, 52(8), 1263-1334. <https://doi.org/10.1016/j.pmatsci.2007.06.001>
- [9] Yanko, T., Brener, V., & Ovchinnikov, O. (2020). Production of spherical titanium alloy powders used in additive manufacturing from titanium scrap. *MATEC Web of Conferences*, 321, 07008. <https://doi.org/10.1051/mateconf/202032107008>
- [10] Sammons, P. M., Gegel, M. L., Bristow, D. A., & Landers, R. G. (2018). Repetitive process control of additive manufacturing with application to laser metal deposition. *IEEE Transactions on Control Systems Technology*, 27(2), 566-575. <https://doi.org/10.1109/TCST.2017.2781653>
- [11] Pasco, J., Lei, Z., & Aranas, C. (2022). Additive manufacturing in off-site construction: Review and future directions. *Buildings*, 12(1), 53. <https://doi.org/10.3390/buildings12010053>
- [12] Tankova, T., & da Silva, L. S. (2020). Robotics and additive manufacturing in the construction industry. *Current Robotics Reports*, 1, 13-18. <https://link.springer.com/article/10.1007/s43154-020-00003-8>
- [13] Halicioglu, F. H., & Koralay, S. (2020). Applicability analysis of additive manufacturing methods on construction projects. *Grđevinar*, 72(04), 335-349. <https://doi.org/10.14256/JCE.2334.2018>
- [14] Ning, X., Liu, T., Wu, C., & Wang, C. (2021). 3D printing in construction: Current status, implementation hindrances, and development agenda. *Advances in Civil Engineering*, 2021, 1-12. <https://doi.org/10.1155/2021/6665333>
- [15] Hossain, M. A., Zhumabekova, A., Paul, S. C., & Kim, J. R. (2020). A review of 3D printing in construction and its impact on the labor market. *Sustainability*, 12(20), 8492. <https://doi.org/10.3390/su12208492>
- [16] Annibaldi, V., & Rotilio, M. (2019). Energy consumption consideration of 3D printing. In 2019 II Workshop on Metrology for Industry 4.0 and IoT (MetroInd4.0&IoT) (pp. 243-248). IEEE. <https://doi.org/10.1109/METROI4.2019.8792856>
- [17] Camacho, D. D., Clayton, P., O'Brien, W. J., Seepersad, C., Juenger, M., Ferron, R., & Salamone, S. (2018). Applications of additive manufacturing in the construction industry-A forward-looking review. *Automation in Construction*, 89, 110-119. <https://doi.org/10.1016/j.autcon.2017.12.031>
- [18] Paolini, A., Kollmannsberger, S., & Rank, E. (2019). Additive manufacturing in construction: A review on processes, applications, and digital planning methods. *Additive Manufacturing*, 30, 100894. <https://doi.org/10.1016/j.addma.2019.100894>
- [19] Ghaffar, S. H., Corker, J., & Fan, M. (2018). Additive manufacturing technology and its implementation in construction as an eco-innovative solution. *Automation in Construction*, 93, 1-11. <https://doi.org/10.1016/j.autcon.2018.05.005>
- [20] Jayathilakage, R., Rajeev, P., & Sanjayan, J. G. (2020). Yield stress criteria to assess the buildability of 3D concrete printing. *Construction and Building Materials*, 240, 117989. <https://doi.org/10.1016/j.conbuildmat.2020.117989>
- [21] McDowell, D. L., & Olson, G. B. (2009). Concurrent design of hierarchical materials and structures. *Scientific modeling and simulations*, 16, 207-240. [http://dx.doi.org/10.1007/978-1-4020-9741-6\\_14](http://dx.doi.org/10.1007/978-1-4020-9741-6_14)



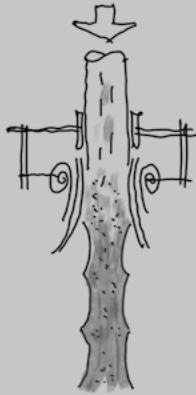
**CONTOUR TECTONICS**  
 The continuous layering of materials gives rise to a distinctive tectonic pattern, closely linked with additive manufacturing (AM) processes. This effect not only influences the haptic qualities of these surfaces but also facilitates the seamless integration of various architectural components, including openings. Ultimately, it leads to the emergence of a new architectural expression.



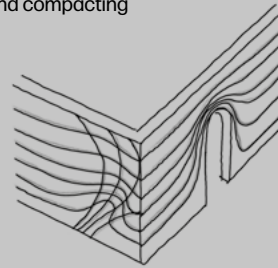
**EXTRUSION COMPACTOR**  
 When printing with liquid materials, the surface characteristics are closely tied to the material's plasticity, shaping a specific texture. To define this surface more precisely, the use of funnels for extrusion could be a viable solution. The extruder plays a dual role by creating surfaces and compacting the material.



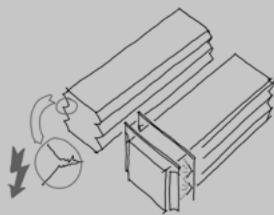
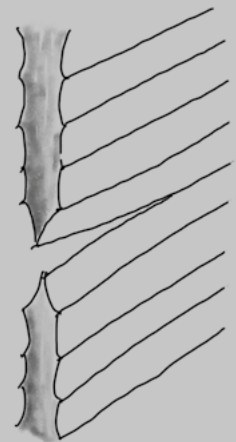
**EXTRUSION SHAPER**  
 Customisation of surface qualities and textures can be achieved by manipulating the surface immediately after extrusion, incorporating devices that engrave shapes such as flushness, wrinkles or free forms.



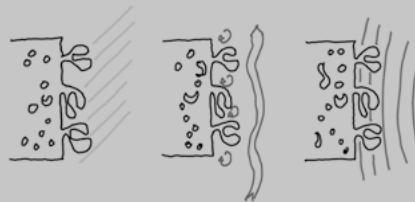
**EXTRUDER TEXTURE**  
 To achieve more freedom in shaping surfaces through AM, incorporate a manipulable outlet nozzle, individually controlled based on the geometry during the extrusion process. This feature holds the potential to introduce a novel layout for creating well-defined surface textures.



**ORGANIC TEXTURE**  
 In the initial stages, it's just a design concept: an organic-like surface. However, delving deeper into the realm of biomimicry reveals a fundamental truth—nature's forms adhere to specific physical or chemical principles to serve their biological functions. This unveils a compelling research field: not mere mimicry, but functioning in harmony with nature's needs.



**MINERAL MATERIAL TREATER**  
 To counteract the problem of cracking in the recesses of extruded materials, a recommended solution involves a post-extrusion surface treatment. This treatment involves the application of water-treated mineral material, effectively minimising the risk of cracking and ensuring its structural integrity.



**MULTIFUNCTIONAL SURFACE**  
 AM unlocks the potential to increase the performance of building surfaces and architectural components. By integrating specific formal and material features, it becomes possible to offer multifunctional capabilities. These include acoustic and light reflection, insulation, and thermal storage.

**LIGHT AND AIR**  
 One of the most thrilling aspects of AM lies in its ability to integrate functionalities. In this context, the concept involves incorporating specific openings, directly into extruded surfaces. This technique not only facilitates illumination but also enhances ventilation, demonstrating the versatility of AM technology.

# CARBON-DRIVEN DESIGN OF 3D CONCRETE PRINTED HORIZONTAL STRUCTURES

Roberto Naboni  
Luca Breseghello

The rapid evolution of 3D printing technology is reshaping the construction industry, offering the potential for environmentally sustainable and architecturally innovative structures. This article explores the pioneering work of SDU CREATE at the University of Southern Denmark in 3D concrete printing. From characterising specialised concrete mixtures to structural design breakthroughs, SDU CREATE's research underscores the promise of 3D concrete printing in reducing carbon emissions, optimising material use, and pushing the boundaries of architectural design. By addressing the complexities of this transformative technology, the research paves the way for a sustainable and creatively diverse future in construction.

## INTRODUCTION

Concrete assumes a dominant role in the global construction industry [1] yet contributes significantly to anthropogenic CO<sub>2</sub> emissions, responsible for approximately 8% of worldwide emissions yearly [2]. Horizontal structures within buildings are a critical factor in this environmental equation. In conventional three- to eight-story constructions, these horizontal elements employ over 40% of the concrete volume [3], pivotal in influencing the built environment's environmental footprint and structural soundness.

Recent years have witnessed a surge in interest within the construction industry regarding digital fabrica-

tion techniques for concrete structures [4, 5, 6]. 3D Concrete Printing (3DCP) has one of the highest impact potentials among these methods. It holds a technology readiness level of 6-7 [7] and is steadily gaining ground in commercial projects. However, it has yet to attain the status of a standard construction method, and various challenges still need to be solved. These challenges encompass the intricacies of 3DCP's printing methods, mechanical behaviour, and the pressing need for comprehensive economic and environmental assessments [9; 10].

3DCP promises to deliver unparalleled construction flexibility and a high level of control over material allocation, positioning it as a transformative technology with the poten-

tial to reduce the environmental impact of the construction sector [11]. Nonetheless, limitations persist. Quality assurance and structural assessment issues often necessitate over-dimensioning structural elements, thus diminishing the intended environmental benefits [12].

Moreover, 3DCP's additive nature, distinct from traditional casting, demands novel engineering approaches for structural elements and building design [13]. Conventional design methodologies often falter in accounting for the geometric constraints of 3D printing, ultimately affecting both the final aesthetics and mechanical performance. Achieving seamless interoperability between 3D modelling and structural analysis software remains challenging for the construction industry [14]. 3DCP necessitates a tighter integration of design, material properties, fabrication constraints, and structural performance. In this context, the development of fabrication-aware models and comprehensive design-to-simulation-to-fabrication workflows, with minimal data loss, emerges as an imperative endeavour to unlock the full potential of this technology.

### 3D CONCRETE PRINTING RESEARCH AT SDU CREATE

SDU CREATE at the University of Southern Denmark investigates sustainable design and manufacturing strategies tailored to take full advantage of 3DCP. Preliminary works involved developing a fabrication setup, characterising a material mix [15], and digital simulation to predict the in-process material behaviour and its outcome [16]. These tools have been exploited in design and fabrication experiments where the printing path and robot code were programmatically manipulated [17]. To enhance the carbon efficiency of structures by tailoring their designs, our research considers the mechanical performance and the specific material characteristics inherent to 3DCP. These are considered by implementing computational design workflows for 3DCP, including pipelines and tools for high-resolution structural designs and engineering. Our work consists of a methodology combining various crucial aspects (Figure 1):

- x Structural performance simulation. We employ Finite Element Analysis (FEA) simulations to assess the structural performance of printed concrete elements at different design stages. Initially, FEA provides insights into stress distribution, offering opportunities for structural optimisation. Once the structural design, including filament size and interactions, is finalised, non-linear FEA is used to predict structural capacity and failure modes, enabling comparisons with structural testing results (Figure 1A).
- x High-resolution in large-scale 3DCP. Large-scale printing filaments, often in the centimetre range, significantly impact material properties and architec-

tural geometry. Our approach involves fine-tuning filament width/height by adjusting robot speed and trajectory with gradient maps. This precision control allows us to manage the sectional attributes of individual wall prints and ensure solid element cohesion (Figure 1B/C).

- x Embedding of steel reinforcements within filaments subjected to tensional stresses, fundamentally obtaining bending-resistant structural elements necessary for horizontal structures (Figure 1D).
- x Structural testing. We subject 3DCP-fabricated structures to testing and validate their performance and integrity. These tests, including 3-point flexural tests, provide essential data on ultimate strength, deformation characteristics, and failure mechanisms while ensuring compliance with safety and durability standards (Figure 1E).

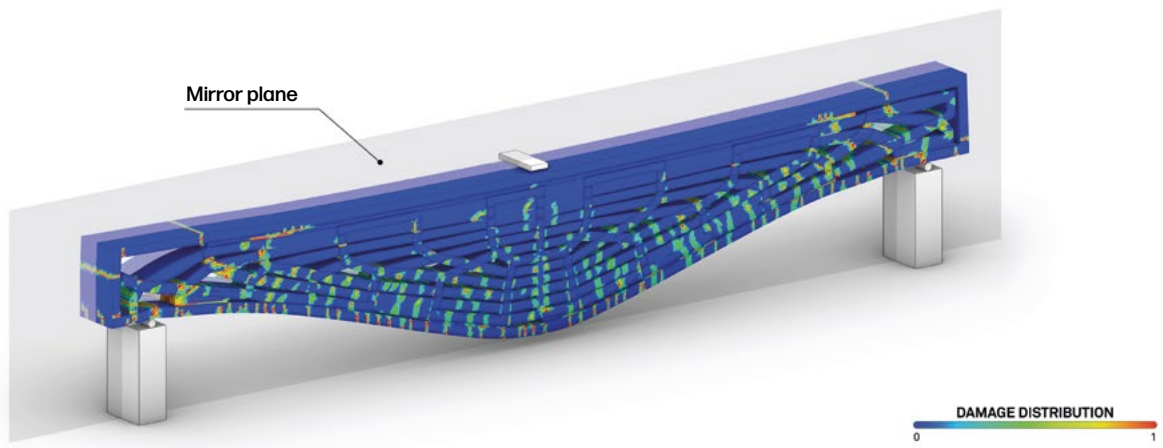
Adopting the above-described methodology, SDU CREATE developed a series of prototypes focused on reducing material consumption and carbon emissions in reinforced concrete horizontal structural elements. These consist of load-bearing beams and slabs, briefly presented in the following sections, providing an overview of our research trajectory.

### GRIDBEAM - LIGHTWEIGHT LOAD-BEARING STRUCTURES

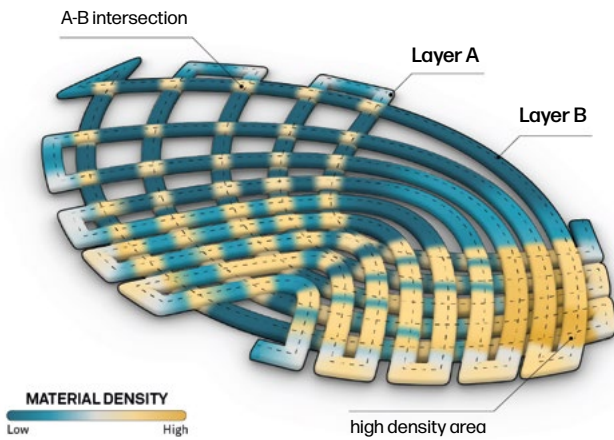
At the core of the first developed prototype lies the concept of a porous structure, essential for minimising material usage within concrete beams by optimising its distribution within their volume. The *GridBeam* developed in [18] incorporates a grid-like orthogonal structure oriented along the longitudinal cross-section plane, resulting in a substantial reduction in material consumption, yielding an approximate 25% decrease compared to a full 3DCP beam. The beam was devised as a simply supported rectangular beam with a length of 3.00 m, a span of 2.76 m, a width of 0.16 m, and a depth of 0.30 m.

To manufacture the designed porous layout, the *Grid-Beam* benefits from a printing process where successive layers are deposited alternately along the two orthogonal grid directions. Notably, at the intersections where the 35 mm wide and 12 mm high layers meet, the motion speed was accelerated to reduce the amount of printing material deposited while maintaining excess material to create a stronger bond between consecutive layers. This approach aimed to balance structural integrity and material usage, introducing new design and fabrication ideas such as porosity and woven toolpaths.

Weighing 231 Kg and integrating around 680 cm<sup>3</sup> of 6 mm reinforcement bars, two specimens of this design were



A



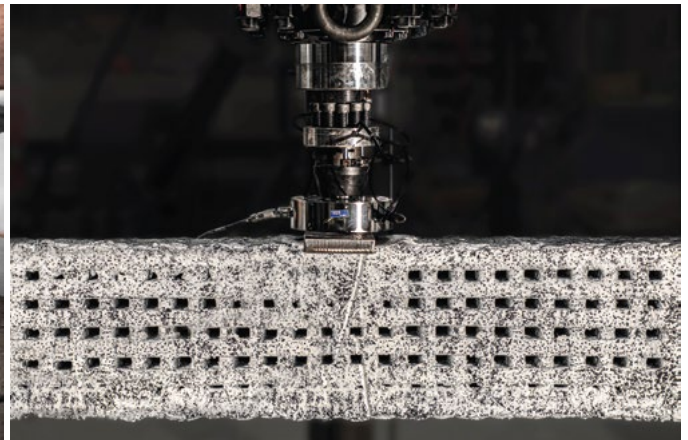
B



C



D



E

Figure 1: Adopted experimental methods exploiting 3DCP: (A) Damage distribution through FEA; (B) Preview of material density in woven layered extrusion; (C) 3DCP with high-resolution control of shape and filament dimension; (D) Insertion of reinforcement bars in the printed filament; (E) Structural testing in three-point bending.

structurally tested in a three-point bending test, achieving an average failure load of 49.9 kN, resulting in a strength-to-weight ratio of 0.22 kN/Kg, higher than the 0.14 kN/Kg of comparative solid 3D-printed beam specimens. Moreover, in a Life Cycle Analysis (LCA), the *GridBeam* presented a 45% lower environmental impact than a full printed beam.

### **3DLIGHTBEAM - STRESS-BASED INFILL DESIGN**

After successfully demonstrating porous loadbearing structures, our work began designing the sectional layout of the same 3.00 meter-long test specimen, whose infill was based on principal stresses obtained through FEA. The design to fabrication and FEA analysis workflow developed in [19] for creating this prototype, namely *3DLightBeam*, strongly emphasises optimising the printing path. Its primary objective was to incorporate a set of geometric and structural optimisation routines to enhance efficiency by reducing material usage and proportionally improving their environmental impact. A computational workflow enabled us to conceive and manufacture tailored beams, capitalising on the inherent design flexibility afforded by 3DCP. *3DLightBeam* utilises stress isostatic curves to enhance the efficiency of beam elements, intended as the ratio between their load capacity and weight. These stress isostatic curves are based on Principal Stress Lines (PSL), instrumental in illustrating the paths of internal forces within a defined loading scenario and design domain. They indicate the spatial directions where stress is purely axial. Structural sections aligned with PSL are particularly advantageous, as they experience minimal to no shear or bending stress locally. Moreover, along the secondary PSL, acting in pure tension, a series of 6 mm reinforcement steel bars were placed in the designed beam, with a quantity measured in a volume comparable to the other experiments presented here.

Building upon a woven toolpath fabrication strategy, the fabrication process implemented a local variation of the filament width based on the resultant stress values by parametrically controlling the robot motion speed. Following an FEA map of the stresses and integrating it with geometric constraints, such as adjacency of filaments, self-intersections and fabrication limitations, such as minimum and maximum filament widths, a set of speeds was generated for each target plane of the robot code.

With an average weight of 198 Kg, the structurally tested specimens of *3DLightBeam* averaged a capacity of 79.5 kN in three-point bending. This resulted in a strength-to-weight ratio of 0.40 kN/Kg, with an 85% increase compared to the *GridBeam* and about 178% compared to the 3D-printed beam with an entire section. The highly porous layout also contributes to carbon efficiency by maximising such elements' surface area and recarbonation potential.

### **3DLIGHTBEAM+. SHAPE AND INFILL-OPTIMISED BEAMS**

The *3DLightBeam+* prototype, a culmination of our ongoing research, represents a substantial improvement in the domain of 3D-printed reinforced concrete beams. The research presented in [21] advances prior work by refining the process of PSL selection and implementing shape optimisation, resulting in the creation of the first reinforced beam with an optimised shape and infill pattern to reduce material consumption and carbon emissions. The design of this prototype employed a linear FEA to computer principal stresses and an evolutionary optimisation process to optimise its section towards the minimisation of its deflection and principal stresses.

These methods have yielded an impressive average bending strength-to-weight ratio of 0.51 kN/kg. This ratio significantly outperforms earlier design iterations, surpassing them by 200% compared to a solid 3DCP beam, 120% when compared to the *GridBeam*, and achieving a 20% improvement over an infill-optimized beam with a rectangular cross-section such as *3DLightBeam*. This progress highlights the advancement achieved with *3DLightBeam+* regarding structural efficiency and material reduction in 3DCP.

### **3DLIGHTSLAB. STRESS-BASED RIBBED SLABS**

*3DLightSlab* is a proof-of-concept ribbed concrete slab designed and fabricated, extending the methods developed in the *3DLightBeam* beams series. Aiming for a lightweight yet structurally efficient concrete structure with a high strength-to-weight ratio, *3DLightSlab* was realised using a workflow that integrates Principal Moment Lines (PML) to generate ribs layout and optimises their depth following resultant bending stresses from an FEA [21]. The prototype was devised as a 3.5 m x 1.6 m rectangular slab supported on two 0.25 m diameter circular columns and features a series of ribs with variable depths between 0.08 m and 0.16 m. The design of the ribs followed the structural analysis results, precisely the magnitude of bending moments present at each analysed location of the ribs. To obtain such changes in the depth of the ribs, the design of the toolpath and the 3DCP fabrication of *3DLightBeam* were characterised by the integration of non-planar and variable heights of the 3D-printed filament. Integrating this with a programmed change in the robot printing speed and following the results of an FEA, the filament width was modulated to place more significant quantities of material where shear stresses were higher. Tested with a distributed load of 3kN/m<sup>2</sup>, the slab did not present perceivable deflection and signs of hairline cracks, fulfilling the requirements indicated by Eurocode. Similarly, two *3DLightSlab* specimens were tested



Figure 2: The *GridBeam* prototype is a three-meter porous beam with a porous pattern and woven layered extrusion.



Figure 3: *3DLightBeam*, a 3DCP lightweight beam that integrates FEA-generated PSL as a design driver.



Figure 4: *3DLightBeam+*, proof-of-concept prototype of a shape- and infill-optimised beam manufactured with 3DCP.



Figure 5: *3DLightSlab*, a 3.5 m x 1.6 m ribbed slab with two punctual supports optimised through PML and non-planar 3DCP extrusion.



with a concentrated load until failure, achieving an average of 17.8 kN, well beyond the standard design load of 4 kN.

The design and successful fabrication of *3DLightSlab* demonstrate 3DCP as a viable technology to overcome the economic implications of complex manufacturing that had previously restricted the utilisation of isostatic slabs since the work of Nervi in the middle of the twentieth century. By integrating the principles of such architectural precedents with the inherent layer-based approach of 3DCP, a new aesthetic dimension has emerged for ribbed concrete floors. This achievement underscores the innovative potential of 3DCP technology in redefining the boundaries of structural design and architectural aesthetics.

## CONCLUSIONS

3DCP represents a remarkable evolution in the construction industry. It offers the potential for stunning architectural designs and a pathway to reducing the industry's carbon footprint. The pioneering work conducted by SDU CREATE showcases the advancements made in material characterisation, structural design, and the realisation of innovative structures.

The presented research showcases the potential for reducing carbon emissions by enhancing the structural efficiency of concrete elements. By addressing typical challenges of shape optimisation, this technology has the power to transform the construction industry while mitigating its environmental impact. Our future research will focus on developing this approach further, involving other peculiar aspects such as (i) printing low-embodied carbon materials, with the development of innovative concrete mixtures designed explicitly for 3DCP, engineered to provide enhanced performance, durability and sustainability; (ii) integration of sensors, to enable real-time monitoring and feedback. This will enhance both the quality and reproducibility of the process and the longevity of 3D-printed building parts; (iii) enhance the automation level through the design-to-production pipeline to render this process more accessible and cost-effective, opening up new possibilities for builders' and developers' adoption.

With ongoing research and innovation, 3DCP is poised to reshape how we build, creating a more sustainable and architecturally diverse future built environment.

## ACKNOWLEDGEMENTS

The experimental work presented in this article was conducted at the CREATE Lab at the University of Southern Denmark. The various projects result from the collaborative efforts of multiple researchers and student collaborators. The authors wish to thank Hamed Hajikarimian (FEA), Sandro Sanin (3D Printing), and Daniele Florenzano (3D Printing) for their contribution to the research presented here. Beams and slabs were tested at SDU Structures Lab in collaboration with Assoc.Prof. Dr. Henrik Brønner Jørgensen. The authors thank industrial partners Hyperion Robotics (3DCP technology) and Weber Saint-Gobain Denmark (3D Printing mortar) for their continuous support of this research.

## REFERENCES

- [1] R. J. Flatt, N. Rousset, and C. R. Cheeseman, "Concrete: An eco material that needs to be improved," *Journal of the International Association for Shell and Spatial Structures*, vol. 32, 2012, pp. 2787-2798.
- [2] IEA, "Technology Roadmap - Low-Carbon Transition in the Cement Industry," 2018. Paris.
- [3] S. A. Miller, A. Horvath, and P. J. M. Monteiro, "Readily implementable techniques can cut annual CO<sub>2</sub> emissions from the production of concrete by over 20%," *Environmental Research Letters*, vol. 11, 2016.
- [4] P. Bischof, J. Mata-Falcón, and W. Kaufmann, "Fostering innovative and sustainable mass-market construction using digital fabrication with concrete," *Cement and Concrete Research*, vol. 161, 2022.
- [5] R. Naboni and I. Paoletti, "Advanced Customization in Architectural Design and Construction," Springer Verlag, 2015.
- [6] A. Paolini, S. Kollmannsberger, and S. Rank, "Additive manufacturing in construction: A review on processes, applications, and digital planning methods," *Additive Manufacturing*, vol. 30, 2017.
- [7] B. García de Soto, I. Agustí-Juan, J. Hunhevicz, S. Joss, K. Graser, G. Habert, and B. T. Adey, "Productivity of digital fabrication in construction: Cost and time analysis of a robotically built wall," *Automation in Construction*, vol. 92, 2018, pp. 297-311.
- [8] G. Ma, R. Buswell, W. R. Leal da Silva, L. Wang, J. Xu, and S. Z. Jones, "Technology readiness: A global snapshot of 3D concrete printing and the frontiers for development," *Cement and Concrete Research*, vol. 156, 2022, pp. 106774.
- [9] G. De Schutter, K. Lesage, V. Mechtcherine, V. N. Nerella, G. Habert, and I. Agustí-Juan, "Vision of 3D printing with concrete—Technical, economic and environmental potentials," *Cement and Concrete Research*, vol. 112, 2018, pp. 25-36.
- [10] A. Perrot and S. Amziane, "3D Printing in Concrete: General Considerations and Technologies," in *3D Printing of Concrete: State of the Art and Challenges of the Digital Construction Revolution*, 2019, pp. 1-40.
- [11] N. Stoiber and B. Kromoser, "Topology optimisation in concrete construction: a systematic review on numerical and experimental investigations," *Structural and Multidisciplinary Optimization*, vol. 64, 2021.
- [12] J. Mata-Falcón, P. Bischof, and W. Kaufmann, "Exploiting the potential of digital fabrication for sustainable and economic concrete structures," in *RILEM Bookseries*, vol. 19, 2019, pp. 157-166.
- [13] R. A. Buswell, F. P. Bos, W. R. Leal da Silva, N. Hack, H. Kloft, D. Lowke, N. Freund, A. Fromm, E. Dini, T. Wangler, E. Lloret-Fritsch, R. Schipper, V. Mechtcherine, A. Perrot, K. Vasilic, and N. Rousset, "Digital Fabrication with Cement-Based Materials: Process Classification and Case Studies," in *Digital Fabrication with Cement-Based Materials*, vol. 36, Springer, Cham, 2022.
- [14] T. Ooms, G. Vantghem, R. Van Coile, and W. De Corte, "A parametric modelling strategy for the numerical simulation of 3D concrete printing with complex geometries," *Additive Manufacturing*, vol. 38, 2020.
- [15] H. Joergensen, P. Douglas, and R. Naboni, "Experimental study on the anisotropic behavior and strength of 3D printed concrete," in *fib Symposium 2021 - Concrete Structures: New Trends for Eco-Efficiency and Performance*, 2021.
- [16] R. Naboni, L. Breseghello, and S. Sanin, "Toolpath Simulation, Design and Manipulation in Robotic 3D Concrete Printing," in *Proceedings of the 26th International Conference of the Association for Computer-Aided Architectural Design Research in Asia, CAADRIA 2021: Projections*, 2021, Hong Kong, China.
- [17] L. Breseghello and R. Naboni, "Adaptive Toolpath: Enhanced Design and Process Control for Robotic 3DCP," in *Computer-Aided Architectural Design: Design Imperatives: The Future is Now. CAAD Futures 2021, Communications in Computer and Information Science*, vol. 1465, Springer, Singapore, 2021.
- [18] S. Gislason, S. Bruhn, L. Breseghello, B. Sen, G. Liu, and R. Naboni, "Lightweight 3D Printed Concrete Beams Show An Environmental Promise: A Cradle-to-Grave Comparative Life Cycle Assessment," *Clean Technology and Environmental Policy*, 2022, Springer.
- [19] L. Breseghello and R. Naboni, "Toolpath-based Design for 3D Concrete Printing of Carbon-efficient Architectural Structures," *Additive Manufacturing*, 2022, Elsevier.
- [20] L. Breseghello, H. Hajikarimian, H. B. Jørgensen, and R. Naboni, "3DLightBeam+. Design, simulation, and testing of carbon-efficient reinforced 3D concrete printed beams," *Engineering Structures*, vol. 292, 2023.
- [21] Breseghello, L., Hajikarimian, H., Naboni, R. 3DLightSlab. Stress-based design-to-fabrication workflow of ribbed 3D concrete printed slabs. *Journal of Building Engineering, Special Issue: Advances in 3D Concrete Printing and Digital Construction Technologies for Building*. In-press.

# THE JOURNEY TO ACHIEVE SUSTAINABILITY AND CIRCULARITY IN ADDITIVE MANUFACTURING OF CONSTRUCTION MATERIALS

Sandra S. Lucas

This study aims to develop sustainable mortars for 3D printing by testing two different strategies. The first strategy involves the use of ground blast furnace slag (GBFS) and volcanic ash (VA) as cement replacement in 3D printing of concrete. Two compositions were prepared, one using CEM III/B cement and the other using 70% CEM III/B cement and 30% VA by weight. The second strategy involves the addition of natural fibres to a cement-based 3D printable mortar to prevent post-printing cracking.

When compared with a printable mix containing Portland cement only, both compositions (CEM III/B and VA) proved to develop higher strength at 28 days. Even though adding volcanic ash can lead to slower strength development, its final strength is higher, and the material also presented lower shrinkage. Replacing Portland cement can reduce substantially the environmental impact of 3DP mortars and this can be achieved without sacrificing long-term durability.

## INTRODUCTION

According to Eurostat, construction and buildings' use accounts for half of the extracted materials and energy consumption and a third of water consumption in the EU, generating 30% of the total waste produced [1]. The European construction sector produces as much as 2 billion tonnes of waste per year with almost 0.9 tonnes still ending up in a landfill, despite the efforts made and the measures the industry is undertaking to decrease these numbers [2]. Securing resources and energy efficiency are key drivers to improving sustainability in buildings and infrastructures. Because attacking the problem downstream is not doing

enough, a solution would be to achieve zero-waste generation by switching to smart manufacturing processes.

The construction industry is entering a new and exciting phase with the development of 3D printing solutions. Concrete materials and structures can now be easily printed into much more complex shapes than before, however, the materials are still quite similar to the conventional concrete that has been used for many decades. The compositions used in 3D printing (3DP) are limited to, so far, basic formulations that do not diverge substantially from a traditional mortar, only its rheological properties are different since they are specifically adjusted to the printing process [3]. Most commercial mixes for 3D printed concrete (3DPC)

still use high amounts of cement which increases the material's embodied energy and carbon footprint. Although 3D printing technology is developing rapidly, the focus has been mostly on the technology and the printability of the 'ink' (cement mortar). Little attention has been paid so far to the environmental performance and sustainability of 3DP buildings [4].

In 3DPC, the whole process is still facing many challenges, such as the quality control of the ink, achievement of a high level of printing quality, good shape stability, proper control of the printability window and lastly, the final quality of the printed product [5]. By replacing cement with more sustainable binders, we are achieving better resource efficiency, reducing the impact of this industry on climate change and contributing to a resilient economy and society. In this paper we present the preliminary results of a new project where we aim to find sustainable and circular solutions for zero-energy 3DP buildings; 1) we investigate the use of alternative binders to produce 3DP materials, and 2) the application of natural fibres as an alternative method for reinforcement of 3DPC.

### USE OF ALTERNATIVE BINDERS IN 3D PRINTING

CEM III/B is a type of blended cement containing approximately 70% blast furnace granulated slag and 30% Portland cement. Because slag is a by-product of the steel industry and is not specifically mined for use in cement production, the carbon footprint of CEM III/B is lower than that of traditional cement.

Table 1 - Compositions tested

Material (wt%)	CEM III/B	30% Volcanic ash
Portland cement 42.5 N	61	4.3
Blast furnace slag	14.2	9.9
Volcanic ash	0.0	61
Limestone powder	13.0	13.0
Sand	66.7	66.7
Superplasticizer (% to total binder)	0.3	0.5
Retarder (% to total binder)	0.2	0.2

In this work, two printable mixes with low cement content were developed (Table 1), one using CEM III/B as a binder and another where part of this binder was replaced with volcanic ash. The mixes were compared with a commercial

3D printable mortar made with Portland cement only. The presence of slag promotes an increase in calcium silicate hydrate (CSH) contributing to higher strength and density (Figure 1) [6]. While volcanic ash contributed to an (expected) slight reduction in the early strength, it has a positive effect on long-term strength development due to its pozzolanic activity. The use of slag also has a positive effect in reducing shrinkage and the partial replacement with volcanic ash did not impact this. The values are similar and significantly lower than the reference mix (Figure 2).

### USE OF NATURAL FIBRES IN 3DCP

Different types of fibres have been tested to compensate for the lack of reinforcement in 3DCP and improve its tensile strength. Because adding short fibres during the printing process is a relatively straightforward solution, this became the method of preference for reinforcement. Other options, including inserting rebars post-printing are far more complex and have not proved so far to be effective.

The types of fibres that have been investigated include steel, glass, carbon and polymer. Each type has its unique properties and can provide different benefits to the mechanical performance of the 3D printed concrete. Steel fibres have high tensile strength and ductility, effectively bridging cracks and reducing post-cracking behaviour, but steel is expensive, has a high embodied energy and can be subject to corrosion. Glass fibres, while lightweight and resistant to corrosion, are brittle and also have high embodied energy. Carbon fibres, commonly used in aerospace and automotive industries, can be very expensive. Polymeric fibres, such as polypropylene, on the other end, are cheaper and easily available but are less effective and can compromise the interlayer bond strength.

In a preliminary study, an amount of 0.5% in weight relative to the binder has been determined to be the optimal content of hemp fibres. The results demonstrate that a printable mix using hemp fibres has comparable flexural and compression strength to a mix using polymeric fibres (Figure 3).

Natural fibres are an attractive option if we are aiming for more sustainable 3D printing due to their renewable and biodegradable properties. They can also provide good tensile strength, flexibility, and thermal insulation. Though their mechanical properties can vary widely depending on the fibre source and further research is needed, they can be grown and harvested sustainably, can be sourced locally and are low-cost, making them an environmentally friendly alternative to synthetic fibres.

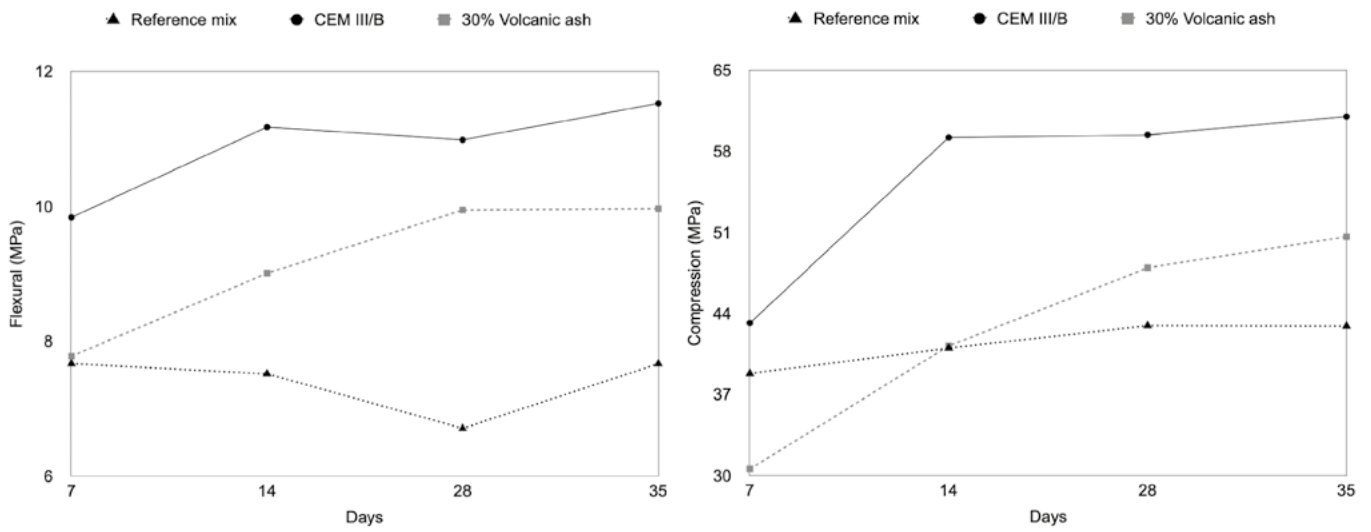


Figure 1: Mechanical strength development of printable mixes containing CEM III/B and volcanic ash, flexural (left) and compression (right).

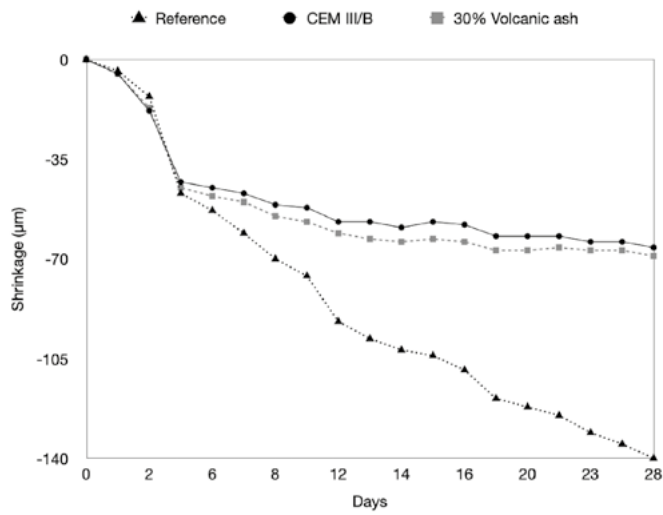


Figure 2: Shrinkage up to 28 days.



Figure 3: Printed sample containing hemp fibres (left) and mechanical strength of 3DPC with PP and hemp fibres (right) [7].

## CONCLUSIONS

The study concludes that using alternative binders and natural fibres shows potential for developing sustainable mortars for 3D printing. The use of GBFS and VA as cement replacements can improve the mechanical properties of the printed specimens, while the addition of natural fibres can prevent cracking in 3D printable mortars. Further research is needed to optimise the printing parameters and investigate the durability and environmental impact of the resulting mortars.

## ACKNOWLEDGEMENTS

This work has received support from the NWO Netherlands through the funding High Tech Systems and Materials HTSM2019 - project number 17967 with the title "Additive manufacturing of sustainable concrete for zero-energy buildings".

## REFERENCES

- [1] European Commission, Database - Eurostat, (2019). <https://ec.europa.eu/eurostat/data/database> (accessed April 5, 2019).
- [2] European Commission, European Construction Sector Observatory, Eur. Comm. (2018). [https://ec.europa.eu/growth/sectors/construction/observatory\\_en](https://ec.europa.eu/growth/sectors/construction/observatory_en).
- [3] F.P. Bos, P.J. Kruger, S.S. Lucas, G.P.A.G. van Zijl, Juxtaposing fresh material characterisation methods for buildability assessment of 3D printable cementitious mortars, *Cem. Concr. Compos.* 120 (2021) 104024. doi:10.1016/j.cemconcomp.2021.104024.
- [4] H. Alhumayani, M. Goma, V. Soebarto, W. Jabi, Environmental assessment of large-scale 3D printing in construction: A comparative study between cob and concrete, *J. Clean. Prod.* 270 (2020) 122463. doi:10.1016/j.jclepro.2020.122463.
- [5] A.S.J. Suiker, R.J.M. Wolfs, S.M. Lucas, T.A.M. Salet, Elastic buckling and plastic collapse during 3D concrete printing, *Cem. Concr. Res.* 135 (2020) 106016. doi:10.1016/j.cemconres.2020.106016.
- [6] C. Shi, D. Wang, L. Wu, Z. Wu, The hydration and microstructure of ultra high-strength concrete with cement-silica fume-slag binder, *Cem. Concr. Compos.* 61 (2015) 44-52. doi:10.1016/j.cemconcomp.2015.04.013.
- [7] N.Z. van Hierden, F. Gauvin, S.S. Lucas, T.A.M. Salet, H.J.H. Brouwers, Use of Hemp Fibres in 3D Printed Concrete, *Constr. Technol. Archit.* 1 (2022) 758-765. doi:10.4028/WWW.SCIENTIFIC.NET/CTA.1.758.

# ADDITIVE MANUFACTURING OF GLASS: TEST SETUPS TO DETERMINE THE COMPONENT STRENGTH WITH PHOTOELASTIC IN-SITU MEASUREMENTS

Philipp Amir Chhadeh

Kerstin Thiele

Maren Dietrich

Christin Lippold

Ulrich Knaack

Jens Schneider

Matthias Martin Seel

This work provides an overview of the existing processes for additive manufacturing of glass and discusses their applicability for the construction industry. A focus is placed on the possibility of additive manufacturing of glass on a base plate and the resulting substance-to-substance bond.

For load-bearing applications in the construction industry or in facades of buildings, knowledge about the component load-bearing capacity is fundamental. In order to investigate this load-bearing capacity experimentally, novel test setups adapted to additively manufactured components are necessary. In this work, the focus is on two test setups to determine the strength of an additively manufactured glass component.

The first setup focuses on the thermal stresses that are present during the printing process and the residual stresses that may remain in the glass product after cooling. Residual stresses that remain within the printed component can reduce the component strength extremely. In order to understand the residual stresses that result from additive manufacturing of glass on a base plate, the stresses due to base plate heating are examined in the tests discussed in this work. Temperatures during heating and cooling are recorded with the help of an infrared camera. Using photoelastic methods, the thermal and residual stresses can be examined. Here, the test setup, material properties of glass, and first results of the investigation of heating and cooling of a base plate using a gas torch are shown.

The second test setup discussed in this work focuses on the load transfer through a substance-to-substance bond of additively manufactured glass components. As the desired application is a load transferring component in facades, this test setup is of high interest as it gives first insights into the load capacity of a printed glass component.

## INTRODUCTION

Glass is a frequently used material in facades because of its many positive properties. In façade systems, mostly flat glass is used. To prevent failure of the glazing due to the brittle material behaviour, plastic is used to avoid hard contact, which can lead to breakage, or to secure and seal the distance between two panes of glass. Additive manufacturing of glass (AM Glass) has the potential to reduce the amount of sealants or adhesives used in building glass facades but also as load-bearing elements. Applications of AM Glass in the construction industry are discussed for example by Seel et al. [4].

In Figure 1 examples are shown how to replace conventional solutions by AM Glass. All these solutions are based on the idea to print glass on a standard flat glass that is usually used in facades, see Chhadeh et al. [9]. In Figure 1a, an AM Glass solution for point bearings is given. Instead of using conventional point bearing systems, a printed glass structure that is directly printed on the flat glass can be used to transfer the load into the load bearing system. In Figure 1b, an AM Glass solution for laminated safety glass is given. Instead of using more than 2 glass panes, the glass panes can be stiffened with AM Glass where necessary. Figure 1c shows an AM Glass solution for vacuum insulating glass panes. Conventionally, metal pillars are used to keep

the glass panes separated. The pillars could be replaced by glass printed directly on the flat glass. Figure 1d shows an AM Glass solution for standard insulating glass. Here, the sealants could be mostly replaced by printed glass. Advantages of the solutions in Figure 1 are higher transparency of the façade and new design possibilities, but also better performance, as sealants and adhesives can be saved, whose properties can change due to ageing.

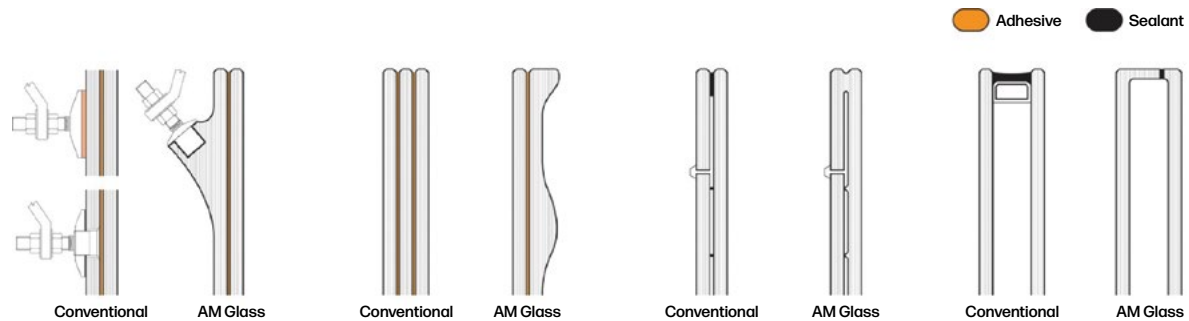


Figure 1: Examples for applications using AM glass [9] © Akerboom.

In order to print glass on flat glass, the base plate needs to be heated up locally to create a load-bearing connection between additive applied glass and the base plate. Several methods for additive manufacturing of glass are currently being researched, most of them capable of creating such a substance-to-substance bond. Table 1 summarises selected types of additive manufacturing of glass and provides information on selected properties relevant for the application in the construction industry. In the following each of the AM Glass processes given in Table 1 are discussed.

Table 1: Summary of types of additive manufacturing of glass and their relevant properties for application in the construction industry.

Institute or Company	Glass Type	Method	Scale	Substance-bond	References
NeptunLab /Karlsruhe Institute of Technology	Quartz Powder	Stereolithography	< 50 mm	No	[3]
Massachusetts Institute of Technology	Soda-lime silicate Nuggets	Fused Deposition modelling	300 mm	No	[1, 2]
Demcon, QSIL	Soda-lime silicate Rods	Fused Deposition modelling	50 mm	Yes	[7]
Technische Universität Ilmenau	Soda-lime silicate / Borosilicate Rods	Laser glass deposition (rods)	50 mm	Yes	[6]
Laser Zentrum Hannover e.V.	Borosilicate / Quartz Fibres	Laser glass deposition (fibres)	< 50 mm	Yes	[5]
Technische Universität Darmstadt Glass Competence Center	Soda-lime silicate / borosilicate Nuggets	Fused Deposition Modelling	300 mm	Yes	[8]



In 2015, Klein et al. [1] developed a glass 3D printer that deposits molten glass on top of each other, allowing free-form shapes to be created. A high surrounding temperature is necessary in this process for the deposited material to bond with the underlying layer. With the first version of their machine, only two axes, x and y, were implemented. In a further optimization of their machine, the authors added a rotation axis to the motion unit to improve the quality of the printed glass parts [2]. With a nozzle diameter of ten millimetres, the viscosity creates a kind of preferred direction for the print. Therefore, it has proven useful for MIT to always keep the print direction in line with the direction of motion. During cooling of the printed glass parts, residual stresses develop within the glass. To reduce these residual stresses after the printing process, the glass unit must be annealed, i.e., heated up to the annealing point. The annealing point is defined to the temperature where the glass composition has a viscosity of  $dPa\ s$ , which is low enough for stress relaxation but high enough to avoid deformations. Research on printing glass onto a glass plate and producing a substance-to-substance bond using this process is not known to the authors of this paper.

Kotz et al. [3] further advanced the traditional 3D-printing technology of stereolithography in order to additively manufacture glass. In the stereolithography process with glass, glass powder and a nanocomposite mixture are cured with a UV-light source. With this method, quartz glass objects can be produced. The shape of the objects can be controlled in detail by the stereolithography process and complex free-form shapes can be created. Through a heat treatment after the 3D printing process, a high quality is produced in strength and transparency or translucency. Research on printing glass onto a glass plate and producing a substance-to-substance bond using stereolithography is not known to the authors of this paper.

Witzendorff et al. [5] use a laser based process to print glass onto a glass base plate creating a substance-to-substance bond. Here through a conveyor, quartz glass fibres are fused onto a quartz glass plate with a laser and deposited on top of each other in the same principle. The base plate is heated by the laser to create a good bond. By controlling the intensity of the laser, different layer heights and wall thicknesses can be achieved. The diameter of the supplied quartz glass fibre also has an influence on possible printable geometries. After the printing process, the geometry is annealed in a postprocessing step to reduce residual stresses. This can be carried out to a complete extent, since the base plate and the fused-on material are the same type of glass and have the same thermal expansion coefficient. Fröhlich [6] upscales the laser process using glass rods as filament. The larger diameter of the borosilicate glass rods results in lower resolution, but also makes it possible to produce larger objects.

The glass manufacturer Qsil is using a glass 3D printer developed by the company Demcon, see [7]. In this device, soda-lime silicate glass rods are mechanically fed into an inductively heated nozzle. The base plate is heated by heat radiating from the heated nozzle. This allows the glass rod to fuse with the glass plate. To maintain the ambient temperature of the process, this printer uses an oven enclosure.

Seel et al. [4, 8] have undertaken preliminary investigations on fused glass deposition of glass onto a glass base plate at the Glass Competence Center (GCC) of the Technische Universität Darmstadt. Here, similar to the artisanal process used by glassblowers, the glass base plate is heated locally with a burner. In this way, the joining area between the base plate and the glass layer is expected to achieve a high quality. The quality of the connection between the face-connected glass rod and the heated glass plate was studied in [4]. The temperatures of the glass plate during fusion and post-processing in the form of annealing has been varied. This made it possible to achieve different qualities of substance-to-substance bond.

### Research objective

Before additively manufactured glass components can be used in facades, the properties of the printed elements must first be determined with regard to the partial safety concept, i.e. with regard to actions and resistances. The focus of this work is therefore the experimental investigation of the resistance of printed glass components. In this work, two experimental setups are introduced, each of which can be used to investigate an aspect that has a major influence on the load-bearing capacity of printed glass components: The level of residual stresses induced after the printing process and the shear transfer across the joining surface. These tests provide the basis for determining partial safety factors. The tests are developed using the printing process available at the TU Darmstadt according to Seel et al. [8]. However, it is possible to adapt the test setup to other printing processes.

Residual stresses are stresses that act in a body at a constant and homogeneous temperature without an external mechanical load being applied. During glass 3D printing on a glass plate, such residual stresses occur and remain in the glass after the glass component has cooled completely. Since glass is a brittle material, the strength of glass components is significantly affected by the micro defects on the glass surface. The residual stresses can, if compressive stresses act on the surfaces, increase the component load-bearing capacity by overpressing the microdefects, or, if tensile stresses act on the surfaces, reduce the component load-bearing capacity or even lead to spontaneous failure. The residual stresses depend mainly on the cooling curve, the temperature distribution, the thermal expansion coefficient, the viscoelastic material behaviour and thus the

viscosity. To investigate the residual stresses that arise, an experimental set-up was developed that makes it possible to observe the thermal stresses and the residual stresses in the compression process.

In order to investigate the printed components, a set-up is chosen in the second experiment to determine the load bearing capacity of the joining area or substance-to-substance bond. The objective is to introduce loads that shear off the added material of the glass base plate. With this the maximum shear stress acting in the joining area can be calculated. The mutual objective is to investigate the resistance of additively manufactured glass components. The overall load-bearing capacity of component and residual stresses as an indicator of reduced load-bearing capacity.

## MATERIAL BEHAVIOUR AND JOINING PROCESS

In the experiments performed in this work, soda-lime silicate glass according to DIN EN 572-1 [11] and borosilicate glass according to DIN EN 1748-1-1 [12] was used. Both glass types are typically used in civil engineering applications. Standard flat glass used for windows is made of soda-lime silicate glass. If special demands like fire or temperature resistance exist, borosilicate glass can be used.

For the production of printed elements, knowledge of the viscosity of the material is fundamental. In the case of glass, the temperature-dependent viscosity can be well described by the Vogel-Fulcher-Tamann equation according to DIN ISO 7884 - 1 [16]. The viscosities and some fixed viscosity points for soda-lime silicate glass and borosilicate glass are given in Table 2 and Figure 2. At higher viscosities than the defined viscosity called strain point, glass behaves linearly elastic and brittle. At lower viscosities than the strain point, glass behaves viscoelastically. At the strain point, mechanical stresses in the glass relax within a few hours, see Shelby [17]. At the annealing point, mechanical stresses in the glass relax after only a few minutes, see Shelby [17]. At the softening point, a glass bar already deforms under its own weight, and the working point defines the viscosity or glass temperature at which the glass is readily deformable, see Shelby [17]. The interval at which two glass bodies join well is shown in Figure 2 as the “area of joining viscosity”. For the shear tests, the viscosities of the glass are relevant, since they determine, in connection with the holding times, the size of the joining areas during specimen fabrication. The size of the joining area is a fundamental factor for the load-bearing capacity.

Table 2: Thermal expansion coefficient and defined viscosity points for soda-lime silicate and borosilicate glass.

Defined viscosity point	Symbol	Viscosities	Soda-lime silicate glass [18]	Borosilicate glass [19]
Working point	$T_w$	$10^4$ dPa·s	1030°C	1260°C
Softening point	$T_s$	$10^{7.6}$ dPa·s	725°C	825°C
Annealing point	$T_A$	$10^{13}$ dPa·s	550°C	560°C
Glass transition point	$T_G$	$10^{13.3}$ dPa·s	530°C	525°C
Strain point	$T_{sp}$	$10^{14.5}$ dPa·s	506°C	518°C

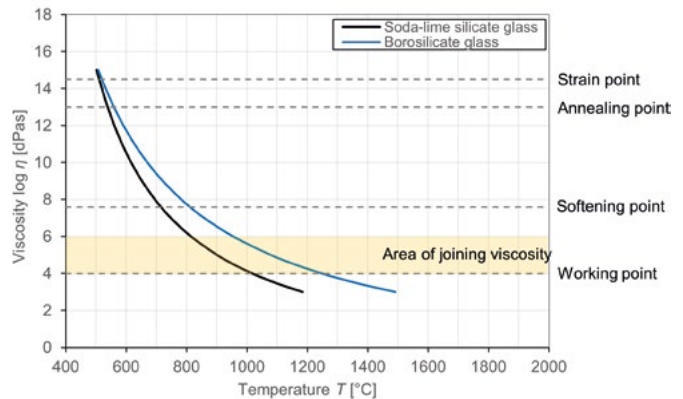


Figure 2: Temperature dependent viscosity of soda-lime silicate and borosilicate glass [18, 19] and the area of joining viscosity [20] © Seel

The viscoelastic material behaviour, which is linked to the viscosities, and the associated relaxation of mechanical stresses in the glass are an important factor influencing the development of residual stresses in the glass. Information on the constitutive material behaviour can be obtained for example from Carré et al [13]. Another reason for the development of residual stresses in glass are density changes in the glass, which depend on the cooling rate. The slower glass is cooled, the higher the density. Since the surfaces of a glass plate cool faster than the glass interior, the glass object may have a greater density at the surface than in the glass interior, depending on the time-temperature profile. In combination with stress relaxation at low viscosities, residual stresses develop in the glass. Works on determining the time-temperature profile include Choudhary et al [14] and Rantala [15].

The coefficient of thermal expansion is relevant for the specimen fabrication for the shear tests as well as an important aspect for the development of residual stresses for this work. The coefficient of thermal expansion depends on the glass composition. Borosilicate glass has a lower thermal expansion coefficient in the glassy state ( $K^{-1}$ ) than soda-lime silicate glass ( $K^{-1}$ ). However, even small changes in the glass composition, which are possible within the compositions according to DIN EN 572-1 [11] and DIN EN 1748-1-1 [12], can have a relevant influence on the specimen

preparation for the shear test. The thermal stresses in an isotropic material due to a sudden temperature change can be determined as follows, stated by Schiffner et al. [20]

$$(1) \quad \sigma_T = \frac{E \alpha_T \Delta T}{1 - \nu} B,$$

wherein  $E$  is the Young's modulus,  $\alpha_T$  is the thermal expansion coefficient,  $\Delta T$  is the temperature change,  $\nu$  is the Poisson's ratio and  $B$  is the geometric factor. The change in temperature during the cool down as well as heating process needs to be controlled to avoid high thermal stress.

If a body is not completely homogeneous, but there are small differences in the thermal expansion coefficients in the body, a permanent stress is created between these different zones in the body, which remains in the body even after cooling. In the case where the glass compositions of the glass plate and the glass applied to it are not identical, these stresses occur. The stresses can be calculated as follows:

$$(2) \quad \sigma_j = \frac{(\alpha_{AM} - \alpha_P) (T_G - T_{OP})}{\frac{1 - \nu_{AM}}{E_{AM}} + \frac{1 - \nu_P}{E_P}},$$

wherein  $\sigma_j$  is the stress in between areas of different thermal expansion coefficients,  $\alpha_{AM}$  is the thermal expansion coefficient of added glass,  $\alpha_P$  is the thermal expansion coefficient of the glass plate,  $T_G$  is the glass transition temperature,  $T_{OP}$  is the operating temperature,  $\nu_{AM}$  is the Poisson's ratio of added glass,  $\nu_P$  is the Poisson's ratio of the glass plate,  $E_{AM}$  is the Young's modulus of added glass and  $E_P$  is the Young's modulus of the glass plate. For the joining process, it is important to ensure that the glass compositions are the same, as the thermal expansion coefficients and Young's modulus can differ significantly between the different compositions of glass.

For the investigation of residual stresses, the coefficient of thermal expansion is important because the residual stresses depend on it, but also because the test performance depends on the coefficient of expansion and the resulting stresses. In order to implement residual stresses in the test specimens, they were locally heated with a burner. If the thermal stresses become too great, the test specimen fractures and the experiment is terminated. Since borosilicate glass has a lower coefficient of expansion, lower thermal stresses are generated and, with the same burner setting, the test specimen can withstand a longer heating time. The lower coefficient of expansion of borosilicate glass is positive for additive manufacturing of glass to a glass plate, as less glass breakage can be expected during manufacturing. However, the higher temperatures required to achieve the desired viscosity, compare Figure 2 or Table 2, are a disadvantage.

## OPTICAL EVALUATION METHODS

The developed experiments for the investigation of residual stresses and shear capacity are used to determine the resistance of a 3D printed glass component. The non-contact stress-optical methods as well as the methods of non-contact temperature measurement by means of an infrared camera, which were used to evaluate the experiments, are explained below.

### Photoelasticity

Glass is a birefringent material when mechanical stresses are applied. That is, local differences in principal stresses can be made visible in polarised light. This phenomenon is referred to as photoelasticity. Depending on the light source and the magnitude of principal stress difference, black and white patterns or coloured patterns indicate the magnitude of principal stress difference present within the glass component. During calibration of a specific test setup, a colour scale can be calibrated to enable the interpretation of the patterns observed.

The retardation of light observed in the experiments can be directly translated to a principal stress difference if some boundary conditions are met depending on the experimental setup, see [21, 22]. The boundary conditions are described below for the test setups used in this work. If all boundary conditions are met, Wertheim's law can be applied, see Equation (3).

$$(3) \quad s = C (\sigma_1 - \sigma_2) t,$$

wherein  $s$  is the retardation,  $C$  is the photoelastic constant which is a material property, and  $\sigma_1$  and  $\sigma_2$  are the first and second principal stress and  $t$  is the specimen thickness.

Photoelasticity is a frequently used method in the glass industry. For example, the quality of thermally tempered glass is easily controlled by use of so-called anisotropy scanners or a Scattered Light Polariscopes, see [23]. In this work, photoelasticity is used as an in-situ method to determine the stress state and its change over time in the experiments. During the tests to investigate the residual stresses, the aim of using photoelasticity is to visualise the thermal stresses during cooling and evaluate the residual stresses that remain in the glass specimen after the cooling process. The test setup used is shown in Figure 3 and described below. During the shear tests, the aim of using photoelasticity is to visualise the load transfer between the actuator and the support through the joining area between glass plate and added glass. The coloured patterns that become visible during the test, visualise the path of principal stress difference and where used to identify possible inhomogeneous joining zone. This could be indicated by a shift in the colour pattern. The setup used is shown in Figure 9 and explained below.

## Measurement of glass surface temperature

In the investigation of residual stresses in glass, in addition to photoelasticity, the glass surface temperature has been measured without contact using an infrared camera. As described above, the development of thermal stresses as well as residual stresses is strongly dependent on the temperature profile.

Glass is a semi-transparent material. That is, electromagnetic radiation depending on its wavelength on the glass temperature can pass the glass or not pass the glass. For instance, for electromagnetic waves with wavelength between 380 and 750 nm, which is visible to the human eye and, therefore, called visible light, glass is almost transparent. For temperature measurements in this work, an infrared camera *VarioCAM<sup>®</sup> HD head* [24] with a band filter transmitting radiation with wavelength of 8  $\mu\text{m}$  was used. Glass is opaque in this wavelength range and the glass surface temperature can be measured.

To evaluate the exact surface temperature from the data measured by the infrared camera, the emissivity coefficient of the measured surface needs to be known. The emissivity coefficient of a surface depends on the wavelength of incident radiation, the surface roughness, the surface temperature and the viewing angle. Detailed information on temperature measurement with infrared cameras and the evaluation of emissivity coefficient can be found in [25, 26]. In this work, the emissivity coefficient was determined by an easy test setup. The glass plates were heated within a kiln which was kept at the desired temperatures for at least half an hour. Then the kiln was opened and the temperatures of the glass plates were measured using the infrared camera. After this, the kiln was heated to the next higher desired temperatures. The emissivity coefficients were approximated by using the Software *Irbis<sup>®</sup> 3.1* [27] corresponding to the infrared camera. It was assumed that the temperature set at the kiln is identical to the surface temperatures of the glass plate. However, this is just an assumption leading to an overestimation of the temperatures measured and thus an underestimation of the emissivity coefficients. The determined emissivity coefficients are given in Table 3.

Table 3: Approximation of emissivity coefficients for soda-lime silicate glass and borosilicate glass at wavelength .

Temperature [°C]	Emissivity coefficient	
	Soda-lime silicate glass	Borosilicate glass
300	0.635	0.643
400	0.693	0.648
500	0.791	0.761
600	0.797	0.778
700	0.839	0.819
800	0.855	0.845

## RESIDUAL STRESSES

### Experimental investigation of residual stresses in glass after printing process

A test setup is developed to measure the glass temperature and the thermal stresses in the glass during heat treatment of the glass specimen. This is achieved via non-contact temperature measurement using an infrared camera and by using photoelasticity. After cooling of the glass, the residual stresses can be measured and correlated with the temperature-time course during the experiment. The temperatures generated during the experiment as well as the slow cooling rates can thus be recorded and correlated with the stresses. In these studies, two glass compositions were investigated: soda-lime silicate and borosilicate glass. Both types of glass were heated with a gas burner in such a way that a maximum temperature was reached for each glass composition without the specimen breaking due to the temperature load. The different coefficients of thermal expansion result in significantly different maximum temperatures for the glass compositions. In the following, the test setup, the specimens examined and the evaluation methods are described. Finally, the results are discussed.

### Test setup

The experiments are set up in such a way that the surface temperatures of the glass specimens can be recorded simultaneously by means of an infrared camera and the thermal stresses within the glass specimen by means of a standard camera using photoelasticity. In Figure 3, the test setup is shown schematically. The test setup was located within a laboratory and the experiments were conducted at an ambient temperature of approximately 20 °C.

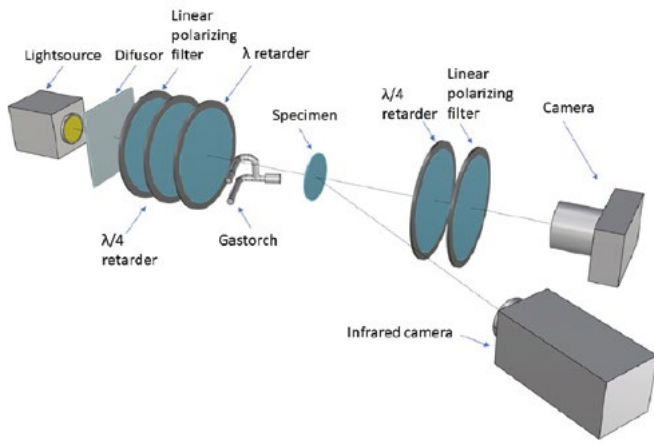


Figure 3: Experimental setup for investigation of residual stresses.  
© Chhadeh

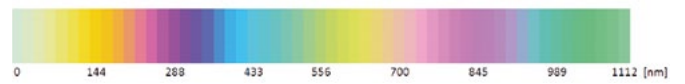


Figure 4: Calibrated colour scale for photoelastic setup shown in Figure 3. The observable colours in the experiments can be mapped to retardation using this colour scale. © Thiele

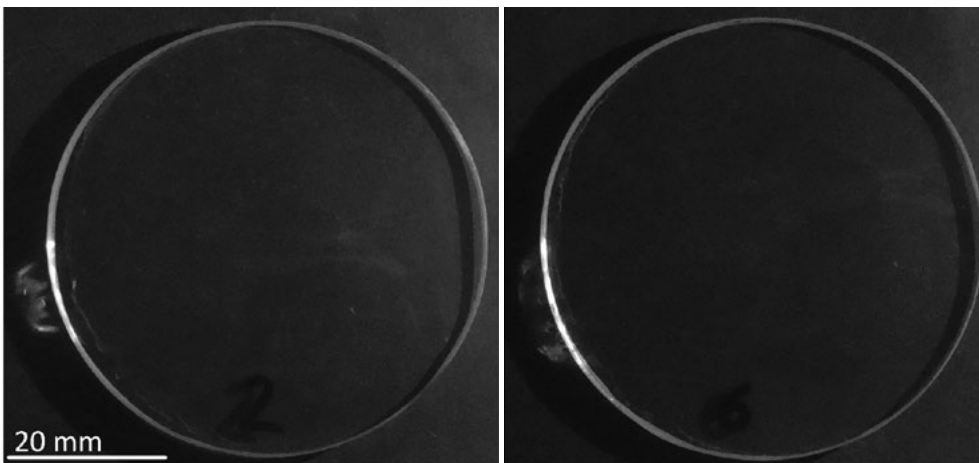


Figure 5: Glass plates with thickness 4 mm and diameter 69 mm used to investigate residual stresses. Left: soda-lime silicate glass specimen; right: borosilicate glass specimen. © Thiele

The test setup is arranged horizontally. This has the advantage that the heat-sensitive polarization filters and cameras are not exposed to waste heat from the gas burner. Furthermore, the horizontal setup allows easier installation of the test specimens, which were installed in a preheated clamp at about 300 °C glass temperature. The disadvantage of the horizontal test setup compared to a vertical setup is the natural convection, which results in an asymmetric temperature distribution. Since asymmetric temperature distribution also occurs via the specimen clamp, and focus was placed on the safe operation of the experiments, the tests were carried out horizontally.

For each experiment, the glass specimen was heated up homogeneously to 300 °C in an external kiln located close to the test setup. The specimen was transported and clamped into the test setup using heat protecting gloves. Then, the standard camera and infrared camera were started, and the specimen was heated locally by using a gas torch. The gas torch was applied manually. It was attempted to heat the specimen in its central point, but due to the manual process, small deviations occurred. Due to the low thermal conductivity of glass, only the centre of the specimen heats up, and the heat is poorly distributed throughout the specimen. If the temperature difference between the centre and the edge of a specimen is too high, the specimen will fracture due to the thermal load. The temperature difference leading to fracture depends on the coefficient of thermal expansion. For this reason, different heating times have been defined for soda-lime silicate glass and borosilicate glass to avoid thermal fracture at the same burner setting. When the defined heating time ended, the gas torch was removed. The specimen was cooled by natural convection.

To evaluate the surface temperature of glass, the data of the infrared camera was post processed using the Software *Irbis*<sup>®</sup> 3.1 [27]. First, the temperatures need to be corrected by applying the coefficient of emissivity of the glass surface. The coefficients applied are given in Table 3. However, as described above this approximation of the emissivity overestimates the temperatures. A new and more accurate measurement of the emissivity is necessary and part of future work.

The photoelastic setup was calibrated using a Babinet-Soleil Compensator, see [35]. For each setting of the Compensator, a photo was taken using the same camera and the same camera settings used during the experiments. This way, a colour scale was created that translates the rgb image made by the camera to the given retardation known from the Babinet-Soleil Compensator. The colour scale is given in Figure 4.

With the help of this colour scale, a value for the retardation can be assigned for each pixel of the photo during or after the test. If the course of the stresses is constant over the thickness, the difference of the principal stresses can be calculated with equation 3. In this experiment, the 4 mm thick

glass is heated from one side with the gas burner. Therefore, theoretically, there cannot be a constant stress profile. The simplifying assumption that there is a constant stress curve across the thickness of the glass can be made due to the small thickness of the glass specimen. The principal stress differences were evaluated using equation 3. The photoelastic constant is assumed to be 2.70 TPa<sup>-1</sup> for soda-lime silicate glass and 3.60 TPa<sup>-1</sup> for borosilicate glass.

### Specimens examined

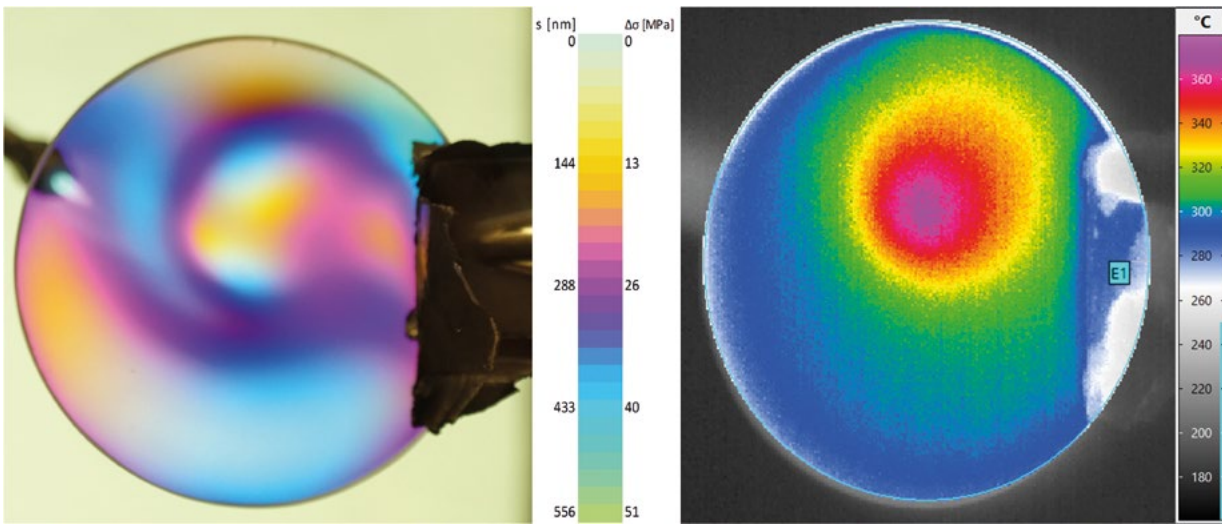
Soda-lime silicate glass plates as well as borosilicate glass plates were investigated. The circular glass plates had a diameter of 69 mm and a nominal glass thickness of 4 mm. The two types of specimens are shown in Figure 5. As discussed above, the lower thermal expansion coefficient of borosilicate glass leads to a longer heating time and therefore higher temperatures. Compared to soda-lime silicate glass, borosilicate glass can resist higher temperature gradients without fracture. Therefore a longer heating time using the same gas torch settings was possible for borosilicate glass. The soda-lime silicate glass specimens were heated by the gas torch for 10 seconds, the borosilicate glass specimens were heated for 60 seconds.

### Results

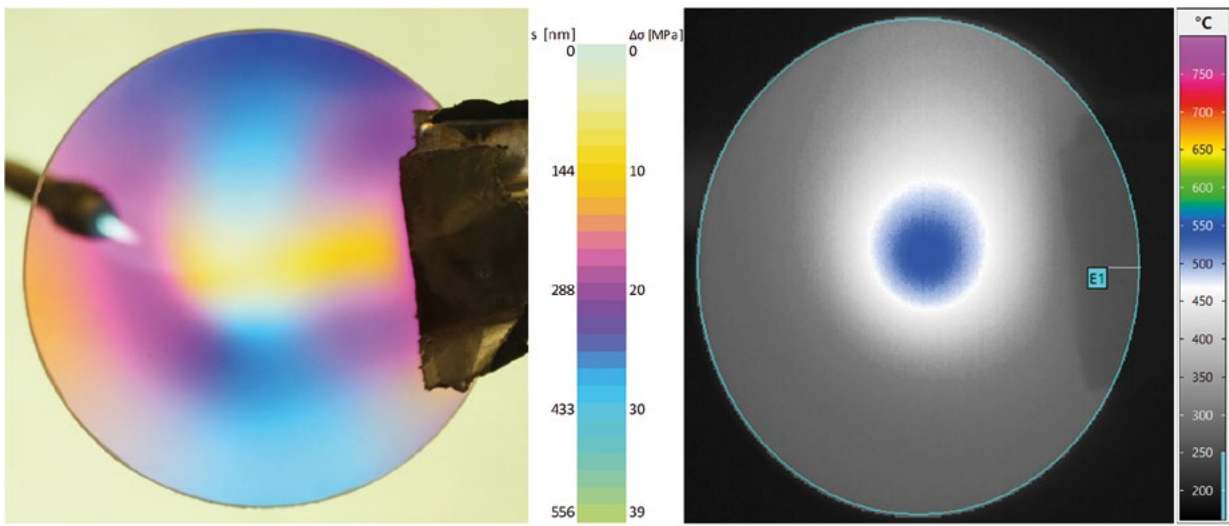
In the visual inspection, the borosilicate glass test specimens have shown significant deformation at the heated area. In some cases, the glass was seen to have melted slightly at the heated area. In the soda-lime silicate glass test specimens, significantly smaller deformations or no deformations were visible. For the sake of brevity of the article, the broken test specimens will not be discussed.

Figures 6 and 7 show the photoelastic images on the left and the thermogram on the right. The two images per figure were taken at the same time. Of the 7 experiments performed with soda-lime silicate glass and borosilicate glass each, only the experiments which reached the highest temperature are shown here. The comparison of the 7 tests each showed similar results and a discussion of all the tests would exceed the scope of this article.

Figure 6 shows the results of the soda-lime silicate glass test at  $t = 10$  s, i.e. at the time when the gas torch heating ended. At this time, the specimen has reached the maximum temperature in the test and is then cooled down again by natural convection. In the photoelastic image, one can see retardations up to a blue, which corresponds to approximately 390 nm in this setup. Using equation 3 a retardation of 390 nm corresponds to a principal stress difference of 35 MPa. From Figure 6 can be seen that the heated area shows little principal stress differences. The glass temperature in this region is about 365 °C, which is below the glass transition temperature. The glass behaves linearly elastic

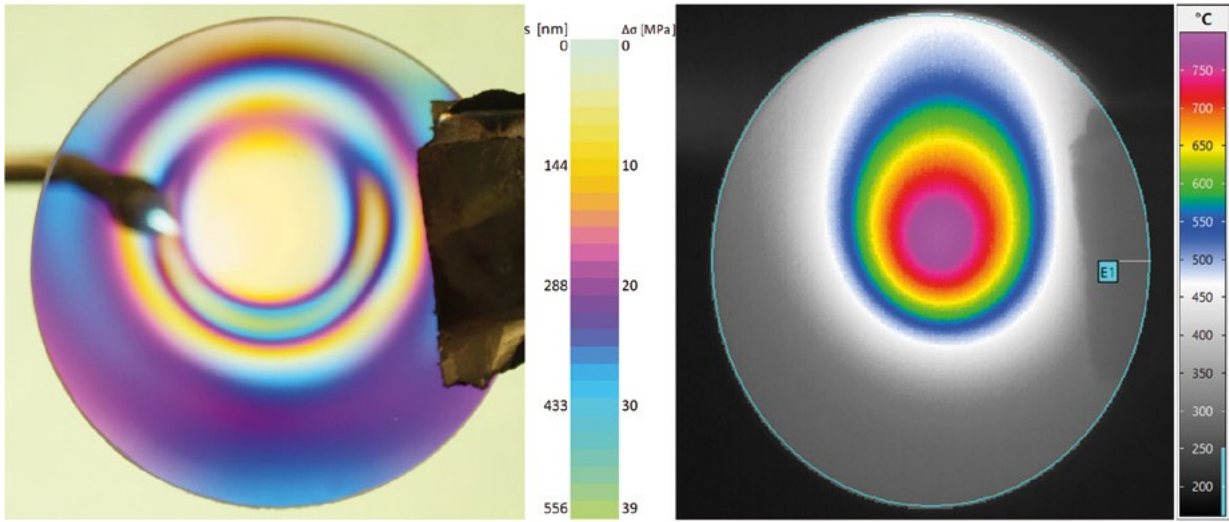


a)  
 Figure 6: Soda-lime silicate glass plate with a diameter of 69 mm heated with a gas torch: a) Thermal stresses at  $t = 10$  s (© Dietrich, Lippold) and b) temperatures at  $t = 10$  s. (© Thiele)



a)

b)



c)

d)

Figure 7: Borosilicate glass plate with a diameter of 69 mm heated with a gas torch: a) Thermal stresses at  $t = 10$  s (© Dietrich, Lippold) and b) temperatures at  $t = 10$  s (© Thiele), c) thermal stresses at  $t = 60$  s (© Dietrich, Lippold) and d) temperatures at  $t = 60$  s (© Thiele).



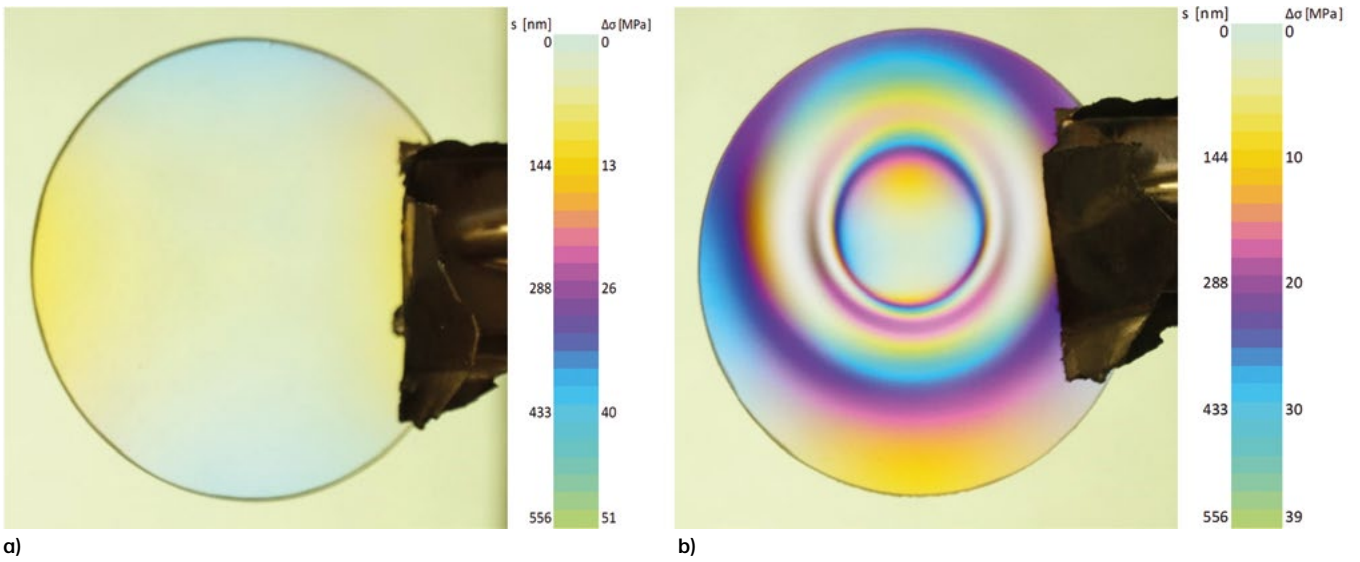


Figure 8: Residual stresses within the specimens after cooling down to room temperature: a) soda-lime silicate glass and b) borosilicate glass. ©Dietrich, Lippold

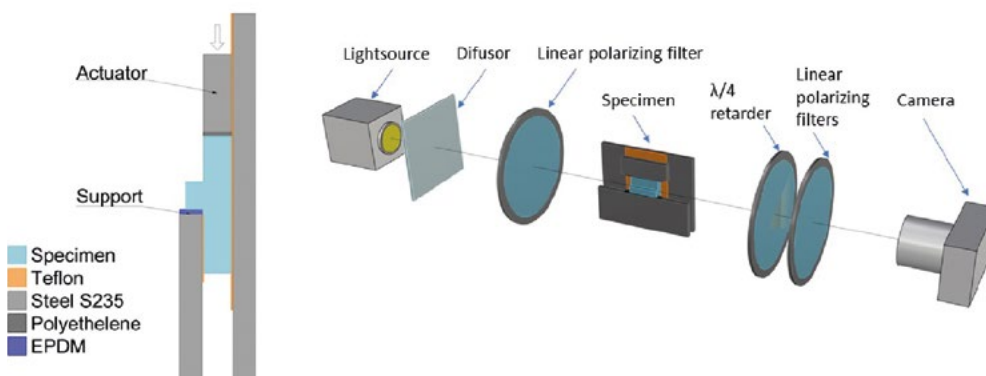


Figure 9: Experimental setup of the shear test © Chhadeh

in this temperature region. Within the heated region, the temperatures are homogeneous and the glass expands homogeneously. This expansion is prevented by the colder edge. In the photoelastic image, a dark colored ring can be seen around the heated area, indicating that high principal stress differences are present. Thermal stresses are present here due to the temperature gradient between the heated area and the remaining area and the corresponding thermal expansion.

Figure 7 shows the results of the investigation of borosilicate glass at the times  $t = 10$  s and  $t = 60$  s. Compared to the tests with soda-lime silicate glass, borosilicate glass shows significantly smaller retardations in the photoelastic image after  $t = 10$  s, although the temperature in the heated region is about  $535$  °C instead of about  $365$  °C. As mentioned above, borosilicate glass has a lower thermal expansion coefficient. Therefore the heated area has a lower thermal expansion compared to the heated area of soda-lime silicate glass. As a result, the resulting stresses are smaller. Due to the larger photoelastic constant, the retardations are smaller. Around the heated area, a maximum principal stress difference of approx.  $25$  MPa is present. The results of the tests with borosilicate glass at  $t = 60$  s are shown in Figure 7c) and d). Glass temperature in this experiment reached a maximum of about  $765$  °C, where the glass behaves viscoelastic. Again, in the photoelastic image, the heated area shows small retardations surrounded by higher retardations. Due to the longer duration of the experiment, the heated area is larger compared to the areas observable at  $10$  s. The largest principal stress difference here is around  $35$  MPa.

Figure 8 shows the residual stresses after cooling to room temperature for the two glass plates discussed. The soda-lime silicate glass plate shows almost no retardations whereas the borosilicate glass plate shows a significant pattern. For residual stresses to form in the glass, the glass must have a temperature above its glass transition temperature before cooling. The residual stresses that form depend on the viscoelastic properties, the cooling rate, the coefficient of thermal expansion and temperature-dependent structural changes in the glass. The soda-lime silicate glass plates could not be heated with the gas torch locally above strain point in this setup, which is roughly around  $506$  °C, without fracture. Therefore no residual stresses could be created using this test setup. But using borosilicate glass, which has a lower thermal expansion coefficient and therefore lower thermal stresses during the experiment, residual stresses could be created. This is due to the higher temperatures reached.

## SHEAR TESTS

### Experimental investigation of the load-bearing capacity of the joining area

A shear test to examine the strength of the substance-to-substance bond between added glass and base plate is conducted. In the following section, the setup of the experiment will be explained. Afterwards the production of specimens and in the end the monitoring concept is explained as well as a discussion of the results.

#### Test setup

Figure 9 illustrates the experimental setup. In the left part of the figure, a schematic drawing of the cross section of the shear test is given. The specimen is placed between two steel plates and supported on one surface of the added fused glass. Here, a two mm thick ethylene propylene diene monomer (EPDM) between the supported surface of the added glass and the steel support is located to reduce stress concentrations at the contact areas. For the same reason, a polyethylene interlayer (thickness  $2$  mm) was used between the specimen and the actuator. To allow the glass specimen to slide freely in the vertical direction between the two steel plates, a low-friction support is created through a layer of Teflon between the vertical steel plates and the specimen. The load speed was selected to  $30$  N/s which translates to  $0.2$  MPa/s mean shear stress according to Equation 4.

In the right panel of Figure 9, a schematic sketch of the photoelastic test setup is given. In comparison to the photoelastic test setup described above, no full wavelength retardation plate was used. Therefore, a different colour scale compared to the setup described above applies to this test setup. The setup was not calibrated but as reference, the interference colour chart by Michel-Levy [28] can be used since the colour sequence is similar.

#### Specimen production

In a study at the GCC, tests with yellow borosilicate glass rods and clear borosilicate glass plates have been conducted to examine the substance-to-substance bond fused glass. The glass rod was placed flat on a glass plate and heated in an oven. The joining areas after different oven temperatures were studied. The heating rate of the oven was selected to  $14$  K/min in all experiments. Then, the temperature was kept constant for  $30$  minutes and then cooled down by natural convection inside the oven without opening the door. Initially, the cooling rate is around  $1.5$  K/min at temperatures higher than  $600$  °C, then drops to  $1$  K/min during  $400$  °C to  $600$  °C and finally, the cooling rate stays around

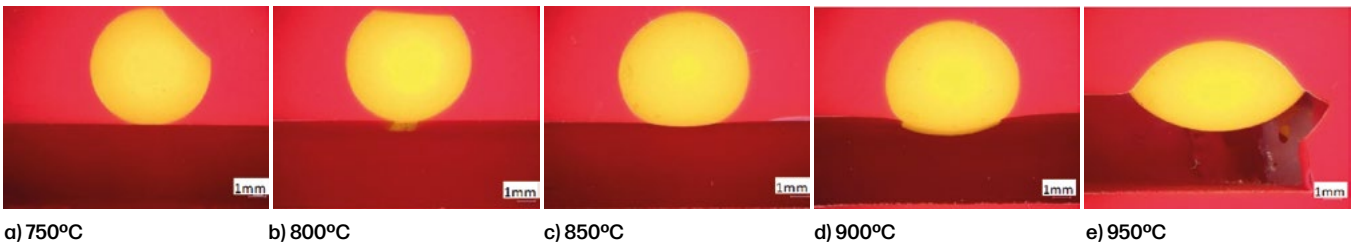


Figure 10: (a)-(e) Preliminary studies on joining Borosilicate rods with glass plates using different set oven temperatures © Seel

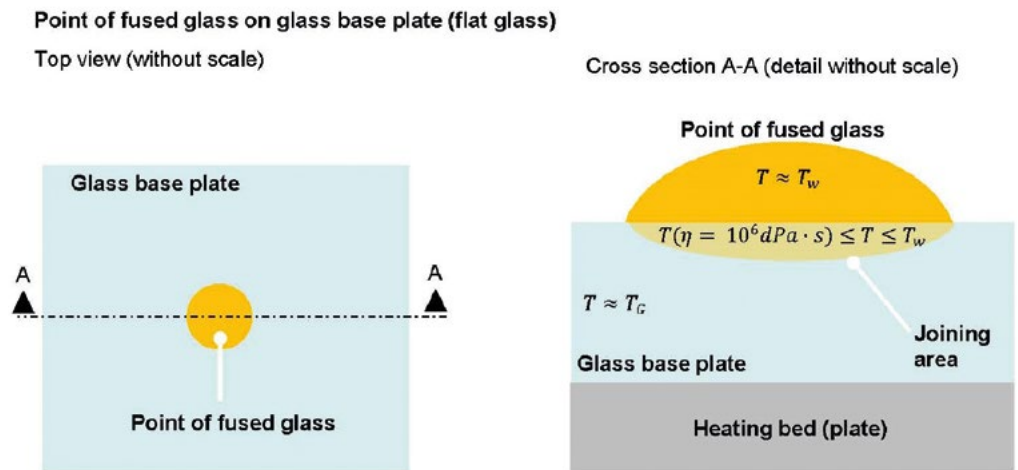


Figure 11: Joining area defining the substance-to-substance bond. © Seel

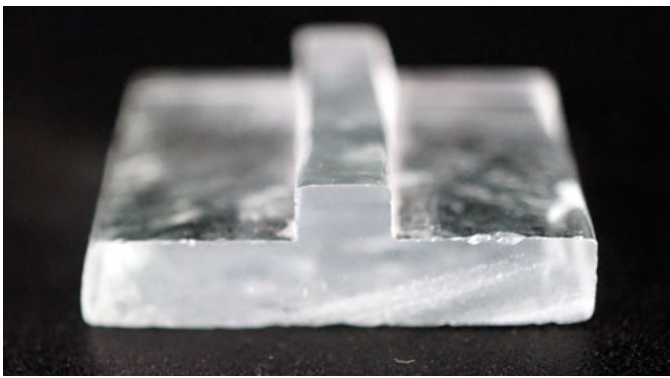


Figure 12: Specimen for experimental tests to investigate under shear loading © Chhadeh.

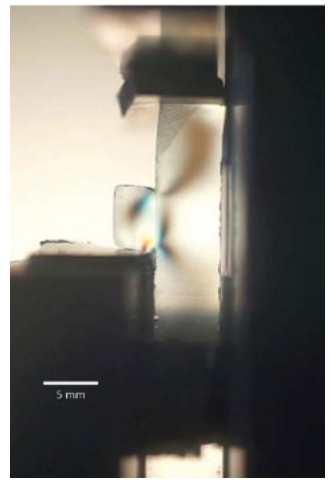


Figure 13: Difference in principal stresses in the specimen under polarised light while loading © Chhadeh.

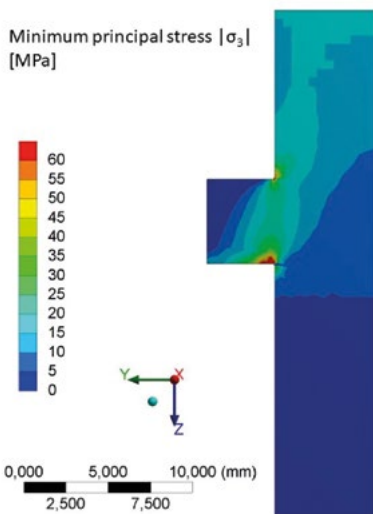


Figure 14: Minimum principal stress in the numerical model © Chhadeh

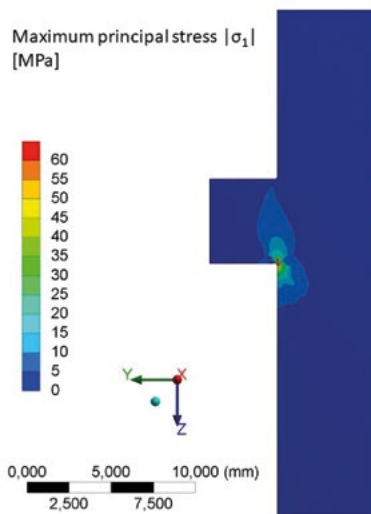


Figure 15: Maximum principal stresses in the numerical model © Chhadeh.

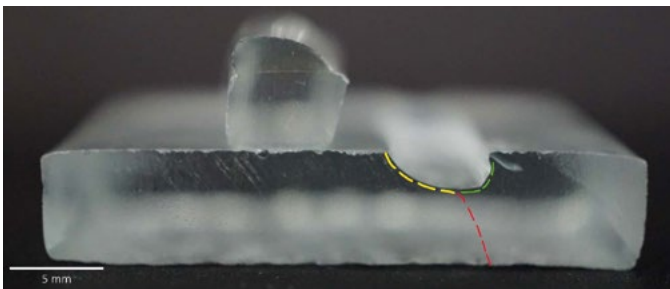


Figure 16: Cracked specimen after shear loading © Chhadeh.

0.5 K/min. Figure 10 shows an overview of the test results. Due to the colouring of the glass rods the interface of the joint can be observed. Below softening point temperatures of the rods (800°C), no bonding between glass rod and glass plate occurred. For oven temperatures above the softening point, the rod fuses to the glass plate. An increase in temperature leads to a larger contact area and more homogeneous bond due to the low viscosity.

An issue of this method is the geometric problem of placing a round object on a plate. Sharp contact angles are the result as shown in Figure 10 (c) and (d). The higher the oven temperature, the flatter the angle at the contact point. Keeping the application of load transferring components in mind, the sharp contact angles will lead to stress concentration and therefore low load bearing capacity of the component.

In Figure 10e, the glass rod has the largest area of contact. Showing that the joint is better as closer the joining temperatures gets to the working point of glass, see Table 2. The disadvantage of this is the decreasing height of the rod, which limits the application. Increasing the temperature of the glass plate and the rod towards the working point will lead to a complete fuse of rod and glass. This also leads to the glass plate losing its rectangular shape, resulting in the surfaces of the glass plate to corrugate and to be non-parallel to each other.

In Figure 2, the joining viscosities are shown. For the application of fusing glass and layering it, it is advisable to reach the joining viscosity directly at the contact area between glass plate and added glass as shown in Figure 11.

To develop a shear test setup soda-lime silicate glass specimens without a sharp contact angle were desired. For this purpose, the glass rod is substituted with a strip of a float glass plate, cut from the base plate. The joining procedure of stacking the strip on top of the plate and heating in the oven is the same as mentioned above.

In the following, temperatures refer to oven temperatures. The soda-lime silicate glass specimens were heated to 750°C for 0.5 hours, using a heating rate of 5K/min and an average cooling rate of 0.8 K/min. The added glass strip has the dimension of 6x4 mm in the cross-section, the base plate 30 x 6 mm in the cross-section. The temperature of 750°C was chosen to have a glass viscosity below the softening point. The 250 mm long specimen was then cut into nine pieces with an average length of 25 mm. The nominal joining area is 150 mm<sup>2</sup>, derived from the width of 25 mm and height of 6 mm on average.

A joining temperature of 750 °C is used below the minimum joining temperature settings based of Figure 11 and Figure 2 as a benchmark test for future printed specimen with soda-lime silicate glass, trying to set minimal achievable bond strength. Figure 12 shows a specimen made by this process.

## Results and Evaluation

The experiment is based on the idea of shearing off the added material. For this purpose, the test specimens presented above are loaded and monitored in parallel by a video recording with polarised light, as shown in Figure 9.

To evaluate the results of this experiment, the applied force can be divided by the joining area to calculate the mean shear stress before cracking, shown in Equation 4. Where  $\tau$  is the mean shear stress [MPa],  $F$  is the applied force [N] by the actuator and  $A_j$  is the joining area.

$$(4) \quad \tau = \frac{F}{A_j}$$

The eccentric loading also creates a bending moment, which increases with the thickness of the glass base plate. Using Equation 5, the bending stress can be calculated and used to evaluate the joining quality. Here  $\sigma_B$  is the bending stress in the component [MPa],  $M$  is the bending moment [Nmm],  $I_j$  stands for the moment of inertia of the joining area [mm<sup>4</sup>], described by  $h_j$  as the height of the joining area [mm],  $w_j$  the width of the joining area [mm] and  $t_{plate}$  as the thickness of the glass plate [mm]. [29]

$$(5) \quad \sigma_B = \frac{M}{2 I_j} h_j = \frac{F \frac{t_{plate}}{2}}{\frac{w_j h_j^3}{12} 2} \times h_j = \frac{3 F t_{plate}}{w_j h_j^2}$$

Both equation 4 and equation 5 consider only the average stress states in the component. Stress concentrations that develop in the contact area cannot be taken into account. The general statement about the average stress state is still suitable for evaluating the joining quality. The occurrence of failure, however, is predominantly determined by the stress concentration, which is correlated to the average stress state.

Figure 13 is an image taken by the above-mentioned camera with the photoelastic setup shown in Figure 9 during load-testing the specimen. To evaluate the test a numerical model using Ansys workbench 2019 R2 [30] was utilised for a comparison. In Figure 14 the absolute values of the minimum principal stresses and Figure 15 the absolute values of the maximum principal stresses are shown.

The stress state in this experiment can be assumed to be constant in the specimen in the direction of the light path. Therefore Wertheims law given in Equation 1 can be applied to determine the principal stress differences. Nevertheless, for the preliminary tests this evaluation was not conducted. Instead, the focus was placed on the evaluation of the colour pattern along the joining zone. A shift in the color pattern would indicate an inhomogeneous joining zone.

Based on the knowledge that there can be no principal stresses in the Y-direction at the free edge, an approach can be made to evaluate the isochromats. In photoelastic

images, the colour change shows that the difference between maximum and minimum principal stress increases. By understanding the mechanics of the experiment and confirming it with the FE results, the difference in the principal stresses increases towards the load input and focuses towards the edges of the added glass strip.

It can also be seen that a load path is formed from the area near the edge of the support to the centre of the load input in Figure 13. Due to the eccentric load application and the thereby induced rotation of the specimen, it can be concluded that the maximum principal tensile stresses are formed in the joining area close to the supported surface. Equation (4) gives an assumption to calculate these bending stresses.

The issue at hand is the stress-convergence at the sharp angle between the fused glass strip and glass base plate. At this point, a stress concentration occurs and leads to failure. To avoid this issue the specimen in further experiments should have rounded corners.

Figure 16 shows a specimen that has undergone the shear test. Cracks follow the path offering the smallest resistance against propagation. Based on the fracture pattern, the crack develops in the area of the notches on the supported side, indicated by the yellow dashed line. In some specimens, the crack then develops through the base plate (red), or, as shown in Figure 16, to the opposite edge of the joint area (green). The fracture mirror was not traceable in the specimens, but the Wallner Lines indicate this crack development behaviour.

Due to the biaxial stress, a mixed failure of mode I and II occurs. Looking at the theory of crack propagation, the initial crack kinks about approximately  $70^\circ$  from the glass pane surface. The experiment is in accordance with the theory described by Erdogan [31], after crack initiation, the cracks always change their direction so that their mode I component attains a maximum. In this case, either through the plate or towards the other notch in a perpendicular direction to the maximum tensile component. In their research on crack growth under combined mode I and mode II loading, Singh [36] state a factor of 0.84 for  $K_{Ic} / K_{IIc}$ . This means that although a mode II failure is induced by the loading, due to the fracture toughness  $K_{Ic}$  being lower than  $K_{IIc}$ , the crack propagation in mode I is being favoured.

Table 4: tests results in form of calculated shear and bending stress

	Minimum value [MPa]	Maximum value [MPa]	Mean value [MPa]	Standard-deviation	Coefficient of variation
Mean shear stress	4	20	10	5.3	0.55
Bending stress	10	59	29	16.9	0.57

In Table 4 the results of the testing of nine specimens are summarised. The mean value at failure of the mean shear stress amounts to 10 MPa based on Equation 4. The result in mean bending stress at failure is 29 MPa calculated by Equation 5. In order to simplify the calculations, only the cross-section of the nominal joining areas were used for Equations 4 and 5. Due to the low amount of specimens and high standard deviation, no characteristic strength values are determined.

There can be several reasons for the scatter of the values. The low fusing temperature during specimen production could lead to inconsistencies in the joining areas. The added glass strips are not perfectly parallel to the edge of the base plate resulting in a stress concentration on one of the corners. Also, the process step of sawing the specimen in parts and polishing them can lead to microscopic fractures.

As a reference, the typical bending stress at failure of annealed soda-lime silicate glass is at 45 MPa with a coefficient of variation of 0.3, see [ (Schneider, et al. 2016)]. A comparison with this value at this point is of limited use. A comparison would have to be made with the edge strength. The edge strength is calculated with a reduction factor of 0.8.

At this early stage, the goal of the research is to determine if it is possible to achieve a strength that could be suitable for applications in the construction industry. One possible application for additively manufactured glass components is brackets, where the thrust would be primarily transferred to the base plate. For a staircase, the example can be calculated as follows: Assuming that the steps are 1.20 m wide and 0.3 m deep, the dead weight of a triple laminate is calculated to be 25 kg. With an ideal live load of 300 kg, consisting of individual and surface loads, the total weight per side is calculated to be 162.5 kg, or 1500 N, which must be supported by each side.

Taking the minimum experimentally determined mean shear stress of 4 MPa, a joining area of 375 mm<sup>2</sup> would be required on each side to support a stair tread under loading. The requirements for process optimization and process scaling can be achieved in the near future through AM Glass, which makes it a feasible application in the building industry.

## CONCLUSION

The two experiments described are concerned with testing the quality of additively manufactured glass structures that are defined by deposition of glass on a glass base plate. For the application of additively manufactured glass components in the construction industry, knowledge about the load-bearing capacity of these components plays a decisive role. They may form a basis on which a safety concept for application of additive manufactured glass components in construction can be developed. As glass is a brittle material this is not an easy task.

Knowledge of the residual stresses generated in the process provides information about any annealing process that may be required and how to monitor it. The shear tests carried out, on the other hand, provide a direct indication of the load-bearing capacity of the components.

The experiments to investigate the residual stresses have shown that the simultaneous measurement of the surface temperature and the thermal stresses that develop during the experiment is possible. The temperature distributions and stress states are comprehensible. Within the heated area the stress state is relatively homogenous. The locally heated area is surrounded by a colder edge that prevents the expansion of the heated area. In the photoelastic images this can be seen by a ring of higher retardation surrounding the heated area. After cooling down, residual stresses can be observed in borosilicate glass specimens only. These specimens have reached a temperature higher than glass transition point. For the development of residual stresses in the glass, the exceeding of the strain point is important. At temperatures below the strain point, the glass behaves linearly elastic. If a glass is not heated beyond this point, residual stresses do not arise. Only at temperatures above the strain point does glass behave viscoelastically, which is a major factor in the development of residual stresses. Further research will be done to optimise the photoelastic setup. By choosing the polarisation filters and retardation plates, the colour patterns in the experiment can be adjusted. For more reliable temperature measurements, the emissivity coefficient needs to be studied in more detail.

For future investigations, the temperature measurement should serve as information for the numerical simulation. The aim is to compare the thermal stresses from the test with the numerical simulation and thus to validate the numerical simulation and the material assumptions made in it. Moreover, the temperature measurement on glass is to be adapted for the investigation of the individual process steps in fused glass deposition modelling process. For a systematic investigation of various influencing parameters, such as the glass thickness, further investigations are to be carried out by means of design of experiment.

The shear test served to determine whether and how much load can be transferred through a fused glass bond.

With polarised light, load transfer path and stress concentration can be qualitatively monitored and matched with FE calculations. Thus allowing the determination of the quality of the joint.

In the future the shear test can be used as a benchmark test to compare different additive manufacturing process settings for their capability of load transfer. The high standard deviation in the experimental results originates on the one hand in the brittle behaviour of glass, but also from the manufacturing of the specimen. The tested specimens have a slight angle deviation leading between base plate edge and fused glass strip leading to higher stress concentrations.

In general, this test has been sufficient to qualify the experimental setup and illustrate the stress distributions in a specimen. It is necessary to consider the above-mentioned challenges in order to improve the methodology of the experiment.

Other options to investigate the joint areas and the AM Glass objects are indentation tests (e.g. Vickers), bending tests in different directions of the fused glass strips and further optical examination under a microscope of the joining area and the fracture behaviours.

The aim of future research is to describe the correlation between the process of fused glass deposition modelling, the temperature measurements during the process and the achievable load transfer. For this purpose, a parameter study will be conducted. These are then to be evaluated with so-called benchmark tests, such as the shear test. In addition to the optical evaluation for quality and anisotropies of the specimens, bending tensile tests are also necessary to characterise the additive manufactured components. The tests can be fundamental for a safety concept for AM Glass in the building industry.

## ACKNOWLEDGEMENTS

The authors like to thank Dariusz Laniewski for his contribution to this work. This work was funded by Deutsche Forschungsgemeinschaft (DFG, German Research Foundation) under grant no. 439726461.

## REFERENCES

- [1] J. Klein, M. Stern, G. Franchin, M. Kayser, C. Inamura, S. Dave, J. C. Weaver, P. Houk, P. Colombo, N. Oxman and M. Yang, "Additive Manufacturing of Optically Transparent Glass," *3D Printing and Additive Manufacturing 2 (3)*, pp. 92-105, 2015.
- [2] C. Inamura, M. Stern, P. Lizardo, N. Oxman and P. Houk, "Additive Manufacturing of Transparent Glass Structures," *3D Printing and Additive Manufacturing 5 (4)*, pp. 269-284, 2018.
- [3] F. Kotz, K. Arnold, W. Bauer, D. Schild, N. Keller, K. Sachsenheimer, T. Nargang, C. Richter, D. Helmer and B. Rapp, "Three-dimensional printing of transparent fused silica glass," *Nature 544*, pp. 337-339, 2017.
- [4] M. M. Seel, R. Akerboom, U. Knaack, M. Oechsner, P. Hof and J. Schneider, "Fused glass deposition modelling for applications in the built environment," *Materialwiss. Werkstofftechn.*, vol. 49, pp. 870-880, 2018.
- [5] P. v. Witzendorff, L. Pohl, O. Suttmann, P. Heinrich, A. Heinrich, J. Zander, H. Bragard and S. Kaierle, "Additive manufacturing of glass: CO<sub>2</sub>-Laser glass deposition printing," *Procedia CIRP 74*, pp. 272-275, 2018.
- [6] F. Fröhlich, J. Hildebrand "Herstellung individueller Strukturen aus silikatischen Werkstoffen mittels Wire-Laser Additive Manufacturing," *ce/papers*, vol. 4, pp. 181-191, 2021.
- [7] Demcon, 17 08 2021. [Online]. Available: <https://demcon.com/>.
- [8] M. Seel, R. Akerboom, U. Knaack, M. Oechsner, P. Hof and J. Schneider, "Additive Manufacturing of Glass Components - Exploring the Potential of Glass Connections by Fused Deposition Modeling," *Challenging Glass 6*, 2018.
- [9] P. A. Chhadeh, M. Seel, R. Akerboom "Additive Manufacturing of glass," in *Print Architecture*, Baunach, AADR - Art, Architecture and Design Research, 2022, pp. 92-95.
- [10] J. Schneider, J. Kuntsche, S. Schula, F. Schneider and J. Wörner, *Glasbau, Grundlagen · Berechnung · Konstruktion*. 2. Auflage, Berlin, Heidelberg: Springer Vieweg, 2016.
- [11] DIN EN 572-1, *Glas im Bauwesen - Basiserzeugnisse aus Kalk-Natronsilikatglas - Teil 1: Definition und allgemeine physikalische und mechanische Eigenschaften*, 2011.
- [12] DIN EN 1748-1-1, *Glas im Bauwesen - Spezielle Basiserzeugnisse - Borosilicatgläser - Teil 1: Definitionen und allgemeine physikalische und mechanische Eigenschaften*, 2004.
- [13] H. Carré and L. Daudeville, "Numerical Simulation of Soda-Lime Silicate Glass," *JOURNAL DE PHYSIQUE IV*, 01 1996.
- [14] M. Choudhary, B. Purnode, A. Lankhorst and A. Habraken, "Radiative heat transfer in processing of glass-forming melts," *International Journal of Applied Glass Science*, 07 2017.
- [15] M. Rantala, *Heat Transfer Phenomena in Float Glass Heat Treatment*, Tampere University of Technology, 2015.
- [16] DIN ISO 7884 - 1, *Glas - Viskosität und viskosimetrische Festpunkte - Teil 1: Grundlagen für die Bestimmung der Viskosität und der viskosimetrischen Festpunkte*, 1998.
- [17] J. Shelby, *Introduction to glass science and technology*, Cambridge: Royal Society of Chemistry, 2005.
- [18] D. Öksoy, L. Pye and E. Boulo, Statistical analysis of viscositycomposition data in glassmaking, 1994: *Glastechnische Berichte* Bd. 67.7, pp. 189-195.
- [19] Schott Glas, "Schott: Borofloat®33. Datasheet," [Online]. Available: <http://www.schott.com/borofloat/german/download/index.html>. [Accessed 17 08 2021].
- [20] U. Schiffner, A. Langer, M. Seibold, G. Wagner, R. Hüther and K. Bröring, in *Fügen von Glas*, Hüttenteschnische Vereinigung der deutschen Glasindustrie, 1995.
- [21] H. Aben and C. Guillemet, *Photoelasticity of Glass*, 1993.
- [22] M. Kufner, in *Spannungsoptische Modellversuche und Dehnungsmessungen am Bauwerk*, Verlag von Wilhelm Ernst & Sohn Berlin München, 1968.
- [23] S. Dix, C. Schuler and S. Kolling, "Digital full-field photoelasticity of tempered architectural glass: A review," *Optics and Lasers in Engineering*, vol. 153, 2022.
- [24] Infratec GmbH, *User Manual VarioCAM HD head Stationary Thermal Imaging Camera*, Dresden, 2021.
- [25] F. Bernhard, *Technische Temperaturmessung*, Berlin, Heidelberg: Springer Berlin Heidelberg, 2004.
- [26] VDI/VDE 3511, *Temperature Measurement in Industry*, 1996.
- [27] Infratec GmbH, *User Manual IRBIS 3.1 Infrared Thermographic Software*, Dresden, 2022.
- [28] Carl Zeiss AG, "Michel-Levy color chart," [Online]. Available: <https://www.zeiss.com.sg/microscopy/local-content/campaign-landingpages/2022/2022-q1/doi-dec/poster-zeiss-michel-levy-color-poster.html>. [Accessed 01 2023].
- [29] D. Gross, W. Hauger, J. Schröder and W. A. Wall, *Technische Mechanik 2 (12)*, Springer Vieweg, Berlin, Heidelberg, 2014.
- [30] Ansys, Inc., "Ansys Workbench 2019 R2 Statisch-mechanische-Analyse".
- [31] F. a. S. G. C. Erdogan, "On the Crack Extension in Plates Under Plane Loading and Transverse Shear," *ASME. J. Basic Eng.*, vol. 85(4), pp. 519-525, 1963.
- [32] J. Luo, H. Pan and E. Kinzel, "Additive Manufacturing of Glass," *Journal of Manufacturing Science and Engineering 136 (6)*, 2014.
- [33] J. Schneider, J. Kuntsche, S. Schula, F. Schneider and J.-D. Wörner, *Glasbau: Grundlagen, Berechnung, Konstruktion*, 2016.
- [34] QSIL GmbH, "QSIL: Materialspezifikation Quarzglas ilmsil PN. Datasheet," 2013.
- [35] Karl Lambrecht Corporation, "Babinet Soleil Compensator" [Online]. Available: <https://www.klccgo.com/bsc.htm>. [Accessed 04 2023].
- [36] D. Singh, K. Shetty "Subcritical Crack Growth in Soda-Lime Glass in Combined Mode I and Mode II Loading", *Journal of the American Ceramic Society* 1990



# SOLAR-SINTERING WITH IN-SITU MATERIAL

Marvin Kehl  
Tom Finger

Hard-to-reach areas on Earth or other celestial bodies are of high scientific interest. The safety of people on-site however, is difficult to guarantee. Providing habitats to protect against extreme weather events, radiation, etc. can be very expensive and may even become impossible due to limitations in the transportation of essential resources. Further, the research team is unprotected during the assembly of shelters, which is an additional safety risk. To reduce the risk of the team and transportation costs of necessary resources, we suggest the construction of habitats by autonomous, solar-powered robots using only in-situ material (ice, sand, regolith,...). For the purpose, the robots use an additive manufacturing technique called solar sintering to fuse the material in layers by melting it with concentrated solar power. The advantage of this approach is the reduction of transportation costs to the weight of the robots. Moreover they can be transported to the targeted area and start printing before the research team arrives.

## INTRODUCTION

The idea to build shelters using additive manufacturing is not new but is already mentioned in William E. Urschels patent for a wall building machine from 1941. [26] The machine was made of an extruder attached to a rotatable and height-adjustable arm mounted on a column in its center. It was filled with lean concrete to build shelters and walls layerwise. The reason why its machine never reached a broader audience was the high operational cost.

Owing to the development of large-format 3D printers, the industry has once again become aware of additive manufacturing in the field of structural engineering. While robotic technology was significantly refined, the basic idea of the pri-

marily used technique MEX (*material extrusion*) still relies on the method of Urchel's approach. Viscous material, mostly concrete or clay, is applied layerwise with an extruder. However, it is no longer necessary to constantly refill material because the machine is able to pump it autonomously from a tank. This reduces the operational expense significantly. In addition, the increase in precision and the possibility of computer-controlled processes allow more complex structures. [7]

Besides to the refinement of the already used techniques of additive manufacturing, new methods are gaining relevance in the field of structural engineering. These include for example WAAM (*Wire and Arc Manufacturing*) for printing steel on large scales and solar sintering, which will be the subject of the following chapters. [23]

## FOCUSING SUNLIGHT AS A SOURCE OF ENERGY

Focusing sunlight as a source of energy to burn or heat materials is an old idea which already used during the roman period. Records of Pliny the Elder described burning-glasses to focus sunlight. [17] Until today it is an easy approach to bring materials to extreme temperatures without contaminating it with components of the heat source. An example for a modern approach is CSP (*concentrated solar power*), where heliostatic mirrors concentrate solar energy onto a power tower. The energy is then used for power generation. [18]

With the upcoming demand for constructions beyond the surface of Earth as well as in hard-to-reach areas of the Earth, new approaches to build with in-situ materials are of interest. Missions like Artimes [2] of NASA (*National Aeronautics and Space Administration*) and the Moon Village [3] of ESA (*European Space Agency*) who are planning permanent bases on the moon, are highly limited by the launch costs per unit mass of needed hardware and construction material. Even with the launch costs reduced to appr. 1500 \$/kg due to new technologies, it is still highly expensive and inefficient to send construction material to other planetary objects. [22]

Therefore, NASA started a new research field called ISRU (*In-Situ Resource Utilisation*) with the goal to produce water, fuel, O<sub>2</sub>, and metals using lunar regolith. With the collection and processing of lunar regolith as an already acquired competence, solar sintering offers a potentially cost efficient way to create building material from lunar regolith without the need of chemical binding materials from Earth. Moreover, the lunar surface is well-suited for the first application of the technology outside of the Earth because it has the same solar constant. Many necessary tests could be performed on Earth beforehand and only have to be scaled to the higher intensity due to no atmosphere. [10]

Solar Sintering is a technology derived from SLS (*selective laser sintering*) and SLM (*selective laser melting*). Both are powder-based additive manufacturing technologies that are broadly used in modern manufacturing industry.

### Selective laser sintering

With SLS, it is possible to print a wide range of materials. The basic technology is to heat granular material using a laser to bind it together. A distinction is made between direct and indirect sintering. In the indirect process, the specific material is coated in a binder that is melted using the energy of a laser and binds the particles during solidification. In the direct process, the raw material is sintered. For the direct process, there is an additional distinction between solid-phase sintering and liquid-phase sintering. In solid-phase sintering, all components stay below their melting point. In liquid-phase

sintering, the material melts partially or only on the grain shell. A heated build volume reduces the energy needed for the laser to melt the material. After finishing a layer, a roll disperses a new layer of material. Since only the required areas of each layer are sintered in this process, the finished objects must be post-processed.

### Selective laser melting

SLM is another variant of powder-based AM. The difference to SLS is that the material is completely melted during the process. As a result, it is possible to achieve almost homogeneous material. Therefore, the material properties of the resulting parts are comparable to classically produced components, which makes SLM the superior AM process compared to SLS. Besides its advantages in the resulting material properties, the challenges typical for SLM are dealing with surface tension, viscosity of the material, and temperature-induced stress, which can cause cracks. [13, 27]

### Solar sintering

The process of solar sintering can be compared to liquid-phase sintering or SLM, depending on how much energy is applied to the material during printing (see section 2.1.4). As in direct SLS and SLM, thin layers of granular material is fused by heating it to partially or completely melt and, hence, fuse it without the need of additional binding material. The difference to the methods previously discussed is the heat source. Instead of a laser, solar sintering uses highly focused sunlight for the printing process. Therefore, the challenge of solar sintering is to produce a constant quality with variable power output of the system, caused by weather, position of the sun, and other environmental conditions. Also focusing the incoming sunlight into a precise controlled, moving, and comparatively small area can be challenging based on the required accuracy. Using the sun's energy directly can decrease complexity and increase energy efficiency. In 2011, Kayser [12] showed that it is possible to print sculptures and vessels from Sahara sand and sunlight using a computer controlled fresnel lens.

### Energy analysis for Solar Sintering

Since the energy output, is highly dependent on external influences, the process of solar sintering must be highly adaptable to them in order to ensure consistent print quality. For this purpose, the focused energy has to be measured constantly and compared to the power output. Adaptions can be made by varying the printing speed or defocusing of the focal point, which results in wider printed layers and therefore less energy per unit area. The interdependencies of these variables are expressed by the following equations, which depends on both the incoming and outgoing energy.

It is also important to define the necessary boundary conditions and assumptions. For this purpose, it is initially determined that the incoming solar energy  $Q_{in}$  is collected on a circular surface of radius  $R_p$ . Also, the collected energy is focused on a circular surface  $A_c$  with radius  $r_c$ . Consequently, the cylindrical volume  $V$  that is heated by the collected energy is defined by the area  $A_c$  and the layer height  $h$ . The following characteristic values are required for the collected energy  $Q_{in}$  and the energy needed to melt the granular material  $Q_{melt}$ .

Incoming energy:

Direct Normal Irradiance:  $S_{DNI}$  [W/2]

System parameters:

Projected area of primary mirror or lens:  $A_p$  [m<sup>2</sup>]

Radius of primary mirror or lens:  $R_p$  [m]

Material parameter:

Efficiency:  $\mu$  [ ]

Density:  $\rho$  [kg]

Area of focal point:  $A_c$  [m<sup>2</sup>]

Radius of focal point:  $r_c$  [m<sup>2</sup>]

Volume:  $V$  [m<sup>3</sup>]

specific heat capacity:  $c$  [J]

Initial temperature:  $T_0$  [K]<sup>kgK</sup>

Melting temperature:  $T_{melt}$  [K]

specific latent heat :  $L$  [J<sub>kg</sub>]

Reduction factors:

Heat Transfer:  $R_{HT}$  [-]

Emission:  $R_E$  [-]

reduction of latent heat:  $\mu_L$  [-]

Using the characteristic values, it is possible to formulate the collected energy  $Q_{in}$  and the energy  $Q_{melt}$  required to melt the given material.

$$(1) \quad Q_{in} = S_{DNI} A_p \mu t$$

$$(2) \quad Q_{melt} = c m \Delta T R_E R_{HT} + \mu_L Q_{latent} \\ = c \rho V (T_{melt} - T_0) R_E R_{HT} + \mu_L Q_{latent}$$

$Q_{latent}$  used in equation (2) is called latent heat. It is a material-dependent additional energy required to perform the phase transition from the solid to the liquid state and is defined as:

$$(3) \quad Q_{latent} = L m$$

To achieve a phase transition of the whole material within the volume  $V$ , the incoming energy  $Q_{in}$  must be equal to the melting energy  $Q_{melt}$ . By setting them equal, it is possible to determine the time that the focal point must remain on the volume.

(4)

$$Q_{in} = Q_{melt} \\ t = \frac{c \cdot \rho \cdot V \cdot (T_{melt} - T_0) \cdot R_E \cdot R_{HT} + \mu_L \cdot Q_{latent}}{S_{DNI} \cdot A_p \cdot \mu}$$

The reduction factor  $\mu_L$  specifies whether the process is more comparable to SLS or SLM. With a reduction factor within the range of  $0 < \mu_L < 1$ , the granular material will not be melted completely. The result is therefore similar to liquid-phase sintering. At  $\mu_L = 1$ , the entire material within the volume undergoes a phase change and the process is comparable to SLM. If the boundary conditions are known, it is also possible to determine the ideal travel speed of the focal point by using the equation (5). [14, 8]

(5)

$$v_{max} = \frac{r}{t} \\ v_{max} = \frac{r \cdot S_{DNI} \cdot A_p \cdot \mu}{c \cdot \rho \cdot V \cdot (T_{melt} - T_0) \cdot R_E \cdot R_{HT} + \mu_L \cdot Q_{latent}}$$

To produce a consistent print quality with varying energy input, the print speed must be adjusted during the process. Hence, the solar irradiation must be measured constantly using sensors. Possible options are for example pyranometers, solar panels and LDR (*light dependent resistors*). Since the prototype uses LDR for alignment (see section 4.5), they should also be used for solar measurements in the future. The advantage here is the reduction of electronic components, as well as the cost reduction of more expensive alternative sensors. [5]

### Solar sintering on the Moon

The solar constant on the Moon is, a on the Earth, 1361 Wh/m<sup>2</sup>, due to its relative proximity to Earth. With a self-revolution time of 655 h and an orbit time around Earth of approx. 655 h, there are approximately 327.5 h of sunlight followed by 327.5 h of darkness. This sums up to around 3930 h of sunlight per year. To calculate the precise hours of available sunlight the exact location for the printer must be known, taking into account mountains, craters etc. The heat capacity for regolith can be expressed after Colozza as:

$$(6) \quad c = 1848.5 + 1047.41 \log(T)$$

For the relevant temperature range of 400 K to 1513 K a mean constant value of  $c = 1250$  J/(kg K) is defined. The latent heat  $L$  of lunar regolith will be assumed as 470 kJ/kg. Other researches predicted values from 161.2 kJ/kg, over 400 kJ/kg to 450 kJ/kg and 480 kJ/kg [16, 1, 24, 19, 21].

## PROTOTYPE DESIGN

In solar sintering, granular material is laid out as a thin layer and melted. As discussed above, the necessary energy for the process is supplied by focused sunlight. In earlier proof-of-concept studies, a stationary lens system using a fresnel lens was employed as the optical system [12, 25]. As a result, the completion of the shelter after printing required post-processing. In order to avoid postprocessing, we propose a printer design that uses mobile devices. Since the critical module of this design is the optical system, this chapter will focus on the design of its prototype.

To begin with, the necessary functions of the robot modules, as well as the advantages and disadvantages of various optical components should be presented.

### Robotic units

Mobile solar sintering should be realized with modular, solar-powered units. The aim of the robot modules is that they act and interact as autonomously as possible once they arrive at their operational area. External intervention should be possible, but only necessary in case of incidents or manual selection of suitable printing areas. Each robot must have a microcontroller with access to sensors, transmitters and receivers for this purpose. This allows each robot to detect its environment, communicate with other units and receive instructions.

The energy supply of the robots should be provided purely by solar panels, which is strongly dependent on the local conditions and must therefore be adapted to them. For a high degree of versatility, the basic modules should be designed with efficient energy management in mind. To achieve this, rovers with modular attachments are planned, which should allow to split processing steps and reduce computing power as well as necessary motors for each robot. Two modules are currently being considered, one for transporting and laying out the in-situ material (carrier) and one for melting the layers (printer). The downside of this method however is that each unit requires an additional transmitter, as well as the related software implementation of a communications system. However, since the modular design can save many motors and redundant components, it's still the preferred design based on the current state of research.

A critical factor for the dimensions and design of the print modules is the choice of the optical parts. In principle, lenses, mirrors, or a combination of both can be considered.

### Optical parts

If lenses should be used, convex lenses or fresnel lenses are suitable for focusing sunlight.

## Convex lenses

Classical convex lenses are typically made of glass or plastic and has a one-sided (convex) or two-sided (biconvex) positive curvature. Incident light is collected and focused towards a focal point. The converging lens can be manufactured with very high precision, resulting in high efficiency. A disadvantage is the comparatively high dead weight with increasing diameter. Moreover, part of the frequency of the sunlight is absorbed when passing through the lens, which leads to reduced efficiency with increasing thickness. [14, 9]

### Fresnel lenses

Fresnel lenses are typically made of plastic and are based on the principle of a convex lens. The difference is that fresnel lenses take advantage of the fact that the relevant refraction of light takes place at the boundary surfaces. Therefore, the curved surfaces are annularly arranged in one plane, which results in a flatter and significantly lighter lens.

The disadvantage is that the stepped surface does not produce continuous refraction and blocks some surface components itself. Compared to a convex lens, the efficiency of a fresnel lens is therefore lower. [14, 9]

Alternatively, mirrors can be used. These reflect incident rays, allowing for their deflection and redirection. An advantage is that light does pass through a medium (unless the mirror is coated on its backside), which means that no losses due to absorption occur.

### Optical system selection

Because the project is based on mobile printing units, it was decided against a single fresnel lens as used in previous projects [12, 25]. In a single lens system, the minimal sun altitude is determined by the lens dimensions and the focal length (Fig. 3). A printer as proposed by *Imhof et al.* [11] requires 5 axis movement to keep the focal point in the same location throughout the day.

To avoid a horizontal compensation, we separate light collection and focal point movement. Similar to a CNC (*computer numerical controlled*) laser cutter, the laser tube is stationary and the laser is reflected along the moving axis and then focused onto the work piece. In the development of the prototype, the following aspects defined the design of the optics system. They serve as KPIs and will be evaluated using the prototype to determine the weaknesses and strengths of the mechanism.

#### 1. Orientation

The optic system has to adapt to the changing position of the sun throughout the day.

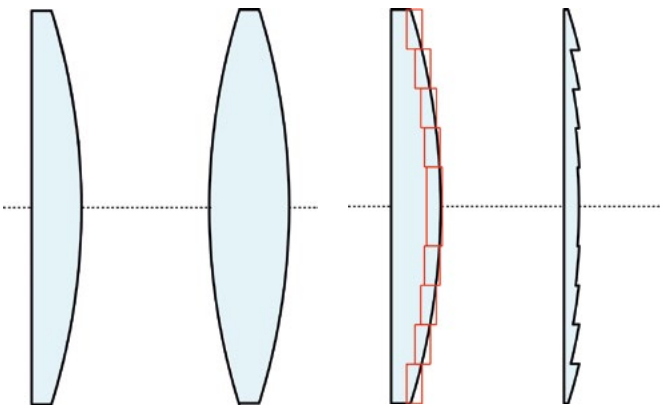


Figure 1: Left: Convex lens - Right: Biconvex lens

Figure 2: Fresnel lens compared to a convex lens



Figure 3: Minimum possible altitude angles limited by the Fresnel lens diameter, focal length and ground clearance.

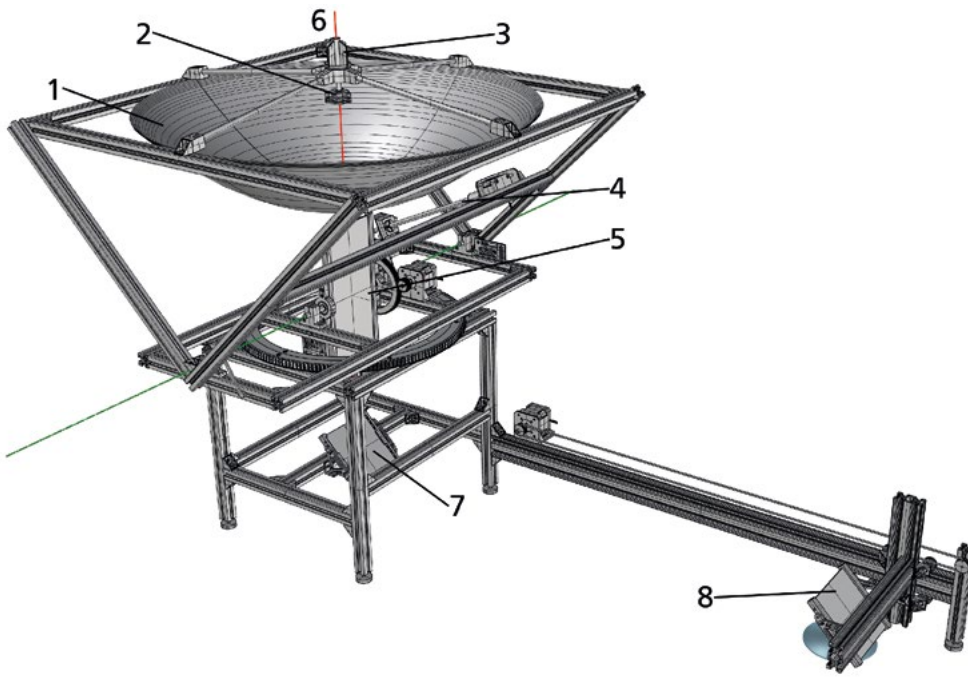
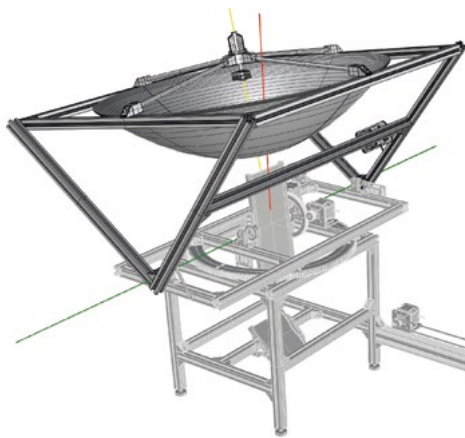
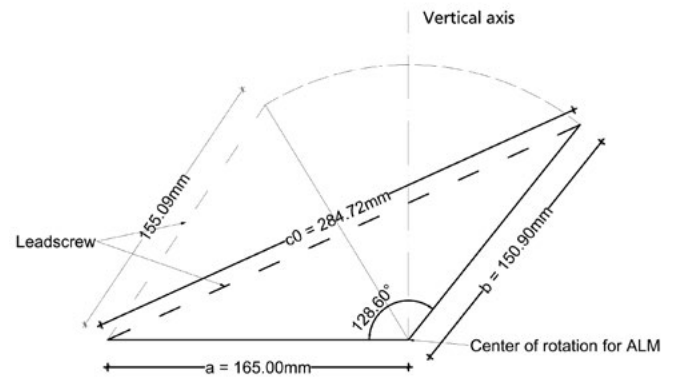


Figure 4: 1-Primary Mirror, 2-Secondary Mirror, 3-Orientation Unit, 4-Lead Screw, 5-Mirror F1, 6-Rotation Axis AZM, 7-Mirror F2, 8-Mirror F3.



(a) Altitude Module



(b) Leadscrew movement to angle relation

Figure 5: Altitude Module with primary mirror, secondary mirror and orientation unit, held in place by 4 threaded rods.

## 2. Area of focused sunlight

The energy output in the focused point is correlated directly with the surface area of the redirected sunlight.

## 3. Area of focal point

The size of the focal point determines how much energy is needed in the first place. A smaller focal point means higher precision of the optical system with a lower minimal energy needed but also less printed material per layer.

## 4. Moving the focal point

The focal point has to be able to move in a single or two horizontal axis to get efficient surface coverage. The focal point also needs to be adjusted in the vertical axis, to control the focal point size.

## 5. Build footprint & mobile mount capability

Mechanism size and available support conditions must be considered when mounted on a rover. In addition, weight is directly related to launch costs.

## 6. Cost-effectiveness

The goal is to create a low-cost mechanism with a high processing volume.

## 7. Energy efficiency

Given the fact that the application will be mounted on an autonomous rover, possibly on a different celestial body, energy consumption by electric parts should be as low as possible.

When using the sunlight as a energy source instead of a laser in conventional SLS, the length of the light path changes constantly. Therefore, a single mirror system is impossible, since the required focal length changes constantly. The secondary mirror has to reflect the optical rays coming from the primary mirror as axis parallel rays, which leads to the fact that also the secondary mirror must be a paraboloid. At the end of the light path the ray bundle gets concentrated into a focal point with a converging lens.

Based on these considerations, it was decided that a mirror system with parabolic mirrors would be the most suitable for the project.

## RESULTS

The aim of the prototype was to built a low cost printing module with mainly standard and commercially available parts. Special parts are 3D printed in PLA. In the following figure the final structure is shown and described top to bottom, following the path of the light.

## Altitude Module (ALM)

The ALM (altitude module, Fig. (5)) handles the altitude angle change of the sun throughout one day. To cover the whole range of motion, the module moves between 0 and  $2\pi$  altitude.

The ALM consists of the primary mirror (1), the secondary mirror (2), and the orientation unit (3). The angle is modulated by a stepper motor driven lead screw (4). The relation between lead screw movement and angle is as followed:

$$(7) \quad c^2 = a^2 + b^2 - 2ab \cdot \cos(\Theta)$$

$$\Theta(x) = \arccos\left(\frac{a^2 + b^2 - c_0^2}{2ab}\right) - \arccos\left(\frac{a^2 + b^2 - (c_0 - x)^2}{2ab}\right)$$

where a, b, c and  $\Theta$  are shown in Fig. (5.b).  $\Theta = 0$  is defined on the vertical axis. With an incline of 2 mm/revolution and the given 1600 steps/revolution of the stepper motor,  $\Theta$  can be calculated according to the steps moved:

$$(8)$$

$$\Theta(s) = \arccos\left(\frac{a^2 + b^2 - c_0^2}{2ab}\right) - \arccos\left(\frac{a^2 + b^2 - (c_0 - \frac{s}{s_r})^2}{2ab}\right)$$

with:

a	fixed length of 165 mm
b	fixed length of 150.9 mm
c	length of lead screw
$c_0$	284.72 mm (home position)
s	steps moved
$s_r$	steps per revolution

The moved steps and angles are always relative to this home position. To reduce self-induced oscillations and unify the load on the lead screw, a spring is mounted between the ALM and the turning table. With decreasing altitude angle, the load induced by the weight of the ALM on the lead screw increases, which is compensated by the spring. The secondary mirror (Fig. (7.a)) is spring-mounted on three screws to allow fine adjustments of orientation and alignment. A central threaded rod allows to adjust the distance between primary and secondary mirror.

The AZM (azimuth module, Fig (6.a)) rotates the ALM along the vertical axis and accounts for the azimuth change over the day. With the mounting on a rover in mind, the azimuth adaption needs to allow full  $360^\circ$  rotations. With a gear reduction of  $i = \frac{200}{20} = 10$ , the AZM rotates  $0.01125^\circ$  per step of the stepper motor.

For the alignment of the concentrated light beam, independent of the position of the sun, the prototype has a rotatable mirror F1 (Fig. (5.a)). Mirror F1 rotates perpendicularly to the rotation axis of the AZM. With a known altitude

angle the mirror aligns itself to always reflect the beam downwards, along the vertical axis.

A limitation of the adjusting mirror is that light cannot be completely reflected for angles of 75° and above. At an angle of 90°, the mirror blocks part of the light as it is illustrated in Fig. (7.b).

With the calculated sun altitude angle of the ALM (Eq. 8) the rotation angle for F1 is expressed as:

$$(9) \quad \Theta_{F1} = \Theta/2$$

A gear reduction of  $i = \frac{100}{20} = 5$  results in 0.0225° per step of the stepper motor. Although the relation is linear and can therefore be realized mechanically, a separate motor was chosen, because it allows to quickly stop the sintering process by deflecting the sunlight away from the intended axis.

To keep the complexity of this prototype low, the gantry only consists of one moving axis. This allows for principal testing and assessment of the precision of the optical system and for melting multiple layers of different materials while keeping the complexity low. Mirror F2 (Fig. (4), 7) redirects the beam 90° towards the moving gantry. Mirror F3 (Fig. (4), 8) moves along the axis, redirecting the beam 90° downwards. The reflectivity will be assumed as  $\mu_r = 0.9$ . The mirrors are mounted with PLA-printed parts and allow adjustment via slotted holes. A converging lens focuses the light beam into the final focal point. The 16 teeth belt pulley and a teeth distance of 2 mm result in 32 mm per rotation or 0.02 mm/step.

### Electrical desing

Four LDRs (light-dependent resistor) are used to determine the orientations of the ALM and AZM. LDRs have different resistances, based on the amount of electromagnetic radiation incident on their photo cell. The higher the light intensity, the lower the resistance. The LDRs are aligned as shown in Fig. 4.6 (a) and separated by walls to ensure different illumination based on the alignment of the module. This means for the movement of the ALM, the mean resistance of the LDR 1 and 2 is compared with the mean resistance of 3 and 4. For the rotation of the AZM, the mean resistance of the LDR 1 and 3 is compared with the mean resistance of 2 and 4. Another approach for a simple and low-cost sun tracking system uses photo cells and was built by *Aiuchi et al.* [4], achieving a tracking error of only 0.6 mrad. Accurate sun tracking is important for sun-concentrating systems. Even a slight tracking error can cause the printing system to fail, due to optical aberrations, especially astigmatism [20].

A Raspberry Pi Pico, connected to A4988 stepper drivers, controls the stepper motors (Nema 17) and processes the input of the LDRs. The rotations and translations are driven by Nema 17 and homed with limit switches. This is necessary as stepper motors have no information about

their current position. The Nema 17 used have 200 steps per rotation (1.8° per step) but are all driven with a microstep resolution of 1/16. This allows a higher accuracy of 3200 steps per rotation, which results in 0.01125° per step. All movements are made relative to the home position. The motor steps provide information about the orientations with the equations discussed above. The azimuth rotation does not require a limit switch, since the horizontal orientation does not need to be known for the system to work. After startup, the initialization program homes all moving axis. With knowledge of the position of all parts, the printer starts the sun tracking program. The Sun tracking will be called passive movement, since it is controlled by the sun's position. The active movements control the position of the focal point and the printing process. In order to run passive and active movement simultaneously, the tasks are executed on different cores of the microcontroller. The active movement for the prototype is limited to console commands, which allows the user to move the gantry. Built-in electronic components are listed in the table below:

Table 4.1.: Basic components of the controller

4x	stepper motor Nema 17 2 A 45 N cm
4x	A4988 stepper driver
3x	RepRap 3-pin end stop
1x	Raspberry Pi Pico
4x	LDR

The schematic circuit used in the prototype can be seen in appendix A.1

### Proof-of-concept studies

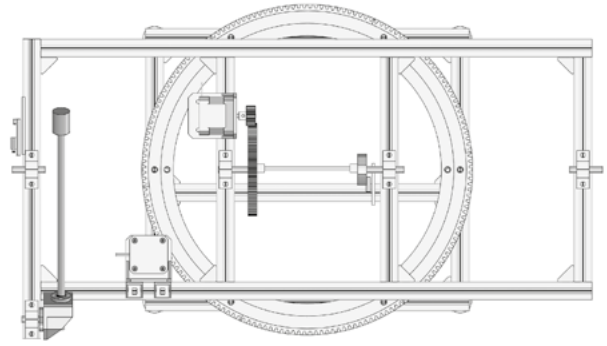
Basic geometric optics simulations were analysed based on 3D vector operations (ray tracing). This approach assumes perfectly flat surfaces and uses basic reflection laws of geometric optics, which allowed a fast analysis of different mirrors, lenses and mechanisms in different positions and alignments. Fig. 4.7 displays the path of light in a system with a parabolic primary and secondary mirror at an altitude of 45°. With a ray density of 961 light rays per m<sup>2</sup>, 260 rays hit the primary mirror. As a result of the ideal parabolic mirrors, all remaining rays reach the main focusing lens Fig. (10).

The mirror available for the prototype is spherical, with a diameter of 25 mm and a radius of 15.5 mm. Spherical lenses and mirrors have disadvantages compared to parabolic components, because of the spherical aberrations. Not all parallel rays are refracted or reflected through the same focal point (see Fig. (10.c)). For reflecting angles, that are not covered by the small angle-approximation, the effect of spherical aberration is not negligible. As a result, the light beam diverges and



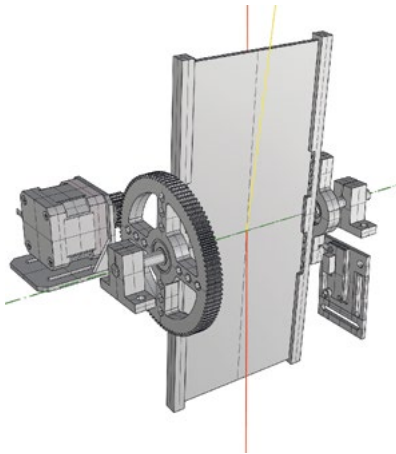


(a) Azimuth Module

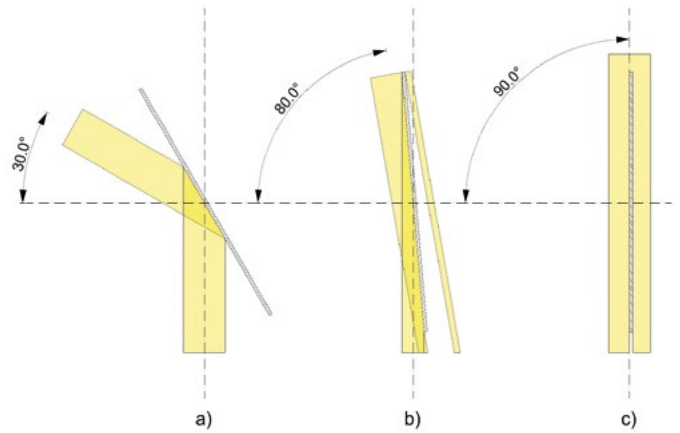


(b) Turntable

Figure 6: Azimuth Module, consisting of the turntable and the Altitude Correction Module.



(a) Altitude Correction Module



(b) Light beam reflection, cases: a) Altitude of the sun is below  $60^\circ$ , b) above  $60^\circ$  and c) at  $90^\circ$

Figure 7: (a) Yellow: direction of the incoming light beam, red: vertical Axis, direction of reflected light beam, green: rotation axis of mirror F1.

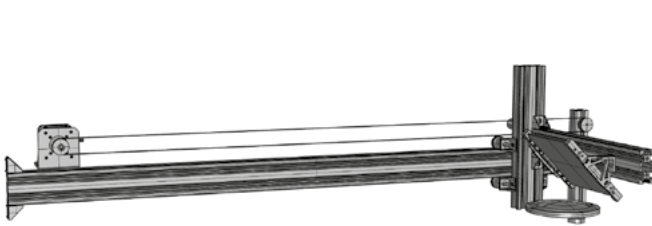
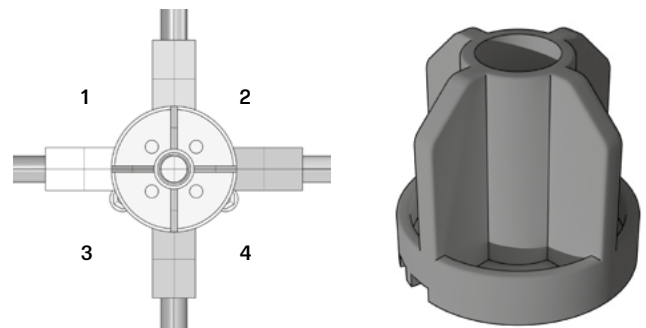


Figure 8: Moving gantry with  $45^\circ$  tilted mirror and converging lens.



(a) Positioning of Orientation Unit, arrangement of LDRs.

(b) Shading of the LDRs.

Figure 9: Functionality Orientation Unit, positions of LDRs, simulated sun shading.

## HABITAT GEOMETRY

only 26.15 % of the rays, compared to the ideal system, reach the focusing lens (manufacturing inaccuracies are neglected in this comparison). Other optical aberrations such as distortions and chromatic aberration are not considered because the system has no imaging function. Chromatic aberrations are not present in reflecting systems, since the law of reflection is independent of wavelength. An aberration similar to an astigmatism is observed, if rays from an off axis source hit the primary mirror. These rays do not converge in the same point in the focal plane.

When a parabolic mirror is chosen as secondary mirror, two orientations are possible (Fig.(10.a) and (10.b)). In both variants, the focal points of the two mirrors must fall onto the same coordinate. A focal length  $f < 0$  has the advantage of not blocking rays on the outside, if the mirror is too large. Convex mirrors are easier to manufacture, since the tool-head has more space to move compared to a concave shape. Larger absolute focal lengths are preferable, reducing surface curvature and therefore limit the reflection angles of the ray. A parabolic mirror with the same diameter but a larger absolute focal length can be better approximated with a circle. This implication reduces the effect of spherical aberration when substituting a parabolic with a spherical mirror. Mirrors with a longer focal length also require less precise manufacturing to get acceptable focusing results, compared to a short focal length.

Every material has its own properties regarding reflectance and transmittance of certain wavelengths of electromagnetic radiation. Reflection specifications are given as an average value  $R_{avg}$  for a distinct wavelength range.

Table 4.2.: Metallic mirror coatings produced by Edmund Optics©[15]

Name	Wavelength Range	Reflection Specifications
VUV Enhanced Aluminium	120 nm-700 nm	Ravg > 88 %
Protected Aluminium	400 nm-2000 nm	Ravg > 90 %
Enhanced Aluminium	450 nm-650 nm	Ravg > 95 %
Protected Silver	450 nm-2000 nm	Ravg > 98 %
Protected Gold	700 nm-2000 nm	Ravg > 96 %

Every coating has also a scratch resistance, which is especially important when evaluating different cleaning mechanisms. To save costs the mirrors used in the first prototype, except for the secondary mirror, are not surface coated and have an unknown reflectance. The secondary mirror is surface coated with an "Enhanced Aluminium" coating.

Prints produced by solar sintering have porous material properties, which means that the resulting material will have better resistance against pressure than tensile or shear forces. Therefore, it is a good approach to choose forms for the habitats that transfer loads to the ground mainly by pressure. As a first design, domes were chosen, since they primarily transfer their dead weight and areal loads by pressure. Despite being relatively simple structures, domes are a challenge for additive manufacturing without any support structure, especially for sintering processes. During the printing process, the printer must print parts of the layers without any support below it. This is necessary because any support structures would again lead to post-processing steps by the arriving team, which should be avoided as far as possible by using the robot modules. To still be able to print unsupported layers, the robotic printer should have a retractable plate that supports the material until it is solidified (see image 5.1). [25]

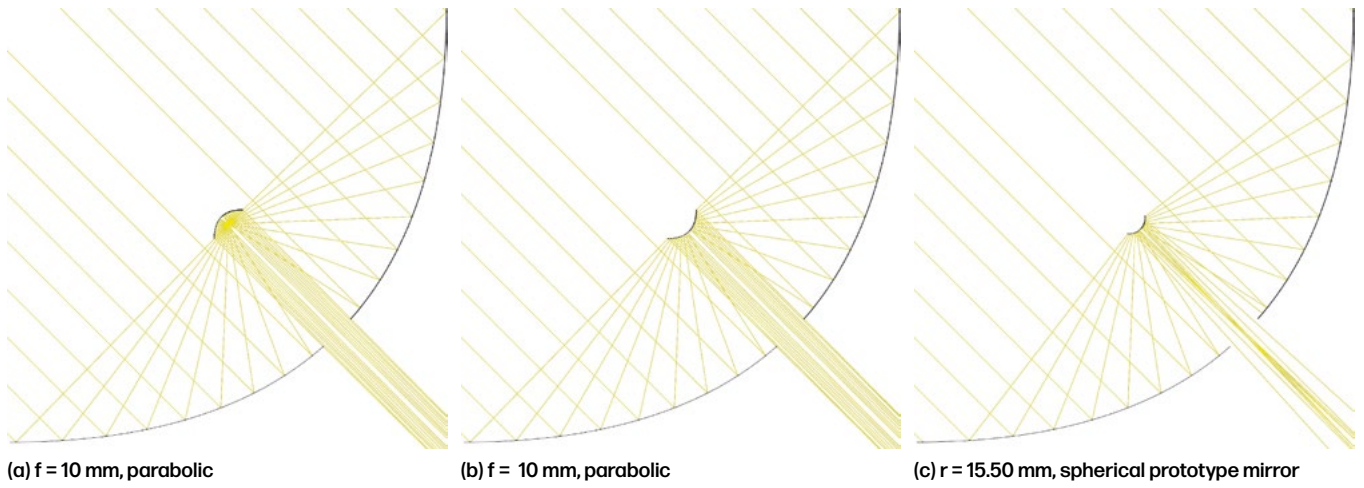
The robots also need to be able to transport material during the printing process. For this purpose, it is necessary that a ramp is created simultaneously as the printing progresses. This allows the robots to reach the current printing layer at any time. For the considered dome it is useful to determine the ramp inversely. This requires two input parameters, the outside radius  $r_a$  of the dome and the necessary minimal width  $d$  of the ramp. To determine the ramp geometry, a two-dimensional spiral is first calculated. The radius of this spiral increases by  $d$  after every full revolution, which ensures that the ramp does not create any overlaps with itself.

$$(10) \quad r_i = \frac{d}{2 \cdot \pi} \cdot \phi_i$$

The maximum radius of the spiral results from the outer radius  $r_a$ , which also allows to determine the maximum angle of rotation  $\phi_{max}$ . The corresponding formula is:

$$(11) \quad \phi_{max} = \frac{2 \cdot \pi \cdot r_a}{d}$$

Equations 10 and 11 allow to describe each point of the two-dimensional spiral in polar coordinates (see figure 12). It is also possible to project the spiral onto the outer surface of the dome, since the distance to the center must always be  $r_a$ . In this case, the conversion into cartesian coordinates is useful:



(a)  $f = 10$  mm, parabolic

(b)  $f = 10$  mm, parabolic

(c)  $r = 15.50$  mm, spherical prototype mirror

Figure 10: Variants of secondary mirrors ( $d = 40$  mm) with primary mirror used in prototype ( $f = 152$  mm,  $d = 609$  mm).

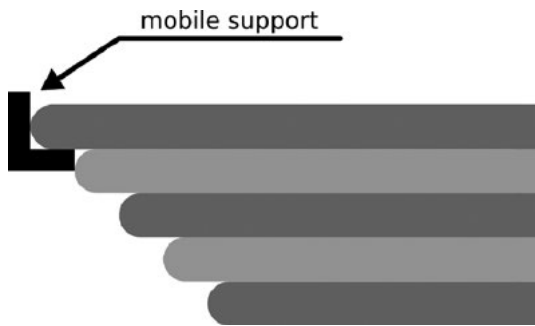


Figure 11: Retractable plate for mobile support of outer layers

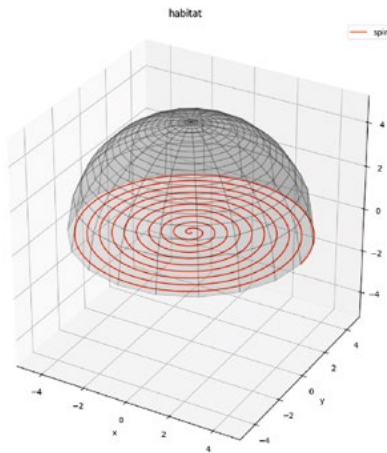


Figure 12: Two-dimensional spiral calculated with formular 10.

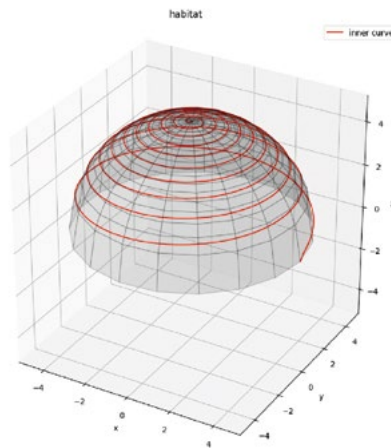


Figure 13: Projected spiral onto the outer surface of the dome.

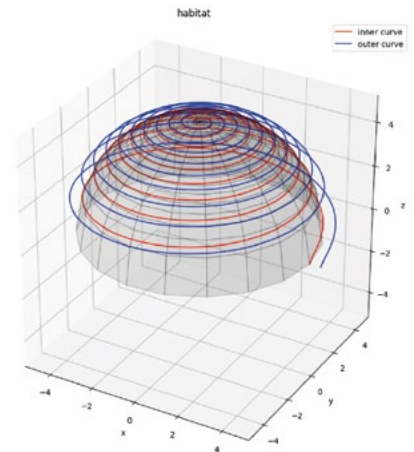


Figure 14: Boundary curves of the ramp.

$$(12) \quad \begin{aligned} x_i &= r_i \cdot \cos(\phi_i) \\ y_i &= r_i \cdot \sin(\phi_i) \\ z_i &= \sqrt{r_i^2 - x_i^2 - y_i^2} \end{aligned}$$

The curve determined and projected onto the dome represents the inner boundary of the ramp, which should be used by the robots to go up and down during the printing process (see Figure 13). To determine the outer curve, the coordinates must be extended with the minimal width  $d$ :

$$(13) \quad \begin{aligned} x_a &= (r_i + d) \cdot \cos(\phi_i) \\ y_a &= (r_i + d) \cdot \sin(\phi_i) \\ z_a &= z_a \end{aligned}$$

It should be mentioned that the z-coordinate remains unchanged. This is justified by the fact that the ramp only needs to be extruded along its normal. A slope in opposite direction of travel is not desired at the moment. With the determined coordinates  $P_{i_i} = (x_i, y_i, z_i)^T$  and  $P_{a_i} = (x_a, y_a, z_a)^T$  it is finally possible to determine the boundary curves of the ramp (see Figure 14).

## REFERENCES

- [1] Yu. A. Abzaev et al. "Investigation of the Melting of Quartz Sand by Low-Temperature Plasma". In: *Glass and Ceramics* 72.5 (Sept. 2015), pp. 225–227. issn: 0361-7610, 1573-8515. doi: 10.1007/s10717-015-9761-z. url: <http://link.springer.com/10.1007/s10717-015-9761-z> (visited on 12/02/2021).
- [2] National Aeronautics and Space Administration. *Artemis*. url: <https://www.nasa.gov/specials/artemis/> (visited on 12/21/2022).
- [3] European Space Agency. *ESA engineers assess Moon Village habitat*. url: [shorturl.at/vBF02](http://shorturl.at/vBF02) (visited on 12/21/2022).
- [4] Kosuke Aiuchi et al. "Sun Tracking Photo-Sensor for Solar Thermal Concentrating System". In: ASME 2004 International Solar Energy Conference. American Society of Mechanical Engineers Digital Collection, Dec. 17, 2008, pp. 625–631. doi: 10.1115 / ISEC2004 - 65025. url: <https://asmedigitalcollection.asme.org/ISEC/proceedings/ISEC2004/37475/625/303756> (visited on 07/13/2022).
- [5] Rodrigo Cassio de Barros et al. "Low-Cost Solar Irradiance Meter using LDR Sensors". In: *2018 13th IEEE International Conference on Industry Applications (INDUSCON)*. 2018 13th IEEE International Conference on Industry Applications (INDUSCON). São Paulo, Brazil: IEEE, Nov. 2018, pp. 72–79. isbn: 978-1-5386-7995-1. doi: 10.1109/INDUSCON.2018.8627176. url: <https://ieeexplore.ieee.org/document/8627176/> (visited on 06/23/2022).
- [6] Pierre-Yves Bely, ed. *The design and construction of large optical telescopes*. Astronomy and astrophysics library. New York: Springer, 2003. 505 pp. isbn: 978-0-387-95512-4.
- [7] Alberto Chiusoli@el. *From the shapeless earth to the earth as house shaped*. url: <https://www.3dwasp.com/en/3d-printed-house-tecla/> (visited on 12/21/2022).

- [8] Wolfgang Demtröder. *Experimentalphysik* 2. 2017.
- [9] Dr. Thomas Halfmann. *Vorlesungsfolien Experimentalphysik 3 - Kapitel 3*. 2021.
- [10] Laura Hall. *Overview: In-Situ Resource Utilization*. url: <http://www.nasa.gov/isru/overview> (visited on 12/21/2022).
- [11] Barbara Imhof et al. "Using solar sintering to build infrastructure on the moon. Latest Advancements in the regolith project". In: *th International Astronautical Congress* (2018), p. 11.
- [12] Markus Kayser. *Solar Sinter*. Kayser Works. url: <https://kayserworks.com/798817030644> (visited on 01/24/2022).
- [13] J.P. Kruth et al. "Lasers and materials in selective laser sintering". In: *Assembly Automation* 23.4 (Jan. 1, 2003). Publisher: MCB UP Ltd, pp. 357–371. issn: 0144-5154. doi: 10.1108/01445150310698652. url: <https://doi.org/10.1108/01445150310698652> (visited on 05/13/2022).
- [14] Horst Kuchling. *Taschenbuch der Physik - 21. Auflage*. 2014.
- [15] Metallic Mirror Coatings | Edmund Optics. url: <https://www.edmundoptics.de/knowledge-center/application-notes/optics/metallic-mirror-coatings/> (visited on 07/06/2022).
- [16] NASA. *Moon Fact Sheet*. url: <https://nssdc.gsfc.nasa.gov/planetary/factsheet/moonfact.html> (visited on 06/23/2022).
- [17] *Pliny the Elder, The Natural History, BOOK XXXVII. THE NATURAL HISTORY OF PRECIOUS STONES, CHAP. 10.—LUXURY DISPLAYED IN THE USE OF CRYSTAL. REMEDIES DERIVED FROM CRYSTAL*. url: <http://www.perseus.tufts.edu/hopper/text?doc=Plin.+Nat.+37.10&redirect=true> (visited on 05/16/2022).
- [18] Solar Energy Development Programmatic. *Concentrating Solar Power (CSP) Technologies*. url: <https://solareis.anl.gov/guide/solar/csp/> (visited on 12/21/2022).
- [19] Scott W. Richter. "Experimental Determination of In Situ Utilization of Lunar Regolith for Thermal Energy Storage". In: *27th Intersociety Energy Conversion Engineering Conference* (1992). Aug. 3, 1992, p. 929277. doi: 10.4271/929277. url: <https://www.sae.org/content/929277/> (visited on 07/07/2022).
- [20] Stefan Roth and Achim Stahl. *Optik: Experimentalphysik – anschaulich erklärt*. Berlin, Heidelberg: Springer Berlin Heidelberg, 2019. isbn: 978-3-662-59336-3 978-3-662-59337-0. doi: 10.1007/978-3-662-59337-0. url: <http://link.springer.com/10.1007/978-3-662-59337-0> (visited on 01/20/2022).
- [21] Samuel Schreiner et al. "Thermophysical Property Models for Lunar Regolith". In: *Advances in Space Research* 57 (Dec. 1, 2015). doi: 10.1016/j.asr.2015.12.035.
- [22] Aerospace Security. *A Space Launch to Low Earth Orbit: How Much Does It Cost?* url: [shorturl.at/abimt](http://shorturl.at/abimt) (visited on 12/21/2022).
- [23] Fachgebiet Stahlbau. *Wire and Arc Additive Manufacturing*. url: [shorturl.at/hrP02](http://shorturl.at/hrP02) (visited on 12/21/2022).
- [24] Tom Benson. *Moon*. url: <https://www.grc.nasa.gov/www/k-12/rocket/moon.html> (visited on 05/24/2022).
- [25] Diego Urbina et al. "Robotic prototypes for the solar sintering of regolith on the lunar surface developed within the Regolith project". In: (Nov. 2017).
- [26] William E. Urschel. *Machine for building walls*. United States Patent Office, 1941.
- [27] C. Y. Yap et al. "Review of selective laser melting: Materials and applications". In: *Applied Physics Reviews* 2.4 (2015), p. 041101. doi: 10.1063/1.4935926. eprint: <https://doi.org/10.1063/1.4935926>. url: <https://doi.org/10.1063/1.4935926>.

# OPTIMIZATION OF 3D PRINTED PAPER PASTE AND ITS PERFORMANCE ACCORDING TO SHRINKAGE FOR THE BUILD ENVIRONMENT

Dunia A. Abdullah Agha

Ulrich Knaack

This Article presents an experimental study to produce 3D printed paper models from pulped cellulose. An optimization for 3D printing paste is investigated in terms of improving shrinkage and deformation after drying to reach a better degree of structural integration, accuracy, and quality. The considerations that are taken to achieve 3D printed paper production are: i) the ability and the ease of extrusion of the mixture, ii) optimization of the mixtures to fit the nozzles for lowest shrinkage and maximum possible buildability. The parameters that were studied are the selectivity of the materials, changing cellulose and filler types, the components proportions of the mixture, and reducing the water content as possible without affecting the extrudability. Finally, models of potential applications are demonstrated with their design as functional products for serving façade engineering. Therefore, such products need ensured 3D models that have been developed and tested to be standing up to the product's requirements and quality. The results show that there is an optimum mixture for each nozzle (1.6mm, 1.2mm and 0.6mm) which are (Paste 11, Paste 12, and Paste 13). Paste 11 has formulation of (Cellulose:15%, water: 69.2%, CMC 7.5%, Lecithin 2.8%, Starch:5.6%). The formulation of Paste 12 is (Cellulose:15.5%, water: 71.5%, CMC 5.8%, Lecithin 2.9%, Starch:3.4%). The formulation of Paste 13 is (Cellulose:13.4%, water: 78%, CMC 3.6%, Lecithin 2.6%, chalk:2.3%). The lowest shrinkage is by paste formulation No.9. However, paste 11 has a diagonal and longitudinal shrinkage strains equal to  $(12.4 \pm 0.7)$  % and  $(1.1 \pm 0.3)$  % respectively.

## INTRODUCTION

3D printing with paper-based materials holds a promising future since it solves some issues for construction with paper cardboard like the bonding process. Additive Manufacturing (AM) is an advanced technology and considered part of the 4<sup>th</sup> industrial revolution [1]. It serves the imagination of engineers and provides the potential of creating any figuration and complex shapes. AM holds the solution to developing the construction with paper material. 3D paper printing gives freedom in design and ease in manufacturing in comparison construction with paper-cardboard for structural engineering. Traditional manufacturing methods for paper

structures are restricted and limited to serve civil engineering or architecture. Even the folding, glueing, and assembly from cardboard is considered a long and not easy process to be applied [1], in addition, it behaves as a composite material due to the employment glue. This is an advantage for additive manufacturing of paper materials, including enhanced geometrical freedom and the efficiency of the behaviour mechanism that could be customised [2], as the "design for functionality" within mathematically optimised topology or as a single consolidated part instead of multiple pieces like the cardboard construction. However, as of today, 3D printing has no recognized standards, specifications, or norms for a comprehensive list of performance requirements and

test methods for a printing mixture [2]. Also, no guidance for the identification and quantification of the printing quality, that consistent measuring methods, is available. However, from industry overlook and scientific experimental overview, the term print quality is usually referred to uniform lines of smooth outlines and have acceptable esthetic with geometric integration and considerable accuracy [3].

Wang et al. 2018 [4], Dai et al. 2019 [5] and Gauss et al. 2021[6] report on the use of cellulose in additive manufacturing and present data according to the nature of the contribution of cellulose in materials developed for AM. These data show that the use of cellulose-based materials with 3D printed materials has encouraging and promising results for shape changing behaviour and as a rheology modifier or reinforcing agent in the field of materials science, engineering, and chemistry. Cellulose and its derivative have been added to the material composition for AM by extrusion as an additive. Whether used as an additive or as a bulk material, it shows the complexity or lack of evidence for using the process. These extrusion 3D printed materials can be (i) thermoplastics, (ii) resins, (iii) other polysaccharides like alginate, chitin and chitosan, (iv) lignin, (v) starch, (vi) solid particles like glass fibre and graphite and (vii) other materials. The role of the addition of cellulose: fillers, reinforcement aids, viscosity modifiers, matrix, binders, plasticizers and excipients. From these reviews, formulation based on cellulosic material serves several key functions when employed in various applications. These functions are dependent on the purpose and the properties that the mixture formulation provides, including its role as a structural component. Each researcher has his invented kind of ideas and purposes that control his results. These results provide strength and rigidity that are required from the materials to employ the application design for. However, despite the advancements in technology, such as additive manufacturing, achieving high-quality and dimensionally accurate results remains a challenge across various materials used in AM. Furthermore, in engineering applications, the ability to scale up production for large-scale products, particularly in building components, is crucial. The starting point in this context involves identifying and utilising suitable formulations and materials that meet these specific requirements. The selection of an appropriate paste formulation is vital to ensure desired performance and compatibility with the intended use.

## EXPERIMENTAL INVESTIGATION

This section describes the selective material used, the manufacturing process and the preparations for testing, as follows:

## Input Materials

The mixture is developed from four components with water, as shown in Table 1. Each component holds a precise purpose and performs a certain function. Cellulose is the central structure of the mixture. Carboxymethyl-Cellulose (CMC) is an organic compound when mixed with water that forms a hydrogel formation. CMC purpose in the formulation is a thickening agent and a rheology modifier. It gives the adhesive effects for the components of the mixture. Lecithin is an organic base of fatty substances. The purpose of utilising lecithin with the formulation of the mixture is to improve the extrudability and flowability. The oily nature of the lecithin assists the cellulose fibres with the other components of the formulation to be easily extruded and increasing its percentage in the mixture helps increase the possibility of the mixture to deform and extrude from the nozzle.

The goal of employing filler within the formulation is to expand the number of interparticle contacts. The filler improves the extrudability and helps by stabilising the hydrogel that is formed by CMC, thus enhancing the buildability. The types of fillers used in this study are three types. The type of the filler was selected to get an optimum designed mixture that gives better results in terms of extrudability, buildability, and confined deformation and shrinkage after drying [2]. One of these filler types is calcium carbonate (chalks,  $\text{CaCO}_3$ ), which is an organic sedimentary rock that dissolves in water. The second type is starch, which is an organic substance. The starch and water mixture acts both like a solid and a liquid as a colloidal solution to a certain temperature then it dissolves with hot water formatting gelatinization. The third type is magnesium sulphate ( $\text{MgSO}_4$ ). Magnesium sulphate absorbs water to crystallise [7].

Table 1: The materials that are used in the mixture formulation [4].

Material	Properties and resource
Cellulose	Type 1: It's from conifer species found in northern forests/Canada from the company (Mercer Stendal). It's Northern Bleached Aspen Hardwood Kraft, NBHK, short fibres, the length of the fibre is 0.75 mm, and the fibre width is 27.4 $\mu\text{m}$ . Type 2: it's Northern Bleached Pine Softwood Kraft, NBSK, and elemental chlorate free, with 2.10 mm fibre length and 28.2 $\mu\text{m}$ fibre width from the company (Mercer Stendal, Germany). Type 3: Powdered cellulose (microcrystalline) from the company "Sigma-Aldrich/Merck", Germany.
CMC	Carboxymethyl-Cellulose from Würzteufel, Germany.
Lecithin	Mivolis lecithin granules from dm chain stores in Germany.
Chalk	Champagner-Kreide/Wolfgang Kenter Kalk-Laden in Germany.
Starch and $\text{MgSO}_4$	Sigma-Aldrich/Merck in Germany.

## Adopted Technology

LUTUM -VormVrij® 3D clay printer version 2.1 was used. The printer is adjusted to fit the paper material instead of a clay paste, through manipulation of the printing parameters. This printer is specified as material extrusion -AM technology, otherwise known as free-form fabrication or fused filament fabrication (FFF). This technology is based on extruding paths through material pumped and extruded through a nozzle and it is built in a layer-by-layer pattern [8].

The material extruded within this printer is semi liquid or highly viscous pasty material that deposits a filament along a defined path. After extrusion, once the material sets, it forms a bond between layers depending on the adhesion strength formulated from the material mix [9]. Then, the material solidified and gained strength to support the following layers printed on top of it. However, certain configurations such as overhangs need a particular arrangement to support the print, depending on the extruded material properties. Such geometrical design cases are treated with a specific slope, others need a supporting material. However, the printing was carried out without using supporting materials. The extruded mixture is supposed to be homogenous and has specific characteristics in terms of viscosity, consistency, and adhesive. These characteristics depend on the designed proportioning of the mixture components and identify the paste in terms of extrude ability and as being self-supported material after extrusion.

## Paste Formulation

Several trials were carried out as shown in Table 2. The aim of the formulation development is to find a suitable mix in terms of i) extrusion capability as a function of nozzle size, ii) buildability by maintaining shape retention and geometry stability when building in the height direction, iii) shrinkage, iv) adhesion properties, v) strength and vi) print quality. Nozzle size has a major influence on the choice of cellulose type to prevent blocking. This is especially the case with fine nozzles. For a 0.6mm nozzle, powdered cellulose is usually used. However, fibrous cellulose is also investigated for 0.6mm nozzle diameter, taking into account that the paste to be formed has a very soft consistency in order to be extruded smoothly without blocking. The mixtures were tested and evaluated using a rheometer according to the rheological behaviour depending on shear rate deformations and viscosity measurement of the mixtures published in [4]. The components of the formulation were prepared using heated water at 40°C, the hot water was used for the purpose of ensuring the effectiveness of the CMC chemically to form a gel and activating the adhesion property. The grained particles of the lecithin were also liquefied alone in the water at 40°C, and shaking with radial movement, the used lecithin was completely dissolved into a liquid state, before being

blended within the mixture to ensure homogeneity and spreading distributary inside the mixture.

Table 2: The proportions and percentages of mixtures formulations that were used through this study [4].

Paste No.	Variable	Cellulose	Water	CMC	Lecithin	Filler
		% by weight	%by weight	% by weight	% by weight	% by weight
1	Changing cellulose and filler type	15.5 Powder	74.6	3.8	3.8	2.3, starch
2		15.5, Pine	74.6	3.8	3.8	2.3, starch
3		15.5, Aspen	74.6	3.8	3.8	2.3, chalk
4		15.5, Aspen	74.6	3.8	3.8	2.3, Mgso4
5	Change proportions	15.5, Aspen	74.6	3.05	2.7	2.7, starch
6	Changing filler type and increasing its percentage	16, Aspen	74	4	3	3, chalks
7		16, Aspen	74	4	3	3, Mgso4
8		16, Aspen	74	4	3	3, Starch
9		13.5, Aspen	64.4	3.5	2.6	15.6, Starch
10		14.8, Aspen	69	3.7	2.8	9.7, Starch
11	Change proportions	15, Aspen	69.2	7.5	2.8	5.6, Starch
12		15.5, Aspen	71.5	5.8	2.9	4.3, Starch
13		13.4, Aspen	78	3.6	2.6	2.3, Chalk

## Deformation & shrinkage measurement

The experimental measurements were performed at TU Darmstadt, Germany. Shrinkage is measured using a microscope Keyence Model VHX-600 Digital. It has a magnification of 20x-200x, and the accuracy of 3D topography mapping is in the micrometre range. Thus, it is used to measure the dimensions before and after drying.

The shrinkage was recorded as the longitudinal and radial deformation of the filaments before and after drying. The radial deformation is assessed by determining the diameter deformation for the filament of each mixture. The result of the deformation is calculated by the difference between the values of the wet filament diameter immediately after printing and the dried filament diameter one week after printing. Each value of the longitudinal and radial deformation is an average of at least twelve measurements distributed on three marked spots (at first quarter, middle, and third quarter) of the filament for each six iden-

tical filaments. The longitudinal deformation is an average calculation for at least six identical printed filaments of 150mm length.

## RESULTS AND DISCUSSION

Shrinkage is the contraction in the size from the printed into the final dimensions, due to:

- x The inhomogeneous crystallisation (of MgSo4) that happens to the material components of the mixture, in which each component behaves differently and that induces a limited shrinkage.
- x Cross-linking between cellulose and CMC causes a moderated shrinkage.
- x Phase change from liquid to solid state during the drying process. Here, water evaporation causes a reduction in volume leading to a noticeable shrinkage. Therefore, controlling the mix formulation by minimising water and solid content has a direct influence on this factor. So, the mix that has limited water content has better shrinkage outcomes.

The shrinkage factor is one of the determinants of print production quality, that is related to dimensional accuracy and aesthetic appearance. That is why it is a limiting factor for designing and optimising the mixture formulation [10]. Figures 1 and 2 illustrate the results for the shrinkage outcomes. The results are under the room temperature, which was climatized to be  $20\text{C}^{\circ}\pm 2$ , and humidity is to be  $60\% \pm 5$ .

Figures 1 and 2 (paste 1, 2 and 3) show the effect of using different types of cellulose proving that it has effective impact on controlling the shrinkage outcomes, due to cellulose properties like the fibre length and width, percentage of curl and fibrillation within single cellulose fibre, and water retention capacity of the cellulose with the others physical properties for each type of cellulose. These factors increase interlocking within the final skeleton of the mixture formulation and help to increase the confinement of the deformation after drying. According to Figures 1 and 2, the properties of long fibre-cellulose provide higher potential than short fibre cellulose or powder-cellulose to bound the shrinkage. Filament of paste 2 has lower shrinkage percentage by 47.85% and by 50.58% in comparison with paste 1 and paste 3.

From Figures 1 and 2, the results of the filaments series (paste 3, and 4) and the series (paste 6, 7, and paste 8) indicated that the filler type has an effective influence on the shrinkage outcomes according to the filler reactivity within the water. Starch is insoluble with the water because the higher temperature which the mixture reaches is less than the temperature reactivity of the starch to gelatinize. Calcium carbonate is soluble in water. Magnesium sulphate

is crystalized with water. It's noticeable that the magnesium sulphate of (paste 4) reduces the diagonal deformation by 39.5% than the starch of (paste 3). Likewise, the results of the diagonal deformation of paste 7 (using Mgso4) are smaller by 38.7% and 40.3% than paste 6 (using chalks) and paste 8 (using starch); respectively. But from another side, Mgso4 affects the recyclability of the paper material, which gives a disadvantage since it is a chemical material. However, using starch in the mixture indirectly reduces the shrinkage when substituting the free water with solid material (less water content); this free water exists from not reacting with the starch due to insolubility; in comparison, this water already reacts with Mgso4. Thus, the paste was solidified, and the shrinkage was reduced. Also, starch is an organic substance and doesn't prevent paper material from being recyclable.

Manipulating the percentages of these components is important to clarify which components have much effect on the shrinkage results, whereas it's noticed that the increase of the lecithin dose in the mix is barely reduces shrinkage, while, increasing the filler percentage has an effective impact on the shrinkage results. The potential of reducing water content in the mixture due to starch as explained above is the aim for the next step to examine the proper percentages for the filler (starch) with the other components in a balance formulation for extrudability purposes. Where, regardless of the effect on the extrudability, the increase of using filler percentage gives a significant decrease in the shrinkage outcomes.

The results of Figures 1 and 2 in terms of the diagonal deformation of paste 9 (using 15.6% starch) are smaller by 42% and 68.4% than paste 10 (9.7% starch) and paste 8 (3% starch); respectively. The explanation is that the filler fills the areas in a distributed way due to fineness and stabilises the CMC which would limit the shrinkage outcomes. However, it is important to find the optimum ratios that achieve all factors that are essential for 3D printing in this study, which are (extrudability, buildability, shrinkage outcomes, and geometrical integration & dimensional accuracy after drying).

Finally, after more optimization and reforming for the component's percentages, the optimum percentages were reached that fit extrudability and limit the shrinkage as possible for the nozzles 1.6 mm, 1.2 mm, 0.6 mm, which is indicated by paste 11, paste 12 and paste 13; respectively.

## POTENTIAL APPLICATIONS ACCORDING TO THE FUNCTIONALITY

Functionality refers to the set of features and capabilities that a product has that enable it to carry out a specific set of tasks or operations. It defines what the product can do and how it can be used to meet the requirements or objectives that are required



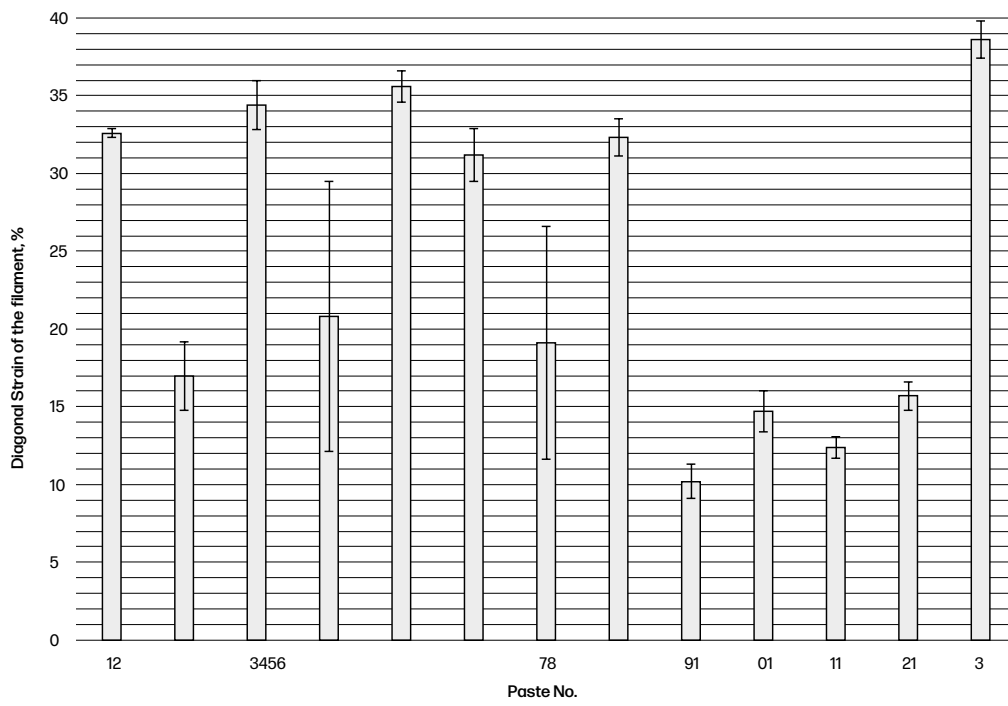


Figure 1: Diagonal deformation of the extruded filament after drying.

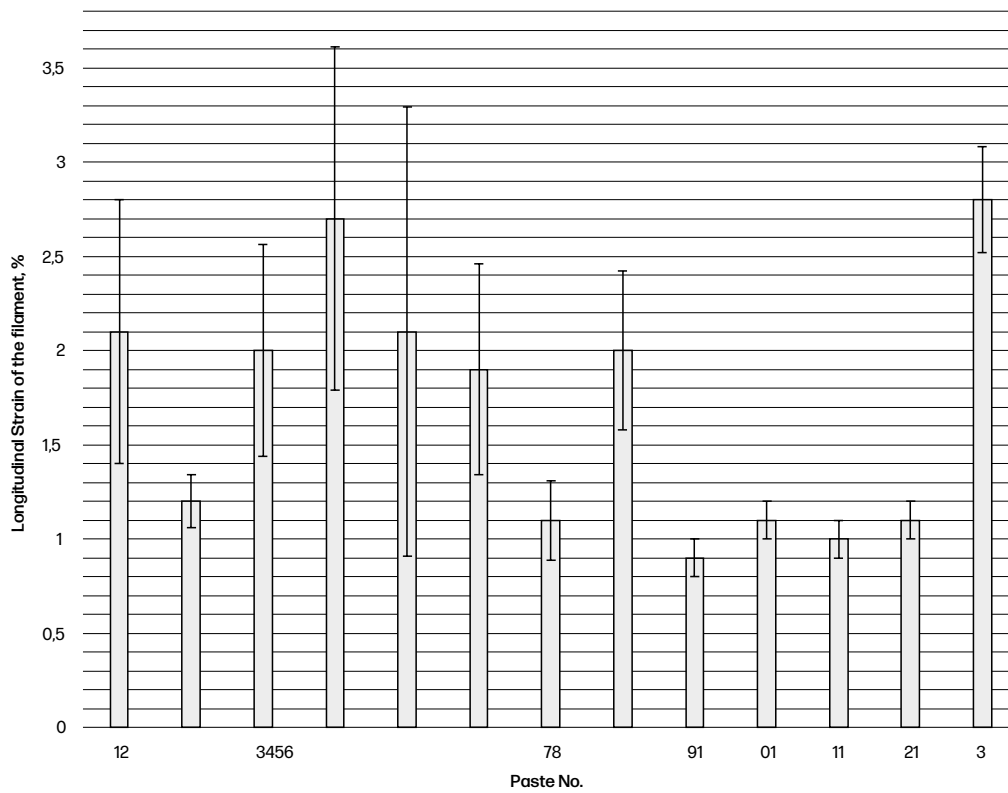


Figure 2: Longitudinal deformation of the extruded filament after drying.

### **Acoustic functionality**

This potential application fits the paper material properties for the acoustical characteristics and could be implemented to benefit the most from additive manufacturing technology. The concept is creating a complex geometry that was designed to optimise the acoustic orientation behaviour within a certain direction. A geometry that is able to trap sound inside, until total dissipation or another one able to diffuse or reflect the sound in a certain orientation. Printed models are shown in Figure 3.

### **Shading system**

The application gives the possibility to design and manufacture a complex muster/ pattern shading muster panel as 3D geometry with aesthetic and recyclable aspects and by benefiting the most from AM. it could be placed inside the gap of the double-glazing system or stuck on the windows. This design supports individuality and uniqueness which would not be reasonable to be manufactured by another technology instead of AM. The shading muster is designed by adjusting the pattern & infill thickness for the benefit of privacy (vision blackout) or shade intensity- light inlet. Figure 4 and 5 displays examples.



Figure 3: 3D paper printed models for acoustical purpose.



a)

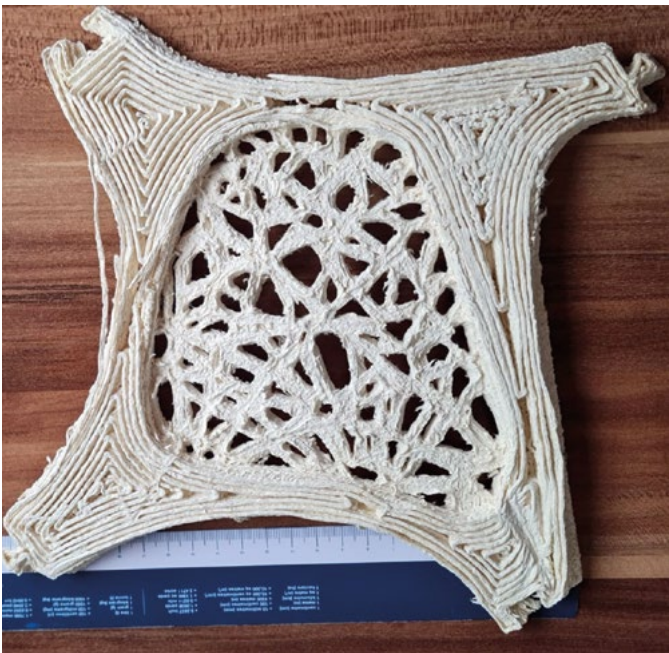


b)

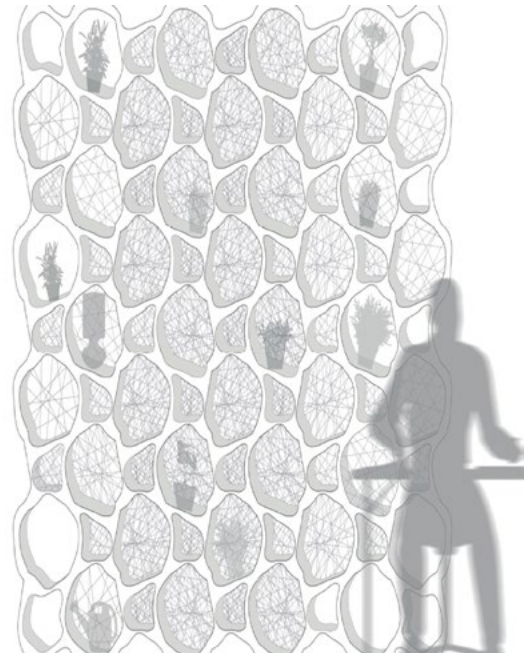


c)

Figure 4: 3D paper printed model for shading and acoustic functionality(a), during printing(b), and its visualisation (c).



a)



b)

Figure 5: 3D paper printed model of shading wall (a) with its visualisation (b).

## ACKNOWLEDGEMENTS

This research is funded by the German Academic Exchange Service (DAAD) as a scholarship grant Funding program/ ID: Research grants - doctorates in Germany, 2018-2023/ (57381412).

## REFERENCES

- [1] H. Bruck, Y. Chen, and S. K. Gupta, Eds., "Manufacturing in the Era of 4th Industrial Revolution," *World Scientific Reference*, vol. 1: *Recent Advances in Additive Manufacturing*, March 2021. DOI: 10.1142/11898-vol1.
- [2] M. Xia, B. Nematollahi, and J. G. Sanjayan, "Development of Powder-Based 3D Concrete Printing Using Geopolymers," in *3D Concrete Printing Technology*, J. G. Sanjayan, A. Nazari, and B. Nematollahi, Eds. Butterworth-Heinemann, 2019, pp. 223-240. DOI: 10.1016/B978-0-12-815481-6.00011-7.
- [3] J. Schirmer, J. Roudenko, M. Reichenberger, S. Neermann, and J. Franke, "Print Quality Assessment by Image Processing Methods for Printed Electronics Applications," in *2018 41st International Spring Seminar on Electronics Technology (ISSE)*, 2018. DOI: 10.1109/ISSE.2018.8443617.
- [4] Q. Wang et al., "3D Printing with Cellulose Materials," *Cellulose*, vol. 25, no. 8, pp. 4275-4301, 2018. DOI: 10.1007/s10570-018-1888-y.
- [5] L. Dai et al., "3D Printing using Plant-derived Cellulose and its Derivatives: A Review," *Carbohydrate Polymers*, vol. 203, pp. 71-86, January 2019. DOI: : 0.1016/j.carbpol.2018.09.027.
- [6] Ch. Gauss, K. L. Pickering, and L. P. Muthe, "The use of cellulose in bio-derived formulations for 3D/4D printing: A review," *Composites Part C: Open Access*, vol. 4, p. 100113, 2021. DOI: 10.1016/j.jcomc.2021.100113.
- [7] D. Abdullah Agha and U. Knaack, "Additively manufactured paper products from cellulose-pulped fibers and its quality according to rheology and 3D printing performance," in *Structures and Architecture Viable Urban Perspective?*, 1st ed., CRC Press, 2022. ISBN 9781003023555.
- [8] B. Redwood, F. Schöffler, and G. Garrent, "The 3D printing Handbook: technologies, Design, and applications," Amsterdam: *3D hubs* B.V., 2018.
- [9] R. Naboni and N. Jakica, "Additive manufacturing in skin systems: trends and future perspectives," in *Rethinking Building Skins/Transformative Technologies and Research Trajectories*, Woodhead Publishing Series in Civil and Structural Engineering, 2022, pp. 425-451. DOI: 10.1016/B978-0-12-822477-9.00004-8.
- [10] C. Thibaut, "Development of fibrous cellulosic materials for the production of bio-based 3D printed objects by extrusion," Université Grenoble Alpes, 2020.

# 3D PRINTING WOOD FOR CUSTOM-DESIGN WINDOW FRAMES

Christopher Bierach

Serdar Aşut

Alexsander Alberts Coelho

Michela Turrin

Ulrich Knaack

Given the urgent sustainability goals, the construction industry is actively seeking renewable and recyclable biobased materials. In this research, cellulose and lignin, the most abundant biopolymers on earth, were studied as fundamental building blocks to create an innovative bio-based material to 3D print elements for the construction industry. Having obtained a 3D printable paste, the study presented in this paper delved into the 3D printing possibilities by using a clay extruder mounted on a robotic arm. A window frame was used as test case, addressing the existing gap in replacing or enhancing current window frames. To better understand the printing process and explore various geometric configurations, a section of a window frame was printed as proof of the concept.

Given the expected population growth to 10 billion by 2050 according to the United Nations [2], alongside the pressing issues of global warming and resource depletion, it's crucial for the built environment to act promptly. This sector is a significant source of human-made greenhouse gas emissions, as highlighted by Pablo Van der Lugt [3]. Buildings globally consume 30% of energy [2] and produce 27% of CO2 emissions, including those from materials like concrete, steel, and aluminum. These materials also contribute to 4% of energy use and 6% of emissions. Overall, the building sector is accountable for a significant 37% of global energy consumption and process-related emissions [4]. To reach global zero net carbon emissions by 2050, utilizing low-car-

bon materials like wood, including hardwood, softwood, and bamboo, is a viable option [3]. These natural materials are anticipated to remain abundant in the next century.

Nevertheless, there are benefits and drawbacks to utilizing wood. Trees take a long time to grow, and wood production generates waste and CO2 emissions from processing and transportation. While wood is valuable, it strains wood resources and forests [5]the current waste wood and paper recycling practices (S1. Timber harvesting requires careful management to avoid overexploitation [6] and Russia boasts the largest forested area in the world. Economic development entails various challenges for the environment, including a lack of forestry legislation or

compliance, poor governance and unrestrained privatisation. This study investigates the role of institutional quality in explaining deforestation using panel-time series data for 75 Russian regions from 2009 to 2019. We apply a one-way autoregressive fixed-effect model with Driscoll-Kraay standard errors due to spatial dependence and time lags across Russian regions. The findings affirm the hypothesis of the environmental Kuznets curve for deforestation, implying that after surpassing a threshold point of gross regional product per capita, deforestation decreases. Poor institutional quality significantly increases the deforestation rate, which remains robust when considering the timber harvesting volume. The results affirm our proposition that the Russian forestry preservation policy is somewhat effective in reducing the deforestation rate. The empirical findings reinforce the importance of improving institutional quality for preserving forest areas toward carbon sequestration and overall Sustainable Development Goal agendas.”,“container-title”:“Forest Policy and Economics”,“DOI”:“10.1016/j.forpol.2023.102949”,“ISSN”:“1389-9341”,“journalAbbreviation”:“Forest Policy and Economics”,“page”:“102949”,“source”:“ScienceDirect”,“title”:“Economic growth, institutional quality and deforestation: Evidence from Russia”,“title-short”:“Economic growth, institutional quality and deforestation”,“volume”:“150”,“author”:“{{‘family’:‘Sohag’,‘given’:‘Kazi’}},{{‘family’:‘Gainetdinova’,‘given’:‘Anna’}},{{‘family’:‘Mariev’,‘given’:‘Oleg’}}”,“issued”:“{{‘date-parts’:[[‘2023’,‘5’,‘1’]]}”,“schema”:“https://github.com/citation-style-language/schema/raw/master/csl-citation.json”}. Thus, the construction industry needs alternative bioresources alongside wood. This research paper explores a new wood-like biocomposite using cellulose and lignin from local biomass waste streams through 3D printing, suitable for the building industry.

Cellulose and lignin are the most abundant natural biopolymers on earth, with cellulose known for its mechanical strength and reinforcement potential included in the 3D printing [7] including 4D (responsive/smart [8]). Lignin, the second most abundant natural material globally [9], holds potential for novel materials [10]. Together, cellulose and lignin mimic timber’s characteristics without relying on trees. 3D printing can allow adjustable mechanical properties and complex structures, offering a renewable, recyclable biocomposite from local biomass for the building industry. Within this overarching research line, that focuses on 3D printed window frames, whether to refurbish existing frames or fabricate new ones for complex buildings. The research follows a bottom-up approach, from developing a biocomposite through blending powder-base cellulose and lignin, to reassembling its structure into a window frame through 3D printing. After conducting tests and experiments with the materials and processes, the results inform and guide the window frame’s design, considering the limitations and advantages of 3D printing with wood waste.

## MATERIAL AND PRINTING PROCESS

Various combinations of cellulose and lignin in different proportions with different binders were studied for use in 3D printing. Among the binders, Methylcellulose outstand in delivering the most promising properties when combined with lignin and cellulose [11]. It formed a consistent paste, exhibiting the adhesion and viscosity needed for cold paste extrusion 3D printing (Figure 1).

With the resulting paste, various 3D printing tests were performed at LAMA (Laboratory for Additive Manufacturing in Architecture), at the TU Delft Architectural Engineering and Technology Department. An LDM WASP extruder XL 3.0 [12] was custom-built to be mounted onto a UR5. To evaluate the potentials and limitations of the cold extrusion 3D printing process multiple factors were considered when designing a set of experiments and tests. Various geometric shapes, including overhangs, overlapping layers, infills, and different forms, were modelled using Rhinoceros (McNeel). Additionally, ‘Robots’ a Grasshopper plug-in was employed to program and simulate the robotic arm [13]. Separately, a slicing software was used to control the rotation of the extruder. The desired shapes were printed using a pressurized system for material extrusion, with a nozzle diameter of 4 mm, a pressure of 2 bar, and a print speed of 2000 mm/s (Figure 2).

First, printing straight and curved elements at a specific height was investigated, while progressively tuning printing parameters and paste formulation. The challenges of printing extruded polygons such as squares, and diamonds were analyzed, including based on their tendency to buckle and eventually collapse during printing. Extruding the paste with 4 mm wide nuzzles at 2000 mm/s allowed producing elements up to 30 mm high, where the structural stability of models with a circular boundary was higher, as expected (examples in Figure 3).

Structural stability during printing increased also based on the design of the infill. Wider layers and reduced layer heights improved stability but obviously came at the cost of increased weight, reduced corner resolution, and a tendency for straight walls to buckle and collapse (Figure 4).

Additionally, studying the overlapping of a single tool-path to connect all its edges enhanced stability. The geometry was contoured at a 3 mm height with a 1 mm overlapping between edges (Figure 5).

Lastly, overhangs were tested to allow more geometrical freedom for the desired printed shape but failed at a 20-degree angle. Despite these failures, a custom infill design was made to provide adequate support without adding extra load on the inclined walls (Figure 6).

These preliminary tests proceeded in parallel with initial mechanical characterization of the 3D printed material, part of which is published in [11], and served to address the research on material development and 3D printing, which



Figure 1: Preliminary studies on extrusion of Methylcellulose with lignin and cellulose using a syringe.

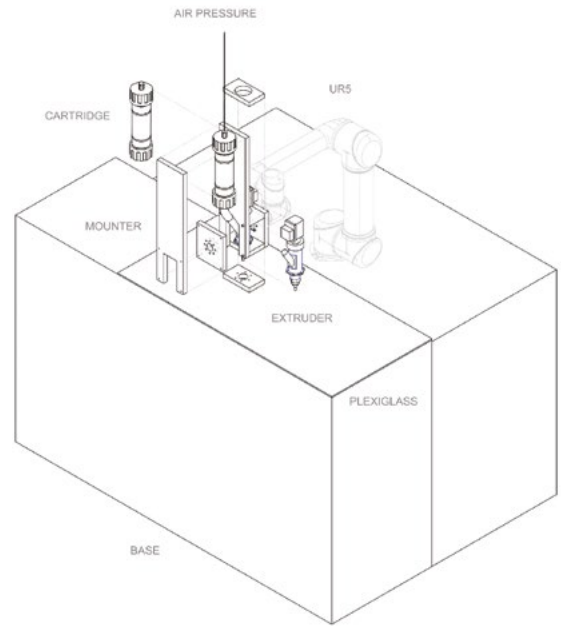


Figure 2: Printing setup with customized tool.



Figure 3: Preliminary geometry testing.



Figure 4: Toolpath testing.



Figure 5: Infill testing.



Figure 6: Overhand testing.

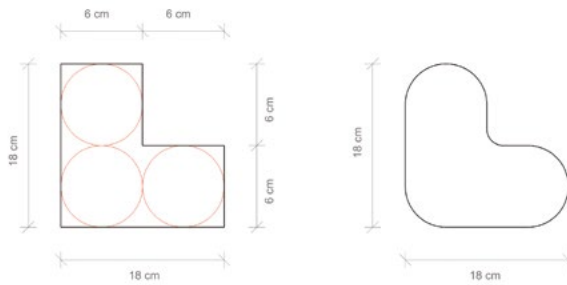


Figure 7: Plan view of straight vs curved edges.

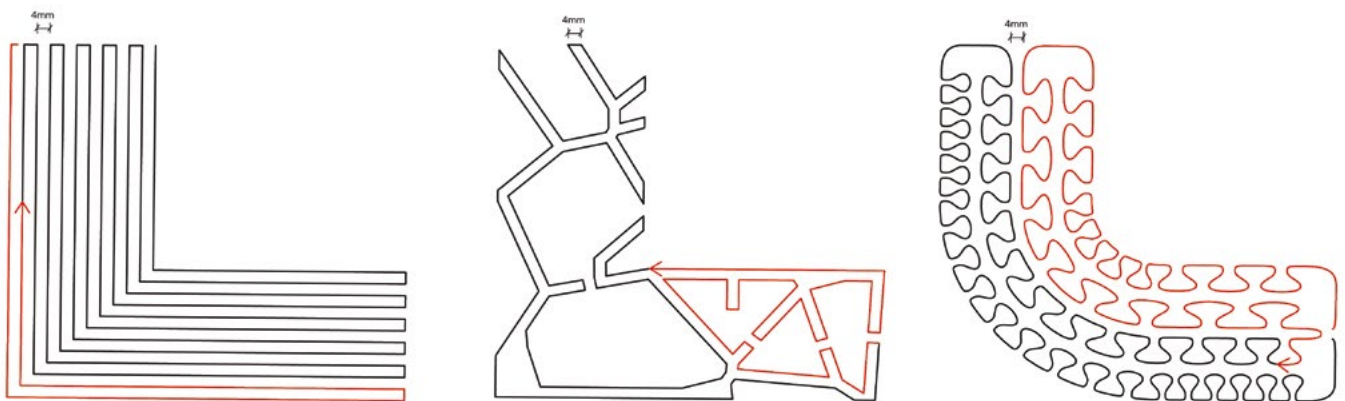


Figure 8: Toolpath restriction [drawing made by author].



proceeded based on iterative loops of testing and reformulating the material and process. They served also to indicate the preliminary boundaries of a design grammar, then used in a design exercise, for which the 3D printing logic was key. Along with the advantages of 3D printing in terms of geometric freedom, the considerations on the better stability of curved structures compared to deformations of straight walls; on the limits of overhang angles; on the shape proportions to facilitate shape stability during printing; on the importance of infills' design to prevent overloading inclined surfaces; and on similar aspects tuned to the specificities of the new material were considered.

## DESIGN CONTEXT

The design exercise is contextualized in a broader vision. The overall context regards the potentials for (i) refurbishment of wooden window frames, and (ii) new window frames for 3DP buildings.

The issue of decaying wooden window frames due to water exposure and other aging factors is a prevalent concern in building maintenance and renovation. When focusing on automation, renovating a decaying wooden window frame with 3DP presents several compelling advantages. Firstly, it can allow preserving the window's original aesthetics with precise replication of intricate details. Additionally, 3D printing offers customization to fit specific dimensions and design preferences, which can ensure a perfect fit as mass-produced frames fail to address individual needs. Moreover, it promotes sustainability and minimizes waste as it can preserve the original frame while only replacing the deteriorated sections. Utilizing 3D printed customized elements with wood can provide effective solutions for the existing building stock, heritage projects and building renovations, where custom solutions are beneficial.

3D printing offers potentials also for new windows frames, for example when including complex geometries or when interfacing complex geometries. This latter occurs for example in 3D printed buildings [14], which currently make use of conventional and standard components. Applying conventional components on 3D printed (concrete) structures sometimes implies a misalignment in architectural language and a technically challenging interface with the surface texture of 3D printed walls [15]. These issues encompass design compatibility, structural integration, waterproofing, insulation, and aesthetics. The intricate, often curved designs of 3D printed walls may not align seamlessly with traditional flat window frames, where a poor connection potentially causes leaks and reduced insulation. A reason for this is that typical elements such as window frames are fabricated via traditional manufacturing processes that lack the advanced construction technology necessary for

producing complex shapes at competitive costs. The tectonics of 3D printed structures invites rethinking traditional components, creating innovative design options for windows and openings too [16]. As 3D printed walls are being increasingly investigated, exploring options to incorporate components like 3D printed window frames can open beneficial avenues.

With this context in mind, the design exercise regarded 3D printed wood in building construction with focus on window frames.

## DESIGN EXPLORATION: LIMITATIONS & ADVANTAGES

The design exercise experimented on a corner part of a window frame, which was designed and fabricated as a proof of concept for the "3D printing wood" process. The first aspect that required reconsideration was the boundary shape of the frame. Reflecting on our earlier tests involving various geometric shapes, it became evident that using straight lines would increase the challenges, for which the use of curved shapes was maximized, in the attempt to distribute stresses evenly during printing and maintaining a consistent material flow. Figure 7 shows an example of the design logic.

As the design exercise was conducted in a preliminary stage of the material development, when exceeding 4 cm in height could have easily resulted in buckling and collapse during printing, the overall height of the printed structure was set to a max of 4 cm per piece. Taller objects were designed by considering the assembling of multiple sections, by first splitting the complete piece into smaller segments later integrated to form a unified whole. At this stage of the material development, another challenge related to the shape fidelity, with the difficulty to predict the deformations during printing, for example due to shrinkage when drying. While research on morphological characterization of the 3D printed material is needed, this preliminary exercise coped with it in an empiric manner. The exercise dealt also with the weight of the overall structure, aiming to minimize the use of material. While in a more advanced phase of the research (when material properties are characterised) computational (topology) optimization opens clear avenues, at this stage the exercise considered general geometric features with focus on printability of elements with inner cavities. The main objective was to create a single and continuous toolpath that could be printed without interruptions. The designed geometry should provide the necessary support for the overall structure, necessitating the path to overlap with itself. A preliminary study was conducted, comparing straight, curved, and Voronoi shapes (Figure 8). The path including most curved elements resulted prefer-

able not only for stability during printing but also to facilitate the inclusion of other printed elements toward minimization of assembling and of use of e.g. adhesives. Consequently, the final toolpath for the cavities was designed by maximizing the use of curved elements.

While the exercise did not aim to technically address the inclusion of sealing gaskets and other needed features, yet it intended to speculate on future approaches for their integration. In this light, it was important to account for the sill, frame, sash, gasket, and glass in the design and printing process (Figure.9). When utilizing a 3D printing approach to wood construction, integrating crucial features that a window frame necessitates, like a sealing gasket, calls for a thoughtful approach to implementing for example locking mechanism using a suitable infill pattern. The frame and sill could potentially be combined into a single printed element. The sash could be excluded since the gasket could be directly integrated into the curved infill of the frame. In this scenario, the single frame and sill would be printed as one piece, and a separate material, semi-flexible, would be employed to print the gasket. At this preliminary stage, this line of thoughts allowed for easy insertion and locking of the gasket into the frame. The glass sheet would then be carefully fitted and held in place by the gasket. Given that window frames required precision between elements and typically had a standard size, considering the nozzle diameter was important. Hence, a 4 mm nozzle was utilized to ensure a higher definition and an accurate model.

## PROOF OF CONCEPT

After studying the parameters for 3D printing with methylcellulose in combination with lignin and cellulose, encountered challenges and potentials became the central driving force to design and fabricate the window frame as a proof of concept (Figure.10). Another limitation is regarding the maximum payload of the robotic arm, which was 5 kg. Consequently, with the custom-built holder weighing 4 kg, there was a small margin of 800 g of material to be used in one single print. Therefore, the design exercise considered these limitations to understand the possibilities of printing a 180x180x100 mm object. Thus, four different parts were printed and later combined. One printed section for one full cartridge would take 40 min to print 21 m of material. After 7 days, the four separate elements were dry and had shrunk by approximately 10 to 15 percent. As expected, the shrinkage of the material challenged the assembling for large objects, resulting in misalignments between the previous and ongoing printed layers, yet offered a test case to better understand the material behaviour. Lastly, it was observed that the printed infill was too dense, affecting the drying time of the pieces as air could not flow easily inside

the cavities. Nevertheless, the curved infill system demonstrated the feasibility of connecting and receiving other components, such as a gasket, without the need for additional sealants or adhesives.

## DESIGN VISION

As the material development proceeds, this design exercise showcased the potential for 3D printing a window frame – for example to replace specific components of a wooden window frame (Figure 11).

Considering the broader context of 3D printed a single window frame, two distinct scenarios are noted, on-site printing and off-site printing. Printing in a facility offered the advantage of a controlled environment, simplifying the printing process. The frame could be easily integrated into the house, either during or after the printing phase, providing better control over material shrinkage, geometrical complexity, and finishing. However, the challenge lay in maintaining the overall quality of the frame while avoiding staggered parts. The integral printing of the frame was pivotal in achieving a satisfactory result. The printed parts, initially done on a flat surface, would later be flipped to a ninety-degree angle for integration into a wall (Figure 12, Figure 14).

This orientation could introduce thermal bridges due to the exposed cavities. Solutions may include filling the cavities with additional material or 3D-printed gaskets, although the airtightness of the printed layers might remain a challenge. On the other hand, printing frames on-site (Figure.13, Figure.15) allowed greater flexibility for 3D printed habitats.

An enhanced recipe, enhancing printability capabilities, could potentially enable printing at greater heights and varied inclinations. In an ideal scenario, the wooden frame would serve as scaffolding for the wall, allowing synchronized printing with two distinct materials. On-site printing permitted staggered printing between both materials, ensuring a perfect fit between components in a wet state (Figure. 16).

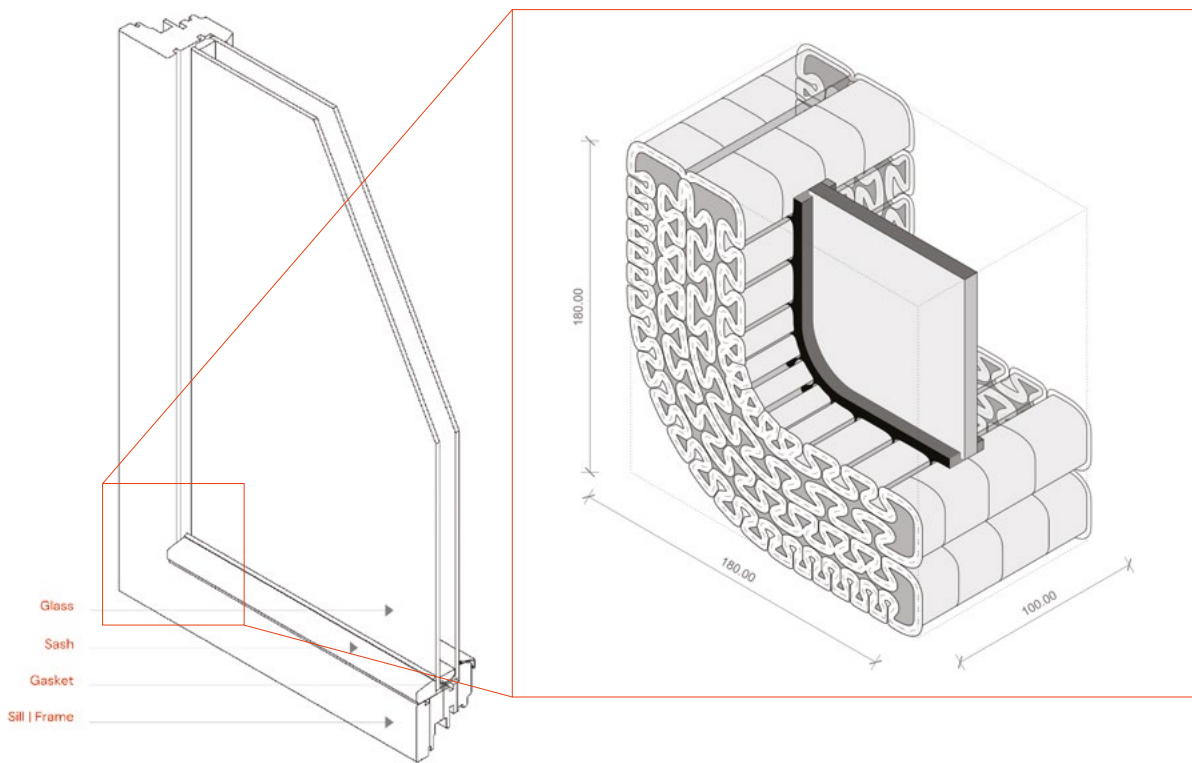


Figure 9: Axonometric view of typical wooden window frame vs 3DP optimized corner of a window frame.



Figure 10: Final 3D-printed window frame.

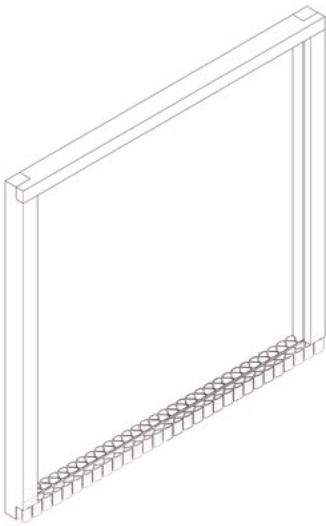


Figure 11: Replace part of the existing window frame with 3DP wood.



Figure 12: 3D printing a window frame horizontally in the factory.



Figure 13: Construction process when placing dried frame to wet printed wall.

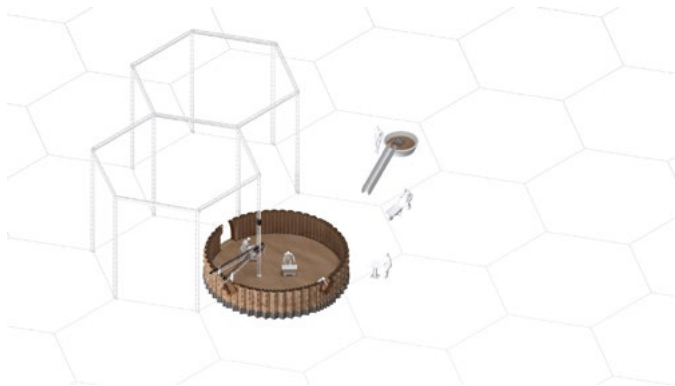


Figure 14: Vertical 3D-printed window frame printed on-site.



Figure 15: Construction process, printing wooden window frame and 3DP wall simultaneously.

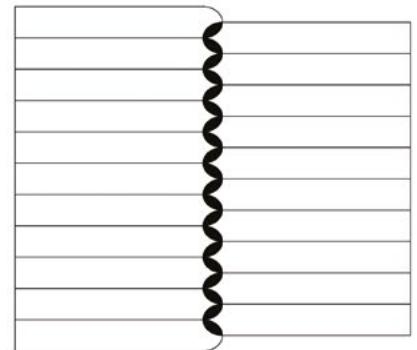
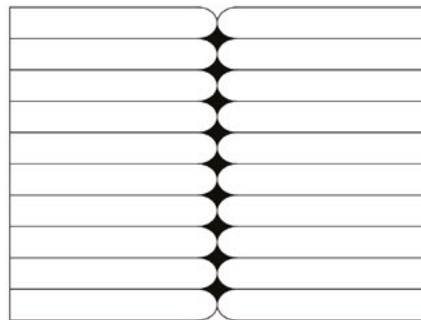
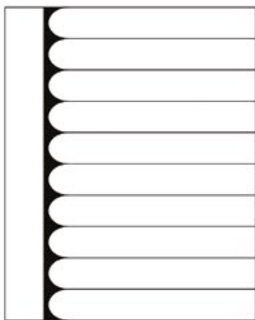


Figure 16: Diagram to describe the connection between flat and 3D-printed elements to 3DP elements when printed separately, and 3D-printed elements when printed together.

## CONCLUSION

The objective of this research was to develop an application as a proof of concept towards using wood-like natural material sourced from recycled materials, customized for 3D printing. This includes preserving existing constructions through non-destructive techniques and employing low-carbon construction methods utilizing natural materials that can be recycled into building components. The main outcome of the material research was a fully bio-based composite using a natural binding agent—methylcellulose—mixed with cellulose and lignin, resulting in a smooth and well-structured paste with viscosity and adherence suitable for 3D printing.

During the printing phase, it was observed that the challenges lay in balancing material behaviour with printability. Design decisions and extrusion parameters played a significant role in addressing these challenges. Curvilinear structures were more stable compared to straight walls, which tended to buckle. Overhang angles were limited, and heavy geometries tended to collapse. Infills needed careful design to avoid overloading inclined surfaces.

These challenges influenced the design and fabrication of a 3D-printed window frame, showcasing the potential for replacing or customizing window frames in 3D-printed buildings. The printed frame was exhibited at the Built Environment Additive Manufacturing (BE-AM) symposium of 2022 [17]. The technology and material are envisioned to be used to replace or create customized window frames. However, it's important to note that the material is still in development, also toward improvements of its structural properties, needed for applications demanding higher strength and stiffness.

Although promising proof of concepts were created, further research and refinement of the material properties are necessary. If the current composite is improved to enhance printability, it could enable printing at different inclinations and offer customization. On-site printing is another potential application, enabling staggered printing with different 3D-printed materials for a perfect fit between components. However, it requires investigation into various printing orientations for 3D printed window frames and their implications on load-bearing capacities. These considerations set the stage for future research into optimal integration scenarios and effective treatment of 3D printed window frames for the building industry.

## ACKNOWLEDGMENT

The “Wood Without Trees” research initiative is an ongoing research line involving the Digital Technologies Section and the Architectural Technology Section of the Architectural Engineering & Technology department at the TU Delft Faculty of Architecture and the Built Environment. The article is based on the master's thesis of the alumni Christopher Bierach and alumni Alexsander Alberts Coelho, supervised by the co-authors. D. Richard Gosselink, the Coordinator of Wageningen UR Lignin Platform, provided valuable guidance and support in sourcing lignin and cellulose materials. The authors appreciate the equipment provided by ir. Paul De Ruiter for 3D printing at LAMA, the TU Delft Laboratory for Additive Manufacturing in Architecture.

## REFERENCES

- [1] "Architectural Engineering and Technology." Accessed: Oct. 10, 2023. [Online]. Available: <https://www.tudelft.nl/bk/over-faculteit/afdelingen/architectural-engineering-and-technology>
- [2] "2022 Global Status Report for Buildings and Construction | UNEP - UN Environment Programme." Accessed: Oct. 02, 2023. [Online]. Available: <https://www.unep.org/resources/publication/2022-global-status-report-buildings-and-construction>
- [3] Pablo Van der Lugt, *Tomorrow's Timber*. Material District, 2020.
- [4] "IEA - International Energy Agency - IEA." Accessed: Oct. 02, 2023. [Online]. Available: <https://www.iea.org/reports/tracking-buildings-2021>
- [5] A. L. Bais, R. Sikkema, M. Vis, P. Reumerman, M. Theurl, and K. Erb, "Assessing wood use efficiency and greenhouse gas emissions of wood product cascading in the European Union," JRC Publications Repository. Accessed: Oct. 02, 2023. [Online]. Available: <https://publications.jrc.ec.europa.eu/repository/handle/JRC103048>
- [6] K. Sohag, A. Gainetdinova, and O. Mariev, "Economic growth, institutional quality and deforestation: Evidence from Russia," *Forest Policy and Economics*, vol. 150, p. 102949, May 2023, doi: 10.1016/j.forpol.2023.102949.
- [7] C. Gauss, K. L. Pickering, and L. P. Muthe, "The use of cellulose in bio-derived formulations for 3D/4D printing: A review," *Composites Part C: Open Access*, vol. 4, p. 100113, Mar. 2021, doi: 10.1016/j.jcomc.2021.100113.
- [8] J. Yang *et al.*, "Cellulose, hemicellulose, lignin, and their derivatives as multi-components of bio-based feedstocks for 3D printing," *Carbohydrate Polymers*, vol. 250, p. 116881, Dec. 2020, doi: 10.1016/j.carbpol.2020.116881.
- [9] D. S. Bajwa, G. Pourhashem, A. H. Ullah, and S. G. Bajwa, "A concise review of current lignin production, applications, products and their environmental impact," *Industrial Crops and Products*, vol. 139, p. 111526, Nov. 2019, doi: 10.1016/j.indcrop.2019.111526.
- [10] S. Bertella and J. S. Luterbacher, "Lignin Functionalization for the Production of Novel Materials," *Trends in Chemistry*, vol. 2, no. 5, pp. 440-453, May 2020, doi: 10.1016/j.trechm.2020.03.001.
- [11] C. Bierach, A. A. Coelho, M. Turrin, S. Asut, and U. Knaack, "Wood-based 3D printing: potential and limitation to 3D print building elements with cellulose & lignin," *Archit. Struct. Constr.*, vol. 3, no. 2, pp. 157-170, Jun. 2023, doi: 10.1007/s44150-023-00088-7.
- [12] "Extruder for ceramics - LDM WASP Extruder XL 3.0," Shop | WASP | 3D printer sales. Accessed: Oct. 08, 2023. [Online]. Available: <https://www.3dwasp.shop/en/prodotto/extruder-for-ceramics-ldm-wasp-extruder-xl/>
- [13] "Home," GitHub. Accessed: Oct. 08, 2023. [Online]. Available: <https://github.com/visose/Robots/wiki/Home>
- [14] "First resident of 3D-printed concrete house in Eindhoven receives key." Accessed: Oct. 02, 2023. [Online]. Available: <https://www.witteveenbos.com/news/first-resident-of-3d-printed-concrete-house-in-eindhoven-receives-key/>
- [15] "Qatar // Expo 2022 Floriade – Expo Pavilion Group." Accessed: Oct. 02, 2023. [Online]. Available: <https://www.expopaviliongroup.com/dubai-expo-2020-algeria-1>
- [16] "OPENINGS IN 3D PRINTING WITH EARTH," IAAC Blog. Accessed: Oct. 02, 2023. [Online]. Available: <https://www.iaac-blog.com/programs/openings-3d-printing-earth/>
- [17] "Booklet 2022," BE-AM. Accessed: Oct. 08, 2023. [Online]. Available: <https://be-am.de/booklet-2022/>

# ADDITIVE MANUFACTURING WITH BAMBOO: MECHANICALLY INFORMED INFILL WALL MADE WITH BAMBOO DUST AND FIBERS

Jasmine Wong

Serdar AŞUT

Stijn Brancart

This paper explores the use of bamboo in Additive Manufacturing (AM), specifically towards the development of a building component. The presented study uses bamboo in the form of dust and fibers, which can be sourced from waste streams. This innovative approach not only offers a solution to the challenges of bamboo's anatomy but also has the potential to use bamboo in a more circular way. With this approach, rather than being discarded at the end of its life cycle, bamboo products can be recycled and transformed into valuable powder and fibers, granting them a second life. By leveraging the benefits of additive manufacturing technology, such as reduced material waste and the ability to fabricate complex geometries, the design aimed to create a mechanically informed infill tailored to the loading condition of the building component. After use, the component can be re-introduced into a new mixture to be used in a new AM application, enabling circular use. The project involves a comprehensive workflow, including material research, design development exploration, manufacturing process exploration and prototyping.

## INTRODUCTION

The rapid population growth contributes to a considerable increase of the amount of raw materials used and produced worldwide [1]. The aim to create more ecologically friendly and sustainable construction processes has boosted interest in the use of bio-based materials. Timber, for instance, has been a prominent choice, but its availability is constrained as the demand should not exceed responsible forestry. Bamboo, a non-wood species, holds promise as a potential substitute to wood due to its rapid growth rate. It is a very adaptable plant that can grow well in a variety of climates and elevations, which enables it to contribute

to the alleviation of demand for wood as a source of raw materials [2].

This research aims to reimagine the use of bamboo. Often, when bamboo-based products reach the end of their life cycle, they are discarded. To enhance sustainability, we propose a method to recycle the material by reducing it into powder and fibers and creating new products with it. A promising technology that can facilitate the increased utilization of bamboo in this manner is Additive Manufacturing (AM). AM techniques, which have seen significant advancements in the past decades, have also made their way into the building sector, traditionally slower in adopting innovations. These additive manufacturing technologies

offer the potential to reduce labor costs, minimize material waste, and enable the fabrication of complex geometries that are challenging to achieve using conventional production methods.

While AM technologies for concrete and steel structures have made significant progress, the research and application of AM with bamboo for architectural purposes still lag.

This research addresses this gap by developing a building component made with bamboo using AM technology. By leveraging the benefits of AM and utilizing bamboo as a renewable and versatile material, this research seeks to promote sustainable practices in the field of architecture.

## BAMBOO COMPLEMENTING WOOD

Humanity is facing a serious resource dilemma as a result of global consumption and population growth as well as an addiction to fossil fuels. This has led to a rise in interest in bio-based materials as a means of creating environmentally friendly and construction and manufacturing processes.

Bio-based materials and goods are made from renewable resources, which, in contrast to many mineral and fossil resources, regenerate more quickly than they are used [3]. A replacement of materials manufactured from renewable resources immediately lowers CO<sub>2</sub> emissions since most bio-based materials are produced with far less energy than materials like aluminum, steel, and concrete and act as carbon sinks by storing carbon during their growth [3].

Although using bio-based products has many advantages, it also has some limitations. Depletion also results from overexploitation caused by demand that exceeds natural reproduction and responsible harvesting.

According to Ashby, the demand for wood will be impacted by material consumption, which is anticipated to increase over the next 25 years at a 2.8% annual rate [4].

Large-scale reforestation initiatives are required to increase the production capacity of the wood sector in order to support this expansion and the effort to increasingly replace techno-cycle materials. Alternatively, faster-growing plants like bamboo, hemp, flax, seaweed, miscanthus; and cork, as well as various types of algae and fungus like mycelium, may play a significant role in this booming bio-based economy [5].

Bamboo production is seen as a promising climate change mitigation technique due to its quick growth cycle (Fig. 1). Bamboo has highly interesting development characteristics because, in its second and third weeks, it grows quickly longitudinally [6].

The main findings of this project emphasize the potential of bamboo as a sustainable material for construction

through AM. A versatile and optimized building material can be created by utilizing bamboo in powdered and fiber form, which can be sourced from waste streams. This waste can include offcuts, trimmings, and bamboo parts that are not suitable for the primary end products or that have reached the end of their life cycle, such as a fractured bamboo pole typically employed in scaffolding.

## MECHANICALLY INFORMED INFILL THROUGH ADDITIVE MANUFACTURING

AM presents a distinct advantage in terms of material waste reduction compared to traditional processes like milling. This advantage arises from its capacity to precisely deposit material solely within the object's volume. The resulting form freedom allows to develop shapes that are more efficient in transferring the loads that are imposed on them, thus reducing resource use. This study applies such a mechanically informed workflow on the design of a self-supporting wall element with integrated bench.

This workflow identifies areas where material is necessary and where it is not, all while optimizing the overall structural efficiency and minimizing material consumption.

The initial concept for this research was to demonstrate the potential of the novel material and fabrication technique. Therefore, the design had to be carefully considered to incorporate the capabilities of the selected mixture and AM technology.

The aim is to create a mechanically informed infill that is tailored to the loads on specific parts of the building component. The design process began through a computational model by lofting different sections of a partition wall and benches on both sides (Fig. 2).

The design was heavily influenced by the novelty of the material and the fabrication process, to allow for a more efficient production process, the study focused on a specific section of the overall design (Fig. 3).

AM enables the realization of complex designs, not only in terms of visual aesthetics but also in terms of performance. Through the use of computational design and performance analysis, the material distribution of the component can be optimized within a specified space, considering loads and boundary conditions. This optimization process involves iteratively refining the material distribution.

To optimize the use of material and create a mechanically efficient infill, it is important to consider that the load on the component is not uniformly distributed. Therefore, it is unnecessary to have the same density in the entire geometry. It is a more efficient approach to create an infill that is mechanically informed and tailored to the loads on specific parts of the component.



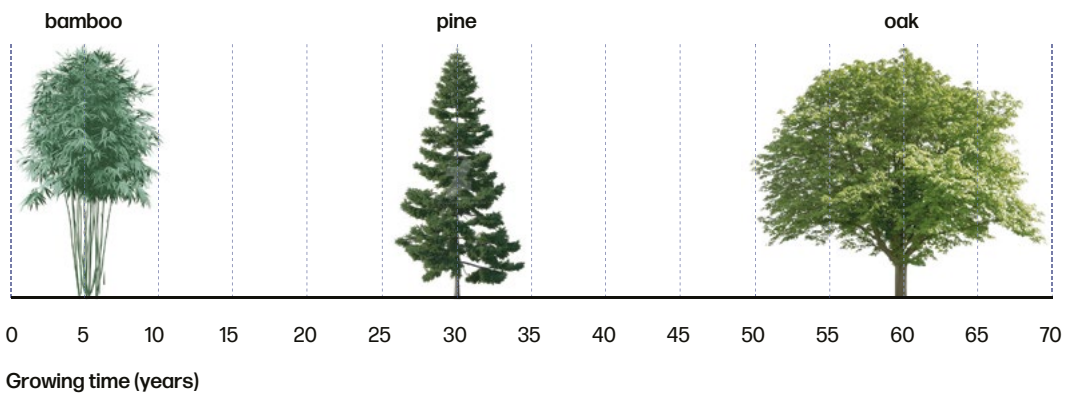


Figure 1: Bamboo, Pine tree and Oak tree growing time [11].

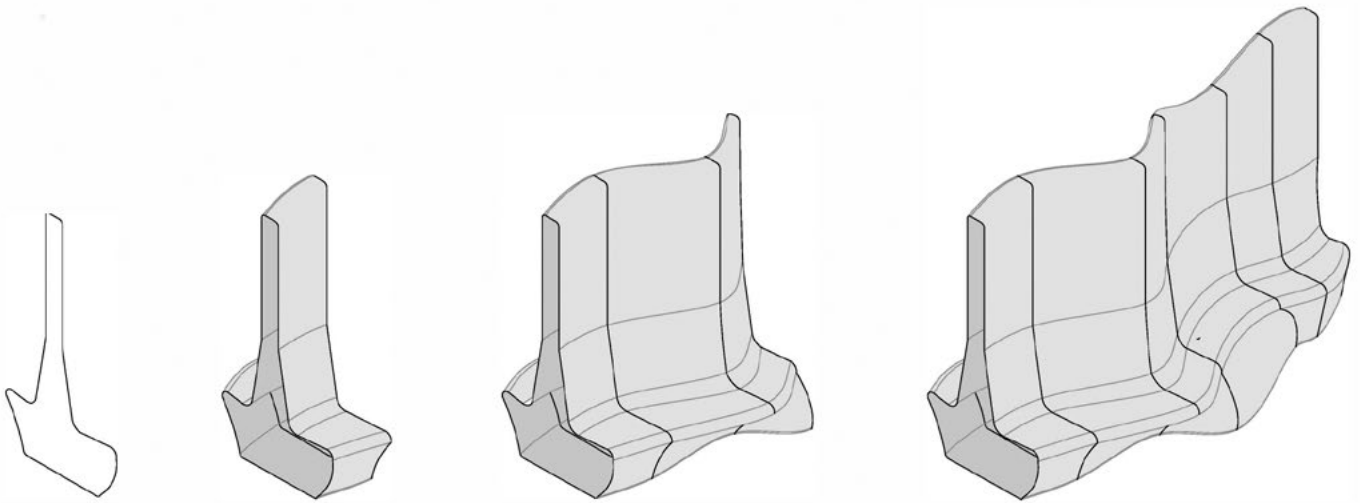


Figure 2: Lofted Design.

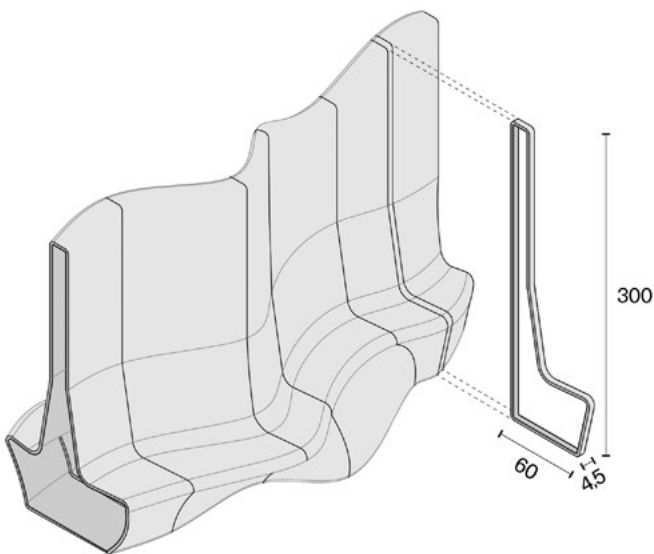


Figure 3: Chosen section.

Figure 4 shows the computational workflow for the mechanically informed infill generation. A structural analysis determines the optimal density distribution within the infill. This analysis involves mapping the density of the infill based on the variable cell size and arrangement. The goal is to identify areas that require higher density to withstand greater loads, as well as regions where lower density can be employed without compromising structural integrity. Once the density mapping is established, the component is designed to generate the toolpath necessary for printing it using a robotic arm.

The workflow begins with generating the mesh geometry of the solid component. After defining the type of support and load conditions a structural analysis generates a color gradient that represents the stress distribution within the component. In this colored mesh, points that are closest to 0% stress are automatically identified as attractor points. The pattern generation is then created, and the center point of each geometry is connected to the closest attractor point. The thickness of the infill is inversely proportional to the distance of the two points, meaning that shorter distances result in thinner thicknesses.

## MATERIALS

The raw materials employed in this research were primarily bamboo fibers and dust (Fig. 5).

Bamboo is a viscoelastic and anisotropic material that exhibits differences in physical and mechanical properties along its three orthogonal axes, with variations being more significant along the length of the culm due to the tapered shape and increasing density with height [7].

Bamboo presents impressive versatility, with the potential for nearly 100% material utilization in most cases. Among its various applications, bamboo culms are the most widely used, finding purpose in products ranging from chopsticks to furniture and crafts [7]. In the construction industry, bamboo can serve as a viable replacement for traditional building materials across several components, including trusses, roof structures, walls, flooring, foundations, and scaffolding [8]. Still its adoption in this industry remains limited due to the challenges posed by its hollow tube anatomy and the lack of established building codes for its use. Furthermore, bamboo's physical and mechanical qualities are affected by moisture content, age, and the location on the stem [7].

Waste can be generated from products at the final stage of their life cycle or from leftovers, cuttings, and parts unsuitable for final product assembly.

## MATERIAL EXPERIMENTATION

Although AM processes and technologies have recently advanced, there are still urgent research needs to create new sustainable materials [9]. The most popular AM process for bio-based materials are extrusion-based techniques, which are also employed in this research project, more precisely liquid deposition modeling (LDM). Although there are many different kinds of pastes, they may all be thought of as viscous liquids that are created by combining one or more solid elements with a liquid. The primary focus of this study is composite pastes. Binders and fillers are the minimum number of constituent kinds required to create composite paste materials [10].

With the goal of formulating a fully bio-based recipe, a series of experiments was conducted to study the behavior of various bio-based binders, both individually and combined in different ratios.

The material experiments aimed to comprehend the behaviour of bamboo dust and fibers when combined with various binders and solvents, with the objective of creating a stable bio-based composite with optimum viscosity and bonding properties suitable for extrusion via LDM technique. This exploration was carried out in two phases.

In the first phase of the material experiments, the focus was on exploring the binding agents that could be used to develop an extrudable paste. Initially, water was used as a binder to test the extrudability of bamboo dust. Therefore, different bio-based and non-bio-based binders were explored as potential alternatives.

The proportions of the binders were determined through empirical research. The binder was first mixed until it reached a glue-like consistency, and then the bamboo dust was gradually added until it formed a paste. The paste was then introduced into a syringe and pressure was applied to extrude the material. This process was repeated for each binder, with the uniformity of each experiment being assessed before the bamboo dust was added.

Material ratios were calculated throughout the material mixing procedure. Then, in order to compare and evaluate the different recipes, material qualities such as extrudability, bio-based content, shrinkage and strength were examined. The most potential recipes were improved upon and classified for comparison.

After the initial phase of material experimentation, it was determined that a second phase was necessary in order to achieve a more comprehensive evaluation of the mix and to refine key parameters for optimal printability in regard to the AM setup.

During the second phase, each binder was exclusively mixed with bamboo dust, as well as bamboo dust combined with fibers, to facilitate an effective comparison process. The results (Fig. 6) indicate the presence of some specimens that broke or bent during the drying process, categorizing them as faulty.

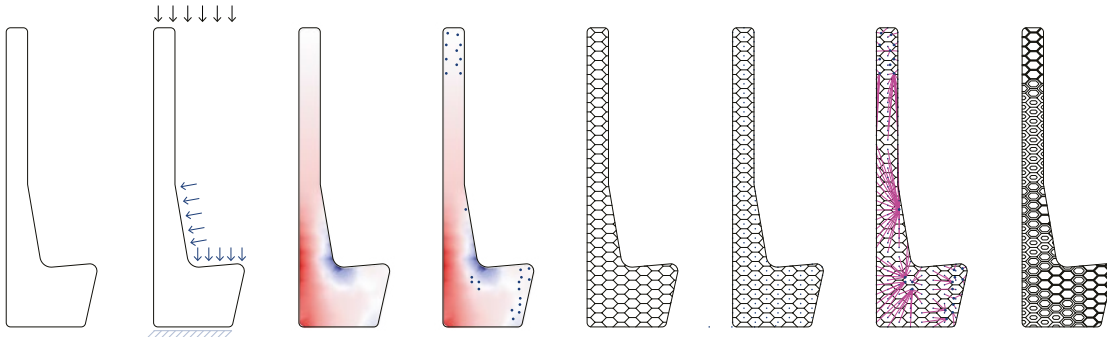
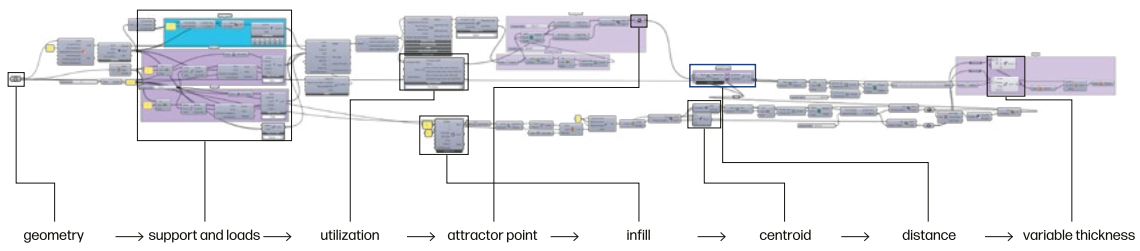


Figure 4: Mechanically Informed Infill Generation.



Figure 5: Bamboo dust (left) and Bamboo fibers (right).

Filler / Binder	Bamboo dust 0100	Green Bamboo dust <i>Sasa tsuboiانا</i>	Dust + Fibers 0100 + 200400 SF	Green Dust + Fibers <i>Sasa tsuboiانا</i> + 200400 SF
Corn starch				
Potato starch				
Tapioca starch				
Gelatin				
Xanthan gum				
Collagen Peptides				
Eco-glue				
Wood glue				

Figure 6: Results of the Second Material Experimentation.



Figure 7: Mixture Procedure.

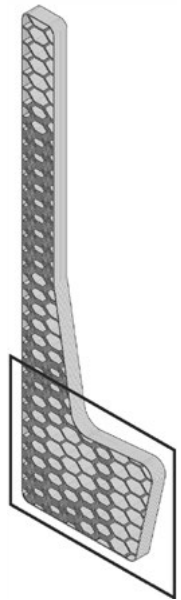


Figure 8: Chosen fragment.

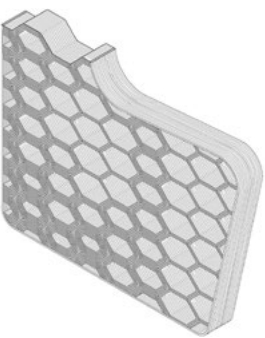


Figure 9: Fragment toolpath.



Figure 10: Printing Process of the Prototype.

The optimal three mixtures, that included the use of potato starch, COLLALL eco-glue and wood glue as binders, were chosen based on a simplified mechanical test and other factors such as printability, cost, and bio-based content. The testing process revealed an interesting correlation between potato starch and eco-glue, as the latter is derived from potato starch. To ensure an effective and efficient testing process, only one binder was chosen for the initial printing test. Consequently, potato starch and eco glue were selected, with potato starch being the more cost-effective option.

The selected mixture is subsequently manufactured in large quantities for the following AM application. This formed the basis for the next phase of the research, which focused on creating an extrudable and printable paste for the AM of a self-supporting wall made from bamboo dust and fibers.

## MATERIAL PREPARATION

A large quantity of the selected mixture made with bamboo dust and fibers and potato starch, needed to be produced in order to proceed with the printability test to explore the potential of the selected mixture through AM. After various iterations of different proportions, the optimal consistency was achieved by using specific amounts of each ingredient.

The process of creating the paste involved several steps (Fig. 7), starting with weighing all the necessary ingredients.

The potato starch was then combined with cold water and mixed until fully dissolved. A pan was placed on a heating stove and the mixture was continuously stirred in it until it boiled. After approximately 7 minutes, a thick paste was formed, and the mixture became transparent. The mixture was then cooled in the mixer for a brief period before adding 1/3 of the dust and starting to mix. Another 1/3 of the dust was added, followed by half of the fibers. The remaining fibers were added, followed by the remaining dust. The mixture was mixed thoroughly until it became a thick paste ready for printing.

By following these steps and using the clay mixer, the optimal potato starch mixture was produced and ready for further testing in the printability test.

## FABRICATION

The printing process involves two crucial factors that need to be controlled: the amount of extrusion and the movement, which are managed by the extruder and 6-axis robotic arm.

In order to streamline the printing process, we utilized the LDM WASP extruder XL 3.0 for controlling extru-

sion. It should be noted that the extruder can only be used with the Delta WASP 40100 Clay according to the manufacturer WASP, and thus, a custom wiring arrangement and extruder holder were constructed to enable the prototyping to be conducted using the robotic arm.

The primary objective of this research is to provide proof of concept for printing with bamboo. To achieve this, a 1:1 scale fragment of the design, explained in the Mechanically Informed Infill section, is prototyped. It was not feasible to print the entire prototype due to limitation of the robot work space, available materials, and tools, therefore a fragment of the overall design was prototyped. The selected fragment corresponds to a specific area within the component, which is determined by the reachable working area of the robotic arm (Fig. 8).

The chosen fragment focuses on the bottom part of the component, as it encompasses the three different types of infill designs. This selection allows for a comprehensive representation of the infill variations within the design and demonstrates the capabilities and potential of the proposed approach. In order to achieve successful printing, it is crucial to generate a continuous and uninterrupted toolpath. To address this requirement, a toolpath was meticulously designed and simulated with the robot arm to ensure optimal printing results (Fig. 9).

Consideration was given to the distances between the walls, taking into account the findings from the printability exploration phase. This approach was implemented to prevent any potential issues such as layer overlapping and ensure the integrity and accuracy of the printed prototype.

The prototype was printed on a PVC film-wrapped printing bed to simplify the removal process once it had dried. It should be noted that the consistency of the material mixture varied from one printing session to another, and even throughout the day. As a result, adjustments were made to the pressure and speed of the extruder based on the observed consistency of the material at each instance.

To prevent excessive extrusion of material, particularly when the cartridge is nearly empty and higher pressure is exerted, a precautionary measure was taken. The cartridge was refilled with material after the completion of each layer, ensuring a consistent and controlled extrusion process throughout the printing procedure. This practice helped to maintain the desired quality and integrity of the printed component (Fig. 10).

Once the component is printed, it underwent a natural drying process, with intermittent application of vinegar to prevent the growth of mold. This step is essential for ensuring the stability and durability of the printed prototype.

While the printed fragment represents a smaller portion of the overall design, it serves as tangible proof of concept and provides valuable insights into the feasibility and potential of printing with bamboo.

## CONCLUSION

This research project represents an innovative approach in the field of circularity and construction automation within the built environment. By exploring the use of bamboo in AM, it showcases the potential for sustainable material use and advanced fabrication techniques. The ability to re-use the printed component in the mixture enables a continuous printing process, reducing the need for new materials. The design process, informed by structural analysis and tailored infill geometry, showcases the potential of AM to optimize material use and create structurally efficient building components. The project addresses the need for renewable and eco-friendly construction materials, as well as the adoption of AM as a platform for material design. Through this innovative approach, the project contributes to the advancement of sustainable construction practices and highlights the possibilities for utilizing bamboo in the built environment.

Overall, this research project demonstrates the potential of bamboo fibers and dust as a valuable material for architecture through AM. The findings emphasize the benefits of incorporating bamboo into the construction industry, including its rapid growth, renewability, and versatile properties. By promoting the adoption of bamboo and AM techniques, the project contributes to circularity in the built environment and supports the transition towards more sustainable and efficient construction practices.

## ACKNOWLEDGEMENTS

We would like to extend our sincere appreciation to Johan Kocks from Bambooder and Alberto Peyron from Made in Bamboo for their generous assistance and provision of the bamboo dust and fibers required for this research. We are also grateful to Paul de Ruiter for his tremendous help in procuring the necessary equipment for 3D printing at LAMA (Laboratory for Additive Manufacturing in Architecture) at TU Delft. His availability and support were instrumental in facilitating the practical aspects of our research.

## REFERENCES

- [1] Craveiro, F., Duarte, J.P., Bartolao, H. and Bartolod, P.J., 2019. Additive manufacturing as an enabling technology for digital construction: A perspective on Construction 4.0. *Sustain. Dev.* 4(6), pp.251-267.
- [2] Borowski, P.F., Patuk, I. and Bandala, E.R., 2022. Innovative industrial use of bamboo as key "Green" material. *Sustainability*, 14(4), p.1955.
- [3] Jones, D., 2017. Introduction to the performance of bio-based building materials. In *Performance of bio-based building materials* (pp. 1-19). Woodhead Publishing.
- [4] Ashby, Michael F. *Materials and sustainable development*. Butterworth-Heinemann, 2022.
- [5] Van Der Lugt, Pablo. *Booming bamboo: the (re) discovery of a sustainable material with endless possibilities*. Materia, 2017.
- [6] Borowski, P.F., Patuk, I. and Bandala, E.R., 2022. Innovative industrial use of bamboo as key "Green" material. *Sustainability*, 14(4), p.1955.
- [7] Correal, Francisco F. "Bamboo design and construction." *Nonconventional and vernacular construction materials*. Woodhead Publishing, 2020. 521-559.
- [8] Yadav, M. and Mathur, A., 2021. Bamboo as a sustainable material in the construction industry: An overview. *Materials Today: Proceedings*, 43, pp.2872-2876.
- [9] Al Rashid, A., Khan, S.A., Al-Ghamdi, S.G. and Koç, M., 2020. Additive manufacturing: Technology, applications, markets, and opportunities for the built environment. *Automation in Construction*, 118, p.103268.
- [10] Bremmer, M., 2020. 3D Printing with Bio-Based Materials: Designing a toolkit to guide makers into sustainable material development.
- [11] Kampinga, C.A., 2016. Bamboo, the building material of the future!: An experimental research on glueless lamination of bamboo.

# GEOMETRY ACQUISITION WITH COMPUTER VISION APPLIED TO WAAM

Juan Ojeda

Ulrich Knaack, Philipp L. Rosendahl

3D printing with metal, applied to thin non-flat surfaces, requires a digital reconstruction of the 3D surface that will be used as a build plate for the wire arc welding manufacturing process. This article describes an experimental workflow of three-dimensional scanning of thin metal plates using a low-cost hardware setup with depth cameras and computer vision. The process allows users to scan, rebuild a 3D model, generate the code for the welding robot, and update the data continuously through the entire welding process. This update is required to analyse and rectify any change of the surface and the height of the welded layers. The result of this article presents the scanning workflow, the CAD 3D model, the method used to check the accuracy of the digital reconstruction, and the application of the collected data transferred as coordinates to carry out the WAAM process over a 1 mm steel plate. The long-term goal of this research is to generate a closed-loop of printing and real-time feedback to change the original printing workflow that is based on an open-loop, typical from off-the-shelf 3D printers.

## INTRODUCTION

Thin metal sheets have been widely used as a construction material for centuries, particularly in applications involving roofing and cladding. As architectural components, according to the structural stiffness required, thin sheets can be strengthened by isotropic or anisotropic stiffening techniques, enhancing the structural capacity by increasing the thickness of the material in certain areas [1]. In industries, such as automotive, aerospace and marine, it has been widely used as it can be formed into complex curvilinear shapes and attached to support structures using techniques such as rivets, bolts, or welding [2]. Steel is currently

characterised as a material capable of adopting complex shapes through the use of robots, using systems such as single-point metal forming [3].

However, the expense and complexity of the manufacturing process stem from the necessity to generate a large number of moulds for forming single panels with intricate shapes and irregular curvatures [4]. Additionally, if there is a better solution, it often involves the development of new tools and manufacturing processes [5]. This further exacerbates the challenge for the industry to adopt such costly alternatives. Moreover, when considering the option to optimise each structural requirement in a unique and specific way, such as increasing the material thickness

locally through additive manufacturing (AM) [6] along the principal stress lines [7] to develop a structurally-informed method of fabrication, the process becomes even more intricate to address.

The article discusses a significant ongoing research project aimed at developing an innovative design for manufacturing technique that combines three essential components: firstly, the free-forming of lightweight metal plates; secondly, the utilisation of depth cameras and advanced computer vision technologies for geometric reconstruction; and finally, the integration of AM on non-planar steel substrates for structural reinforcement. The focus of the article is on the development of a workflow to digitally reconstruct the intricate free-form geometries of steel plates, which plays a crucial role in planning and guiding the welding robot's path during the manufacturing process. By combining cutting-edge technologies and unconventional manufacturing approaches, this research project aims to revolutionize the production of lightweight facade components, with the potential to advance the construction industry's practices significantly.

### Additive Manufacture

AM is a resource-efficient process that is right now in the spotlight of the industry [8], where it is changing it completely with a high-speed development that has had a projected growth of CAGR 18.2% [9]. AM is used with 3D printers and robotic arms and allows for the customization of the production of final parts, reducing material waste, and adjusting according to the customer and designer's needs. As Colegrove et al. [10] describe, it is a collection of manufacturing processes where components are manufactured by breaking a CAD model down into layers, each of which are then deposited using a variety of techniques [11] that are either powder or wire based. The benefits are that today it is possible to realise high shape complexity without increasing the production costs, contrary to traditional technology [12], and opens up the possibility of load optimised design [13] printing non-planar layers onto existing objects with curved surfaces [14].

### WAAM

Related to metal 3D printing there are different technologies of AM like selective laser melting, direct metal laser sintering, binder jetting, metal sheet lamination, metal material extrusion and directed energy deposition (DED). DED consists of an energy source (usually an Electron Beam, Laser, or Arc) that is directed towards a plate or other substrate material on which it impacts wire or powder feed material and melts, leaving deposited material on the substrate. Wire arc additive manufacturing (WAAM) is a manufacturing-process of DED, based on gas-shielded metal arc welding (GMAW) that uses welding/filler wire made of carbon

steel or stainless steels that are melted by the electric arc and then solidifies in lines or spots [8]. The common setup considers a welding torch, a motion six-axis robotic arm, shield gas, and a controller for welding parameters and wire feeding. This setup allows to achieve multiple scale parts, with less geometrical restrictions that can be produced in a continuous process (Figure 1).

Users of WAAM however should be aware of issues which still need research [15] and some common limitations of AM like the print size of the bed and the part, the wait time or interpass time between printed layers, the cooling system, the end effector alignment, and a geometry that is defined by an overhang angle of 35 degrees [16]. Other ongoing challenges, which are still in the quest for a standard solution, is that WAAM applied to lightweight metal sheets involves dealing with thermal deformation. Deformation, which can cause imperfections in the shape of the weld bead, structural performance, as well as prevent the correct electrical contact that must be achieved to guarantee an adequate level of process quality by ensuring the distance of the contact tip to the workpiece [17].

### FREE-FORM GEOMETRY RECONSTRUCTION

Unlike traditional 3D printing processes that start on a flat-bed, within a controlled environment, printing on non-flat free-form substrates, or directly on site, involves a digital reconstruction of the surface or the built environment enabling the spatial coordinates to be extracted and thus generate the basis for the robot's motion code.

In the context of geometric reconstruction for AM, extensive research has been dedicated to monitoring metal printing using 2D scanning systems as a post-process to assess manufacturing quality. These studies aim to identify and address issues like porosity and inhomogeneity in printed parts [19]. However, there is relatively limited research focused on reconstruction prior to the printing process, with one notable case by Sheng et al. [18], which however relies on costly scanning hardware, such as the Microsoft HoloLens 2, priced at over €3,000.

Furthermore, the scanning equipment commonly used in the literature often includes turntables and expensive laser scanners that come with substantial costs, making them financially impractical for projects with limited budgets, particularly those outside of an established production line. Hosseinaveh et al. [20] also highlight the presence of time-consuming processes, such as using projectors to display patterns on objects or placing multiple coded markers on surfaces. These methods are employed to obtain and overlay a sufficient number of 2D images from different scenes to facilitate the creation of a point cloud.



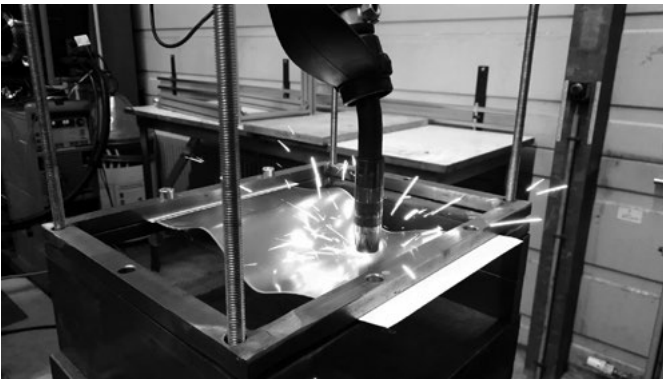


Figure 1: WAAM reinforcement of thin, lightweight, free-form steel sheet.

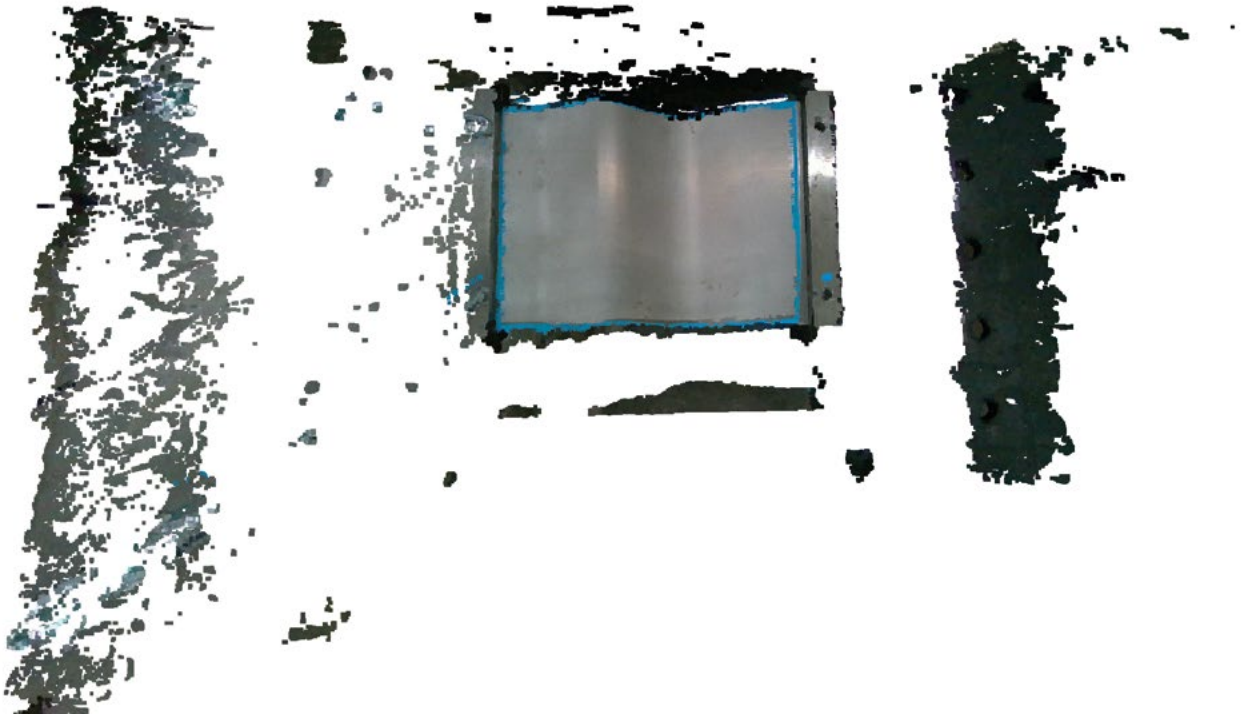


Figure 2: Visualisation of a Point Cloud: This image shows a point cloud consisting of 405,418 points captured using the Intel Realsense Viewer v2.53.1. The capture was performed with a Intel Depth Camera D405, and the visualisation was accomplished using Open3D.

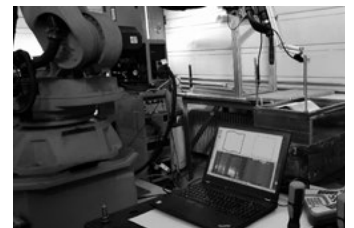


Figure 3: Geometry reconstruction hardware and software setup.

In this project, a capture and reconstruction process of a 1 mm free-form metal surface was carried out under normal WAAM laboratory conditions, without considering special lighting adjustments for the use of a depth camera that was simply attached to the robot's end effector.

To achieve an efficient and fast approach, the decision was made to work with real-time capture and analysis of a single frame instead of capturing a continuous stream of images to create a point cloud. This resulted in a reduction of data volume to analyse and significantly minimised the time needed for capturing and reconstructing the metal surface. A point cloud would involve post-production processes and result in over 400,000 points (Figure 2), whereas the single frame can be adjusted to provide less than 500 points. This drastic reduction in data allowed achieving a response time of less than 2 seconds between capture and reconstruction.

## METHOD

To test this technology, a 1 mm steel plate, chalk markers and blue masking tape were used. The hardware setup included an Intel Realsense D405 Depth camera, which was configured to run at a resolution of 1280 x 720 pixels, and connected to a personal computer using a USB 3.0 to Micro B Camera Cable. The total cost of this scanning hardware setup was less than €310. Additionally, a Fronius CMT Advanced 4000 R welding device and a 6-axis robot arm Comau Smart NM 16-3.1 were used in the setup. For software, the following tools and libraries were utilised on the personal computer: Python 3.9.12-64 with pyrealsense, numpy, opencv, flask, and ghops\_server libraries, Conda 4.13.0, OpenCV 4.5.5, Rhinoceros 3D 7, and the Intel RealSense SDK 2.53.1.4623. These components together formed the setup used for testing and experimentation in this study (Figure 3).

The sheet metal, measuring 190 x 345 mm, was subjected to plastic deformation by pressing it into a wooden mould. This mould was meticulously crafted using a CNC router. The pressing process caused the sheet metal to adopt the shape of the mould, and this plastically deformed configuration was the starting point for the subsequent geometric reconstruction process.

Due to the reflective nature of the metal surface and the limitation of the D405 camera to RGB technology, it was decided to implement a manual process of stamping coloured dots on the metal surface as a first step. This approach allowed a precise and clear definition of the points to be analysed, overcoming the challenges posed by the reflective properties of the metal. By introducing these coloured dots, a clean data acquisition process was achieved from the outset, ensuring accurate and reliable data for further analysis and reconstruction.

The process of filtering and extract the coordinates of the points on the surface of the sheet metal by colour involves several steps (Figure 4): (1) A colour detection routine is used to identify the blue colour on the sheet metal; (2) Once the blue colour is detected, a mask is applied to the image, distinguishing the regions that will be analysed with white pixels and those that won't with black pixels; (3) Contour Detection: The algorithm detects the contours of each point within the white regions of the mask. These contours represent the points on the surface of the sheet metal; (4) Geometric Centre Extraction: For each contour, the geometric centre is extracted. This centre pixel serves as the reference point for extracting the x, y, and z coordinates of the points on the sheet metal; (5) Coordinate Transfer to Grasshopper: The obtained series of coordinates are transferred to Grasshopper using Hops plugin. Hops facilitates communication between different platforms and brings the coordinates into the Grasshopper environment; (6) Reconstruction in 3D Space: Using the received lists of x, y, and z coordinates, the points are reconstructed in a 3D space relative to the camera's position, which is typically the mid-point between its two lenses; (7) Orientation Transfer: The orientation of the points is then transferred to a work plane relative to the Rhinoceros framework. This work plane can be adjusted according to the robot's location or desired work frame, and; (8) Geometric Reconstruction: The set of points is used to define a series of curves that connect the points, enabling the digital visualisation of the surface.

The workflow demonstrates notable success in achieving precision and accuracy in geometry reconstruction [Figure 5], as the resulting scanned object is consistent with the intended shape. This is evident in the visually apparent alignment with the intended shape. However, a critical consideration is the time consuming nature of the pre-processing stage when more points need to be marked, requiring manual application of the pattern for each scan. To mitigate this problem, a new approach is taken that minimises reliance on the physical pattern. Instead, a digital pattern is generated and projected onto the image, optimising the scanning process for greater efficiency.

The next version of the workflow introduces improvements and optimizations. Instead of using blue dots drawn over the surface, blue masking tape stripes are now applied to create a rectangular contour along the edges of the steel plate. (1) Blue color detection on the steel plate; (2) Mask Generation: A mask is generated to filter the relevant information; (3) Contour detection is then performed, resulting in a precise outline with an abundance of geometrically defining points; (4) However, this detailed contour with a large number of points can lead to inefficiencies in subsequent processes an approximation function is applied to simplifies the number of segments defining the polyline, preserving its essential shape. As a result, the simplified contour retains the critical features of the original shape but with significant-

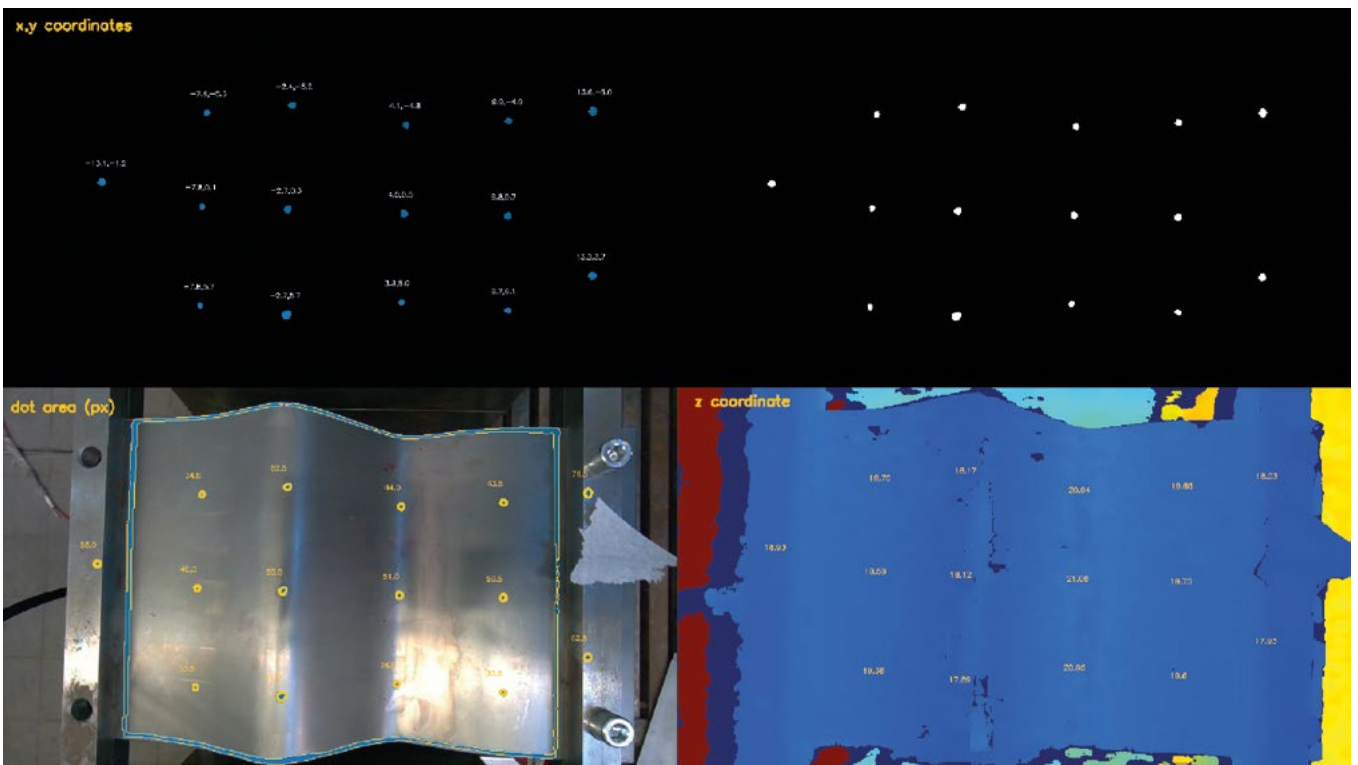


Figure 4: This image shows an overlap of steps in the data acquisition process. Mask by colour detection showing the x and y coordinates from each moment of each blue dot. Binary mask generated with the colour mask as an input. Contours from the binary image with the area size of each blue dot (the area allows to filter the contours by size). Depth colour image with the z value of each blue dot.

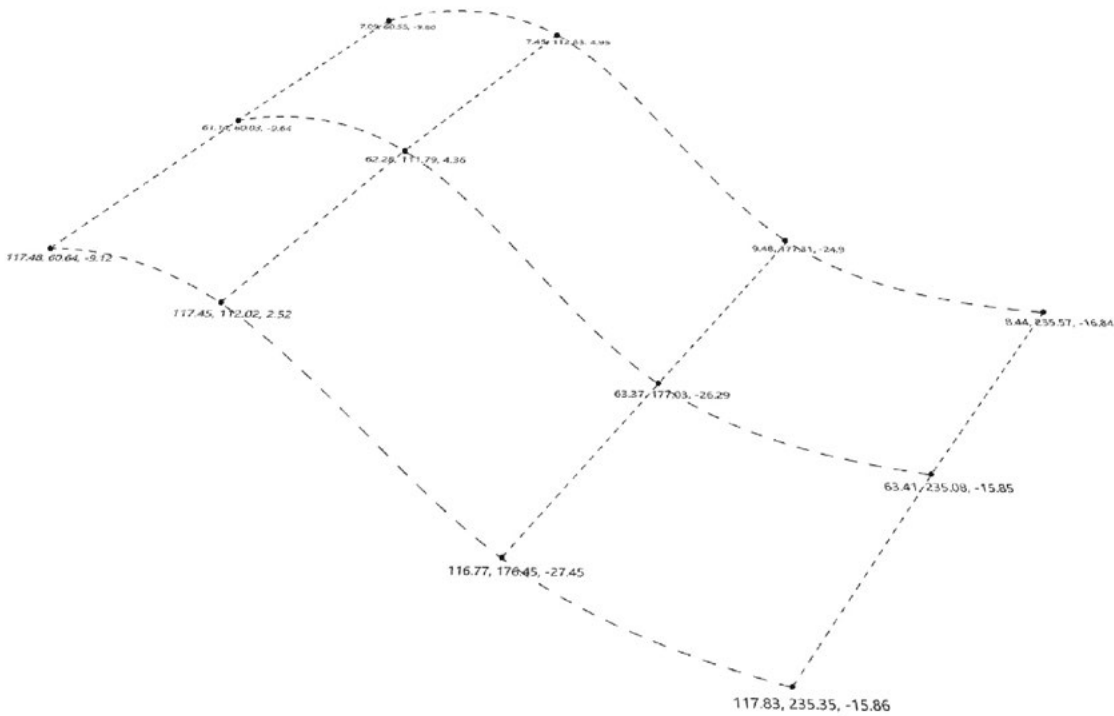


Figure 5: Digital model with the points coordinates extracted with the Depth Camera.

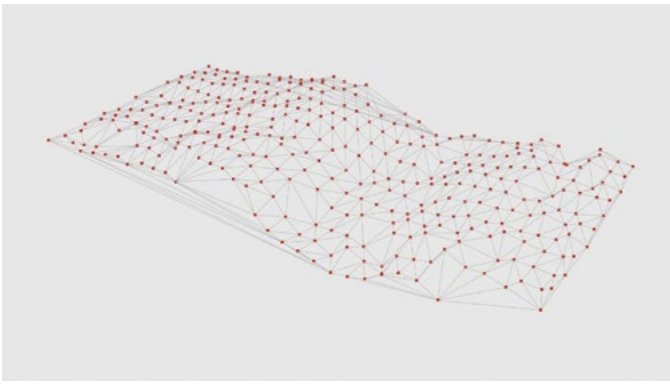


Figure 6: The image shows the inaccuracies in the position of the reconstructed points. The misalignments and discrepancies are obvious and indicate that the current reconstruction process needs further improvement.

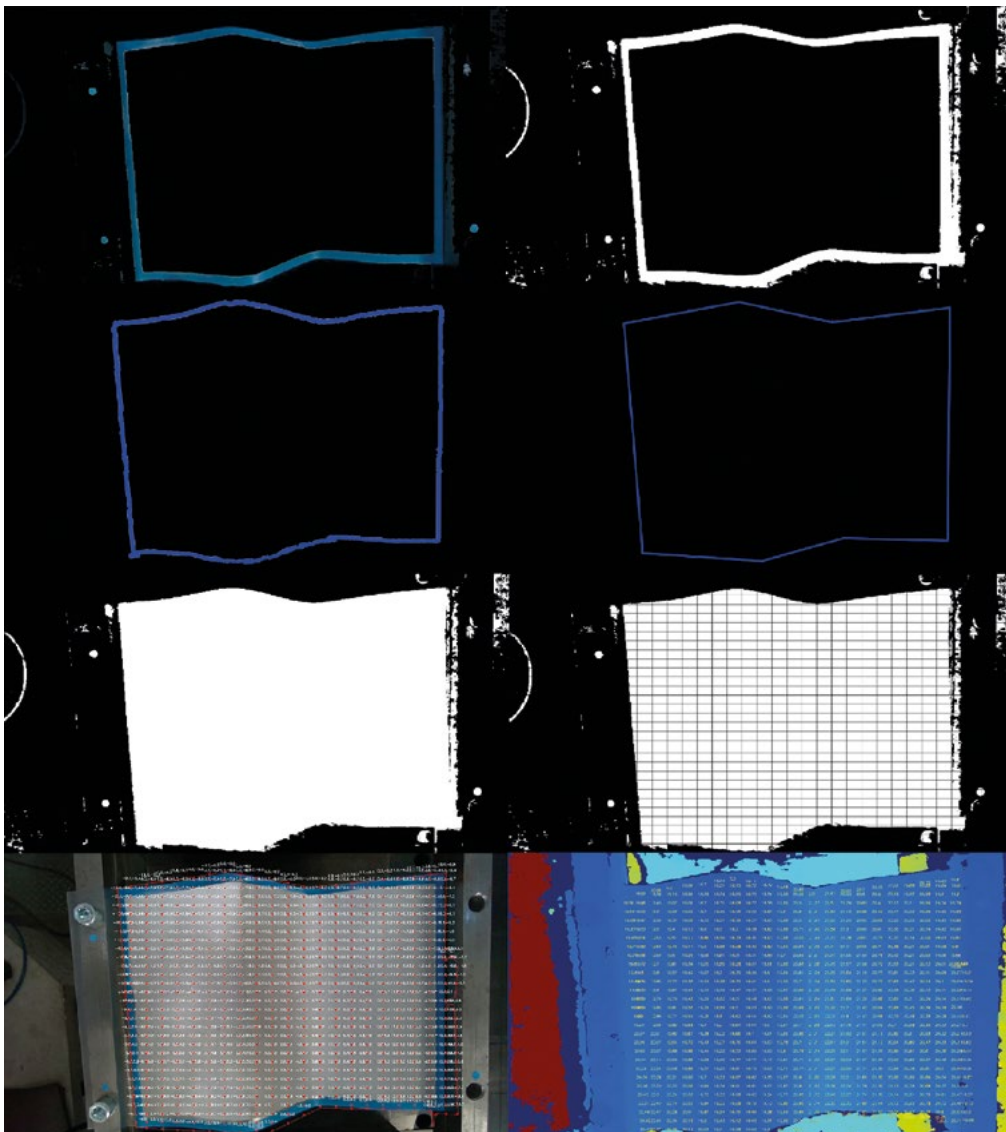


Figure 7: The image shows all the steps involved in extracting a series of point coordinates without applying coloured points. The grid of points is generated digitally, applying a grid of lines, which allows to extract all intersections by using the Harris Corner Detection algorithm.

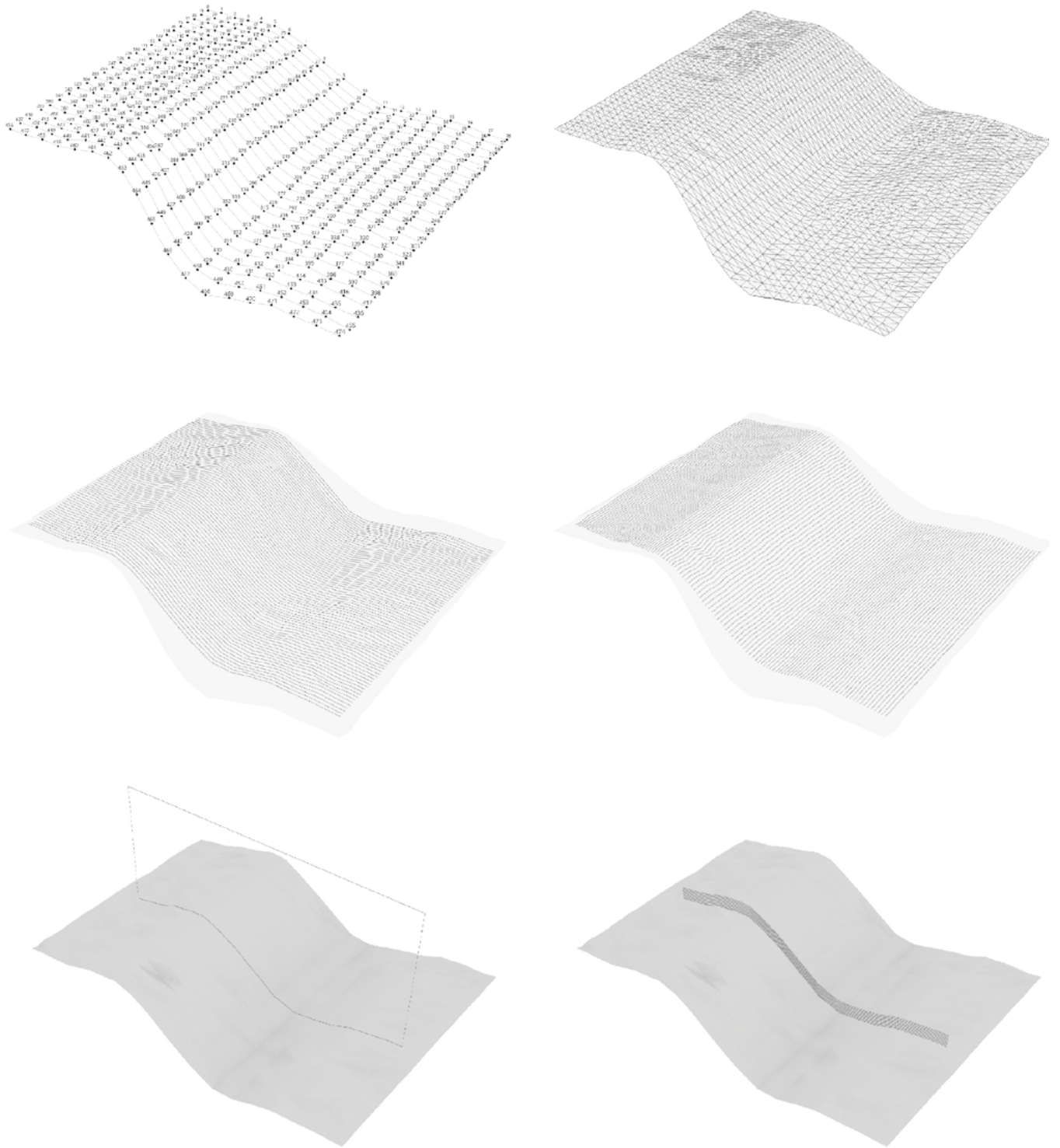


Figure 8: Digital model reconstruction.

ly fewer points. By simplifying the contour, the subsequent steps in the workflow become faster and more efficient; (5) The simplified contour is used to generate a binary mask, filling the entire surface of the plate with white pixels. This infill becomes the background for a black grid of lines projected over the white mask; (6) The Harris Corner Detection algorithm [22] is applied to detect each point situated at the intersection of the vertical and horizontal lines; (7) The centres of each grid intersection are extracted, and the x, y and z coordinates are then obtained and sent to Grasshopper. This digital process effectively marks the points similarly to how they were previously marked manually point by point, resulting in an improved and efficient methodology for reconstructing geometric information and transferring it to Grasshopper for further analysis and design.

However, in this case, the reconstruction result is not accurate [Figure 6]. The process led to irregular coordinates on the scanned surface. To investigate this issue, several tests were performed by changing the physical location of the experiment. These tests revealed that the errors are caused by the type of light reflection that occurs at certain points of the plate and the variations in lighting conditions within the environment.

In the final iteration (Figure 7), only one adjustment was made to the metal surface, which was the application of a white spray (scanning spray AESUB). This spray disappears completely from the surface after 4 hours or can be easily removed by hand. Surprisingly, the results of this last iteration are as good as those obtained with the dot pattern painted on the surface. By using the white spray coating instead of painting the dot pattern, we have eliminated the need for manual dot placement and subsequent removal. This not only reduces the time and effort involved in the scanning process, but also provides the freedom to adjust the dot density to meet the specific requirements of each scan.

The accuracy and quality of the reconstruction is not compromised with this new approach, as the results remain comparable to the method that considers the blue marker. In addition, the temporary nature of the spray coating ensures that it leaves no trace on the surface after a few hours or can be easily wiped away by hand when no longer needed.

After a rigorous and reliable scanning process, the obtained coordinates are transferred to Grasshopper, where they are used to reconstruct the accurate geometry of the metal plate (Figure 8). The key input points are then utilised to generate a Delaunay mesh [23], effectively capturing the essential features of the plate.

To ensure that the mesh precisely represents the plate's surface, a cleaning step is performed, extracting only the relevant faces and edges. Subsequently, the mesh is sliced into contours at 2 mm intervals, creating a digital surface. This digital surface acts as a canvas for projecting the lines and curves that will serve as the path for the

welding robot during the welding process. Each line is transformed into a series of correlative planes that determine the direction of movement and the angle of the end effector over the sheet metal's surface.

This integrated workflow results in an accurate reconstruction of the metal plate's geometry. The Delaunay mesh efficiently captures its essential features, while the contouring and projection steps create a digital surface that guides the welding robot precisely along its intended path. The seamless transition from scanned data to the welding phase ensures that the robot adheres precisely to the metal plate's contours.

Thanks to the reliable geometric information obtained from the scanning phase, this streamlined and efficient process guarantees a high-quality welding application.

## CONCLUSION

From the curves projected on the surface, it was possible to generate a code that allows the robot to locate itself using the coordinates of the first plane that defines the curve, start the welding process (Figure 9) and move through each of the points that describe the profile of the freeform plate. The number of points and layers sent to the robot can vary depending on the type of robot movement and the required height of the printed wall. A continuous motion was used to define the motion that connects the different coordinates.

The workflow proves that it is possible to generate a low-cost setup of a depth camera and computer vision algorithms to perform an accurate geometric reconstruction of a metal plate, which is a faster alternative to the tactile measurement and reconstruction methods used in the past [2] [18] to generate the coordinates that define a robot movement.

The next challenge is to create closed-loop systems in which tasks are generated to correct the path that the robot follows in order to avoid defects or correct imperfections during the execution of the task. These imperfections can be related to voids in the welded surface or deformations in the plate due to high temperatures and internal stresses.

## ACKNOWLEDGEMENTS

Supported by: Federal Ministry for Economic Affairs and Climate Action on the basis of a decision by the German Bundestag.

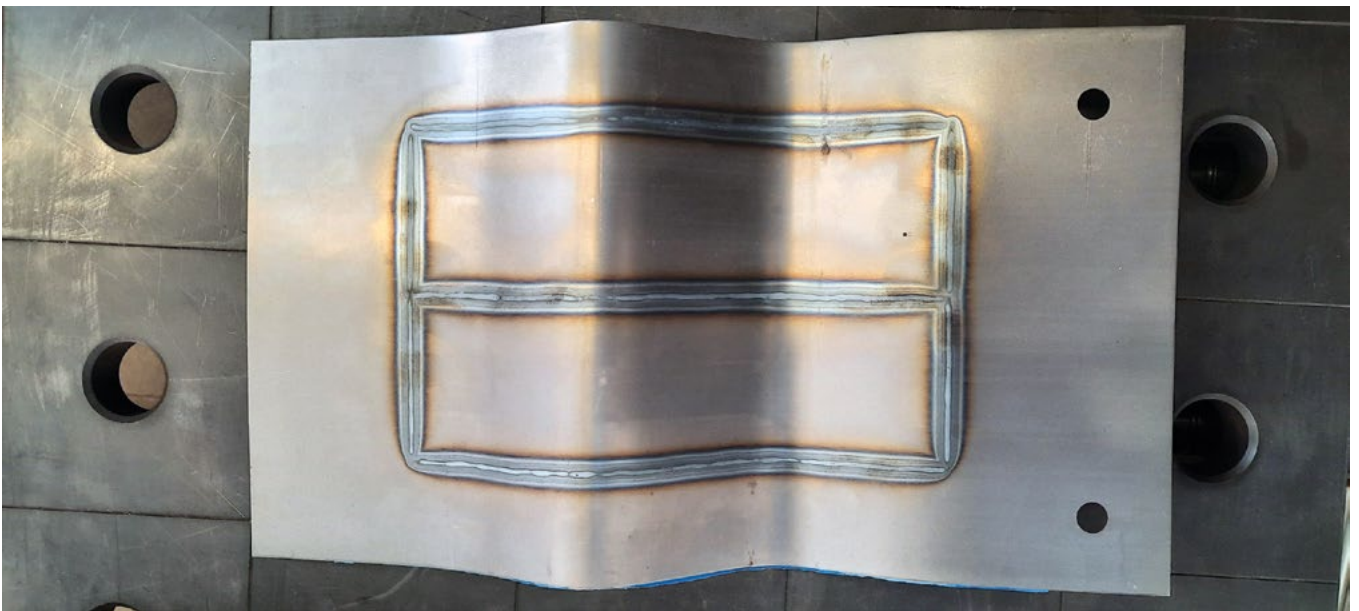
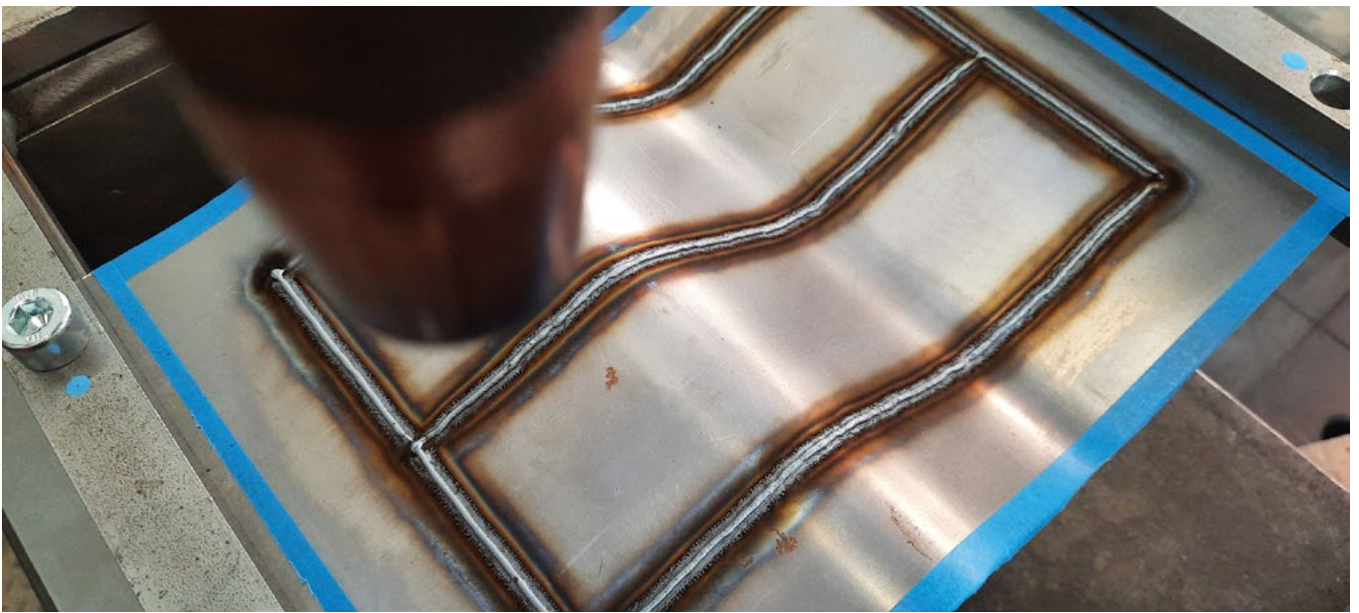


Figure 9: Top: 3D metal printing process result after performing the described geometry scan and reconstruction workflow. Bottom: Back side of the 1 mm metal plate surface.

## REFERENCES

- [1] P. Nicholas, M. Zwierzycki, E. C. Nørgaard, S. Leinweber, D. Stasiuk, M. R. Thomsen, and C. Hutchinson, "Adaptive robotic fabrication for conditions of material inconsistency: Increasing the geometric accuracy of incrementally formed panels," in *Fabricate 2017*, UCL Press, 2017, pp. 114-121.
- [2] C. Borg Costanzi, "Hybrid WAAM - reinforcing sheet metal," in *Print architecture!*, O. Tessmann, U. Knaack, C. B. Costanzi, P. L. Rosendahl, and B. Wibranek, Eds. AADR, 2022.
- [3] A. Bårsan, R. Sever-Gabriel, and R. Breaz, "Incremental forming using KUKA KR210-2 industrial robot - research regarding design rules and process modelling," in *MATEC Web of Conferences*, vol. 343, N. F. Cofaru and M. Intă, Eds., 2021, DOI: 10.1051/mateconf/202134308005.
- [4] E. Castañeda, B. Lauret, J. M. Lirola, and G. Ovando, "Free-form architectural envelopes: Digital processes opportunities of industrial production at a reasonable price," in *FDE 3*, vol. 1, 2015, pp. 1-13, DOI: 10.3233/FDE-150031.
- [5] G. Lee and S. Kim, "Case Study of Mass Customization of Double-Curved Metal Façade Panels Using a New Hybrid Sheet Metal Processing Technique," in *J. Constr. Eng. Manage.*, vol. 138, no. 11, 2012, pp. 1322-1330, DOI: 10.1061/%28ASCE%-29CO.1943-7862.0000551.
- [6] C. Borg Costanzi, *Reinforcing and Detailing of Thin Sheet Metal Using Wire Arc Additive Manufacturing as an Application in Facades*. Wiesbaden: Springer Fachmedien Wiesbaden, 2023.
- [7] K.-M. M. Tam, J. R. Coleman, N. W. Fine, and C. T. Mueller, "Robotics-Enabled Stress Line Additive Manufacturing," in *Robotic Fabrication in Architecture, Art and Design 2016*, D. Reinhardt, R. Saunders, and J. Burry, Eds. Springer International Publishing, 2016, pp. 350-361.
- [8] N. A. Rosli, M. R. Alkahari, M. F. bin Abdollah, S. Maidin, F. R. Ramli, and S. G. Herawan, "Review on effect of heat input for wire arc additive manufacturing process," in *Journal of Materials Research and Technology*, vol. 11, 2021, pp. 2127-2145, DOI: /10.1016/j.jmrt.2021.02.002.
- [9] T. Wohlers, R. I. Campbell, O. Diegel, J. Kowen, N. Mostow, and I. Fidan, *Wohlers report 2022: 3D printing and additive manufacturing: global state of the industry*. D. L. Bourell and J. Van Rensburg, Eds. Fort Collins, Colo.
- [10] P. A. Colegrove, F. Martina, M. J. Roy, B. A. Szost, S. Terzi, S. W. Williams, and D. Jarvis, "High Pressure Interpass Rolling of Wire + Arc Additively Manufactured Titanium Components," in *Advanced Materials Research*, vol. 9996, Aug. 2014, DOI: org/10.4028/www.scientific.net/AMR.996.694.
- [11] A. Gibson, D. Rosen, B. Stucker, and M. Khorasani, "Introduction and Basic Principles," in *Additive Manufacturing Technologies*, Springer International Publishing, 2021, pp. 1-21.
- [12] G. Costabile, M. Ferab, F. Fruggiero, A. Lambiase, and D. Pham, "Cost models of additive manufacturing: A literature review," in *International Journal of Industrial Engineering Computations*, vol. 8, 2017, pp. 263-282.
- [13] J. Reimann, P. Henckell, Y. Ali, S. Hammer, A. Rauch, J. Hildebrand, and J. P. Bergmann, "Production of Topology-optimised Structural Nodes Using Arc-based, Additive Manufacturing with GMAW Welding Process," in *Journal of Civil Engineering and Construction*, 2021, DOI: 10.32732/jcec.2021.10.2.101.
- [14] L. Pelzer and C. Hopmann, "Additive manufacturing of non-planar layers with variable layer height," in *Additive Manufacturing*, vol. 37, 2021, p. 101697, DOI:10.1016/j.addma.2020.101697.
- [15] T. A. Rodrigues, V. Duarte, R. M. Miranda, T. G. Santos, and J. P. Oliveira, "Current Status and Perspectives on Wire and Arc Additive Manufacturing (WAAM)," in *Materials (Basel, Switzerland)*, vol. 12, no. 7, 2019, DOI: 10.3390/ma12071121.
- [16] J. Heerdegen, "Non-linear fabrication: A dialogue between architecture and robotic wire-arc additive manufacture," Master's thesis, Victoria University of Wellington / Te Herenga Waka, 2021, DOI:10.26686/wgtn.16644829.v1.
- [17] S. Radel, A. Diourte, F. Soulié, O. Company, and C. Bordreuil, "Skeleton arc additive manufacturing with closed loop control," in *Additive Manufacturing*, vol. 26, Mar. 2019, pp. 106-116, DOI:10.1016/j.addma.2019.01.003.
- [18] Y.-T. Sheng, S.-T. Liong, S.-Y. Wang, and Y.-S. Gan, "3D printing on freeform surface: Real-time and accurate 3D dynamic dense surface reconstruction with HoloLens and displacement measurement sensors," in *Advances in Mechanical Engineering*, vol. 15, no. 1, 2023, p. 168781322211484, DOI:10.1177/16878132221148404.
- [19] Z. Li, X. Liu, S. Wen, P. He, K. Zhong, Q. Wei et al., "In Situ 3D Monitoring of Geometric Signatures in the Powder-Bed-Fusion Additive Manufacturing Process via Vision Sensing Methods," in *Sensors (Basel, Switzerland)*, vol. 18, no. 4, 2018, doi:10.3390/s18041180.
- [20] A. Hosseininaveh Ahmadabadian, A. Karami, and R. Yazdan, "An automatic 3D reconstruction system for texture-less objects," in *Robotics and Autonomous Systems*, vol. 117, 2019, pp. 29-39, DOI:10.1016/j.robot.2019.04.001.
- [21] J. Ojeda, "OpenCV-RealSense\_scanGeometry (Version 0)," Zenodo, 2023, DOI:10.5281/zenodo.8205361.
- [22] G. Bradski, "The OpenCV Library," in *Dr. Dobb's Journal of Software Tools*, 2000, pp. 120-125.
- [23] L. Perumal, "New approaches for Delaunay triangulation and optimisation," in *Heliyon*, vol. 5, no. 8, 2019, DOI: 10.1016/j.heliyon.2019.e02319.



# CONCRETE AM: STATUS OF THE DEVELOPMENT OF A ROBOTIC ARM-BASED EXTRUSION SETUP

João Ribeiro

Bruno Figueiredo, Paulo J. S. Cruz, Aires Camões

The integration of Additive Manufacturing (AM) technologies into the production of architectural components has demonstrated a great potential to meet the demands of customisation and optimisation that have been highlighted by the evolution of digital processes in architectural design.

This paper provides an overview of 3D Concrete Printing (3DCP) extrusion systems, presenting a series of experiments with cement-based mixtures, with a view to progressively increasing the manufacturing scale. A comparative analysis is established between the experiments carried out at the School of Architecture, Art and Design of the University of Minho (EAAD-UM), and other 3DCP projects in order to better understand the main control parameters of the technology and to aid in the understanding of related topics in other scientific areas.

The work presented aims to contribute to the knowledge of 3DCP processes, identifying potential applications and overcoming the issues inherent in the transition between experimental studies in AM and the more challenging contexts of the construction industry.

## 1. INTRODUCTION

Following applications in other industrial areas such as automotive, aerospace and naval industries, computer controlled AM has proven to be a very versatile process, allowing namely automated production of intricate/multi-functional geometries without increasing the associated costs and, therefore, offering a more adequate response to the new needs raised by the development of digital technologies in architectural design. The adoption of these tools in the construction sector has not kept up with the speed of integration seen in other emerging fields, encountering various obstacles for the application of these tools in real-world contexts.

It is in this context that the Advanced Ceramics Laboratory (ACL), from EAAD-UM, has been working since 2016. As presented in ACL's project portfolio [1], the research developed since then, mostly using small/medium scale ceramic extrusion processes, demonstrates the ability to create customised complex geometries in a fast and automated manner, while also proving to be an economical and sustainable process in that raw material waste is reduced.

Despite the significant achievements, it is denoted that the scale-up in order to fit real contexts sometimes translates into manufacturing problems that require additional care [2]. Although AM processes can produce objects with a margin of error of tenths of a millimetre, deformations in extruded objects are frequent during their manufacture,

drying and/or firing stages. In particular in the case of ceramics, a large part of the geometric alterations comes directly from the dehydration shrinkage process. An example of this is noted in the prototype of the *Ficus Column*, a biomorphic inspired column illustrated in Figure 1 at various scales [3]. Although in the prototype discretised at 1/5 scale it was possible to calculate the shrinkage and its compensation in the digital model, allowing perfect links between printed elements, the same was not possible when printing at 1/2 scale. In this case the need to subdivide the column into smaller elements, adjusted to the working area of the printer and the size of the oven firing chamber, caused ribs of the column to be undone providing a non-uniform shrinkage (affected by friction at the base, freedom at the top, self-weight, etc.), which provided the buckling of the structure and the deformations pointed out in Figure 1.

In contrast, as mentioned by Craveiro et al. (2019) [4] in recent years, perhaps due to the type of material traditionally employed in construction, or the great shortage of skilled labour or even the introduction of new environmental sustainability targets, there has been a growing effort in the exploration of 3D Printing Concrete techniques (3DCP). In this sense, we believe that in order to increase the scale of production and adapt it to current construction contexts, a change in the material is determinant. Although we believe in the added value of Ceramic AM in certain architectural contexts, the elimination of intermediate stages such as the firing of the pieces, or the capacity to produce larger components, are seen as essential for the profitability of the demands of components aimed at industrial contexts.

Based on a 2016 report by the World Economic Forum [5], entitled “Shaping the Future of Construction”, on the “likelihood of integrating new technologies” into construction, we believe that the adoption of contour printing strategies for buildings will not have a major future impact. On the contrary, it is stated that the probability of integration in construction of “3D printing of components” is considered moderate and of integration of “prefabricated building components” is extremely high. In this sense, we orient the work towards prefabrication in off-site environment of discrete elements, later transported to be assembled in construction site context.

Having as ultimate goal the production of components by AM capable of being integrated into the construction of a building, this work is methodologically tabulated by an empirical investigation into two interrelated elements: the machinery and the material. Based on experimental work, it presents particular developments in each – 2. *Extrusion System* and 3. *Material* – as well as seeks the intrinsic relationship between them by presenting the main conclusions drawn – 4. *Material vs. Technology*. Finally, some additional cares that must be taken into account concerning the application in real contexts are presented, namely at the level of the structural reinforcement of the produced components – 5. *Designing to build*.

## 2. EXTRUSION SYSTEM

While material properties are absolutely crucial for the viability of AM processes, the remaining print configuration is the basis of any extrusion test and must also be subject to constant evolution. Starting from consolidated models, namely as exposed by Da Silva (2017), Buswell et al. (2018) or Gosselin et al. (2016) [6, 7, 8], in general, the printing process comprises three essential, sequential and usually continuously interlinked steps: (1) the production/mixing of the material with automated or non-automated dosing; (2) the pumping of the material to the extruder tip; and (3) the deposition of the layered material, with continuous filaments, along a given printing path. Figure 2 illustrates a typical 3DCP configuration using a continuous supply system comprising a dry pre-mixing (Stage 1), mixing with water (Stage 2), a screw pumping system (Stage 3) and an industrial robotic arm as manipulator of the extrusion head equipped with a helical spindle (Stage 4).

### 2.1. Small-scale equipment

Although due to its cost-effectiveness, high accuracy and ease of control, currently many medium/large scale 3DCP exploratory projects use industrial robot-based systems as printhead manipulators, the first tests were conducted using an alternative extrusion system, by hacking a ceramic 3D printer – a Lutum® Mini – composed by a simple Cartesian kinematics, where three servomotors control the movement of the extrusion head according to X, Y and Z coordinates, providing a working area of approximately 450mm in each direction (Figure 3a).

Originally, at the level of the extrusion head, the ceramic paste extrusion flow is controlled by another servomotor connected to a spindle with helical ribs, simultaneously with the air pressure exerted on the cartridge. For the extrusion of cementitious materials, the same operating principles allowed to generate two different extrusion methodologies: producing a set of components to use the servomotor to control the extrusion flow with an auger (Figure 3b); using the cartridges used for ceramics for an extrusion regulated by air pressure (Figure 3c). In both systems a prior preparation of the cementitious mixtures is required before starting the extrusion process.

#### 2.1.1. Extruder for air pressurization

The system based on air pressure extrusion also employs the cartridge used in AM with ceramic paste, but now uses it for the deposition of the material to be extruded. Bearing in mind that, in this case, any cementitious mixture will have a lower yield strength than the ceramic paste, flowing naturally by action of the gravitational force, it became impossible the normal coupling of the cartridge to the extrusion head.



Figure 1: *Ficus Column System* manufactured in ACL at 1/5 and 1/2 scale.

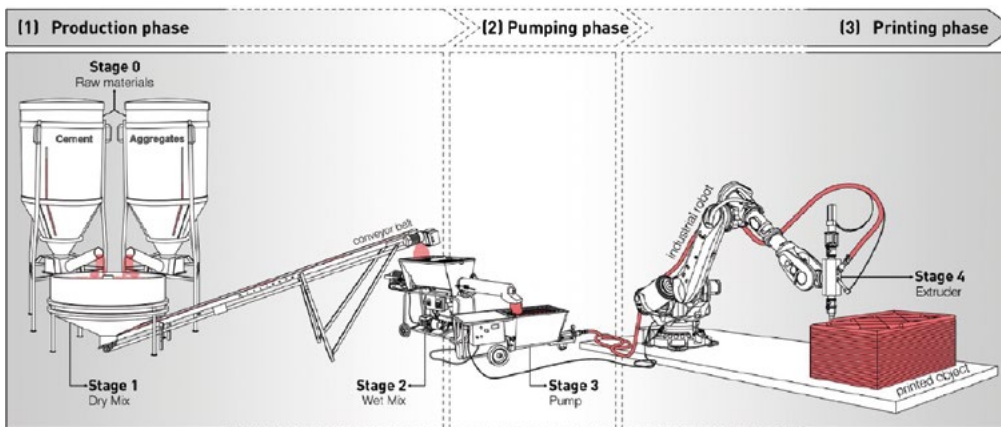
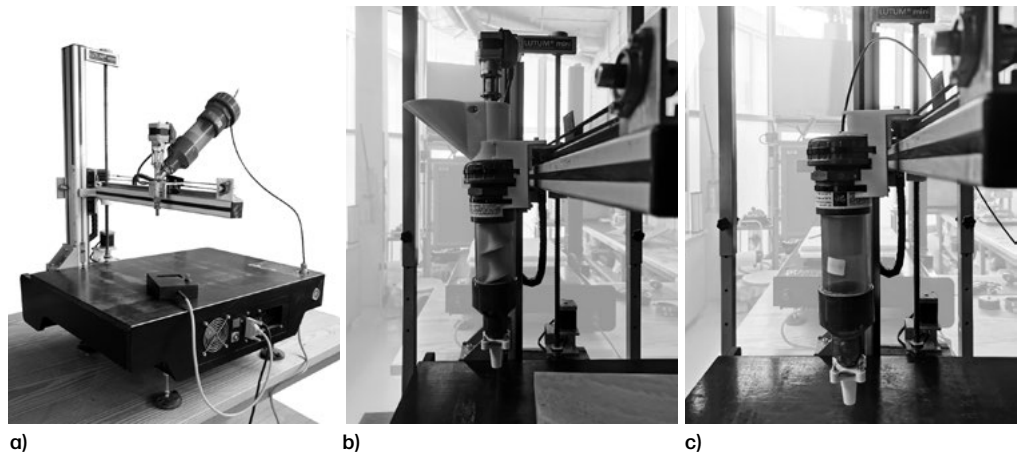
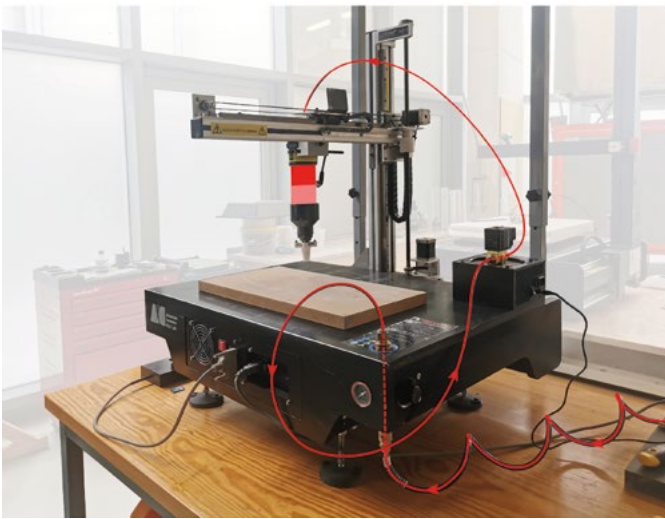


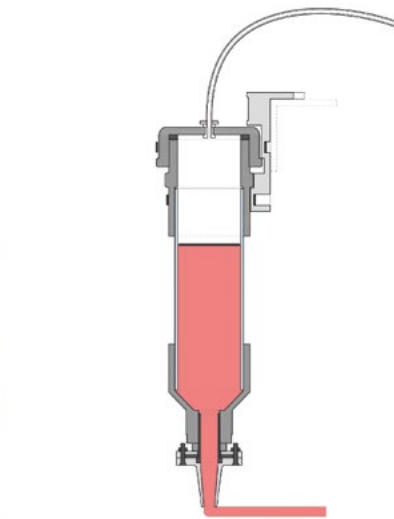
Figure 2: Layout of the print configuration to be mounted in the ARENA Space.



a) b) c)  
 3: Lutum® Mini - 3D Clay printer machine (a), custom extruder with an auger controlled by a stepper motor (b) and custom extruder for air pressurization (c).



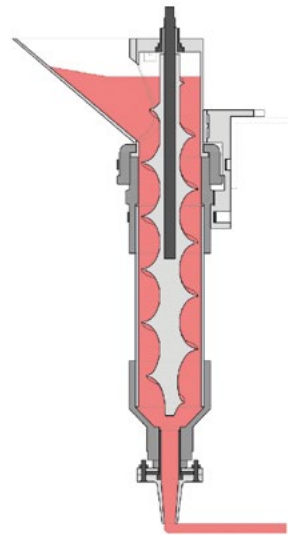
a)  
 Figure 4: Custom extruder for air pressurization (a) and section of extruder head (b).



b)



a)  
 Figure 5: Components of custom extruder with an auger - 1st attempt (a) and section of extruder head without the step motor on top (b).



b)

In this sense, similarly to the extruder with the spindle, it was decided to directly attach the cartridge to the printer arm (Figure 4).

After the cartridge is closed and correctly fixed on the equipment, a hose connected directly to the top of the cartridge, injects air, pushing a plastic plunger that presses the material through the extruder tip. In this step it is essential that an effective seal of the cartridge is ensured.

Control of the air pressure exerted is carried out directly on the base equipment. The Lutum<sup>®</sup>, used as an extrusion manipulator, has a manometer for analogue air pressure control. Thus, the compressed air circuit, supplied by a compressor with 10 bar maximum pressure, is connected to the equipment, allowing the pressure to be regulated as required (for safety reasons, always below 5.5 bar). Since, unlike the ceramic AM, in this case the driving force is only the air pressure, a solenoid valve has been added to the circuit, which allows the cartridge to be more quickly pressurised and depressurised.

Detecting that the capacity of the cartridge (approximately 0.6 litres) was not adequate for tests in which continuous extrusion was required, a larger cartridge of approximately 2.7 litres was used. In this particular case, the load limitation of the equipment arm made it necessary to fix the cartridge on an autonomous gantry structure, and the connection to the extruder tip was made through a hose. To fix the customised extruder tip, brass fittings were used and a customised support was manufactured.

Nevertheless, even though promising results were initially obtained, after a set of extrusion tests, the use of air pressure as a propulsive force for cementitious mixtures was discontinued due to difficulties in maintaining a regular extrusion, as well as production limitations associated with the use of cartridges with limited capacity.

### 2.1.2. Extruder with an auger

The spindle extrusion process included the modelling, development and production of a set of components. For a greater capacity to resist the effort inherent to the extrusion process, a cartridge was used as the main body of the extruder. The remaining components were designed and produced to fit in it: an inverted cup to fix the stepper motor on top, an attached material dispenser, a ribbed spindle with geometry adjusted to the internal section of the cartridge (with 57mm diameter and 350mm height), extruder tips with variable section and geometry, a support to fix it to the printer arm (the last two are common to both extrusion systems), etc. All the customised elements were 3D printed using FFF (Fused Filament Fabrication) technology, but for greater precision between the different parts of the extruder, standard brass threaded connections were used. Figure 5 shows the parts produced for the first test of the extruder and diagrams their assembly.

In this solution the material to supply is placed manually through a feed hopper at its top and the cementitious mixture is progressively pushed by the helical auger through the extruder tip. Since an operator is simultaneously adding material during extrusion, extra care must be taken to avoid excessive vibrations in the tool during this process, however, it is not necessary to interrupt extrusion for refuelling.

The experiments carried out using the power of the servo motor originally fitted to the Lutum<sup>®</sup> extruder, Nema 17, showed a regulated extrusion process, however it demonstrated a very limited extrusion capacity, making frequent blockages of the motor even when using more fluid mixtures. Following tests to improve the extrusion apparatus, experiments using a stepper motor with a higher torque capacity, Nema 23, produced better results. This change made impossible to use the Lutum as a manipulator due to the carrying capacity of its arm.

## 2.2. Medium-scale equipment

The initially developed auger extruder was adapted and connected to a short reach robotic arm (KUKA KR10 R1440-2) as an end-effector tool. This robot, by having a higher load capacity than the ceramic printer, allowed the use of a motor with higher torque capacity, resulting in a higher extrusion capacity.

Regarding the extruder tip section, different geometries and dimensions were tested. Given the scale of the prototypes produced, namely for compressive strength tests, and for reasons of uniformity, the tests used a circular section tip with 12mm diameter. Figure 6 illustrates the extruder head and its articulation with the robot.

### 2.2.1. Digital control

While the tests performed with the Lutum<sup>®</sup> Mini printer followed the same G-code generation process normally used for ceramic printing and for most 3-axis AM systems, the use of the robot required the use of the *KUKA Robot Language* (KRL). To this end, a computational environment was defined to assist the AM production of architectural components. For the programming of the robotic arm it was used *KUKA/PRC* - a parametric robot control plug-in for Grasshopper. This plug-in allows the control of robots from computational models, giving the possibility to develop the digital design model and simultaneously, in the same API environment, generate the necessary commands for the robot to execute the intended task. At the same time, the printing bases where the extruder will act were calibrated in the robot control unit, as well as the extruder tool dimensions, among other calibrations necessary for a correct use of the extruder in accordance with the robot.

With the use of the extruder attached to the robotic arm, there was a need to replace the controller used in the

3D ceramic printer, namely to control start, stop and speed commands of the extrusion flow. In order to synchronise these commands with the robot movement, and due to the hardware limitations of the robot controller, which does not have digital outputs for controlling external hardware from the KRL code, it was necessary to resort to an external controller. The solution was to use an Arduino UNO board – a microcontroller board with an integrated processor, that allows to send or receive information to the computer via USB. At this stage, the board was used to control the parameters that were previously ensured by the 3D printer controller sending data from the computer to control the stepper-motor of the extruder, and in future developments being able of receiving information from temperature and flow sensors. In addition to the Arduino board, a power supply (24V) and a “step-driver” was attached to the top of the extruder to allow the communication between the Arduino and the stepper motor.

For a smarter communication between the computer and the Arduino microcontroller, *Funken* was used – an “open source” Arduino library, initially created by Stefás et al. (2018) [9], with the aim of simplifying communication between Arduino-based hardware and different software. In this specific case, *Funken* bridges the gap between the Arduino and the Grasshopper, making it possible to send start and pause commands and control the speed of rotation for the stepper motor that controls the extrusion flow. In order to coordinate the extruder and the robot’s movement, defined by the KRL code, it was necessary to read the robot’s position in real time. This was done using *Kuka Var Proxy* – another “open source” software that allows ethernet-tcp communication with Kuka robots. This software made it possible to read various robot variables in real time, in particular the current position defined by the angular relationship between its axes.

### Full-scale equipment

After acquiring more experience in controlling the KUKA KR10, for the implementation of the extrusion system controlled in an automatic way using a mortar pump, and no longer needing the proximity of the operator to the robot/extruder (since this system can be supplied outside the robot working area), we moved on to the use of the KUKA KR120 2700-2 – a robot with a similar interface but with a longer range that allows an effective response to larger components.

The printing setup was based on the diagram outlined in Figure 2. As far as equipment acquisition is concerned, and bearing in mind that intensive production is not foreseen, it was decided at this stage to carry out the entire mixture production using a single machine. Thus, the extrusion system, illustrated in Figure 7, is formed by three interconnected pieces of equipment: (1) a planetary

mixer, (2) a mortar pump and (3) the industrial robotic arm equipped with an end-effector tool. The connection between the pump and the extrusion tool is made through a 25mm diameter mortar hose.

At the level of the end-effector tool, a direct extrusion system – a cylindrical steel tube with two threaded ends – was fixed to the robot flange. The lower end for fixing an extrusion nozzle and the upper end for connecting a “Camlock” type coupling for connecting the mortar hose. Different extrusion nozzles were also produced and tested, varying the output diameter of the material, with the 20mm section being assumed to have the best results so far.

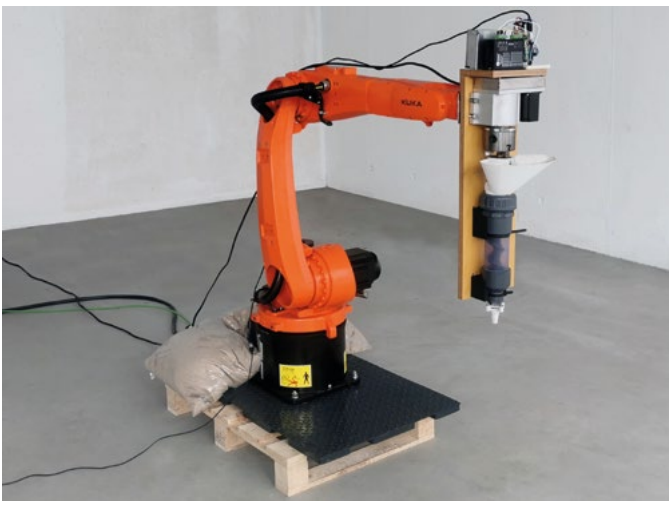
In a parallel, steps have been taken to allow the communication and adjustment of printing parameters, correction or optimization actions of the extruded filaments in real time through the reading of a camera installed in the extruder (Figure 7b). For this purpose, the previously mentioned “open source” software *Kuka Var Proxy* and the *Funken Library* was used.

## MATERIAL

Concrete is the most used material in the building industry. Its composition is based on the mixture of aggregates, of various granulometries, with a binding paste composed of water and cement and/or mineral additions. The mixture hardens naturally as a result of a chemical reaction between the binder and water, but chemical additives can be added to achieve the desired workability (i.e. accelerators, retarders and fluidizers). Furthermore, during the mixing process, other additives can be added, namely, pigmentation for aesthetic purposes.

The technological advancement towards automation and the constant investment in the field of construction material science has enabled the optimisation of production, transport and placement of the material. Being able to reach quality standards and be suitable for specific circumstances is highly dependent on a set of precautions. In accordance to Lage (2013) [10], this includes the selection of materials, determining compositions based on systematic tests, homogenizing the mixture, controlling the concreting process, using appropriate equipment, etc., making it possible to use concrete in any environment and under different conditions, such as extreme temperatures (high or low) and even underwater.

Despite the extensive studies improving the behaviour of cementitious materials for the most diverse structural and architectural applications, their integration into AM poses new challenges which necessitates a reconsideration of the core components of the material – binder, aggregates, water and additives/adjuvants. Le et. al (2012) [11] recognises progress in the construction industry in de-

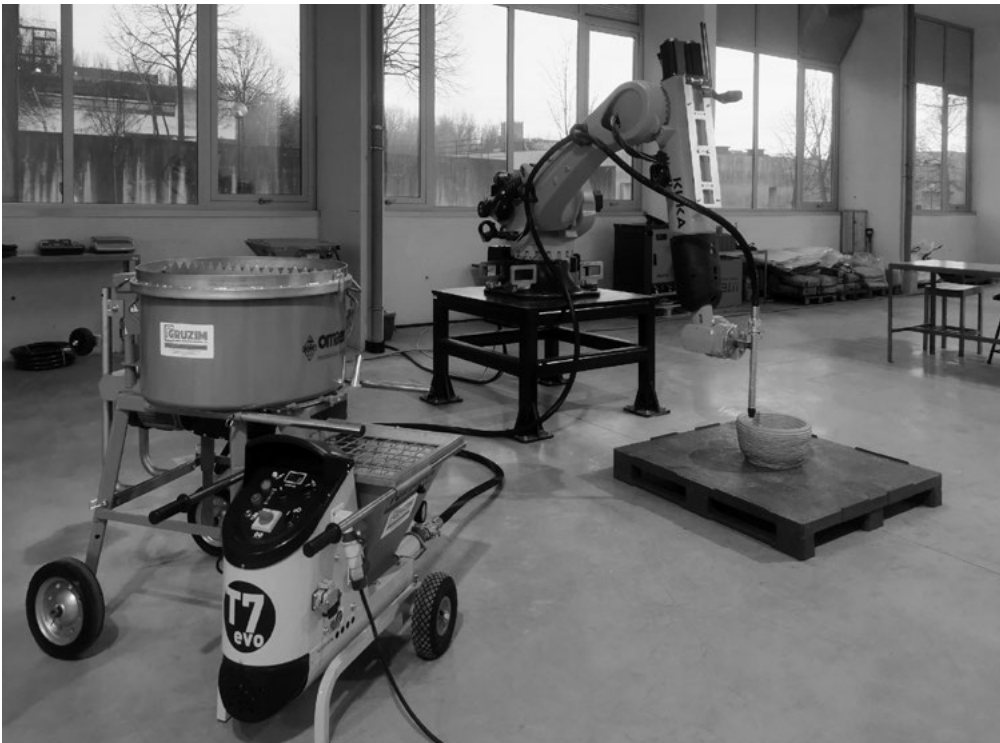


a)



b)

Figure 6: KUKA KR10 robotic arm equipped with the extruder (a) and the printer head (end-effector tool) (b).



a)



b)

Figure 7: Configuration of the extrusion system conformed by a planetary mixer with 120 liters, a Turbosol T7 mortar pump connected to the end-effector tool on the KUKA KR120 2700-2 robot (a) and detail of this extrusion tool, including the attachment of a camera (b).

veloping material properties that match the requirements of AM processes. For example, self-compacting concrete, which is composed of fine aggregates and a high amount of cement, is used to form fluid but consistent mixtures. On the other hand, sprayed concrete and GRC mortars provide a custom mix that is suitable for continuous pumping and extrusion of the material through a nozzle. However, there are several other essential characteristics that must be taken into account to guarantee the success of the extrusion process and the quality of the printed objects. These characteristics will be discussed below.

### 3.1. Rheological behaviour of the material

Regarding the behaviour of the material in the fresh state, printable mixtures must guarantee a uniform flow during all stages of the process: production, pumping and printing. Their refinement is based on the coordination of two key factors: the optimisation of the material's behaviour in the fresh state and its compatibility with the employed printing technology [12].

Taking into account the empirical knowledge evident in other researches [11, 12], the optimal characteristics for 3D printing are measured from four properties that attest to its feasibility: (1) extrudability; (2) buildability; (3) workability; (4) open time.

- (1) Extrudability is defined by the ability of the concrete to be pumped and flow continuously through the hoses from the mixer or hopper to the print head, providing a uniform extrusion through the nozzle, layer by layer throughout the process until the element is fully built.
- (2) Buildability has to do with checking the properties of the material immediately after the deposition process: the extruded filaments must be able to retain their shape and bond to the previous layers, avoiding any kind of collapse or excessive deformation of the printed object.
- (3) Workability is observed in the ability of the newly mixed concrete to be moved, deposited and finished maintaining an acceptable degree of homogeneity, even if some loss of its basic characteristics is observed. A factor usually directly related to the workability degree of the mixture is its fluidity.
- (4) Open time refers to the period of time that the material, once mixed, remains with the necessary degree of workability and fluidity to be continuously pumped through the hoses to the extrusion nozzle without stopping or clogging. The control of the open time is a particularly relevant aspect to guarantee an adequate extrusion and construction capacity.

The main difficulty in the fine-tuning of cementitious mixtures for AM processes is related with the need to coordinate antagonistic characteristics in the extrusion process. For instance, the right fluidity for pumping and extrusion without blockages is needed but if it's too fluid, the printed filaments will be weak and structure could sag or collapse. According to Zahabizadeh et al. (2019) [12] one of the main challenges of 3DPC is also the rheological and mechanical balance of the printable mixtures in the fresh and hardened state, which depends heavily on the material, method, geometry and machine settings.

### 3.2. Cementitious mixtures

Wider research on cement-based mixtures used in 3D printing revealed a diverse set of recipes. Preliminary tests allowed to conclude that different brands, models and characteristics of the raw materials could originate different results from the ones originally described. In this sense, we have selected as a reference the compositions resulting from the two systematised investigations mentioned above [11, 12].

The first experiments were performed using compositions with different quantities of: cement, sand, water and superplasticizer. As a reference, we considered the proportions referred to in the mentioned papers: binder/aggregates ratio of 40/60 and water/binder ratio of 0.31 (reference value). A Type II cement of strength class 32.5 was used, without addition of fly ash or silica fume.

After this, the mixtures were progressively tuned to improve the behaviour during extrusion. Table 1 lists two mixtures tested, varying the type of cement. Then, variations were introduced by increasing the amount of water (approximately 8%) and removing superplasticizer and retarder.



Table 1. Mixtures used for testing

Mix	Units/ caption	Binder		Aggregates	Water	Additives/Adjuvants		Total
	Raw Materials	CEM II	Silica Fume	Sand (2mm)	Water	Superplasticizer	Retarder	
CEM I 42,5 R with Superplasticizer (a)	Kg	1,320 Kg	0,147 Kg	2,200 Kg	0,381 Kg	0,018 Kg	0,007 Kg	4,073 Kg
	Ratio Binder- Aggregates	40%		60%	26% of the binder*	1,25% of the binder	0,50% of the binder	
	Binder composition	90%	10%	* It was used dry sand and it was necessary to add another 0.035 kg of water to make the mixture possible to extrude, making up 28.40% of the Binder (19°C temperature / 14°C water temperature).				
CEM II 32,5 N with Superplasticizer (d)	Kg	1,320 Kg	0,147 Kg	2,200 Kg	0,337 Kg	0,010 Kg	0,007 Kg	4,020 Kg
	Ratio Binder- Aggregates	40%		60%	23% of the binder*	0,70% of the binder	0,50% of the binder	
	Binder composition	90%	10%	*26,28% of the binder if we include an estimate of water present in the sand (17°C temperature / 14°C water temperature).				

Figure 8 illustrates the differences obtained in the production of four specimen with different mixtures: (a) CEM I 42.5, with superplasticizer and retarder; (b) CEM I 42.5, without superplasticizer and retarder; (c) CEM II 32.5, without superplasticizer and retarder; (d) CEM II 32.5, with superplasticizer and retarder. Although compression test results have not yet carried out, it is possible to verify that mixtures with the correct dosage of superplasticizer and setting retarder remain more stable, providing more controlled extrusions. The lower amount of water added to these mixes is also expected to result in higher compressive strengths.

Additionally, polypropylene fibres (Sika Fiber M-12) were added to the mix (d) during mixing process (0.15% of binder weight). Although no improvements were expected in the compression tests, this addition also improved the extrusion capacity, increasing the cohesion of the extruded strands and consequently also providing a better buildability.

Finally, in order to achieve faster mixing processes, a optimised mortar for 3DCP developed and marketed in 25 kg bags by Weber - Saint Gobain (Weber 3D 160-1) was tested. This pre-mix obtained good extrusion capacity with water dosages of between 10.8% and 11.5%, depending on the mixer and extruder used.

### 3.3. Laboratory Tests

Besides the visual assessment of the capacity/characteristics of a given cementitious mixture, tests were made in order to assess and quantify with greater precision the particularities of each mortar, namely their viscosity.

The flow table test was carried out according to BS EN 1015-3:1999 for approximately two hours on two mixtures with and without superplasticiser. It was observed that both lose workability and extrudability approximately 30 minutes after the start of the test, at which point the spread of both mixtures is less than 175mm (Figure 9).

Due to the complexity of concrete composition, its rheology is only satisfactorily described, for instance, by using a Brookfield viscometer or a rheometer, as it allows the simultaneous measurement of two characterisation parameters. If none of these equipments is available, workability is, in general, evaluated using more expedite tests, which allow for a partial determination of the intrinsic rheological properties of the material. In this sense, considering cementitious mixtures as a Bingham fluid, their rheological behaviour could be satisfactorily translated into a linear relationship evaluated by gauging at least two parameters, both with physical meaning: the yield strength and the viscosity. Ma et al. (2018) [13] presents a set of tests that can be used to evaluate the fresh and hardened properties of concrete, which can help the design of the material. This will be an essential step to make the behaviour of the mixture more predictable. Regarding the mechanical characterisa-

tion of the mortars, tests of compressive strength, capillary absorption and immersion absorption will also be carried out in next stages of the research.

## 4. MATERIAL VS. TECHNOLOGY

A reliable extrusion process combines the study of the most predictable material configurations with a set of relevant information about machine operation and extrusion processes. Assuming as main goal the adjustment of the printing process according to the performative/aesthetic properties required for a given project, the experimental program developed so far sought to identify the variables and parameters that condition the printing process. The focus is the intrinsic relationship between the behaviour of the material and the extrusion system, allowing a practical notion of the conceptions previously exposed. Since the extrusion tests were divided in time, the extruders initially presented allowed conclusions to be drawn which were directly or indirectly applied in subsequent tests.

### 4.1. Speed vs. amount of material deposition

The relationship between the extrusion travel speed and the amount of material deposition (controlled by the auger rotation speed or pressure that controls the material flow) is one of the most determining factors in the AM process, especially with regard to the mechanical behaviour and final appearance of the object produced. These variables, which can be adjusted individually, must be correctly coordinated and serve, together with the layer height and the extruder tip section, to define the exact amount of material that will be deposited at each moment and in each part of the object.

By adjusting these values, it is possible to obtain specific variations. For the same travel speed and layer height, an increase in the material flow will imply a substantially thicker extrusion strand. Conversely, keeping the material flow and layer height stabilized and increasing the travel speed during printing will result in a thinner layer, corresponding to the value of increased speed. In this sense, we can state that for the same geometric translation in coordinates we can obtain substantially different objects.

From another point of view, keeping the same printing settings, a change in the layer height has great repercussions on the printed geometry. Figure 10 illustrates two specimens printed using the same printing settings (12mm extruder nozzle, 20mm/s travel speed and 0.25bar air pressure) but with a variation of layer height. In addition to a more uniform side finish, specimen "b" shows a better relationship between thickness and filament height (thickness = height layer  $\times$  2).

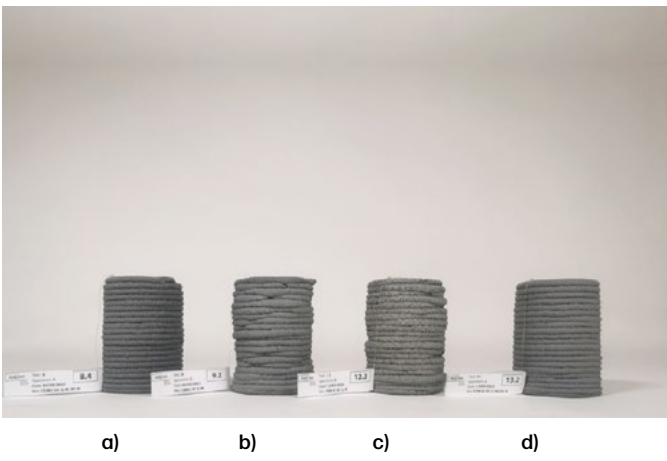


Figure 8: Printing tests of the same specimen with different material mixtures.

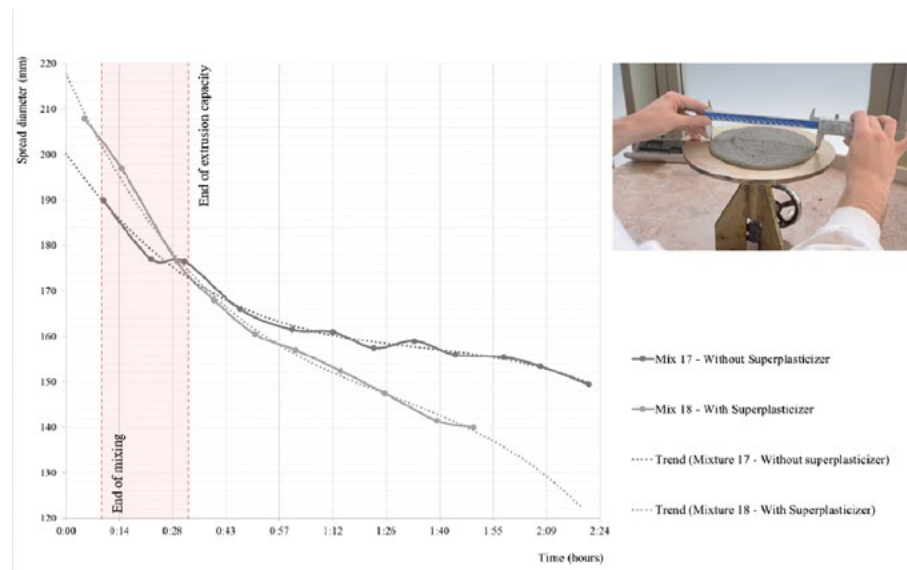


Figure 9. Result of the Flow Table test carried out on the 2 mixtures over approximately 2 hours.



Figure 10: Two samples of a specimen printed with the same print settings, using a layer height of 6mm (a) and a layer height of 10mm (b); Section of specimen "b" after 28 days (c).



Figure 11: The influence of the interlayer waiting time on the manufacturing of cylindrical concrete specimens printed in spiral (Specimens presented in order of printing time); The last specimen (presented on the right) was printed about 35 minutes after the first one, by setting the speed to 50%.

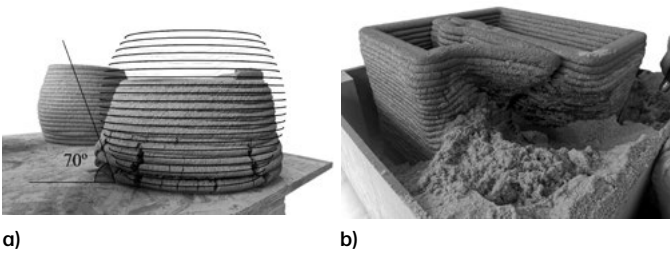


Figure 12: Test specimen of the maximum printable degree of curvature (a) and printed prototype using sand as support material (b).

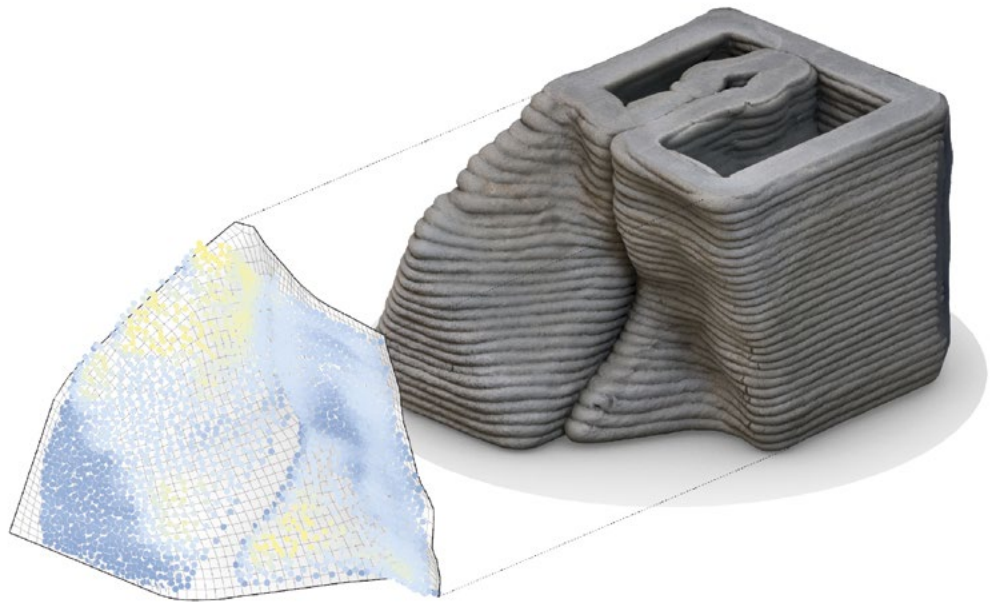


Figure 13: Comparative analysis of the photogrammetry model obtained with the target geometry.

Alternatively, a similar ratio between nozzle diameter and layer width could be created. This option was followed in the tests keeping a layer height of 10mm (to privilege the printing definition), using a circular nozzle with 20mm diameter and a standard speed of 10cm/s, it was agreed a layer width of 40mm (thickness = nozzle diameter x2).

Insufficient delivery rates lead to gaps in the printed layer that may result in buckling or collapse of the object due to the lack of support for the upper layers. Conversely, excessive delivery rates lead to an “overflow” of material that results in uneven surfaces or deviations in the desired geometry and, in the worst case, can also cause the element to break by requiring too much support for the lower layers. The synchronisation between the print speed at a given moment, the material delivery rate and the desired layer section thus represents a major challenge for the optimisation of the printing process.

#### 4.2. Time

Increasing the manufacturing speed is usually associated with increases in layer thickness, changes in the extruder tip section or increases in the equipment’s movement speed. Fluctuations in these parameters change the resolution of the models produced as well as their physical/mechanical characteristics, so they should be tested according to the desired geometry and finish. Very high layer heights or acute curvature radii performed at excessive speeds are likely to generate conflicts with the kinematics of the machinery, which may, by excessive vibration, generate unstable structures and, in the limit, lead to the collapse of the manufactured model.

Moreover, particularly with regard to cementitious mixtures, the “time” issue is not limited to the longer or shorter production time (which can be optimized), but mainly to its influence on the material’s characteristics. In addition to the aforementioned open time, an excessive waiting/resting period after the deposition of a layer often results in poor chemical bonds between subsequent layers - a problem commonly referred to as Cold Joints [14]. This issue is naturally more problematic in accelerated mixes (mixes activated by injection of a setting accelerator during extrusion). The use of non-accelerated mixes, extruded directly, did not represent a problem. Microscopic analysis might help to verify. Contrarily, given the small scale of the specimens printed in this study, a problem we experienced was generated by an insufficient waiting period. As shown in Figure 11, this issue can cause the collapse of a structure due to lack of support of the lower layers [15]. In concrete and mortars, the “time” in which the material remains suspended must be taken care of and tested so that the viscosity of the layers, already deposited and to be deposited, are as close as possible to the ideal conditions for their correct bonding.

#### 4.3. Extrusion path

The extrusion path is defined by the translation of the model into vector data - a set of continuous points along paths of superimposed extrusion layers - subsequently compiled in a code readable by a 3-axis printer or robot. The control code generated, G-code or KRL, results in an approximation of the initial shape to the constraints of the printer and the characteristics of the material, gathering a set of basic information needed for the printing process: information related to the speed and kinematics of the printer, the height and number of layers, etc. parameters that must be adjusted to the nozzle diameter, the extrusion flow, among other characteristics that are not defined by the code.

Although three-dimensional models are usually the result of the most used design methodologies, the preparation of the print presupposes the translation of this geometry into a succession of contour curves, usually defined by a series of parallel slices spaced by the layer height previously defined. Since the code generation for the robot’s path is performed only through a list of points, the generated curves are divided into a set of equidistant points. After tests, in order to keep the accuracy of the printed geometries without making the information too heavy, we defined a distance between points of 5mm.

All the print settings directly affect the match between the digital model and the printed prototype. Features such as the layer width should be predicted and compensated when generating the print paths. Furthermore, geometries with more forced angles revealed a tendency to a lower correspondence between the digital model and the printed prototype, which may cause the rupture of the printed object due to the subsidence of the lower layers and lack of support for the upper layers. Figure 12a illustrates the rupture of an ovalised specimen with an angle of 70°.

On the other hand, Figure 12b reflects the printing of a prototype test with varied inclinations beyond the limit previously gauged. In this case, taking into account favourable results of the use of sand as a support material for complex geometries reported by Ahmed et al., 2022 [16], some support tests were performed in the areas of greater instability after the deposition of the concrete, before it acquired strength capacity. After the beginning of the curing process, the sand was removed, and this technique revealed not only a great increase in the fabrication success rate, but also minimized the geometric deviation to the digital twin. Figure 13 illustrates an analysis performed based on the prototype photogrammetry where it is reflected that the largest deviations (in yellow) happen when the curvature occurs inwards, where no sand was placed. In the opposite direction, the deviation in the convex curvature is minimal.

## 5. DESIGNING TO BUILD

The design principles initially identified pointed to the production of discretised elements, produced in the laboratory for subsequent transportation and placement in-situ. Considering this methodology, all the elements produced must be thought out giving an effective response to each step of the process.

If at the printing level, the main themes are presented in the previous sections, at the level of transport and placement there are two essential factors to take into account: (1) the scale and portability of the elements produced and (2) the integration of solutions for reinforcement and connection between parts.

Regarding scale, besides the limitation of the robot working area, it was decided to limit the size of all printed elements to the handling capacity currently existing in the laboratory. This factor is deeply dependent on the available transport equipment, the type of geometry and the weight of the produced elements. In order to facilitate the lifting of prototypes impossible to handle manually, provisional fixing systems are being integrated during the production phase.

On the other hand, the implementation of strategies to reinforce of 3DCP architectural components is currently a topic of great importance when talking about large-scale components, as in the case of reinforced concrete in traditional construction systems, cementitious materials alone do not have sufficient tensile capacity and ductility to ensure the requirements of building construction.

One of the main difficulties in the application of reinforcement is the adaptation of traditional models to a whole new range of possibilities and complex geometries that can be achieved through digital manufacturing processes. Therefore, as framed by Asprone et al., 2018 [17] and Kloft et al., 2020 [18], it is extremely relevant to define new reinforcement criteria, developing the methodologies traditionally used in the construction sector, in order to adapt them to the specificities of the 3DCP technique.

In the case study illustrated in Figure 14 two solutions of structural reinforcement were integrated [19]. On one hand, at the material level, Weber 3D 160-1 mortar was used which contains in its composition reinforcement fibres, being expected an increase of the shear stresses resistance. On the other hand, at the level of the geometry of the pieces, we defined a reinforcement strategy based on post-tensioning systems applied on site, this limited the printing problems. For that, a set of ducts - voids that cross continuously the whole geometry of the elements - were contemplated in its internal structure in order to facilitate the placement of steel cables posteriori. Similarly, to other examples, such as the ones presented by Salet et al. (2018) and Vantyghe et al. (2020) [20, 21], the system used explores a mechanical principle where the concrete will always remain under compression. In this sense, the additional application of

prestressing allows conferring load capacity to elements that normally would also involve tensile forces.

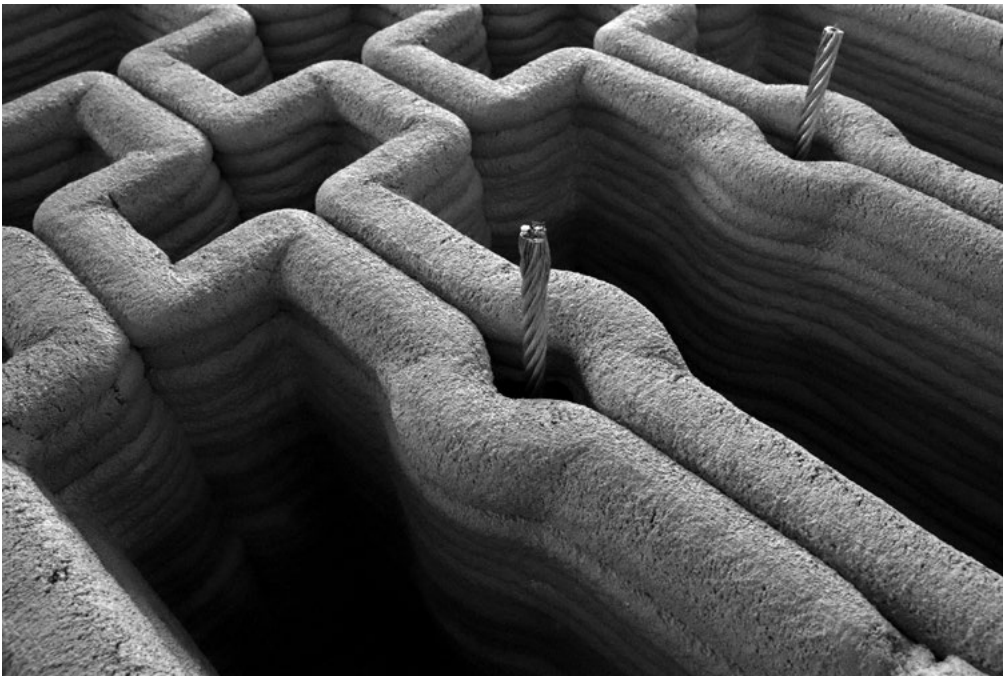
## 6. CONCLUSION AND FUTURE WORK

This study presents frames an investigation into the use of cementitious materials mediated by AM processes for the prefabrication of architectural components. Besides presenting different extrusion systems developed, and a set of cementitious mixtures applied, the work lists a series of principles and functional relationships to assist the extrusion process domain, namely regarding the characteristics that should be sought in the material and how these should be communicated to the extrusion technology. Finally, thinking about applications in real contexts, a practical case is illustrated where structural reinforcement solutions were integrated, namely post-tensioning solutions.

As future work, we foresee an investment at two levels: (1) the development of the extrusion system with spindle for application in the KR120 robotic arm in order to improve the reliability of the process, namely by allowing the pumping of the material in a more fluid state and by adding a setting accelerator during extrusion; and (2) the optimisation of a set of mixtures for this purpose, taking into account not only the functional but also the aesthetic properties. For that we will try to increase the complexity of the cementitious composition by increasing the amount of reinforcement fibres together with other additives that favour the pumping capacity of the material. Personalised strategies of concrete pigmentation are also being thought, in order to provide the new mixtures, besides an increased mechanical resistance, with unique visual characteristics that can be applied in real projects.

## 7. ACKNOWLEDGEMENTS

This work is financed by the Project Lab2PT - Landscapes, Heritage and Territory laboratory - UIDB/04509/2020 through FCT - Foundation for Science and Technology and by FCT Doctoral Grant with the reference SFRH/BD/145832/2019. This work is co-funded by the European Regional Development Fund (ERDF) through the Operational Competitiveness and Internationalization Programme (COMPETE 2020) of the Portugal 2020 Program [Project No. 47108, "SIFA"; Funding Reference: POCI-01-0247-FEDER-047108. We are grateful to the School of Architecture, Art and Design of University of Minho for hosting and supporting the ARENA Laboratory. We are also grateful to Saint-Gobain Weber for its monitoring and supply of the material.



a)



b)

Figure 14: Integration of ducts into the geometry of each part to post-tension the entire structure (a) and diagram of two-piece assembly (b) [19].

## REFERENCES

- [1] "Advanced Ceramics Laboratory, Guimaraes, Portugal", <https://www.aclab-idegui.org> (accessed Sep. 17, 2021).
- [2] P.J.S. Cruz, B. Figueiredo, J. Carvalho and J. Ribeiro, "From rapid prototyping to building in real scale: methodologies for upscaling additive manufacturing in architecture," in *IASS Symposium 2019 - 60th Anniversary Symposium of the International Association for Shell and Spatial Structures and Structural Membranes 2019 - 9th International Conference on Textile Composites and Inflatable Structures, FORM and FORCE*, Barcelona, Spain, October 7-10, 2019, C. Lázaro, K.-U. Bletzinger and E. Oñate (eds.), International Centre for Numerical Methods in Engineering (CIMNE), 2019, pp. 103-112.
- [3] J. Moreira, B. Figueiredo, and P.J.S. Cruz, "Ceramic Additive Manufacturing in Architecture - Computational Methodology for Defining a Column System," in *The Age of the 4th Industrial Revolution - 37th eCAADe and 23rd SIGraDi Conference*, Porto, Portugal, 2019, J. Sousa, D.C. Henriques and J.P. Xavier (eds.), 2019, pp. 471-476, DOI: 10.5151/proceedings-ecaadesigradi2019\_455.
- [4] F. Craveiro, J. P. Duarte, H. Bartolo, and P. J. Bartolo, "Additive manufacturing as an enabling technology for digital construction: A perspective on Construction 4.0," in *Automation in Construction*, Jul. 2019, vol. 103, pp. 251-267, DOI: 10.1016/j.autcon.2019.03.011.
- [5] World Economic Forum, "Shaping the Future of Construction - A Breakthrough in Mindset and Technology," in *Industry Agenda*, Ref. 220416, Prepared in collaboration with The Boston Consulting Group, Switzerland, 2016.
- [6] W.R.L. da Silva, "3D concrete printing: from material design to extrusion," Presented slides in *Annual Civil Engineering Workshop at Ecole Centrale de Lille (ACE Workshop 2017)*, 2017.
- [7] R. A. Buswell, W. R. Leal de Silva, S. Z. Jones, and J. Dirrenberger, "3D printing using concrete extrusion: A roadmap for research," *Cem. Concr. Res.*, vol. 112, pp. 37-49, 2018, DOI: 10.1016/j.cemconres.2018.05.006.
- [8] C. Gosselin, R. Duballet, P. Roux, N. Gaudillière, J. Dirrenberger, and P. Morel, "Large-scale 3D printing of ultra-high performance concrete - a new processing route for architects and builders," *Mater. Des.*, vol. 100, pp. 102-109, 2016, DOI: 10.1016/j.matdes.2016.03.097.
- [9] A. Stefas, A. Rossi, and O. Tessmann, "Funken: Serial Protocol Toolkit for Interactive Prototyping," 2018, DOI: 10.52842/conf.eacaade.2018.2.177.
- [10] R. Lage, "Equipamento de fabrico, transporte e colocação de betão em obra", Master's thesis, Instituto Superior Técnico, Universidade de Lisboa, Portugal, 2013.
- [11] T. T. Le, S. A. Austin, S. Lim, R. A. Buswell, A. G. F. Gibb, and T. Thorpe, "Mix design and fresh properties for high-performance printing concrete," *Mater. Struct.*, vol. 45, no. 8, pp. 1221-1232, 2012, DOI: 10.1617/s11527-012-9828-z.
- [12] B. Zahabzadeh, V. Cunha, J. Pereira, and C. Gonçalves, "Development of cement-based mortars for 3D printing through wet extrusion," in *IABSE Symposium 2019 Guimarães - Towards a Resilient Built Environment - Risk and Asset Management*, pp. 540-547, 2019.
- [13] G. Ma and L. Wang, "A critical review of preparation design and workability measurement of concrete material for large-scale 3D printing," *Front. Struct. Civ. Eng.*, vol. 12, no. 3, pp. 382-400, 2018, DOI: 10.1007/s11709-017-0430-x.
- [14] T. Wangler, E. Lloret, L. Reiter, N. Hack, F. Gramazio, M. Kohler, M. Bernhard, B. Dillenburger, J. Buchli, N. Roussel and R. Flatt, "Digital Concrete: Opportunities and Challenges," in *RILEM Tech. Lett.*, vol. 1, pp. 67-75, 2016, DOI: 10.21809/rilemtechlett.2016.16.
- [15] R. J. M. Wolfs and A. S. J. Suiker, "Structural failure during extrusion-based 3D printing processes," *Int. J. Adv. Manuf. Technol.*, vol. 104, no. 1, pp. 565-584, 2019, DOI: 10.1007/s00170-019-03844-6.
- [16] Z. Ahmed, R. Wolfs, F. Bos, and T. Salet, "A Framework for Large-Scale Structural Applications of 3D Printed Concrete: the Case of a 29 m Bridge in the Netherlands," *Open Conf. Proc.*, vol. 1, pp. 5-19, 2022, DOI: 10.52825/ocp.v1i.74.
- [17] D. Asprone, C. Menna, F. P. Bos, T. A. M. Salet, J. Mata-Falcón, and W. Kaufmann, "Rethinking reinforcement for digital fabrication with concrete," *Cem. Concr. Res.*, vol. 112, pp. 111-121, 2018, DOI: 10.1016/j.cemconres.2018.05.020.
- [18] H. Kloft, M. Empelmann, N. Hack, E. Herrmann, and D. Lowke, "Reinforcement strategies for 3D-concrete-printing," *Civ. Eng. Des.*, vol. 2, no. 4, pp. 131-139, 2020, DOI: 10.1002/cend.202000022.
- [19] J. Ribeiro, J.M. Silva, A. Morais, B. Figueiredo, P.J.S. Cruz, "3DCP for Complex Sites: Robotic Fabrication of Custom-Fit Slabs in Irregular Pontoons," in *Proceedings of Digital FUTURES – The 5th International Conference on Computational Design and Robotic Fabrication*. CDRF 2023, 2023.
- [20] T. A. M. Salet, Z. Y. Ahmed, F. P. Bos, and H. L. M. Laagland, "Design of a 3D printed concrete bridge by testing," *Virtual Phys. Prototyp.*, vol. 13, no. 3, pp. 222-236, 2018, DOI: 10.1080/17452759.2018.1476064.
- [21] G. Vantighem, W. De Corte, E. Shakour, and O. Amir, "3D printing of a post-tensioned concrete girder designed by topology optimization," *Autom. Constr.*, vol. 112, p. 103084, 2020, DOI: 10.1016/j.autcon.2020.103084.



# THE FLUSH INTEGRATION OF ADDITIVELY MANUFACTURED CERAMIC COMPONENTS IN BUILDINGS

Alexander Wolf

While technologies to additively produce building components made from concrete, steel or earth are getting closer and closer to market-maturity, additive manufacturing of ceramic components is still bound to certain limitations in its process. Nevertheless, the additive manufacturing of individualised parts and pieces is seen as a valuable addition to usual manufacturing-processes and may enable the integration of specialised components into common ceramic systems. To fully exploit the technology, an appropriate way to deal with limitations like the instability of the green body or the appearance of printed surfaces must be found. This article aims to identify these limitations and give advice for the further exploration of the process.

## INTRODUCTION

The additive manufacturing of buildings and their components is taking foot in the construction industry. Common building-materials such as concrete, steel, plastics, glass and ceramics can nowadays be processed additively into large elements, but the associated technologies show different degrees of maturity. While on one hand, entire buildings are already being created from concrete [1], steel [2] or earth [3] many projects in the field of ceramics are rather to be seen as art and avant-garde [4], still being far from market-maturity. In particular, the production of individual, specialised components represents a useful addition to the

usual mass production of simpler geometries[5] and therefore seems to be a favourable technology for the ceramic industry to introduce in their production. The technology of Robocasting [6] as the most promising manufacturing technology for large elements so far [4, 7] is accompanied by various process-related limitations, for which appropriate countermeasures have to be found.

The use of ceramics itself as a building material dates back at least to 5,000 BC, when the first buildings were constructed in Mesopotamia using bricks made of fired clay [8]. Over the centuries, other applications of ceramics in construction have appeared, such as roof tiles or bathroom ceramics, and the relevance of such products

seems to be unbroken even today. With an annual production worth €5.5 billion [9] the ceramic industry still acts as a key player in the European building-material industry.

While in ancient times ceramic building-products were mostly manufactured by hand, with the upcoming industrialization production-processes have been widely automated, which resulted in a huge increase of productivity. Even though these, in view of the overall history of ceramics, rather recent developments are assuring big outputs and reasonable unit-prices, the processes used nowadays are still somehow limited in terms of their geometric output.

Bricks are commonly produced through extrusion, meaning that the raw material is pressed through a mouth-piece, which prescribes the bricks' geometry in X- and Y-direction. The so produced strand of material is afterwards cut into equal sized sections, resembling the Z-direction and resulting in the final bricks. Even though there are many possibilities for shaping in X- and Y- direction, the appearance in Z-direction can only be determined as the later height. Therefore, this process can be described as 2 ½-dimensional as it is shown in Fig. 1 on the next page.

Roof tiles, on the other hand, are formed in a two-step production. After a rather flat piece of clay material is first extruded, then shaped by a stamp into its final form [10]. This process, in comparison with the aforementioned, is in principle capable of producing 3-dimensional objects. Its limitations derive from the fact that after shaping the stamp has to retract from the green body, which does not allow any undercutting geometry as seen in Fig. 1 on next page.

Bathroom ceramics, for instance, are often shaped through slip-casting, a moulding process which uses a low-viscosity ceramic slurry [7]. Using segmented moulds (Figure 2), this method allows undercutting to a certain degree and can therefore be seen as a process with a rather high degree of geometric freedom. Unfortunately, this method also needs multiple steps to be carried out and therefore does not generate the high output of the other two processes.

The additive manufacturing of ceramics can be described as a layerwise stacking of a geometries' cross-sections to achieve a final result (Figure 3). Its application on the product of ceramic building elements is strongly connected with the introduction of a digitalized "industry 4.0" and therefore has even been described as "the fourth generation of brickwork" [7]. Several different procedures to produce 3D-printed ceramics have been developed so far [11], but only Robocasting [6] seems to be a promising candidate for its use in the construction industry [4], [7]. The technology's capability of creating shapes without much of preliminary labour makes it suitable to produce complex geometries, unique pieces or small series [5], but lacks efficiency when there is a demand for fast production and high output-rates.

Even though Robocasting has been around for 25

years since its introduction in 1998, an adaptation for building purposes mainly took place within the last decade. So far, at least 35 projects have been carried out, mainly creating rather artsy pieces of architecture and often lack proper scientific documentation [4]. Especially the process-related properties of Robocasting have to be investigated to assure a scalability and adaption to the demands of the ceramic building-industry. The present work addresses, classifies and discusses these demands and properties.

## PROPERTIES OF THE MATERIAL

Clay as a natural material comes in innumerable varieties, depending on where it was sourced [12]. All of them have in common, that a mixture of minerals and water forms a more-or-less viscous paste, which is formed into a green body, that hereafter is dried and fired. The properties of the later product are dependent by the used mixture as well as the firing temperature, which usually ranges from 900-1800°C [10]. Overall, additively manufactured ceramics should, in terms of material, integrate into conventional systems, e.g., as special bricks in masonry bonds. This may be assured by:

- I *Usage of the same raw material as in conventional products*  
Due to many ceramic companies running their own clay pits, or at least relying on a certain group of suppliers, it is advised that raw materials used in additively manufactured components should be the same as in regular products.
- II *Keeping the ceramic paste close to the production standard*  
As the printers prevalent on the market operate with much less pressure than e.g., an industrial brick-extruder, certain alterations regarding the viscosity or graininess of the paste might be necessary to assure printability.
- III *Keeping the firing-process close to the production standard*  
The firing process should only be altered to ensure corresponding properties of the final AM-product in comparison with the conventional one.

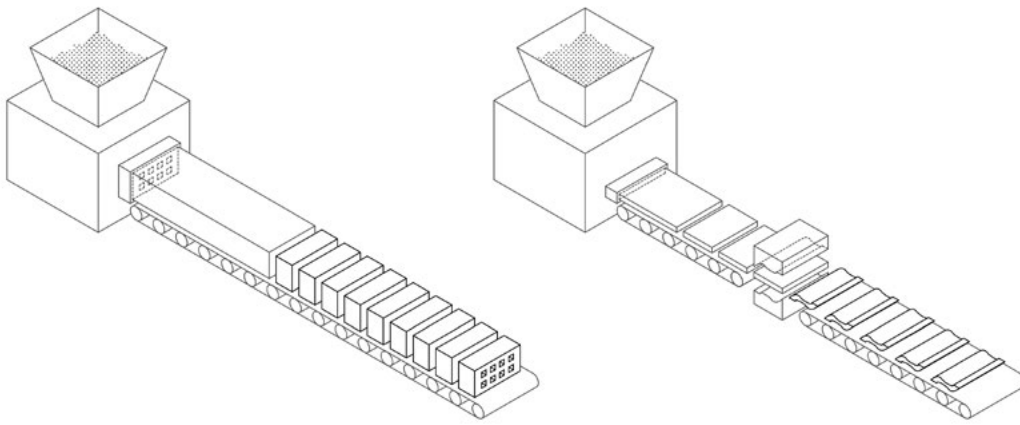


Figure 1: left: extrusion-process as used for bricks. right: extrusion/  
stamping-process as used for roof tiles

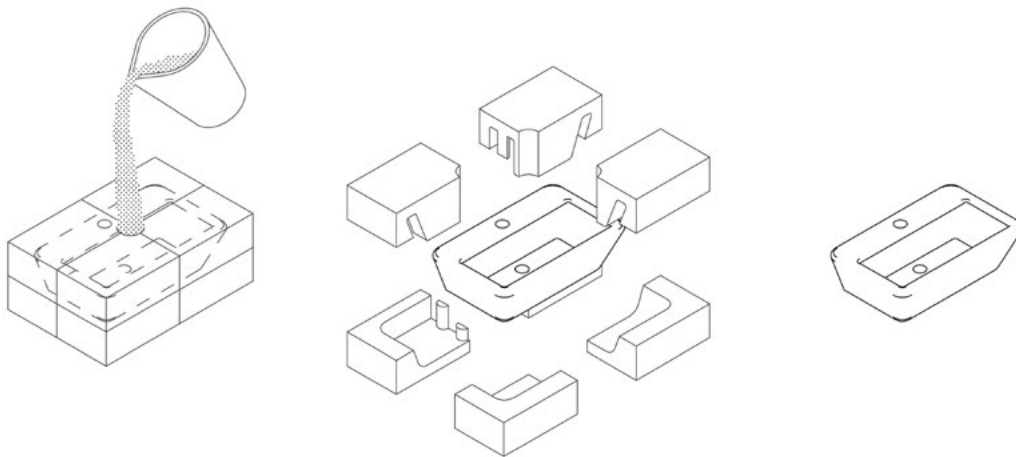


Figure 2: slip-casting process as used for bathroom-ceramics.

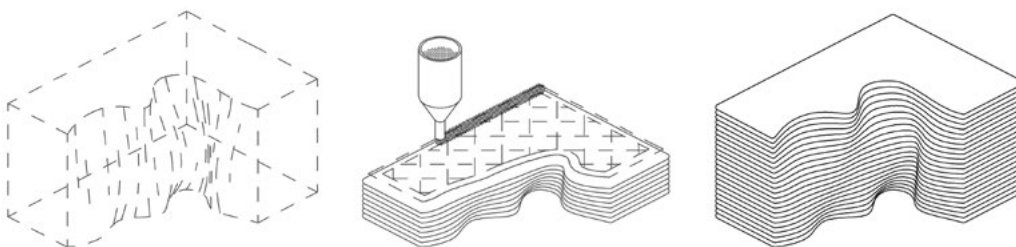


Figure 3: Robocasting-process left: the digital model. middle: fabrication  
along paths. right: final object

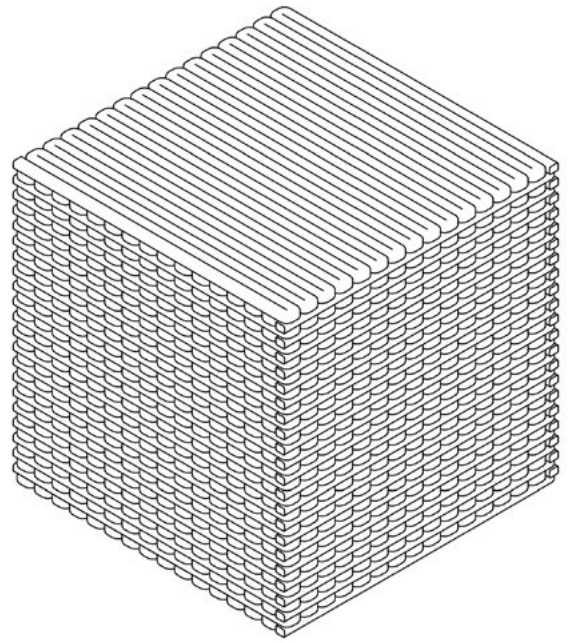
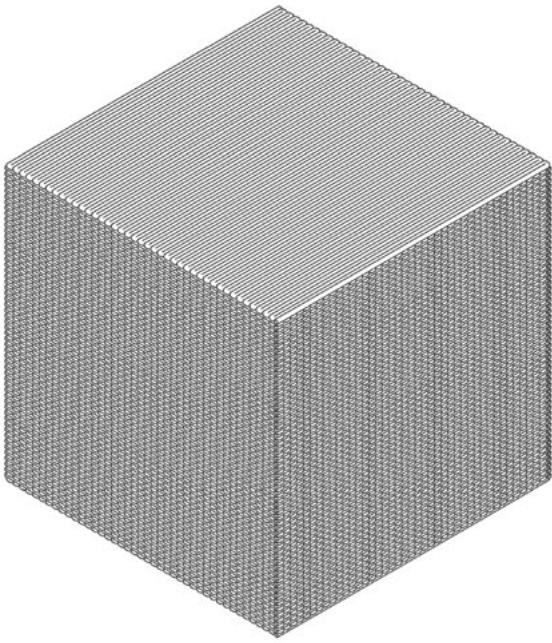


Figure 4: Printpaths. left: nozzle 3 mm Ø / layer-height 2,25mm. right: nozzle 8mm Ø / layer-height 6mm .

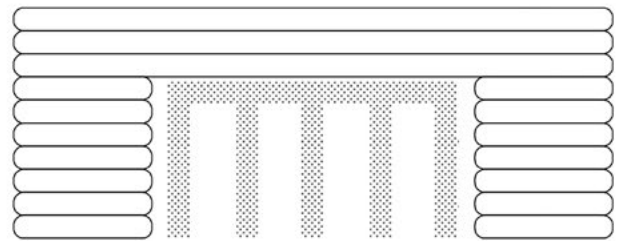
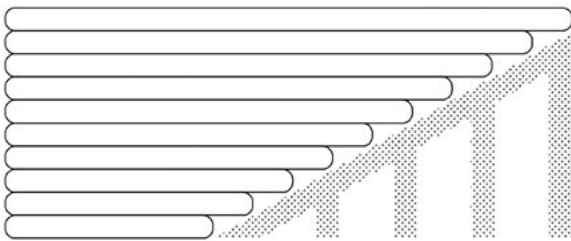
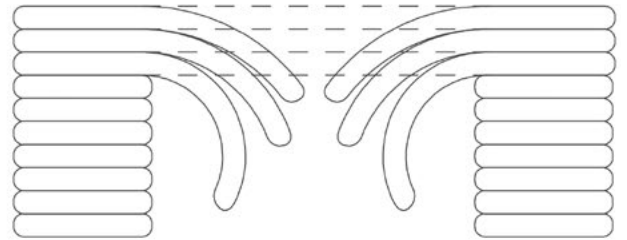
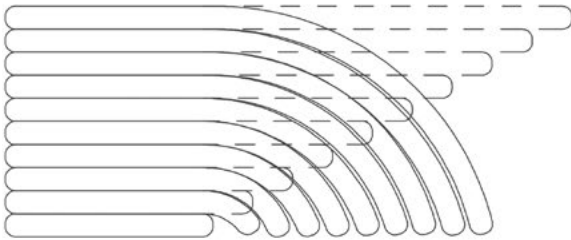


Figure 5: Failure-patterns of unsupported prints. left: overhang. right: bridging.

## SIZE OF THE FINAL PRODUCT

One of the biggest challenges of the implementation of AM in the building industry is the large size of the components. While many other ceramic AM processes produce small parts like dental prostheses or electric isolators, one of the smallest parts in the building industry is the brick. According to DIN 105 [13], many brick-formats derive from the 1DF, which has a size of 240x115x52mm, but is nowadays rather to be seen in facing shells. In times of thick, thus highly insulated walls, formats like the 21DF, measuring 425x365x238mm become more and more common. Although not standardised, roof tiles range in sizes around 450x250x65mm and a medium-size sink as an example for bathroom ceramics is to be planned taking up 650x550mm of space [14].

Commercially available ceramic printers such the Lutum 5 [15] or DeltaWasp40100 [16] models on the other hand provide build volumes of 400x460x800mm and Ø400xh1.000mm, respectively. The mentioned printers can be equipped with extruder-nozzles ranging from 1.2 up to 8 mm in diameter, which has a significant impact on the printing time. It can be assumed, that for commercial exploitation of the process, short printing times are favourable, therefore:

- IV *Usage of the biggest nozzle possible*  
Bigger diameter nozzles result in bigger strands of clay to be disposed of, which results in reduced printing time. On the other hand, bigger nozzles may negatively affect the smaller details of a geometry. Depending on the desired outcome a balance between those two aspects must be found for each individual project.

Figure 4 illustrates the influence the choice of the nozzle can make on the outcome. While both cubes measure 250x250x250 mm, the one on the left is sliced with a 3 mm nozzle, whereas the right one is sliced with an 8 mm nozzle. As maximum layer-height is 75% of the nozzle's diameter has proven as a best practice to quickly fabricate robocasted parts for building-applications. This results in layer heights of 2,25 mm and 6 mm, respectively. Therefore, a printing path of in total 2.303.250 mm cumulative length (resulting from 111 layers, each with 83 strands) would be necessary to process the print job with the smaller nozzle, while with the bigger nozzle could process the same geometry with just 325.500 mm (42 layers with 31 strands each) of path, which would be about seven times faster. On the other hand, it is clearly visible in the image that surface-quality is negatively affected by larger nozzles, which will be discussed in the paragraph "finishing of the product's surface".

## GEOMETRIC FREEDOM

Although additive manufacturing in general is praised again and again for its geometric freedom [17-19], much of this depends on the process used. Whereas for instance powder-based technologies come with an inherent support material that ensures the creation of overhangs, bridges, and cavities, robocasting as an extrusion-based process lacks this feature. Since the paste is not hardening fast enough to provide stability for subsequent layers, this at some point results in the collapse of the green body (Figure 5) and causes the loss of the whole print. Although cavities and overhangs have already been realised in the projects carried out so far, until now it has not been documented how the results were achieved [4]. Nevertheless, it must be mentioned in this context that by using finite-element simulation, the collapse of ceramic printed geometries has been made predictable [19]. Therefore, the exploration of two topics is advised:

- V *Development of strategies to counteract the limitations in overhang and bridging*  
Depending on the specific cases when overhanging or bridging may occur strategies to counteract their effects have to be developed. This may include the adaptation of techniques already known from FDM printing, as well as exploring other options.
- VI *Preliminary simulation of geometries prone to collapse*  
Besides the development of support strategies, an adaptation of the aforementioned simulation methodology and a follow-up adjustment of the geometry may contribute to achieving favourable printing-results.

## FINISHING OF THE PRODUCTS SURFACE

As typical for AM processes, depending on their height, the layers of a geometry become more or less visible (Figure 6, left side). Following the advice from paragraph "size of the final product" to use the biggest nozzle possible will surely promote this effect. Also, some of the aforementioned support strategies may leave visible marks on the surface which is supported. In backing bricks for instance, this may not be a big issue, or maybe even seen favourable as it provides a good subsurface for plaster to adhere. Facing bricks, roof tiles, or bathroom ceramics on the other hand, have visible surfaces for which these surface patterns may be unsatisfactory. Consequently, two subjects may be explored further:

VII *Development of methods to post-process printed surfaces*

Methods to flatten these surfaces need to be researched and tested. For instance, grinding down as well as filling up (Figure 6 middle & right side) those surfaces may take place in green, dried, or even fired state of the object.

VIII *Investigation on the applicability of coatings and other surface-treatments*

Even though glazing as a famous way to treat ceramics has been tested with additively manufactured objects [20], there are many ways surfaces are treated. Common techniques like engobing, sanding and scorching may be tested, too.

It must be mentioned at this point, that making the visible layers an inherent part of the design is a common way in AM to deal with his effects. Although a certain aesthetic quality is not denied in these approaches, the criterion of a flush integration is seen as the main topic of this paragraph.

## CONCLUSION

It has been pointed out, that many questions regarding the process have to be explored further, before additively manufactured ceramics may make their way into the market. In terms of materials, the use of already used raw materials provides a good approach on their integration, but the paste mixtures might be altered to achieve printability. Regarding component size and efficiency, a big printing nozzle is advised, even though this might affect surface quality. The development of support strategies appears to be crucial to achieve a higher degree of geometric freedom, but also may negatively affect surfaces. To eliminate such flaws when it comes to a visible usage of these components, methods to post process printed ceramics should be investigated. Also, commercially available printers do not appear to meet the requirements of the industry in the long term. The development of industrial-grade machines seems inevitable to set up efficient production.

## PRODUCTION TECHNOLOGY

As touched in paragraph “size of the final product”, commercially available printers barely exceed the necessary build-volumes for ceramic building components. Even though slightly bigger machines can be built on demand [21], industry will sooner or later have to aim for:

IX *Development of industrial-grade machinery*

The printers prevalent on the market do not meet the requirements of industrial production. Besides larger build-volumes, a constant supply of clay-paste needs to be implemented in such systems. Also, a 24/7 operation of the machines might be ensured in set-ups known as “print-farms”.

X *Training of CAD/CAM-skilled personnel*

Even though CNC-technology has been around since the 1970s, the brick industry so far has not been much affected by this. To digitally design and additively manufacture ceramic components may arise to a very specialised job-profile in the near future.

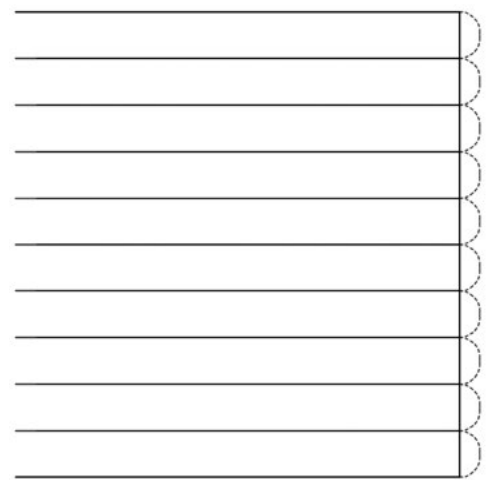
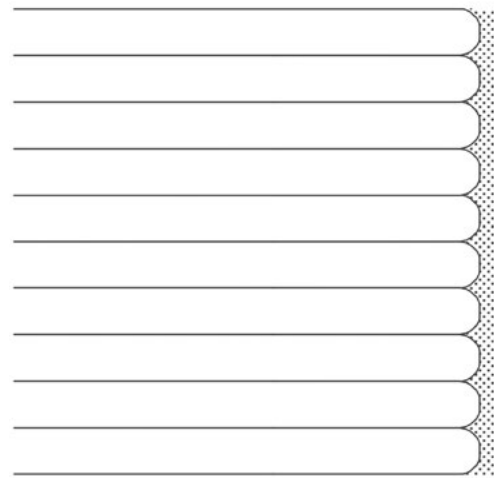
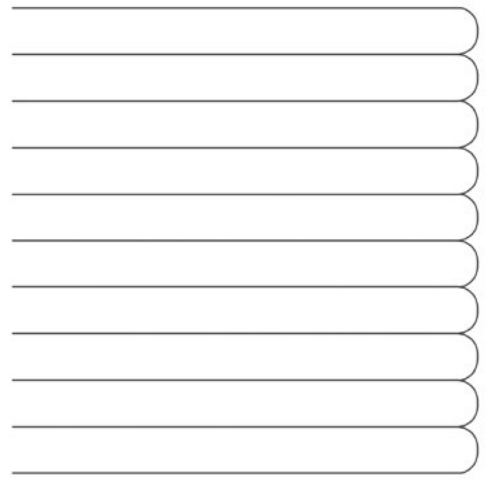


Figure 6: Surface-finishing. left: untreated. middle: filled up. right: smoothed down.

## REFERENCES

- [1] Peri GmbH, "Press release PERI builds the first 3D-printed residential building in Germany," 2020. <https://www.peri.com/en/media/press-releases/peri-builds-the-first-3d-printed-residential-building-in-germany.html> (accessed Aug. 16, 2021).
- [2] G. van der Velden, "MX3D : A 3D METAL PRINTING COMPANY," in *Built Environment - Additive Manufacturing Symposium 2019*, 2019, pp. 73-78. [Online]. Available: <https://be-am.de/>
- [3] A. Chiusoli, "Tecla," 2021. <https://www.3dwasp.com/en/3d-printed-house-tecla/> (accessed Mar. 04, 2021).
- [4] A. Wolf, P. L. Rosendahl, and U. Knaack, "Additive manufacturing of clay and ceramic building components," *Autom Constr*, vol. 133, no. September 2021, p. 103956, 2022, DOI: 10.1016/j.autcon.2021.103956.
- [5] P. L. Rosendahl and A. Wolf, "The business case for 3D printing in the built environment," in *Structures and Architecture A Viable Urban Perspective?*, 2022, pp. 254-259, DOI: 10.1201/9781003023555-31.
- [6] J. Cesarano, "Robocasting provides moldless fabrication from slurry deposition," *Ceramic Industry*, vol. 148, no. 4, pp. 94-100, 1998.
- [7] D. De Witte, *Clay Printing - The Fourth Generation Brickwork*. 2021.
- [8] J. Achtziger, G. Pfeifer, R. Ramcke, and K. Zilch, *Mauerwerk Atlas*. 2001, DOI: 10.11129/detail.9783955531652.
- [9] Tiles & Bricks Europe AISBL, "Bricks and tiles European manufacturing," 2021. <http://www.tiles-bricks.eu/industry> (accessed Apr. 26, 2021).
- [10] H. Backe, W. Hiese, and R. Möhring, *Baustoffkunde*. 2013.
- [11] Z. Chen *et al.*, "3D printing of ceramics: A review," *Journal of the European Ceramic Society*, vol. 39, no. 4. Elsevier Ltd, pp. 661-687, Apr. 01, 2019, DOI: 10.1016/j.jeurceramsoc.2018.11.013.
- [12] A. Deplazes, *Architektur konstruieren vom Rohmaterial zum Bauwerk : ein Handbuch*, 3rd ed. Birkhäuser, 2005.
- [13] Deutsches Institut für Normung, "DIN 105-1 Mauerziegel Teil 1: Vollziegel und Hochlochziegel der Rohdichteklassen >1,2." 2002.
- [14] T. Jocher and S. Loch, *Raumpilot*. Wüstenrot Stiftung, 2012.
- [15] VormVrij3D, "Lutum 5," 2023. <https://vormvrij.nl/brutum/products/lutum-5/>
- [16] 3DWASP, "DeltaWasp 40100," 2023. <https://www.3dwasp.com/en/ceramic-3d-printer-delta-wasp-40100-clay/>
- [17] A. Paolini, S. Kollmannsberger, and E. Rank, "Additive manufacturing in construction: A review on processes, applications, and digital planning methods," *Additive Manufacturing*, vol. 30, no. September, p. 100894, 2019, DOI: 10.1016/j.addma.2019.100894.
- [18] I. Larikova, J. Fleckenstein, A. Chokhachian, T. Auer, W. Weisser, and K. Dörfler, "Additively Manufactured Urban Multispecies Façades for Building Renovation," *Journal of Facade Design and Engineering*, vol. 10, no. 2, pp. 105-126, 2022, DOI: 10.47982/jfde.2022.powerskin.7.
- [19] V. Sangiorgio, F. Parisi, F. Fieni, and N. Parisi, "The New Boundaries of 3D-Printed Clay Bricks Design: Printability of Complex Internal Geometries," *Sustainability (Switzerland)*, vol. 14, no. 2, 2022, DOI: 10.3390/su14020598.
- [20] StudioRap, "New Delft Blue," 2019. <https://studiorap.nl/#/poortmeesters> (accessed Feb. 25, 2021).
- [21] VormVrij3D, "Brutum," 2023. <https://vormvrij.nl/brutum/>



# ADDITIVE MANUFACTURING EARTH-BASED COMPOSITE: DEFINING OPTIMUM COMPUTATIONAL METHODOLOGY FOR BUILDING SHELL GEOMETRY

Mohamad Fouad Hanifa

Bruno Figueiredo

Paulo Mendonça

Investigating the use of Additive Manufacturing (AM) in the construction of shell structures using earth-based materials is a challenge that attempts to combine the effectiveness of an innovative manufacturing system with an optimal structural system and a material resource with a low embodied carbon footprint. It is proposed to focus on the definition of an optimal structural optimization method for an AM self-supported shell system through computational strategies based on logical similarities between the brick assembly process and the extrusion layer path. The ideal topology for any structure with a given set of shell boundary conditions is naturally encoded by principal stress lines which are pairs of orthogonal curves that show internal force trajectories and consequently idealised paths of material continuity. The relationship between geometry and structural behaviour is investigated for shell-thin surfaces with overhangs. The structural integrity of the shell during the printing stage while the material is still wet or uncured is analysed as well as the printed-dried results and loads are taken into consideration to evaluate their structural properties. Finally, characteristics including structure balance, strength, local inertia, global inertia, and stiffness are also evaluated physically and digitally to infer the shell's structural performance.

To accomplish architectural design expression, structural performance, and efficiency, generative design methods are often incorporated into conceptual design. While using different techniques these initiatives aim to capitalise on the crucial connection between architectural geometry and structural behaviour and can inspire innovation in both. Efficient structures might involve sophisticated geometric solutions that can be formally appealing. However, because of a dearth of design tools that can efficiently combine architectural and structural considerations, the implementation of structural-led exploration has often fallen short of expectations [1].

## **Additive Manufacturing in AEC**

The use of additive manufacturing AM technologies in the Architecture, Engineering, and Construction AEC sector offers several benefits, including improved worker safety, effective resource use, and shortened construction times and costs. These benefits also consider crucial factors to control material transport parameters and manufacturing processes, as shown in Table 1 different case studies of AM structures in different countries. Additionally, it results in more reasonably priced and environmentally friendly construction, which is an important factor to mention as a beneficial point of using AM in areas with rapid population expansion. However, applying AM technologies at the build-

ing scale presents several opportunities and challenges, including enhancing structural strength, minimising support structure to produce more complex geometries, increasing printing speed, lowering material consumption, and improving printing quality and shape accuracy. Trials in building construction by AM in concrete have recently taken place in China, the US, and Russia. In all these projects, vertical walls are constructed using AM, whereas other building components, such as roofs, are constructed using conventional building techniques [2]. Vaults and shells are a great structural solution for using less material in building, but they are frequently unaffordable due to the labour and formwork requirements. Furthermore, after construction is finished, this formwork often ends up in landfills as garbage [3]. Over the past ten years, there have been major advances in technologies for AM in concrete and earth enabling the creation of multi-storey printed structures. Even said there are still few examples of AM roofs despite the existence of conventional models [4]. Reinforced Masonry shell techniques have been used in AM using both concrete and earth in small-scale prototypes [5]. The complexity of toolpath design and the absence of reliable structural simulation methodologies to quantify and validate non-planar printing have prevented full-scale 3D printing of spanning structures [6].

Table 1: Case studies of different AM structures on site [20].

Project Name	Guard House La sphere	First Residential House	The BOD	3D Housing 05	PRVOK	ICON-House ZERO	Project Milestone "platte kei"
Architect	Archétude	PIK companies group/Apis Cor /	COBOD	LOCATELLI   CLS ARCHITETTI	Michal Trpák	Lake Flato	Houben & Van mierlo
Printing material	Concrete	Concrete	Concrete	Concrete	Concrete	Concrete	Concrete
Project location	Harfleur , France	Stupino , Russia	Denmark Copenhagen	Milan , Italy	Prague , Czech Republic	Austin TX , USA	Eindhoven , the Netherlands
Climate zone	Temperate	Polar / Subpolar	Temperate	Temperate	Temperate	Subtropical	Temperate
Manufacturing method	Pre - fab	In - situ	In - situ	In - situ	Pre - fab	In - situ	Pre - fab
Type of Robotic printing	IRA	IRA	GP	IRA	IRA	GP	IRA
Geometric complexity	Double curvature	Single curvature	Single curvature	Single curvature	Single curvature	Single curvature	Double curvature
Reinforcement implementation	Steel rods	Steel rods	Steel rods	Not applied	Steel grate	Steel rods	Steel rods
Printing Time	21h	24h	1day 4h	2days	22h	10 days	-
Printed Elements	Wall elements	Walls	Walls	Walls	Walls	Walls	Wall elements
Printing Environment	Controlled exterior climate tent	Controlled exterior climate tent	Exterior climate	Exterior climate	Controlled interior climate	Exterior climate	Controlled interior climate
Reference	[23]	[25]	[26]	[27]	[28]	[22]	[29]

Project Name	TECLA	GAIA	DIOR Concept store	The House of Dust	TOVA	Clay Rotunda	Casa Covida
Architect	MC Architects	WASP	WASP	Alison Knowles	Posgrado 3D printing Architecture IAAC	Gramazio Kohler Research	Emerging Objects
Printing material	Earth	Earth	Earth	Earth	Earth	Earth	Earth
Project location	Massa Lombarda Italy ,	Massa Lombarda Italy	Dubai , U.A.E	Wiesbaden Germany	Barcelona , Spain	Bern , Switzerland	Colorado
Climate zone	Temperate	Temperate	Subtropical	Temperate	Subtropical	Temperate	Temperate
Manufacturing method	In - situ	In - situ	In - situ	In - situ	In - situ	In - situ	In - situ
Type of Robotic printing	IRA	IRA	IRA	IRA	TIRA	IRA	IRA
Geometric complexity	Double curvature	Single curvature	Single curvature	Double curvature	No curvature	Double curvature	Double curvature
Reinforcement implementation	Not applied	Not applied	Not applied	Not applied	Not applied	Not applied	Not applied
Printing Time	8 days 8 h	4 day 4h	-	-	49 days	50 days	-
Printed Elements	Double Dome	walls	walls	walls	walls	walls	walls
Printing Environment	exterior climate	exterior climate	Building walls	Building walls	exterior climate	Controlled interior climate	exterior climate
Reference	[21]	[24]	[30]	[31]	[32]	[33]	[34]

Given the current climate crisis, CO<sub>2</sub> overproduction, and the problematic material sourcing associated with the production of concrete, cob (earth-reinforced by natural fibres) outperforms and represents a realistic option for construction in the twenty-first century. In a temperate area, AM cob is an alternative to AM concrete for narrow-span constructions. Larger spans are not possible with clay due to a lack of reinforcing and its limited structural performance. Furthermore, when comparing the material features, cob has higher insulating values, although concrete has better mechanical properties, making prefab constructions easier to construct. When comparing the LC CO<sub>2</sub> of the two materials, cob has a 91% smaller carbon footprint than concrete [20].

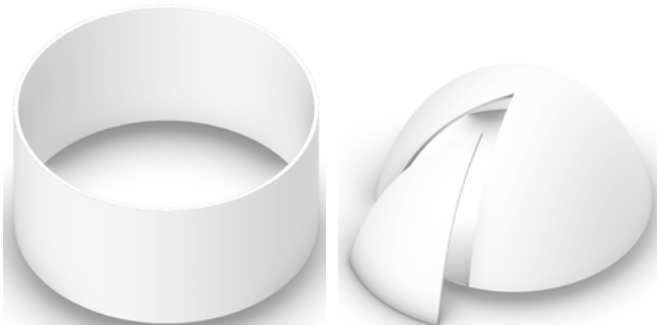


Figure 1: Earth formations with representative morphology [20].

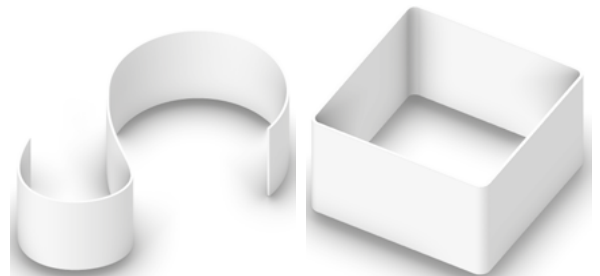


Figure 2: Concrete formations with representative morphology [20].

## Earth-based Materials for Additive Manufacturing

When utilised appropriately, the earth may offer solutions that are structurally, thermally, and acoustically efficient, furthermore being building material with low costs and minimal environmental impact. Untreated raw earth, however, has several limitations and drawbacks when compared to other conventional building materials (such as concrete or fired clay), as discussed in Table 2: low resistance to compression and tensile loads, vulnerability to water erosion, low resistance to dynamic loads, and high cracking during the drying process. [7,8,9]. This material has been actively modified to produce earth-based composites with increased compressive, tensile, and flexural strength using chemical stabilisers and fibre reinforcement [10]. The key issue in the attempt to combine the world's oldest construction material with the newest construction processing techniques is to assure their stability during the entire process [4].

### Earth-based Composites

Earthenware powder, aggregate (sand), fibre (straw), earth binders, and water are all components of earth-based composites. The qualities of the printing medium must be carefully researched and formulated in accordance with both its wet and hardened stages. Extrudability, buildability, and workability over time are the three fundamental requirements that must be satisfied for a 3D printing process to be successful, as shown in Figure 11. This calls for the material to deposit in layers with the least amount of deformation and flow effectively through the system without using excessive force [11,12].

### Natural Fibres & Earth Binders

Fibres are widely employed in earthen construction. In general, fibres can be easily combined with earth-based mixtures that present a viscous plastic state. By spreading stresses, the fibres increase tensile strength, decrease density, speed up drying, and prevent cracking.

Fibres vary in shape, size, strength, elasticity, and bond strength with earth, therefore the potential benefits with different types of fibre will change, as will the amount of a certain fiber required. The typical proportions vary from 1 to 4% by weight, signifying a volume in bulk that can be as large as the volume of soil. In this work, natural polyamide fibers such as sisal, vegetal fibre raffia, jute, and straw were combined with two types of earth binders' sodium silicate, and sodium hexametaphosphate that cast with different types of earth binders as shown in Figure 5 [35].

## Extrusion Systems

In this research, a comparative analysis of two material extrusion methods was conducted: Screw-extrusion and Ram extrusion. These methods represent distinct approaches to transporting and compressing material for AM purposes.

Screw-extrusion employs an auger screw mechanism to propel and compress the material toward the nozzle, a crucial point in the AM process. This rotational positive displacement pump, functioning through the rotation of the screw, moves material along the axial direction of the screw Figure 3 and Figure 7 using Lutum 4 VormVrij 3D Printer Auger extrusion system can be configured vertically or horizontally and involve a material hopper that holds the material for extrusion. The rotation of the screw within the hopper draws the material into the system. Notably, the WASP Company's Delta 3MT and 12MT printers utilize this method for experimenting with AM earth-based materials.

On the other hand, Ram extrusion relies on the application of a linear force to a piston within a cylinder ram filled with the material. Upon surpassing a pressure threshold, the accumulated pressure drives the material through the nozzle. This approach is also referred to as a linear actuator. Linear actuators generate force through the method of Pneumatic force, where a pneumatic cylinder induces linear motion and exerts force on the extrusion plunger and Electromechanical force, which employs mechanisms like lead screws or screw-jacks to transform motor-driven circular motion into the linear motion required for material extrusion as extruder is developed by 3DPotter as shown Figure6, Figure 8.

While both systems aim to achieve material extrusion for AM, they diverge in their mechanisms of force generation and material transport. Screw-pump extrusion capitalizes on rotational motion and positive displacement, whereas Ram extrusion employs linear forces through pneumatic or electromechanical means. The choice between these methods can significantly impact the efficiency, precision, and feasibility of additive manufacturing processes using earth-based materials.

In order to solve the shortcomings of the pneumatic system the use of the electromechanical extrusion method was considered for complex composites that consist of large size natural fibres between (0.5-1) cm. A commercial small screw-jack extruder supplied by 3D Potter® [11].

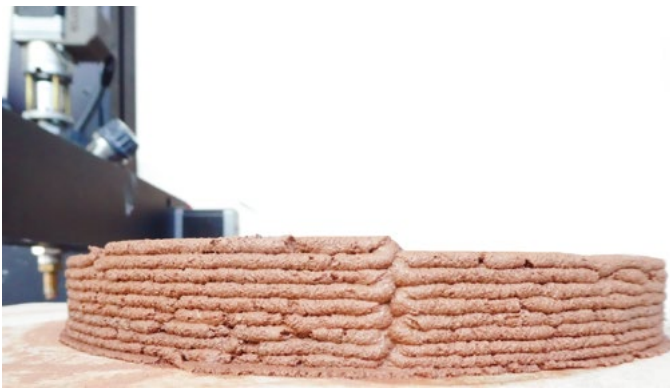


Figure 3: Extrudability test of Earthenware (Eco-clay) composite using Lutum® 4 VormVrij 3D Printer nozzle size 8mm.



Figure 4: Extrudability test of Earthenware (Eco-clay) composite consists of Fibre(straw), Aggregate (Fine sand), and Binder (Sodium silicate).

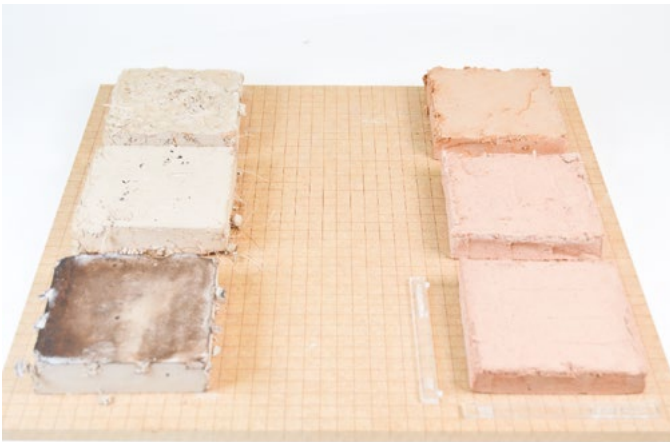


Figure 5: Different brick Earth-based composites cast by mold 10x10x2 cm.



Figure 6: Ram extrusion system consists of (1) Anti rotation, (2) stepper motor, (3) cartridge, (4) screw, (5) Clamp brace, (6) plunger, (7) earth-based composite, (8) nozzle adapter, (9) nozzle 15mm.

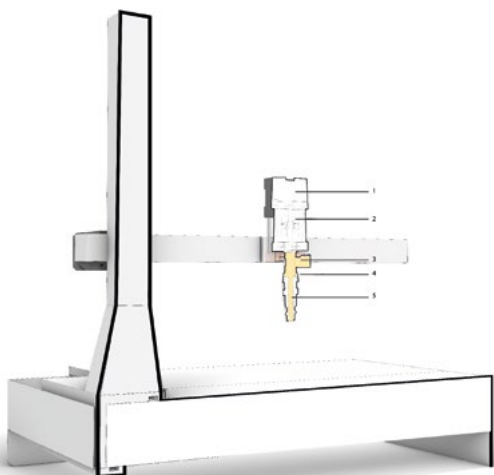


Figure 7a: Lutum (R) 4 Screw ceramic extrusion system consists of (1) stepper motor, (2) bearing, (3) ceramic inlet, (4) nozzle adapter, (5) auger screw.



Figure 7b: The utilization of stoneware clay composite without fibre extrusion with a Screw system has demonstrated significantly higher efficiency when it comes to additively manufacturing large-scale prototype.

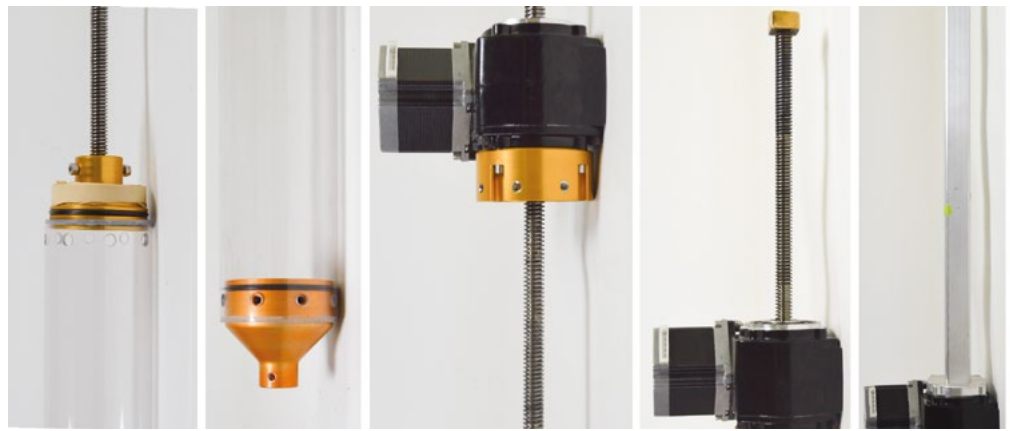


Figure 8: Ram extrusion system is developed by 3D Potter®.

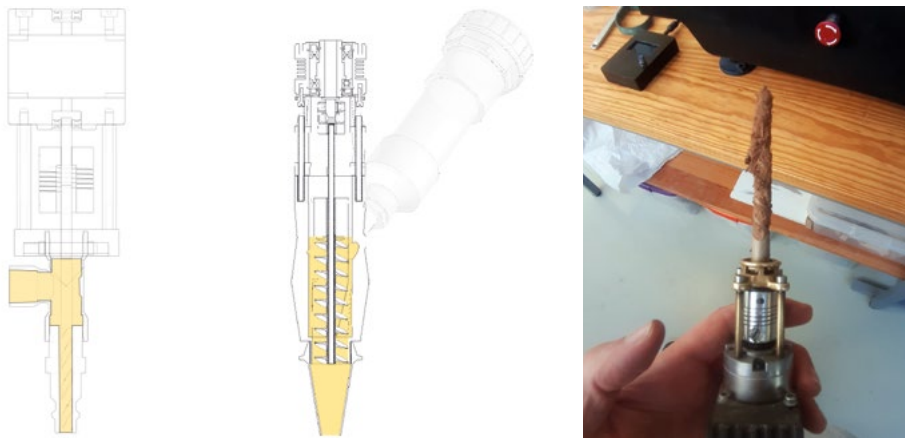


Figure 9: The challenge of maintaining feeding continuity during the printing process arises due to the utilization of composites containing oversized fibers within the screw Lutum® 4 extrusion system. This has spurred the exploration of a novel extruder concept, as illustrated in the figure.



Figure 10. A 6-axis KUKA robot was used to provide a workspace for the specimen extrusion procedure.

## AIM

The aim of this research is to comprehensively review the current state of additive manufacturing (AM) shell structure with a particular focus on earth-based materials. By synthesizing previous studies and tests on earth-based composites for AM also investigate the feasibility of enhancing the physical properties of these composites through the incorporation of natural fibers, binders, and stabilizers with defining the most suited extrusion system of these composites. The overarching objective is to contribute to the development of optimized computational design techniques or methodologies for AM shell structures by Considering the results of research on digital simulations and physical tests to qualify the optimal computational method for the definition of a design and the configuration into shell surface topology.

## AUTOMATED EXPERIMENTS EARTH-BASED COMPOSITE EXTRUSION

This part of the article explores the additive manufacturing potential of different earth-based composites, creating scaled cylindrical structures with dimensions of 10 cm diameter and 20 cm height. Two types of clay, namely earthenware (Ecoclay) and stoneware (Barcelo's clay), were utilized as the foundational materials for these composites. To enhance the mechanical strength of the resulting structures, we introduced sodium silicate as a binder during the mixing and extruding operations. This addition of sodium silicate aimed to augment the cohesion and robustness of the pieces, enabling better formability and structural integrity[19].

A critical aspect of achieving optimal extrudability and workability of Earth-based materials is the process of deflocculation. Deflocculation transforms a clay slurry from a thick and viscous consistency into a more fluid or plastic, pourable state. This process enhances the material's flowability, making it well-suited for extrusion-based additive manufacturing techniques. We employed sodium alginate as a deflocculant agent, effectively modifying the clay slurry's rheological properties. Furthermore, sodium alginate contributed significantly to the mechanical strength and water stability of the earth-based composites. By altering fundamental physical parameters like liquid limit, plastic limit, and plasticity, sodium alginate played a pivotal role in improving the overall engineering properties of the materials, particularly relevant for applications where structural stability is crucial[17].

Addressing the challenges posed by the engineering properties of loess an Earth-type characterized by loose accumulation and high collapsibility. To overcome these limi-

tations and enhance the suitability of loess for engineering applications, we introduced sodium hexametaphosphate as a dispersing agent. This compound has proven effectiveness in stabilizing earth dispersions, serving as both a surface complexant and a means of achieving particle size analysis in earth or soil studies (ASTM D422 - 63). In tandem with sodium hexametaphosphate, a polyacrylic acid with sodium ion side groups (PAAS) was also employed to further stabilize the earth's dispersions, contributing to improved extrudability and print quality[16].

In summary, the research demonstrated the feasibility of utilizing various earth-based composites, including earthenware and stoneware clays, in additive manufacturing processes. Through the strategic incorporation of sodium silicate binders, deflocculants like sodium alginate, and stabilizing agents such as sodium hexametaphosphate and PAAS, we successfully enhanced the workability, and engineering properties of the composites as shown Figure 11. In addition, Arabic gum, a product derived from the acacia tree, takes a pivotal role in soil or earth stabilization and composite reinforcement within construction applications. Acting primarily as a flocculant, Arabic gum facilitates the formation of cohesive flocs by binding clay particles together within the earth matrix. This process significantly contributes to augmenting the dry compressive strength of the composite, thereby mitigating water absorption and reducing shrinkage tendencies. However, the solubility of Arabic gum in water limits its effectiveness in protecting against prolonged moisture exposure to harness its benefits effectively, other natural additives such as sisal, jute, straw, and raffia vegetal fibers[15]. These natural fibers serve as reinforcement elements, enhancing the overall structural integrity of the composite. Alongside these fibers, aggregates such as fine sand and stone dust complete the composition, forming a balanced blend that combines the mechanical advantages of reinforcement with the stabilizing effects of Arabic gum and other binders. Through this tailored formulation, Arabic gum contributes to the creation of durable and resilient building materials that find utility in various construction scenarios[13].



Figure 11: The process of extruding diverse earth-based composites and enhancing them with binders, stabilizers, and reinforcing fibers is undertaken with the overarching goal of improving the overall quality of their physical and mechanical properties. The resulting composites have increased structural integrity, durability, flowability, extrudability, and performance qualities in the printing process as fresh state also in the drying state.



Figure 12: This figure shows the extrusion process of stoneware clay following amounts Table 2 composite code SSFEM - G.



Figure 13: This figure shows the extrusion process of earth-based composite using earthenware following the Table 2 amounts composition code SASHEXAGSSFEM - K.



Table 2. Characterizing Earth-Based Composite Material Matrix: Physical Properties and Carbon Footprint.

Amounts Kg/m3										
Compositions code	SSFEM -A	SSFEM -B	SSFEM -C	SSFEM -D	AGSSFEM -E	SSFEM -F	SSFEM -G	SSFEM -H	SHEXAGSSFEM -J	SASHEXAGSSFEM -K
Clay type	SW 0.0024	SW 0.0024	EW 0.004	EW 0.004	EW 0.004	EW 0.004	SW 0.0024	EW 0.004	EW 0.004	EW 0.004
Aggregates Type	FS 0.0006	FS 0.0006	FS 0.0937	FS 0.531	FS 0.456-SGD 1.0	FS 1.018-SGD1.426	FS 1.562-SGD2.0	SGD4.666	FS 1.018-SGD 1.426	FS 0.0676-SGD 1.677
Binder Type	-	-	SS 0.0008	SS 0.0062	SS 0.0055	SS 0.0342	SS0.0061	SS 0.0166	SS 0.0166 - SHEX 0.040	SS 0.0114 - SHEX 0.010- SA 0.0334
Stabiliser type	-	-	-	-	-	AG 0.5555	AG 0.5555	AG 0.5555	AG 0.5555	AG 0.2539
Fiber Type	SI 0.0344	SI 0.1724	SI 5.747	RV0.066	JU 0.1923	SI 0.3448	-	JU 0.0447	SI 0.0688	CS 0.091
Water	W 0.4	W 0.4	W 1.6	W 1.0	W 0.27	W 1.995	W 1.15	W4.688	W 0.141	W 0.367
Total Kg/m3	0.437	0.575	7.446	1.608	2.484	5.378	4.72	10.3771	3.269	2.617
Physical Properties										
Hardness	Average	Average	Average	Average	High	High	High	-	High	High
Extrusion	Good	Good	Good	perfect	Perfect	Perfect	Perfect	Not extrudable	Perfect	Perfect
Drying Time	36h	30h	48h	32h	40h	44h	38h	-	48h	35h
Cracking	No cracking	No cracking	cracking	No cracking	No cracking	No cracking	No cracking	-	No cracking	No cracking

EM: Earth - based Matrix.

FEM: Fibre reinforced Earth-based matrix.

SSFEM: Fibre reinforced Earth-based matrix stabilized with sodium silicate.

AGSSFEM: Fibre reinforced Earth-based matrix stabilized with sodium silicate & Arabic gum.

SHEXAGSSFEM: Fibre reinforced Earth-based matrix stabilized with sodium silicate , Sodium hexametaphosphate & Arabic gum.

SASHEXAGSSFEM: Fibre reinforced Earth-based matrix stabilized with sodium silicate , Sodium hexametaphosphate,Sodium alginate & Arabic gum.

Table 3. Earth-based composites ingredients density and carbon footprint kgCo2/kg eq.

Composition ingredients	Density kg/m3	KgCO2/KG
Earthenware EW	860	0,021
Stoneware SW	1650	0.029
Fine sand FS	1600	22.7
Stone granite dust SGD	1500	0.107
Sisal SI	1450	0.0005
Chopped Straw CS	43.5	0.061
Raffia Vegetal RV	750	0.0007
Jute JU	1300	0.57
Water W	1000	0.298
Sodium silicate SS	2400	0.91
Sodium hexametaphosphate SHEX	2480	3.206
Sodium Alginate SA	1000	2.7

# COMPUTATIONAL DESIGN METHODOLOGIES FOR (AM) SHELL SYSTEM

## Introduction

The construction industry's widespread implementation of earth or concrete AM technology in the future will be heavily reliant on breakthroughs in printing methods, materials science, reinforcement techniques, and design tactics. Nonetheless, current technology allows for the printing of structures of a decent scale that do not require formwork simplifying construction and lowering costs & time. For these structures to be functional, their geometry must be tailored to the behavior of the printed material, transforming them into compression-dominant structures. An examination of historical precedents revealed that building designs meeting such requirements integrated load-bearing wall systems with shell structures derived mostly from arches, especially vaults and domes [36].

## Historical form typology to slicing strategies

The Middle Age Gothic stone vaults had to be erected formwork-free due to a lack of wood resources for carpenters. Masons produced these constructions with minimal equipment by using specific mortars, brick-laying assemblies, and geometries. The history of Persian architecture has contributed to the development of long-lasting vault constructions using distinct Persian vaulting techniques [36].

The Persian vault system is a way of dividing square or rectangular limits into smaller triangular pieces and then changing the initial boundary into a circular boundary as the foundation for the construction of a dome to entirely cover large spans without the use of formwork.

This article introduces an exploration featuring two meticulously tested methods, both executed at a 1:10 scale, analysing the Potkaneh and rib-reinforced AM approaches. The objective of this study revolves around harnessing the intrinsic potential of analysis-building typology of historical structural elements, specifically Persian and gothic vaulting, to bolster the efficacy of the additive manufacturing process also to extract specific mixed slicing strategies that support the AM process. Additionally, the incorporation of rib elements further augments the stability and global inertia of the structure [37].

The slicing approach used has a direct impact on the success of AM by changing the structure's local stability throughout the printing process. There are many ways to slice a geometry for AM. The slicing thickness and slicing angle, which might be constant or variable, distinguish these approaches. 3D topology printing is an excellent method for reducing local cantilevers between printing laces while increasing the interface between succeeding laces.

The simplest approach to creating a dome as known Vaults and domes are shells formed by translating or rotating arches through layer corbeling, which is attainable if the foundation arch is pointed with an appropriate slope. Aside from the regular use of corbeling to deposit material in circular layers until the pointed dome is reached, a composition of niches resembling Potkaneh, a type of Persian squinch, can be obtained using corbeling to make a structure consisting of a dome supported by bearing walls. In Persian architecture, the introduction of squinches or pendentives as transition elements can provide a way of reducing stress in the connections between the wall and the circular base.

This article solely examines the horizontal slicing technique (1) in relation to emulating historical building typologies and transitioning from masonry to earth-based additive manufacturing as shown in Figure 17. is an attempt to investigate the Earth AM design space by using examples of masonry constructions-built centuries ago with no temporary support. As a result, costs, construction delays, and waste after completion are all reduced. Identifying and categorizing masonry solutions for constructing shell structures makes it easy to identify which factors to experiment with while transitioning to AM. Additionally, to clarify computational design methods with particular criteria drawn from historical vaulting techniques.

The distance and the slicing angle are the two most important aspects of the slicing process. Slicing plane distances and angles might be fixed or changeable depicting the various slicing procedures for the same shape.

## Automated Experiments - Extrusion shell surface

### Objective

The core aim of these experiments centers on investigating key aspects of additive manufacturing (AM) applied to simplified self-supported geometries characterized by circular and square boundaries at a scale of 1:10 using a nozzle size 3mm.

The study encompasses the following goals:

**Analysis of Catenary Arch Profile within dome or shell surface:** Through digital simulation, the research endeavors to uncover the range of minimum and maximum overhang angles achievable within AM This analysis provides insights into the geometric limits and structural behavior starting from simple shapes into such complex as shell surface during the additive manufacturing process.

**Exploration of Buildability:** By systematically experimenting with diverse strategies the study assesses the feasibility of applying Various approaches to enhance both local and global inertia of the geometry by translating ancient vaulting methods that increase the surface area and reduce stresses within the shell surface by adding ribs and pendentives, thereby addressing challenges related to sta-

bility and structural integrity. The investigation encompasses both digital and physical examinations to ascertain the viability of the proposed methodologies.

In pursuit of these objectives, this research seeks to contribute to the comprehension of AM's capabilities in crafting intricate architectural forms and to identify strategies that optimize the construction of complex shell structures with circular boundaries.

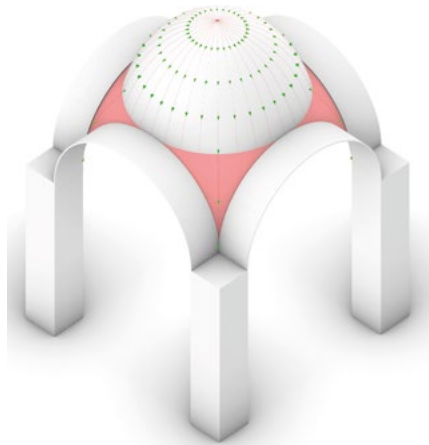


Figure 14: In dome construction, the transition between curved and planar surfaces is made. Squinch in Persian domes, pendentives in Western domes.

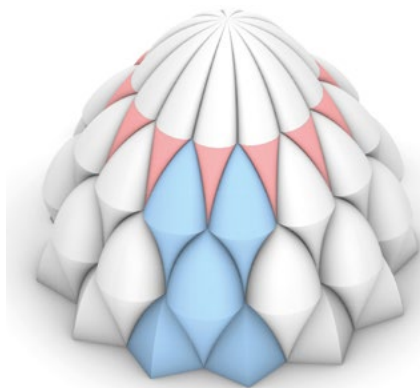


Figure 15: Potkaneh vaulting method.

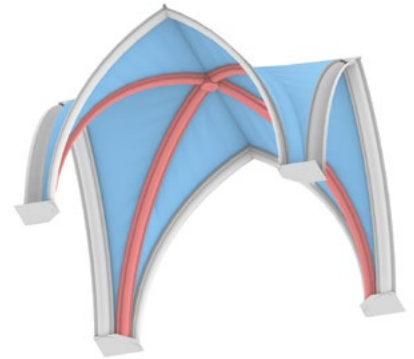


Figure 16: Gothic vaulting: (a) primary building components, (b) rib network configuration, and (c) various infill patterns

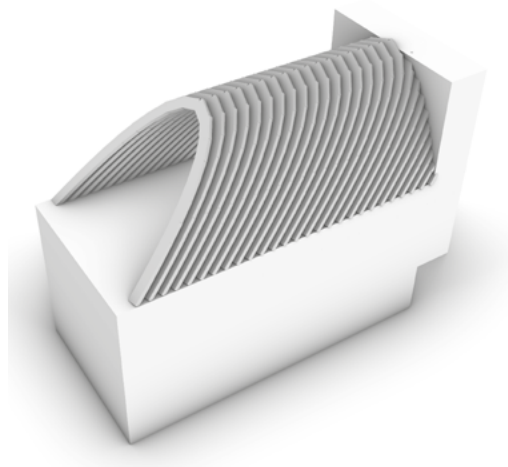


Figure 17: Deriving a slicing strategy inspired by the architectural features of Nubian vault construction within the context of masonry building typology.

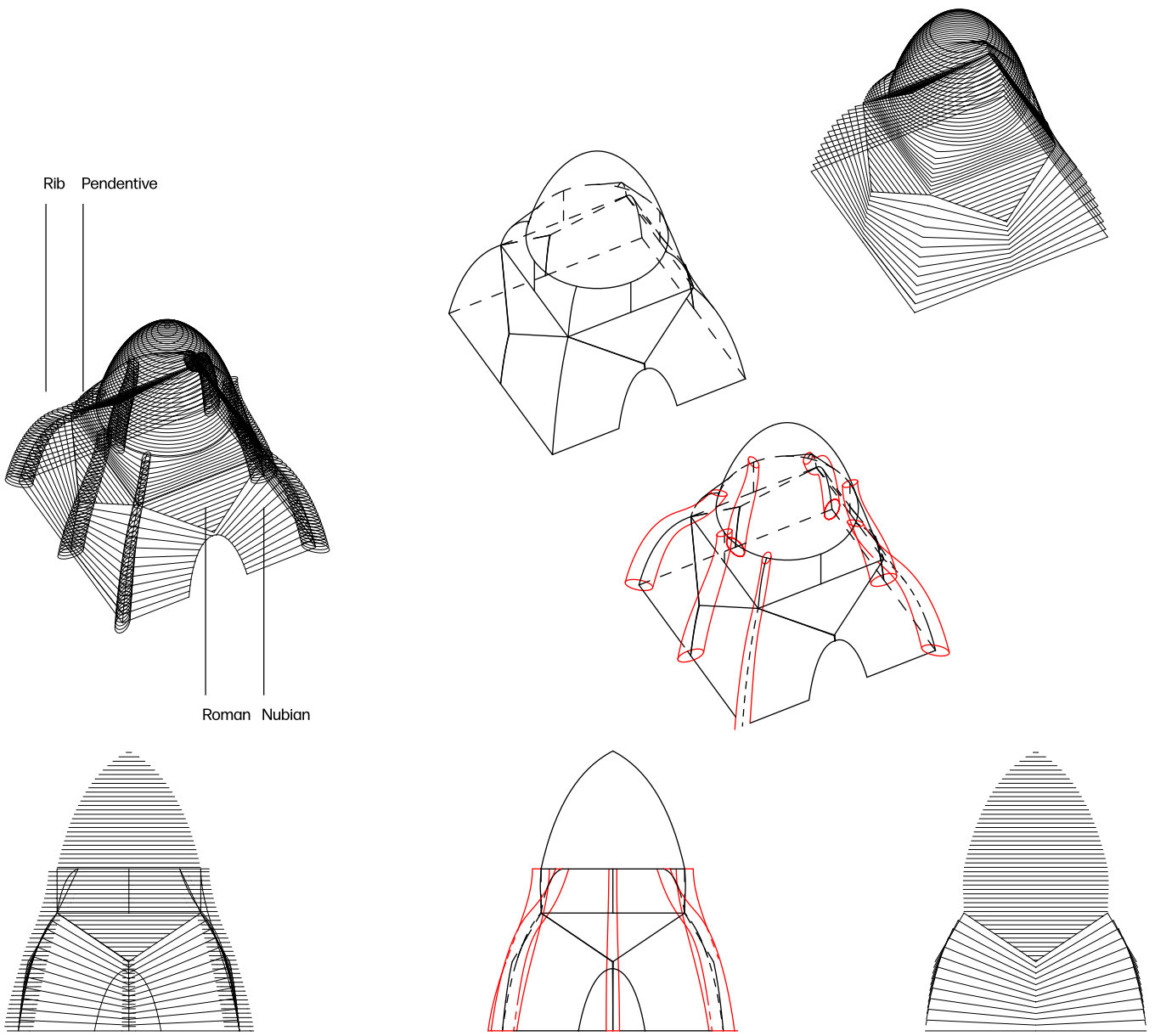


Figure 18: Formulating a slicing strategy rooted in the amalgamation of diverse historical building typologies.

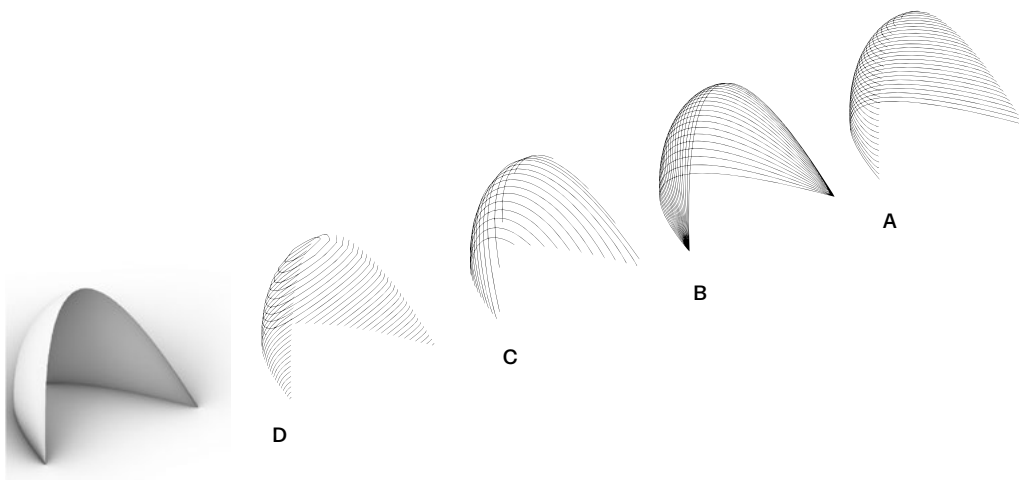

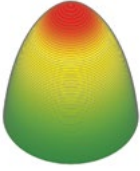
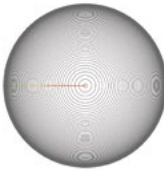


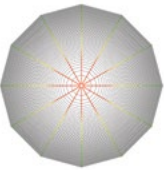





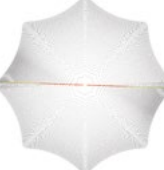











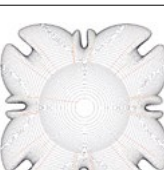


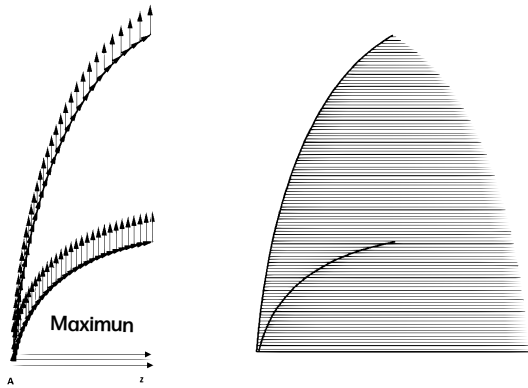
Figure 19: Various methods for slicing shell geometries are contingent on parameters like slicing distance and orientation angles.

Table 4. Design framework for earth-based composite AM shell surface.

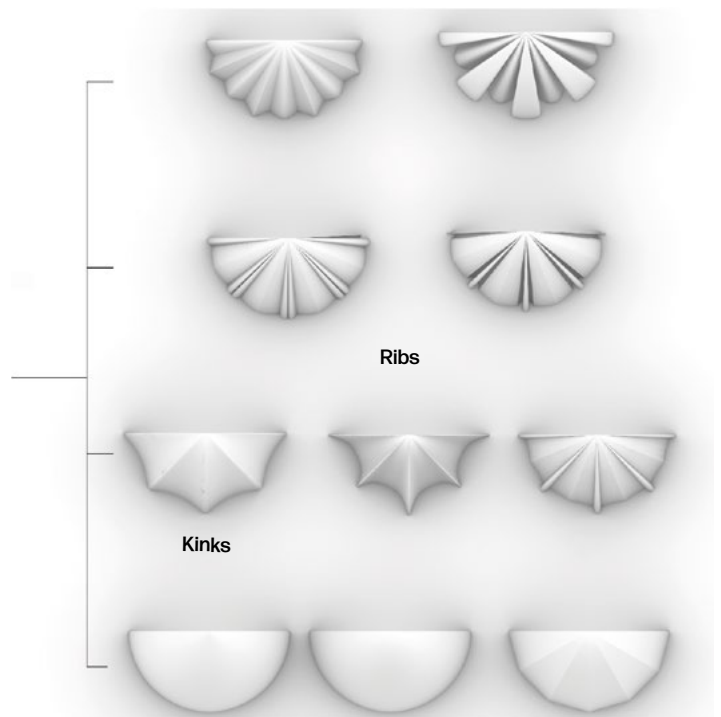
Shell Structure system		Analysis	Slicing	Computational Method	
Boundary	Form	Overhang Angle	Horizontal	Rib reinforced	Potkaneh vaulting
Circular				Not applied	Not applied
Faceted				Not applied	Not applied
Circular				Applied	Not applied
Circular				Applied	Not applied
Circular				Applied	Not applied
Circular				Applied	Not applied
Square				Not applied	Applied
Square				Applied	Not applied

### 4.3.2. Methodology

Minimum overhang angles



a)



b)



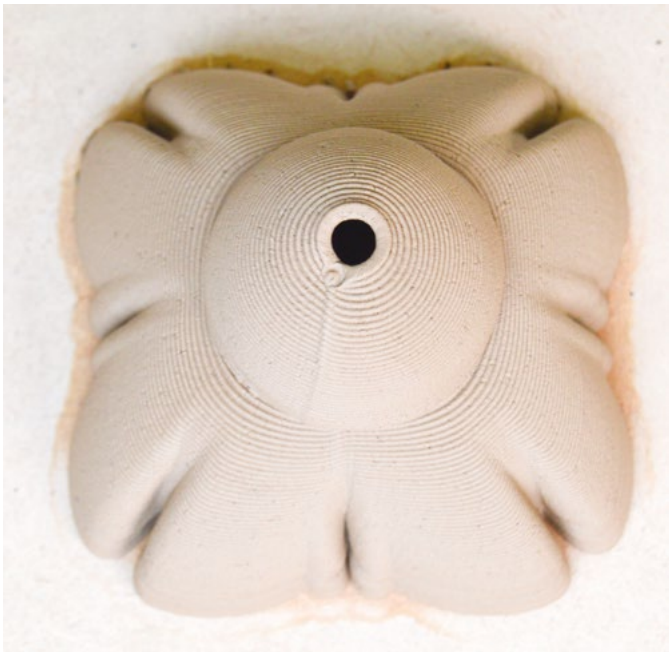
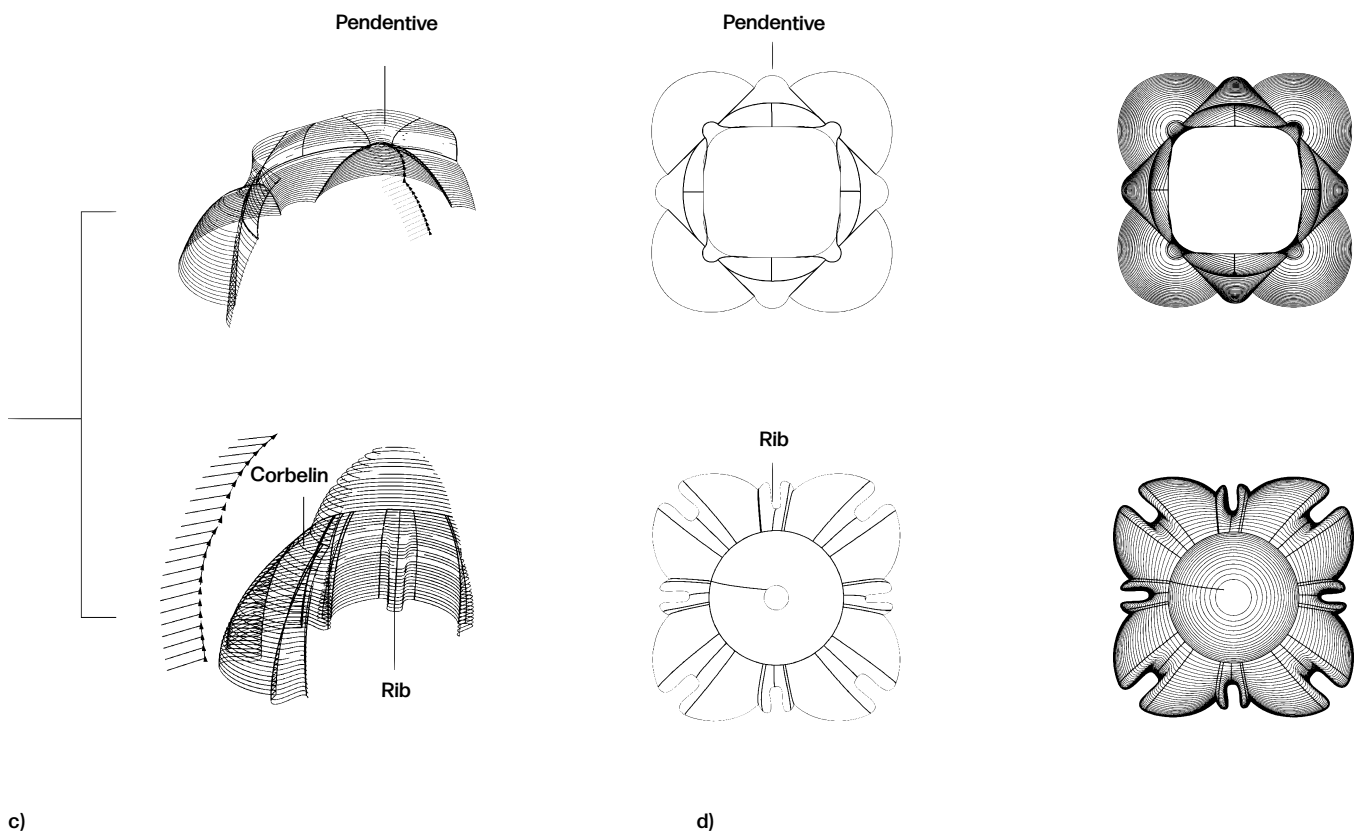


Figure 20: Multiple iterations of additive manufacturing half-domes were conducted, wherein each prototype's design was systematically adjusted to enhance both local and global inertia. This optimization was achieved by strategically modifying the surface area, resulting in improved stability during the printing process.

### **The conditions of the boundary and global geometry**

The range of geometries that can be produced is extensive, as demonstrated by the examples of brick structures created without or with little temporary support as shown in Figure 14, Figure 15, and Figure 16. Table 4 suggests primitive shapes depending on boundary conditions particularly the structure's supports and a chosen profile. This profile can be square or turned to make a shell or dome faceted or unfaceted. A robot eliminates this geometric barrier because of its precise precision in space. As a result, the goal geometries for this article must be as close to the sum of the structure's self-weight and anticipated external loads related to the object function as possible [36] [37].

### **The establishment of the Rib shell network**

Through the allocation of thickness, we transform the surface into a shell structure. This shell is then subjected to external loads and analyzed using Finite Element Analysis (FEA). From the FEA results, we derive the primary stress distribution across the surface, ensuring material integrity and identifying the optimal topology. Our goal is to strategically position ribs along two perpendicular axes. Leveraging this stress field information, we create a comprehensive parametric representation and subsequently generate a quad-mesh with edges aligned to these axes. Within this quad-mesh, we extract a network of ribs, maintaining uniformity through quadrangulation. This network encompasses a variety of elements, including branches, circles, and curves. [38].

## **DISCUSSION AND CONCLUSION**

Expanding the vocabulary of AM complex structures using sustainable materials as earth-based composite by mimicking building typologies from masonry structures into mixed slicing process considering horizontal and non-planar AM methods opens up a wide range of new possibilities for waste reduction, decreased construction time, and increased geometric flexibility, as well as enhances the behavior of the material composite by studying binders, stabilisers, and material reinforcement helps to increase the buildability, flowability, and durability. Our findings show that structural and material improvement reduces the failure of building complex structures such as shell in AM which have a strong promise in construction-scale printing. The optimised toolpath geometry through different slicing tactics also opens up new design possibilities for printed structures, where the look of path patterns can be further

controlled by aesthetic constraints defined by the architect. Reducing overall path length can also allow for faster deposition, reducing the risk of structurally deteriorating. In the future, Form-finding layer-by-layer processing and overhang simulation could be combined to generate varying shell thicknesses, lowering material usage and print times. This systematic study used a traditional material composite and its related embodied knowledge to foster digital innovation with a low-cost and sustainable alternative robotic AM method and a hardware extrusion system is developed for this sake.

### **Limitations and future work**

The primary challenge of AM earth-based composites to build complex structures as shells is to ensure the stability, flowability, and buildability of the material deposition whereas the structure scale considering the deposited layer size also the extrusion system that should give continuous material feeding has a dominant role in achieving the best material and machine behavior.

When AM shells the stresses in the material are higher than for a standard vertical wall with the potential apparition of tensile stress and bending moment whereas The failure risk of the structure is possible during the process according to this fact the material formulation and the printing set-up have to be optimised in order to successfully complete the fabrication. The simulations in this paper show vast inputs including geometrical aspects such as the boundary, layer distance, and overhang angle conditions to achieve an accurately AM-optimised structure.

The process of creating reliable toolpaths for shell structures during the AM process can be challenging. Future work can be outlined to address this issue :

Proposing A novel computational method takes into consideration the orientation of the toolpath relative to the principal stress lines in order to enhance the structural integrity of the shell system. By aligning the toolpath perpendicular to these stress lines, the resulting structure exhibits improved mechanical properties. Furthermore, the toolpath is generated with respect to the supporting computational technique such as rib reinforcement of the structure to ensure stability during the printing process.

### **ACKNOWLEDGMENTS**

This work was financed by Minho University, Lab2PT, Landscapes Heritage and Territory laboratory through FCT (Foundation of Science and Technology) as a Doctoral Grant with the reference 2021/07670/BD. The Institute of Design of Guimaraes was hosting and supporting the *Advanced Ceramics R&D Lab & ARENA LAB* on the use of their facilities and equipment to achieve the research proposal tests and prototypes.



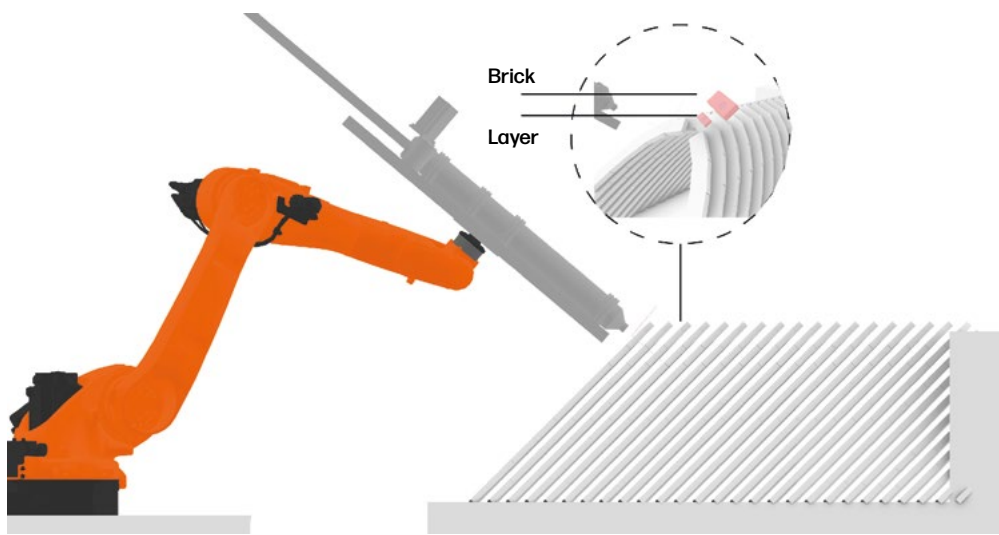


Figure 21: This figure shows the similarity between assembling masonry brick structure Nubian vault and the extrusion layer path.

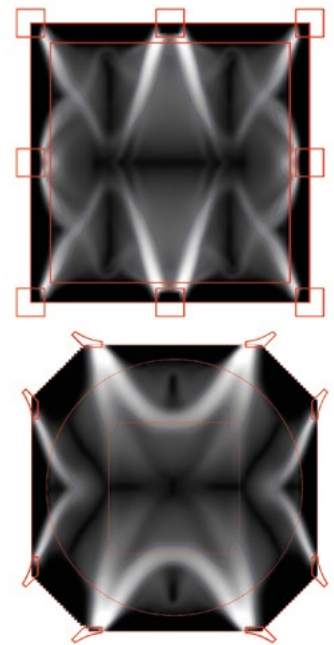


Figure 22: The primary goals encompass using the 'topos' plugin for topological optimization to replicate the rib cross-section, and harnessing the stresses present in the initial shell surface to inform the placement of ribs and determine their precise mass

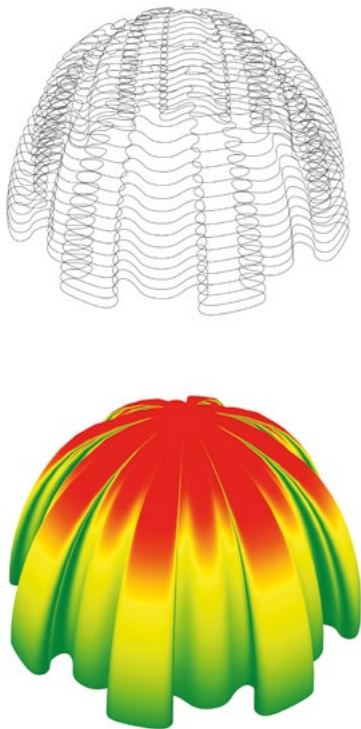


Figure 23: Extrusion test of shell geometry scale 1:10 using nozzle 15mm following the rib reinforced computational method with simulation of overhang angle.

## REFERENCES

- [1] Kam-Ming Mark Tam, C. T. STRESS LINE GENERATION FOR STRUCTURALLY PERFORMATIVE ARCHITECTURAL DESIGN. *ACADIA*, 108-109(2015).
- [2] J. S. N. Duarte. Designing Shelters for 3D-printing. *eCAADe*, 31-38. (2018)
- [3] G. Bertino. Fundamentals of Building Deconstruction as a Circular Economy Strategy for the Reuse of Construction Materials. *applied sciences*, 939. (2021)
- [4] L. C. Lancaster, Ed., "Complex Vault Forms of Brick," in *Innovative Vaulting in the Architecture of the Roman Empire: 1st to 4th Centuries CE*, Cambridge: Cambridge University Press, pp. 70-98. (2015)
- [5] R. Rael. *Earth Architecture*. Princeton, Architectural Press. (2009)
- [6] Alexander Curth, T. B. (2021). Multi-objective optimization of 3D printed shell toolpaths. *ResearchGate*. Retrieved from [https://www.researchgate.net/publication/355652674\\_Multi-objective\\_optimization\\_of\\_3D\\_printed\\_shell\\_toolpaths](https://www.researchgate.net/publication/355652674_Multi-objective_optimization_of_3D_printed_shell_toolpaths)
- [7] F. Aymerich, L. Fenu and P. Meloni, *Constr Build Mater* 27 (1) 66-72. (2012)
- [8] V. Sharma, H. K. Vinayak and B. M. Marwaha, *Constr Build Mater* 93 943-949. (2015)
- [9] L. Miccoli, U. Müller and P. Fontana, *Constr Build Mater* 61 327-339. (2014)
- [10] C. Galán-Marín, C. Rivera-Gómez and J. Petric *Constr Build Mater* 24 (8) 1462-68. (2010)
- [11] M. Gomaa, 3D Printing System for Earth-based construction: Case Study of Cob Mohamed. *Automation in Construction*, 124. (2021)
- [12] A. Perrot a, e. D., 3D printing of earth-based materials: Processing aspects. *Construction and Building Materials*, 670-676. (2018)
- [13] G Silva, L. Q. (2019). Development of a stabilized natural fiber-reinforced earth composite for construction applications using 3D printing. *IOP Conference Series: Materials Science and Engineering*, 706. doi:10.1088/1757-899X/706/1/012015
- [14] Niels de Beus, M. C., Carbon Footprint and Sustainability of Different Natural Fibres for Biocomposites and Insulation Material. Germany: RENEWABLE CARBON PUBLICATIONS. (2019)
- [15] CRA Terre, A. E.-U. (n.d.). *Additives to clay - Organic*. France: Practical Action . Retrieved from [https://ia600308.us.archive.org/15/items/PracticalActionTechNotes/Practical\\_Action-additives\\_clay\\_organic.pdf](https://ia600308.us.archive.org/15/items/PracticalActionTechNotes/Practical_Action-additives_clay_organic.pdf)
- [16] Yves Jorand, L. A. (2015). Earthen construction: an increase of the mechanical strength by optimizing the dispersion of the binder phase. *ResearchGate*. doi:10.1617/s11527-015-0595-5
- [17] Jia1, Y. Z. (2020). Improvement of loess characteristics using sodium alginate. *Bulletin of Engineering Geology and the Environment*, Springer. doi:<https://doi.org/10.1007/s10064-019-01675-z>
- [18] R.Yahaya1, 4. S. (2016). WATER ABSORPTION BEHAVIOUR AND IMPACT STRENGTH OF KENAF-KEVLAR. SAGE
- [19] Hansen, T. (2019). *Binders for Ceramic Bodies*. Retrieved from [digitalfire.com/article/binders+for+ceramic+bodies](https://digitalfire.com/article/binders+for+ceramic+bodies)
- [20] M.Bochem, Brug, S., N.Duister, I.Kaan, & Gemert, M. (2022-2023). *Comparison of 3d printed earth & 3d printed concrete for small spans*. Research in Urbanism and Architecture. IS-SUU. Retrieved from [https://issuu.com/mwvjangemert/docs/comparison\\_of\\_3d\\_printed\\_earth\\_3d\\_printed\\_concre](https://issuu.com/mwvjangemert/docs/comparison_of_3d_printed_earth_3d_printed_concre)
- [21] 3D printed house TECLA - Eco-housing - 3D Printers I WASP. (n.d.). Retrieved October (23, 2022), from <https://www.3dwasp.com/en/3d-printed-house-tecla/>
- [22] ICON's House Zero I ICON. (n.d.). Retrieved October 21, 2022, from <https://www.iconbuild.com/housezero>
- [23] RP, B. B. (2020, sep 19). *SPHÈRE: a 3D printed building in Harfleur (76)*. Retrieved from [batinfo: https://batinfo.com/en/actuality/sphere-a-3d-printed-building-in-harfleur-76\\_16826](https://batinfo.com/en/actuality/sphere-a-3d-printed-building-in-harfleur-76_16826)
- [24] Press Release\_3D printed house\_Gaia\_WASP.docx. (n.d.). Retrieved October 23, 2022, from [https://www.dropbox.com/sh/vvktzj4bfhjzfy/AADMZtYJt7bg-rkN0015jZaSa?dl=0&preview=Press+Release\\_3D+printed+house\\_Gaia\\_WASP.docx](https://www.dropbox.com/sh/vvktzj4bfhjzfy/AADMZtYJt7bg-rkN0015jZaSa?dl=0&preview=Press+Release_3D+printed+house_Gaia_WASP.docx)
- [25] Vesna Mila Z. Čolić Damjanović, N. J. (2018). Housing of the Future: Housing Design of the Fourth Industrial Revolution. *ResearchGate*. doi:10.1109/EFEA.2018.8617094
- [26] Bod, T. (2022, August 11). *cobod*. Retrieved from [cobod: https://cobod.com/projects-partners/the-bod-building/](https://cobod.com/projects-partners/the-bod-building/)
- [27] Massimiliano Locatelli, C. A. (2018). *3dhousing05*. Retrieved from [3dhousing05: https://www.3dhousing05.com/](https://www.3dhousing05.com/)
- [28] Wang, J. (2020, August 2). *apartmenttherapy*. Retrieved from [The First 3D Printed House in the Czech Republic Could Float on Water: https://www.apartmenttherapy.com/burinka-3d-printed-house-czech-republic-36803935](https://www.apartmenttherapy.com/burinka-3d-printed-house-czech-republic-36803935)
- [29] Ranjit, J. (2021, may 11). *parametric-architecture*. Retrieved from [Project Milestone: 3D-Printed Home Designed By Houben & Van Mierlo: https://parametric-architecture.com/project-milestone-3d-printed-home-by-houben-van-mierlo/](https://parametric-architecture.com/project-milestone-3d-printed-home-by-houben-van-mierlo/)
- [30] L., M. (2021, Nov 9). *WASP 3D-Printed Dior Pop-up Store Using Eco-Friendly Materials*. Retrieved from [3dnatives: https://www.3dnatives.com/en/wasp-3d-printed-dior-store-eco-friendly-materials-091120216/#!](https://www.3dnatives.com/en/wasp-3d-printed-dior-store-eco-friendly-materials-091120216/#!)
- [31] Knowles, A. (1967-2021, sep 26). *The House of Dust*. Retrieved from [tinybe: https://tinybe.org/en/artists/alison-knowles/](https://tinybe.org/en/artists/alison-knowles/)
- [32] Ikiz, S. U. (2022, sep 12). *Spain's First Building Made With Earth And A 3D Printer: TOVA*. Retrieved from [parametric-architecture: https://parametric-architecture.com/spains-first-building-made-with-earth-and-a-3d-printer-tova/](https://parametric-architecture.com/spains-first-building-made-with-earth-and-a-3d-printer-tova/)
- [33] Gramazio Kohler Research, E. Z. (2020-2021). *Clay Rotunda, SE MusicLab, Bern*. Retrieved from [gramaziokohler: https://gramaziokohler.arch.ethz.ch/web/e/projekte/430.html](https://gramaziokohler.arch.ethz.ch/web/e/projekte/430.html)
- [34] Paula Pintos, R. R. (2020). *Casa Covida / Emerging Objects*. Retrieved from [archdaily: https://www.archdaily.com/963516/casa-covida-emerging-objects](https://www.archdaily.com/963516/casa-covida-emerging-objects)
- [35] G Silva, L. Q. (2019). Development of a stabilized natural fiber-reinforced earth composite for construction applications using 3D printing. *IOP Conference Series: Materials Science and Engineering*, 706. doi:10.1088/1757-899X/706/1/012015
- [36] Gonçalo Duarte, N. B. (2020). Learning from historical structures under compression for concrete 3D printing construction. *Journal of Building Engineering, scienceDirect*, 116.
- [37] Mahan Motamedi, R. O. (2020). Supportless 3D Printing of Shells: Adaptation of Ancient Vaulting Techniques to Digital Fabrication. *ResearchGate*. doi:DOI: 10.1007/978-3-030-29829-6\_55
- [38] BOMMES D., ZIMMER H., KOBELT L.: Mixed-integer quadrangulation. *ACM Transactions On Graphics (TOG)* 28, 3 (2009), 77.5

# CERAMIC AM FUNCTIONAL STRUCTURES

João Carvalho

Bruno Figueiredo

Paulo J. S. Cruz

The manufacture of architectural components driven by digital design tools and Additive Manufacturing (AM) allows the achievement of highly evolved constructive systems, capable of answering to specific contexts and demands, resulting in unique solutions with high geometric and material performances. It is not a new method to build the same architecture, but a set of techniques that enhance new formal, spatial and material conditions [1], integrated in a logic that transcends the architectural project as we know, establishing itself as fundamental to overcome some of its limitations. In this sense, it is presented as research to the design and construction of 3D framed structures constituted by discretized ceramic components produced by PEM (Paste Extrusion Modelling) and post tension systems. For the execution of the connecting elements between ceramic components were tested metallic and wooden parts to work in collaboration with ceramic elements, counteracting their weakness to traction efforts. The outcome is a hybrid framed structure made of ceramic, wood, steel, and concrete, taking advantage of the specific properties of these materials.

The potential that Additive Manufacturing (AM) can bring to architecture has been highlighted during the last few decades with a large number of examples exploring different approaches and materials. Traditionally called 3D printing, AM consists in the production of objects by the successive deposition of material, layer by layer, where it is necessary, making it a more sustainable system when compared to traditional methods and even to contemporary subtractive methods where, generally, there is a big waste of material during production processes.

As Guilherme Wisnik (2016) [2] points out, contemporary architecture is currently undergoing a transition from a focus on mechanical form to an emphasis on performative behaviour. A passage that embodies Reyner Banham's (1969) [3] idea of architecture as a mean to the production

of “well-tempered environments”, elevating the architectural project to more than a simple formal or structural determination. Basically, as proposed by Marjan Colletti (2010) [4] this contemporary manifestation of digital architecture materialises a fusion of poetic expression and instinctual understanding, merging cultural traditions with technological advancements and progress, striving for a more efficient and adapted built environment.

In addition to the potential benefit regarding the economy of means and sustainability, AM also allows mass customization, having few restrictions about the plurality of geometries that are possible to manufacture. The limitations are related to the material and the production equipment. Since the material is only deposited where it is needed and this process is computer controlled, the pro-

duction of a series of different objects does not depend on the existence of moulds or formworks, eventually takes the same time to produce and has the same cost as a standard mass production.

Supported by computational design logics, AM allowed new fields of research and development in architectural design, building materials and construction industry, enabling geometric freedom that can result in the design of geometries with specific requirements, optimising the design and functions of traditional systems [5].

In 2016, a report from the World Economic Forum [6] on the impact of new technologies in the future, based on the results of the “Future of Construction Survey”, states that “contour crafting of buildings” is unlikely to be developed, having little impact on the construction industry. Comparatively, the probability of the production of components by AM and “advanced building materials” is considered moderate, and the production of prefabricated components is extremely high.

There are currently several examples that unquestionably prove the potential of this digitalization on the production of architectural components and their implications and limitations when applied to common structural elements. Concrete AM of columns of the Concrete Choreography project by Anton et al. (2020) [7] and the project of a post-tensioned concrete girder designed by topology optimization by Vantuyghem et al. (2020) [8] make clear that it is possible to add formal complexity, reduce material usage and merge structure and infrastructure in a single element without compromising any of them. Despite this, the lack of studies focusing on the connection between vertical and horizontal structural elements (columns and beams) is still evident.

Following Miguel Fisac’s Bones System designed in the 1960s [9], that consists on discretized pressed concrete beams with hollowed sections similar to bone structures, this investigation comprises the development of a set of prototypes aiming: a) the design of a simple framed structure; b) the topological optimization of beams and columns; c) the definition of connection elements; d) the discretisation of structural elements into smaller components; e) the design of the internal structure and creation of the numerical control code that informs the production machines.

## METHODOLOGY

Considering the implications associated with the PEM of ceramic materials, namely the need to fire the components and the limited working volume of the production/firing equipment, the entire system was discretized into smaller elements to meet these requirements. Thus, the methodology applied in this study begins by analysing the discretisation of the general model into components, proceeds to the interconnections between each of these components considering the mate-

rial constraints and ends with the dynamic behaviour of the system when subjected to load-bearing efforts. The used methodology follows a set of rules considered fundamental to reach relevant data for the definition of fully functional systems, capable to respond to mechanical requests, be easy to produce and assemble, as well as environmentally friendly compared to systems with similar behaviour. For that and taking into consideration the restraints that ceramic PEM have, namely geometric deformations, on these initial tests the system must be as simple as possible, both functional and geometrically, focusing on the definition of joints and overall structural scheme. In addition, the discretisation methods that may vary in future conceptions are strict to simple slices of the overall component, avoiding unnecessary complexity that could compromise the results of preliminary tests.

### Problem definition

Considering the problems related to the use of ceramic AM on architecture and construction, that goes from material composition to the limited built volume of the production equipment, this study aims to contribute with solutions for the design and manufacture of high performance ceramic gantry structures. In this sense, and since we are dealing with discrete components and a complete structural system, there is a need to correlate these two scales. For that, it is important to study the reaction that the material has when increasing or decreasing the size of the components as well the response of the assembled systems when subjected to efforts. Additionally, there are common problems that condition the use of ceramic materials in the construction of structures, their fragile behaviour that results in low fracture toughness and bad behaviour when subjected to traction forces.

### Material

The material used to produce the ceramic components was a fine stoneware paste (130-MP) without chamotte and with 35% of water content, as it proved to be the most suitable and compatible with the 3D printer extrusion system used – a Lutum® 4.0XL. Tests carried out on previous studies show that this specific material when fired at 1260°C can reach up to 175 MPa of compressive strength [10].

### Fabrication

PEM comprises the formation of objects from a paste material that is extruded on a regular or irregular basis, layer by layer. The extrusion of the ceramic material is controlled by a rotating spindle that regulates the outflow of material. The material intake system uses compressed air to compact and transport the ceramic material to the extruder, where the spindle is located. Depending on material characteristics and the equipment settings, the deposition flow, speed,

layer height and layer thickness must be changed accordingly. The 3D printer allows the control of each parameter automatically (from the numerical control code) and manually in real-time (from the machine's control interface). The produced ceramic components use basic configurations for the execution of mid-size components. Extrusion thickness of 3 mm and 1,5 mm height. The pressure applied to the ceramic paste on the cartridge was 5,0 bar with a printing speed of 50 mm/s. These values, namely the air pressure, have in consideration the plasticity of the ceramic paste.

## PRELIMINARY TESTS

The characterisation of the materials proved to be essential to understand and mitigate the events that occurred in the phases of test, production and assembly. Prior to any geometric or systemic definition, a set of ceramic specimens were defined and produced by LDM, to clarify the behaviour of the ceramic material alone and in conjunction with complementary materials. Given the production method and its inherent characteristics, particularly regarding the size of the components, it becomes necessary to discretise constructive elements into smaller pieces that conform to the production equipment volume standards. In this context, the connections and unions gain particular importance, becoming an integral part of the project. In order to attain the desired characteristics for the constructive elements, the connection material must offer the necessary ductility that ceramics inherently lack, all the while upholding relatively strong mechanical properties, particularly when it comes to withstand compressive forces, to maximise the ceramic's potential. Using the aforementioned stoneware as base material, we explored additional materials that could function as connections between the various ceramic pieces to create a unified structural element.

### Complementary materials

For the execution of the necessary additional components was defined a material palette that could compensate for the previously mentioned ceramic downsides, like its fragility, and help to get the better behaviour of the entire system. Wood (laser cut oak), rubber (SBR), mortar (Sika adhesive mortar for ceramic), glue (acrylic adhesive) and concrete (C-30), as well metallic elements for the nodes and post tensioning were tested. These materials are used either to separate ceramic pieces, to glue them together or to give resistance to traction efforts.

The first set of tests was carried out having in mind the search for the best material to serve as a separating element between ceramic components, something fundamental considering that ceramic is a material that, although extremely resistant to compression efforts, is also

very fragile, especially if the applied tension is not uniform, which can cause early ruptures, jeopardising the integrity of the system. For this purpose, cylindrical ceramic pieces with approximately 70mm in diameter, 40mm in height and with 9mm thick walls – composed by three vertical layers of 3mm each – were fabricated. For better connection between the pieces, a ledge was predicted at the base and top of the pieces. This ledge is obtained by varying heights of the layers of the wall. Later, these pieces were associated with materials that could serve as separation elements (Figure 1). As previously mentioned, the inclusion of other materials was tested, namely wood, rubber, mortar, glue, and concrete. Based on this aggregation, a series of test specimens were developed, comprising: a) simple ceramic element; b) two stacked ceramic elements; c) three stacked ceramic elements; d) two ceramic elements stacked with a layer of separation material; e) three ceramic elements stacked with two layers of the separation material; f) two ceramic elements filled inside with concrete; g) three ceramic elements filled inside with concrete; h) cylindrical test pieces of solid concrete; i) cylindrical hollow concrete test specimens (Figure 2).

Three test pieces were developed for each series, making a total of 51 test specimens. The main objective of these tests was to determine which material is best suited to work together with ceramics having as a base point the results obtained by the concrete specimens. The concrete used in the test specimens was a traditional C-30 mixture.

### Mechanical behaviour

The results obtained during the compression tests show the potential of using this material in structures with bearing capacity (Table 1). Based on the values achieved by concrete, the most used material for the construction of supporting structures, we realise the enormous difference in the capacity that exists between both ceramic and concrete. Even without the introduction of elements to separate ceramic pieces, as are the cases of C2 (approx. 80mm height) and C3 (approx. 120mm height), respectively with two and three stacked components, which could reduce drastically the capacity of the ceramic set, the resistance values (in MPa) were substantially higher than those presented by the equivalent concrete specimens, CM/CH80 and CM/CH120. Also, the results obtained from test pieces that used rubber (C2R1/C3R2) and acrylic glue (C2A1/C3A2), as a separating element between ceramic pieces, show the instability that these two materials give to the system by causing accentuated deformations and misshapen settlements, leading to total rupture of the ceramic pieces. In contrast, the materials studied by specimens C2M1/C3M2 and C2W1/C3W2, respectively mortar and wood, present very positive values in the way they avoid part of the weaknesses of the ceramic material and can present resistance values higher than those presented by concrete specimens.

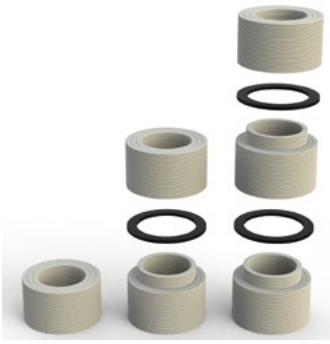


Figure 1: Ceramic test specimen and separation material (rubber).



Figure 2: Complementary materials test specimens.



Figure 3: Hybrid beam.

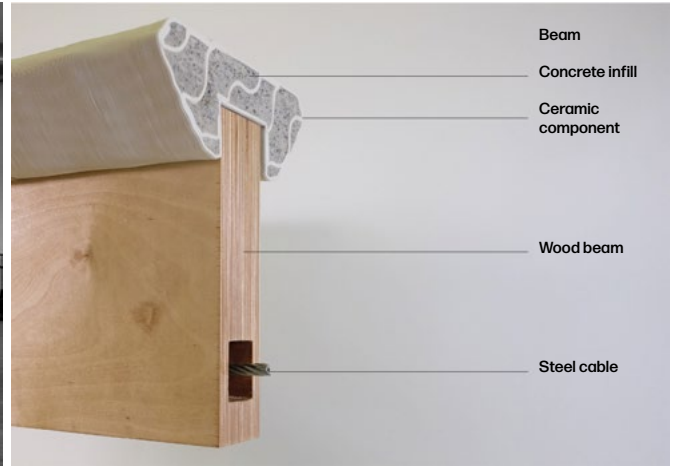


Figure 4: Hybrid beam (section).



Figure 5: Connection between columns and beams.

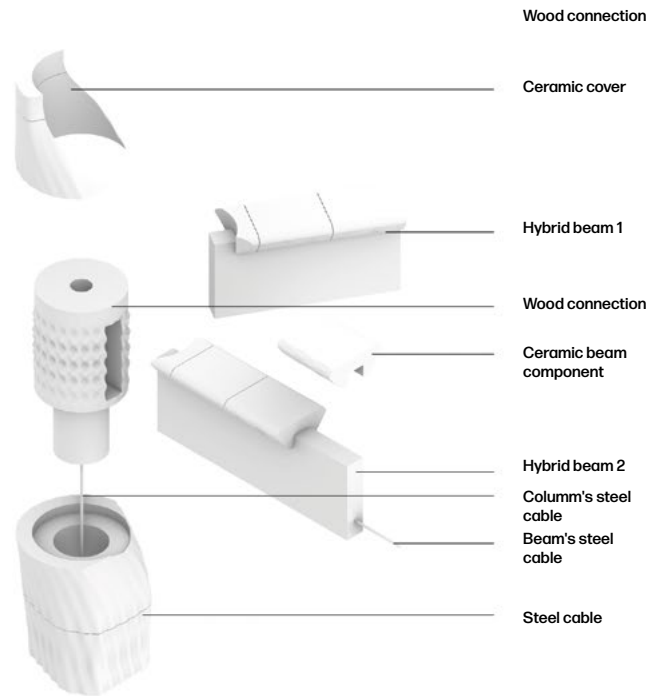


Table 1: Complementary materials compression tests.

Code	Test probe	Connection Height [mm]	Connection Section area [mm <sup>2</sup> ]	Average Load [kN]	Standard Deviation [MPa]	Standard Deviation [%]	Average Load [MPa]
C1	Ceramic [1]	0	1870	313,1	12,9	7,7%	167,4
C2	Ceramic [2]	0	1870	120,1	15,8	24,6%	64,2
C3	Ceramic [3]	0	1870	57,5	8,5	27,7%	30,7
C2M1	Ceramic [2] & Mortar [1]	3	1870	78,2	8,8	21,1%	41,8
C3M2	Ceramic [3] & Mortar [2]	6	1870	78,2	8,3	19,9%	41,8
C2A1	Ceramic [2] & Acrylic adhesive [1]	1	1870	67,7	8,1	22,4%	36,2
C3A2	Ceramic [3] & Acrylic adhesive [2]	2	1870	71,5	5,1	13,4%	38,2
C2R1	Ceramic [2] & Rubber [1]	2,75	1797	80,3	8,4	18,8%	44,7
C3R2	Ceramic [3] & Rubber [2]	5,5	1797	51,0	6,4	22,5%	28,4
C2W1	Ceramic [2] & Wood [1]	6,08	1690	165,3	5,9	6,0%	97,8
C3W2	Ceramic [3] & Wood [2]	12,16	1690	128,0	28,7	37,9%	75,7
C2C80	Ceramic [2] & Concrete [80]	1 (acrylic adhesive)	1870	189,0	10,8	10,7%	101,1
C3C120	Ceramic [3] & Concrete [120]	1 (acrylic adhesive)	1870	124,3	12,0	18,0%	66,5
CM80	Concrete Massive [80]	no connection	5026	129,1	6,3	24,5%	25,7
CM120	Concrete Massive [120]	no connection	5026	107,3	3,7	17,4%	21,3
CH80	Concrete Hollowed [80]	no connection	2211	47,5	3,3	15,3%	21,5
CH120	Concrete Hollowed [120]	no connection	2211	40,3	6,4	35,2%	18,2

## PROTOTYPES

The prototypes developed during this investigation had as final objective the verification of the applicability of the structural systems formed by ceramic components, pointing out advantages, flaws and indicating the path for future resolutions and for the qualification of this as an alternative and sustainable answer to the traditional systems.

### Columns

5 types of columns were developed, each having a different purpose and representing an additional performative function. Although they are presented as being of different types, in their constitution and way of operation there is no change, being the formal variation an element that points to the study of a system that integrates several functions. The columns, in addition to the structural role, which later will relate to the beam, there was also a demand to give these elements functions that were not limited to the load support, as are the cases of: a) structural reinforcement; b) thermal insulation; c) passage of infrastructural networks; d) ventilation. Additionally, two types of discretisation were also tested: a) one component at each level; b) three components per level. Here, on column prototypes, the focus was mainly on the functional side, leaving out the structural performance, since the responses to this were expressed by the tests presented in the previous section 3. *Preliminary tests.*

## Beams

The hybrid beam (Figure 3) is presented as a result of the study carried out on the horizontal elements of an architectural structure. The beam, with a 6 metres span, studies the use of discretized ceramic elements in a linear element where traditionally there are different types of mechanical efforts, such as compression, traction, bending and cutting. In this sense and considering the inherent characteristics of the ceramic material, we concluded that we should not fight the laws of physics, trying to make the material adapt to these efforts, but rather to develop a system that would take advantage of the strengths of the ceramic material. The hybrid beam was born precisely in this commitment of balance between its mechanical capacity and the functional request.

The beam presented here is made up of 4 main elements, each with a specific function, which responds to each of the previously exposed requests (Figure 4). Running through the entire body of the beam, in the centre, we have a wooden core that simultaneously provides tensile strength and constitutes a ductile base for fixing the ceramic components. Inside the wooden beam, a steel cable runs in a channel positioned in the lower area to reinforce the response to traction efforts, which may use a self-tensioning system (Estévez-Cimadevila et al., 2019). Fixed to the wooden beam, at the top, ceramic pieces of variable geometry are placed, responding to compression efforts and counteracting bending, which is why they have more mass in the central area (ceramic components are designed according to bending scheme).

The ceramic pieces are fixed to the wood using screws and a fourth element that serves to consolidate the entire system, a concrete infill. In this case, concrete appears as a binder of the parts that respond to compressive stresses with the part that responds to tensile stresses, while at the same time provides additional strength to the system.

### Connection between columns and beams

The connection between beams and columns is perhaps the most important element achieved in this investigation as it constitutes the main advance developed. This element has the function of connecting, distributing loads and consolidating several separate elements into a single, solid system, with high performance capacity. Once again, and following the logic found for the formalisation of the beam, wood was used to build this element (Figure 5).

It results from a relatively simple design and functional mechanism – the overlapping of two cylinders of different diameters, with a longitudinal hole and a set of cavities specially created to receive the body of the beams.

The connection to the columns is made in its last two components, where each of the connection cylinders rests. The hole in the centre allows the passage of a steel cable that will consolidate the column and prevent it from having lateral movements due to the compression of all its components.

The connection to the beams is made in the cavity left for this purpose, and it is also possible to join these elements through the steel cable that runs inside the beam, and which will connect to each of the wooden connectors at the ends.

## RESULTS AND DISCUSSION

The developed system comprises the use of discretised ceramic components to create functional frame structures with load bearing capacity. Considering the results of preliminary tests on the ceramic material, namely its weak resistance to tensile and bending efforts, in addition to a well-known fragile condition, led us to look for a set of complementary materials capable of having high mechanical performance and at the same time providing ductility to the ceramic set. The result of this study was the selection of wood as the best material to work with ceramics.

The system we present here constitutes a step forward in the search for more sustainable construction systems, adapted to a given reality. Each of its constituent elements can be customised and have its own performance, form, or function, differentiated, but integrated into the same logic.

As future work we point to the effective testing of the presented structure, as well as the inclusion of performative and infrastructural systems in the built set.

## ACKNOWLEDGEMENTS

This work was financed by the project Lab2PT – Landscapes, Heritage and Territory laboratory, reference UIDB/04509/2020 through FCT – Fundação para a Ciência e a Tecnologia and the FCT Doctoral Grant with the reference SFRH/BD/138062/2018. We are also grateful to Instituto de Design de Guimarães for hosting and supporting the activities of the Advanced Ceramics Laboratory on the use of their facilities and equipment, and for all the assistance provided by the technician Samuel Ribeiro.

## REFERENCES

- [1] Rahim, A. (2010). Interiorities. *Architectural Design*, 80 (2) - Exuberance: New Virtuosity in Contemporary Architecture, 24-31.
- [2] Wisnik, G., (2016). "Inmersión contra imagen: desenfocando el mundo". In Plot nº32, August-September, Buenos Aires: Grupo Vórtice, 2016, p. 10-12.
- [3] Banham, R. (1969). *The architecture of the well-tempered environment*. London: The Architectural Press.
- [4] Colletti, M. (2010). Digitalia – The Other Digital Practice. *Architectural Design*, 80 (2) - Exuberance: New Virtuosity in Contemporary Architecture, 16-23.
- [5] Sarakinoti, M-V., Konstantinou, T., Turrin, M., Tenpierik, M., Loonen, R., Klijn-Chevalerias, M. L. and Knaack, U. 2020, 'Development and prototyping of an integrated 3D-printed facade for thermal regulation in complex geometries', *Journal of Facade Design and Engineering*, 6 (2), pp. 029-040
- [6] Renz, A. and Solas, M. Z. 2016, 'Future of Construction Survey Results', in Almeida, P. R., Buhler, M., Gebert, P., Castagnino, S. and Rothballer, C. (eds) 2016, *Industry Agenda, Shaping the Future of Construction – A Breakthrough in Mindset and Technology*, World Economic Forum, Switzerland: World Economic Forum, pp. 51-54
- [7] Anton, A., Bedarf, P., Yoo, A., Dillenburger, B. (2020). Concrete Choreography. In Burry, J., Sabin, J., Shiel, B., Skavara, M. (Eds), *Fabricate 2020* (pp.286-293). London: UCL Press.
- [8] Vantghem, G., De Corte, W., Shakour, E., & Amir, O. (2020). 3D printing of a post-tensioned concrete girder designed by topology optimization. *AUTOMATION IN CONSTRUCTION*, 112. <https://doi.org/10.1016/j.autcon.2020.103084>
- [9] González Blanco, F. (2007), *Miguel Fisac: Huesos Varios*. Fundación COAM, Madrid.
- [10] Cruz, P. J. S., Camões, A., Figueiredo, B., Ribeiro, M. J. and Renault, J. 2019, 'Additive manufacturing effect on the mechanical behaviour of architectural stoneware bricks', *Construction & Building Materials*, 238, pp. 1-17



# DESIGN OF WAAM-STEEL NODES FOR RELIABLE CONSTRUCTION

Maren ERVEN

Jörg Lange

Wire Arc Additive Manufacturing (WAAM) is a promising manufacturing process for steel construction. There is great potential in producing structures that connect multiple components, referred to here as steel nodes, to facilitate fabrication and assembly. This article describes the potential of WAAM steel nodes, briefly presents the research that has been done by the authors in three main areas, and then addresses the influence of the printing process on the material properties of the node structures. For this purpose, five different slicing strategies for the realisation of an intersection are investigated based on three tensile specimens each. A hardening process is shown that leads to different microstructural formations in and around the intersection centre. The behaviour can be simulated and confirmed using FE. The results are summarised in suggestions for the design of WAAM steel nodes.

## INTRODUCTION

In recent years, Additive Manufacturing (AM) has developed rapidly in the construction industry. For structural steel Wire Arc Additive Manufacturing (WAAM) is promising, as it focuses on the production of large components [1]. The WAAM process can be classified as Direct-Energy-Deposition-Process (DED). With the help of welding robots or CNC systems, the melted filler wire becomes the component by welding multiple layers on top of each other (Figure 1). It can print 3D steel structures comparatively quickly. As a direct deposition process no extra material is needed and waste is reduced. Investigations show good material behaviour nearly equivalent to hot-rolled steel [2–4].

## WAAM STEEL NODES

Compared to hot rolled beams, which are produced in an automated process, joints are mainly made by hand and are difficult to automate due to their high degree of individuality. Although they are rather small parts, connections between elements in steel structures are a significant performance factor of a building structure. The more complex they become, the more time is needed to build the entire structure. Therefore, the simplicity of these connection points determines the economy of the whole structure. However, it often conflicts with the desire of architects and building owners for unusual, exceptional shapes.



Figure 1: WAAM Printing process and printed specimen. [5]

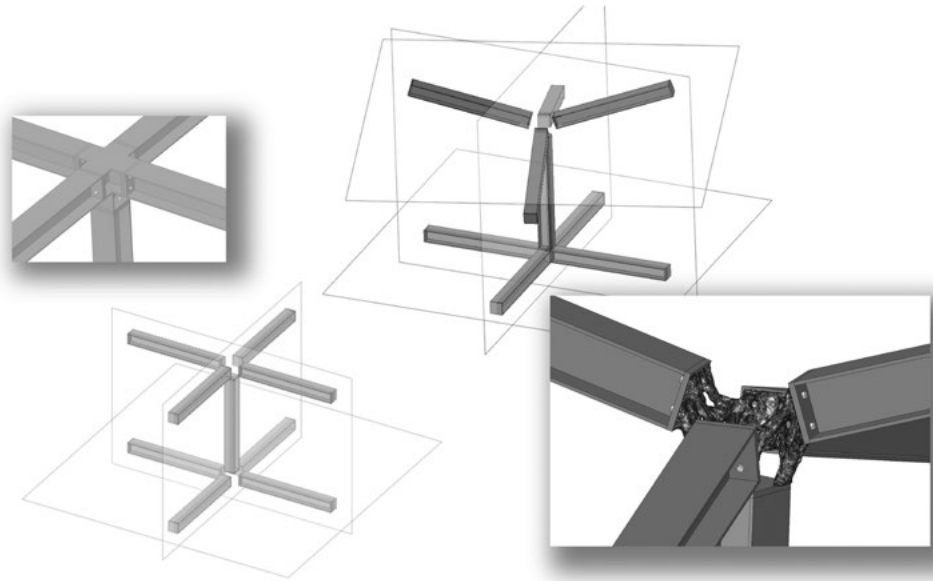


Figure 2: Freeform node leaving the conventional rectangular structural pattern

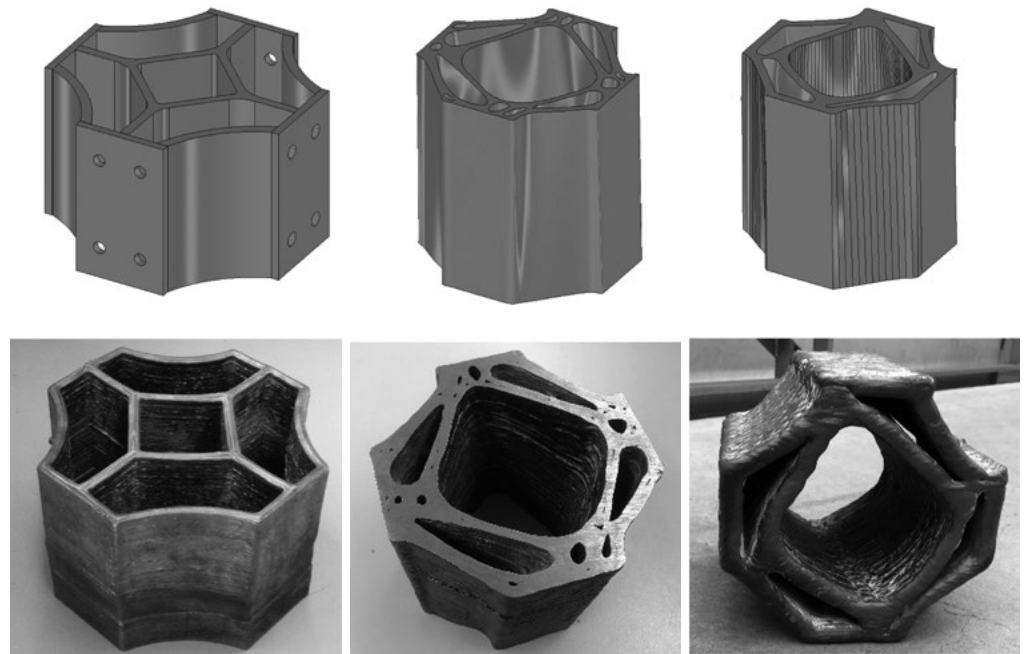


Figure 3: Designed and printed Nodes

With additive manufacturing and especially with WAAM, it can be possible to combine both desires and ensure simple assembly and preparation of the remaining components while creating unusual load-bearing structures. The complexity is shifted from the overall structure to the few 3D printed nodes (Fig. 2). These node structures are individually adapted to their geometric installation situation as well as to the loads acting at this point. It saves material and production time and, additionally, shows the observer how the forces act.

In order to make such a WAAM steel node a reality, the following question is investigated: What must a design process for WAAM steel nodes look like in order to take advantage of the new method, ensure the required static load capacity, and verify it in a cost-effective manner? To answer this question, three main topics are considered: Form Finding, Connection Means, Material Behavior. The importance of these three areas and some of the published results are briefly presented below. The article then discusses in detail the results on the influence of different slicing approaches on the material behaviour.

### **Form finding**

The goal of the node structures under investigation is not to simply replace any conventional node. Rather, the goal is to use the new technology to achieve a clear advantage over the conventional design. Particularly in the case of simpler connections, material should be saved significantly or an advantage within the assembly should result from the new manufacturing method. Especially when the complexity of a node increases and the manufacturing effort becomes very large, it may be reasonable to think about an additively manufactured alternative. Therefore, geometry and load conditions were determined for which an additively manufactured alternative seems reasonable [2, 5, 6]. In the context of form finding, it is also important to consider the limitations and effects of the printing process. For this purpose three nodes were designed, printed and tested, see Figure 3 [2,5].

### **Printed material**

WAAM already shows very good properties comparable to hot rolled steel in material tests, which were mainly made from straight sheets [2-4]. However, additive structures are often not simple sheets, but can have shape changes over their height; there is overhanging material, intersections in different directions and variable wall thicknesses. It is therefore necessary to investigate how the printing process and the slicing affect the behaviour of the component.

### **Connection means**

The aim of the investigated node structures is to form an assembly point that can be attached without much effort. Furthermore, the node should take the complexity of the connection and provide the need of as little preparation as possible for the connecting elements. So, the idea is to use standard connections such as flag plates and head plates which are bolted. In order to use the connections safely, it is necessary to check whether the printed material behaves in a special way in interaction with the bolts or whether the same behaviour can be assumed as for hot rolled steel.

The literature [7, 8] and own investigations show that the printed material behaves comparably to hot rolled steel in interaction with bolts. For this purpose, both double-lap shear tests (see Figure 4) and tensile tests on head plates were carried out [9]. Although the welding direction has a small influence on the load-bearing capacity in the shear tests, the failure mode, i.e., the way the component fails, is the same for both loading directions compared to hot rolled steel (see Figure 4). The differences in load-bearing capacity can be explained by the slightly anisotropic material behaviour resulting from the printing process, which will now be discussed in more detail in this article.

## **MATERIAL BEHAVIOUR OF WAAM STEEL**

WAAM is an additive manufacturing process that uses a welding process to build up steel layer by layer. WAAM systems can use stationary 3- or 5-axis CNC systems or 6-axis welding robots. Robot systems have lower accuracies than CNC systems, depending on the stiffness of the robot. However, robots offer greater flexibility in terms of installation space, especially when large structures are to be manufactured on existing components. For research on WAAM with carbon steel, the institute of Steel Construction and Materials Mechanics at TU Darmstadt has a Comau 6-axis welding robot and a Fronius CMT Advanced 4000 R power source.

The welding process used, the wire and the welding parameters, along with other environmental influences, affect the resulting material and thus its material behaviour. Hartke (2014) [10] shows that a lower line energy leads on the one hand to better control of the geometric properties and on the other hand to better material properties. In addition, the material behaviour depends on the direction of the weld and the acting direction of the load. More precisely, the material behaves slightly anisotropically, especially in the plastic range, as shown in Figure 5 (with the welding parameters given in table 1).

Table 1: Process Parameters

Process	CMT Cycle Step
Wire Material	G3Si1
Gas	82 % Ar, 18 % CO <sub>2</sub>
Wire-Feed-Speed (nom.)	6.5 m/min
Travel-Speed	0.5 m/min
Cooling time	45 - 60 s
Welds per Layer	3

## INVESTIGATIONS ON SLICING STRATEGIES

The arrangement of the paths - the slicing - is decisive for the behaviour of the printed material. In order to investigate to which extent path planning with the same welding parameters influences the material behaviour, different variants are compared with each other. It is clear that the path planning should ensure that the printed material forms a unit without voids. In this respect some studies can already be found in the literature, which aim to find the optimum spacing of welds [11-13].

However, even assuming that the optimum spacing of several welds that are to form a straight plate is maintained, the material behaviour changes depending on the number of welds [12-14]. Thus, the material behaviour determined from a wall made from one weld cannot be directly transferred to a structure built from multiple welds. Due to the increased heat input, the strength increases and the ductile range decreases.

In addition to the influence of the number of welds, crossing points, where welds frequently have to start or end, are also of great importance. These can be designed in different ways. Again, provided that the end result is a structure without voids, Grebner [15] developed five different slicing strategies for a right-angled intersection (see Figure 6) which were investigated with tensile tests.

The investigated intersection is created by three welds in one layer and is also produced with the previously considered welding parameters. While in strategies 1 to 3 the structure is outlined, in strategies 4 and 5 one direction is welded through and the other connected. While strategies 1 and 5 use the same path planning for each layer, in the strategies 2 to 4 the paths change each layer. For comparison, a reference wall without a crossing point is also printed with 3 welds per layer using the same welding parameters.

Three tensile specimens of the geometry DIN 50125 - A 10 × 50 were extracted from the printed bodies for each direction of the intersection. While one could still identify

the strategy at the top layer of the printed structure, on the turned specimens the slicing strategy was no longer visible to the naked eye. Further, no pores could be seen in the samples either. However, the results of the tensile tests show a dependency on the slicing strategy (Table 2). Compared to the reference specimen, there is a significant increase in strength as well as a decrease in ductility for all strategies. Further, the failure in all specimens did not occur in the middle, but in the outer region of the parallel length (Figure 7).

Table 2: Mean Values of the Tensile Tests

	Yield strength in N/mm <sup>2</sup>	Tensile strength in N/mm <sup>2</sup>	Elongation at fracture in %
1_A	517.1 ± 4.7	576.0 ± 5.9	25.7 ± 0.7
1_D	510.6 ± 4.8	571.8 ± 3.8	26.6 ± 0.6
2_G	512.0 ± 7.3	576.2 ± 4.3	25.7 ± 2.1
5_A	487.0 ± 5.5	558.0 ± 4.6	25.7 ± 0.7
5_D	532.2 ± 8.1	594.6 ± 7.5	21.8 ± 0.1
3_G	526.5 ± 17.3	585.8 ± 13.6	26.3 ± 0.3
4_G	494.0 ± 1.4	567.0 ± 1.2	27.0 ± 0.6
Reference	465.3 ± 4.0	533.9 ± 3.7	33.1 ± 1.0

The difference between the strategies is particularly evident by comparing the different directions in slicing strategy 5 in Figure 7. The graphs of the through-welded direction are significantly higher than those of the welded-on direction. In all graphs of the tensile specimens distinct jags appear in the area of strain hardening as it is noticeable for 5\_D at around 2 % and 5 % in Figure 7. Compared to the reference specimen, no yield plateau is formed, but strain hardening occurs almost directly.

One reason for the deviating behaviour compared to the reference specimen could be a hardening of the intersection point due to the repeated heat input. This results in different microstructural regions in the specimen, depending on how much heat has arrived at the different parts. Thus, the centre of the intersection receives the greatest energy input and is therefore hardened the most. The further away the area is from this heated centre, the less the area is hardened. The described distinctive stiffness drops in Figure 7 speak for three different material areas, which plasticize one after the other due to the different strengths.

The behaviour can be simulated with the help of a finite element analysis (FE analysis). In the FE analysis, the tensile specimen is geometrically modelled according to the dimensions in the standard. Within the measuring range, the solid is divided into areas to which three different materials are assigned (see Figure 8 - red, orange and yellow areas in the specimen). The material behaviour is defined elastically the same for all three materials, the plastic behaviour is defined by an offset of the yield strength corresponding

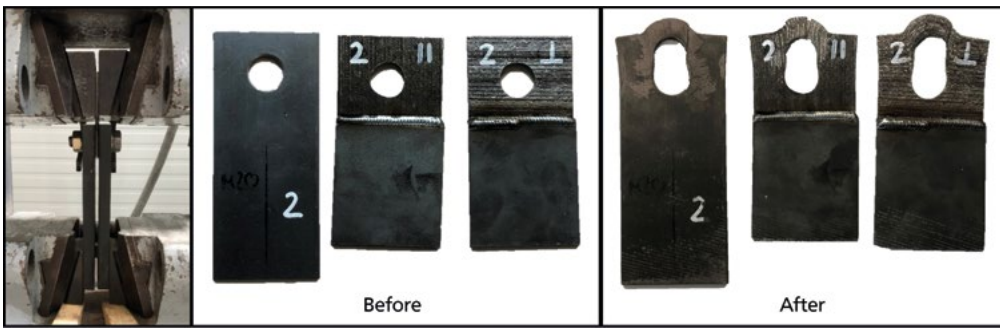


Figure 4: Double-lap shear tests Specimens before and after testing.

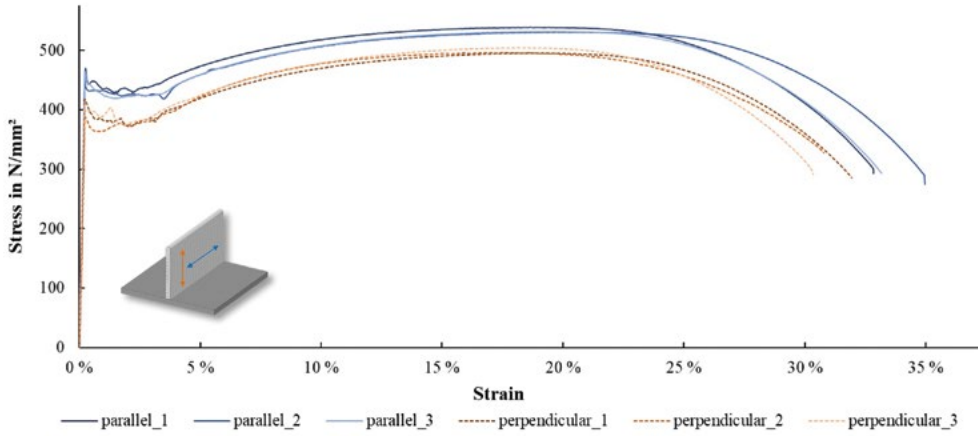


Figure 5: Stress-Strain-Curve Tensile Tests in parallel and perpendicular direction.

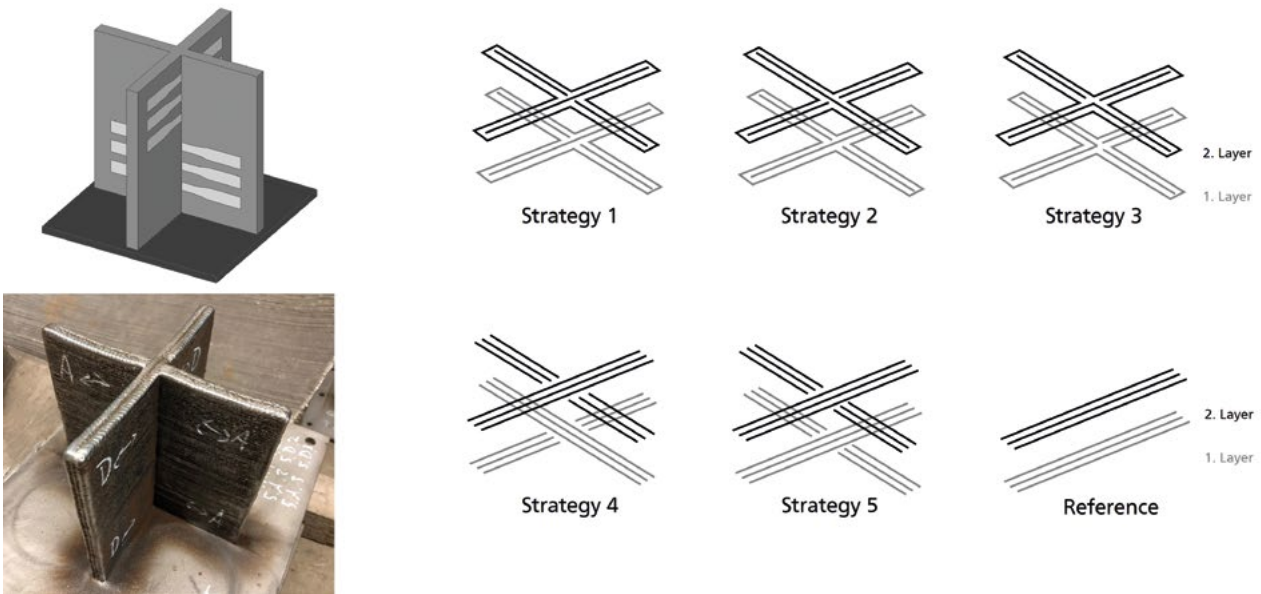


Figure 6: Investigated Printing strategies.

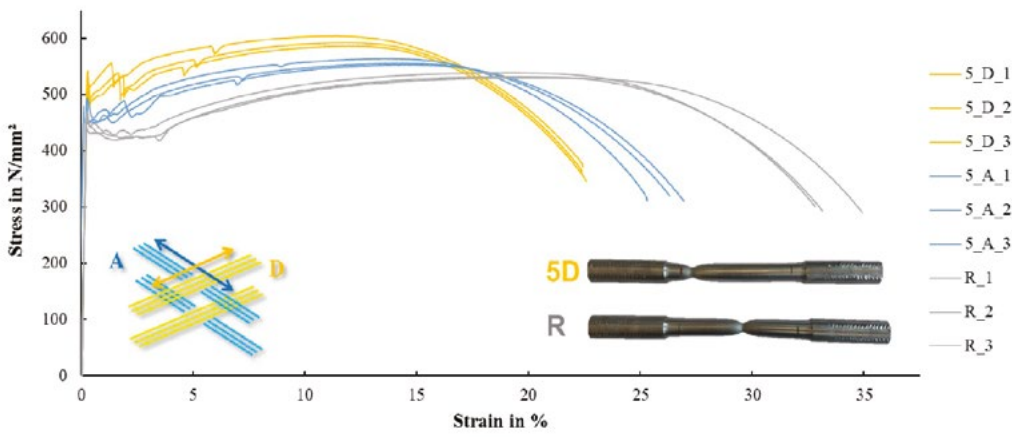


Figure 7: Comparison of reference, welded-trough and welded-on direction.

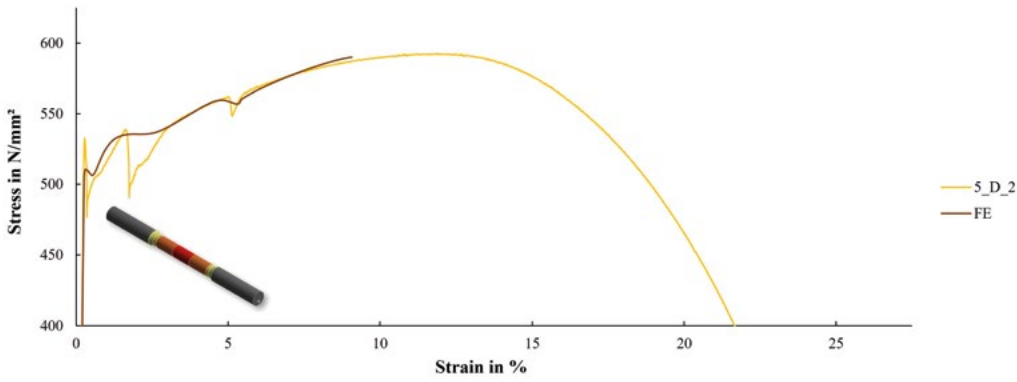


Figure 8: Finite Elements Model with different areas.

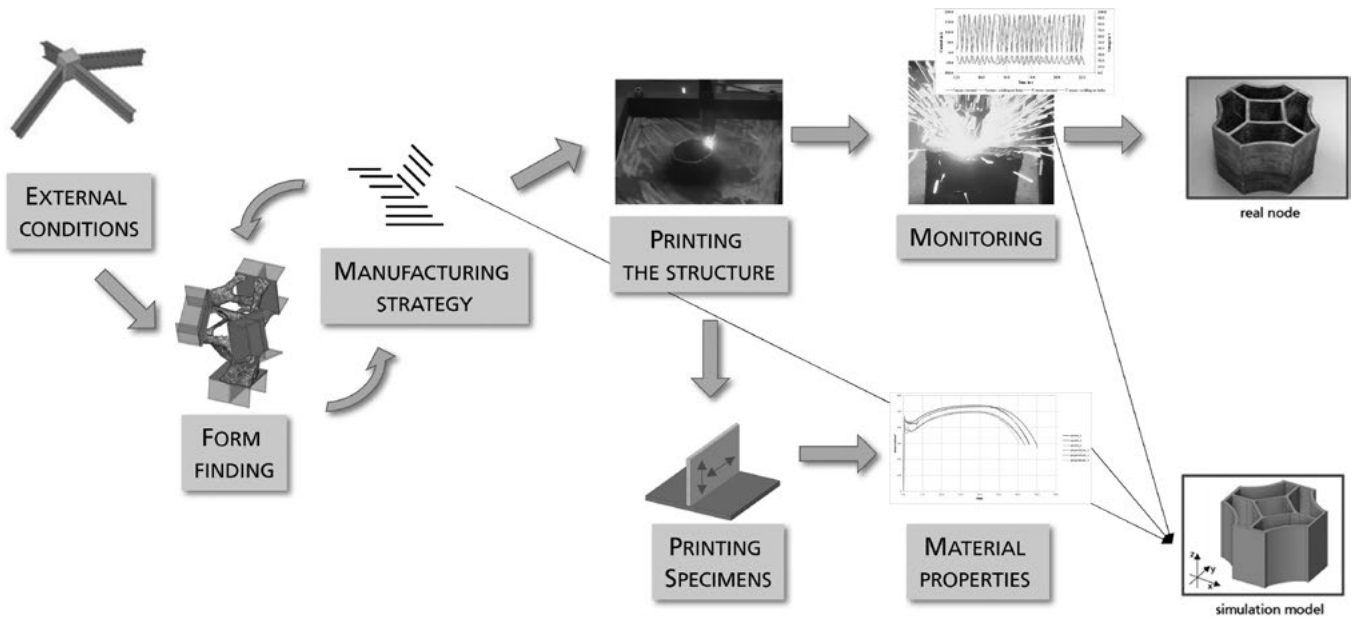


Figure 9: Proposed Workflow to identify the load-bearing capacity of a WAAM-steel node

to the value of the stiffness drop. The red region is assigned a corresponding high yield strength (550 N/mm<sup>2</sup>), while the yellow region is assigned a low yield strength (505 N/mm<sup>2</sup>) and the orange region a medium yield strength (530 N/mm<sup>2</sup>). This allows the behaviour of the specimen to be mapped well (Figure 8).

Due to the lower strength, the specimen fails in the yellow range. However, this area is not completely within the measurement range, so the strain at necking is not fully recorded and there is a significantly lower strain at fracture compared to the reference specimen. Furthermore, the multi-material model and the lower strength at the edge explains the off-centre failure point of the specimens.

The investigations show that crossing points, if care is taken not to create voids, increase the strength of the structure at this point. Therefore, if the body is dimensioned in the elastic range, the material values of a reference specimen made from an additively manufactured plate can be used to calculate on the safe side. If plastic reserves are to be used, which seems reasonable for material saving reasons, geometrically interesting points, such as intersections, should be given special consideration.

### CONSEQUENCE FOR THE DESIGN

From the aspects of investigation presented, rules for the design of WAAM steel node structures can be derived. First of all, material should only be used where it is necessary, taking into account all load cases that may occur. However, the printability of the structure should be considered as well. The investigations show that bolts can be used in additively manufactured structures without having to establish completely new design rules. However, they should be used as efficiently as possible. Further, the presented investigations show that the printing process and path planning strongly influence the material properties. Therefore, to determine the load-bearing capacity of a printed structure, the slicing strategy must be considered.

The following workflow (Figure 10) is proposed to describe the load bearing capacity: After the external constraints are known, a suitable structure can be found, e.g., by using topology optimization. The structure is adjusted with respect to the printing boundaries. If shape and manufacturing strategy match, the structure can be printed. With the process parameters intended for this purpose, a straight sheet should be printed for extracting tensile specimens. From these specimens, material properties can be derived, which are adapted with regard to the slicing strategy and transferred to a simulation model of the node. During the printing process, the current and voltage curves can be recorded in order to detect process irregularities occurring during the process and transferred into

the simulation model [16]. This simulation model can then be used to identify the load-bearing capacity of the node without destructive testing.

### SUMMARY

WAAM is an additive manufacturing process that seems very suitable for steel construction. Especially for the production of highly complex nodes it offers a reasonable alternative. The form-finding process has already been described in detail in previous articles. However, for use in real structures, the load-bearing capacity of these nodes must also be known. Therefore, the influence of the slicing strategy on the material behaviour is investigated. If it is known to what extent the material is quantitatively influenced by the slicing strategy, the load-bearing capacity of the nodes can be simulated using the workflow proposed in the article.

### ACKNOWLEDGEMENT

We would like to thank the companies Fronius Deutschland GmbH, Messer Group GmbH, WDI Schweißtechnik GmbH and Comau Deutschland GmbH for their kind support.

The nodes in Figure 3 were developed in cooperation with the companies Cognition Factory, GEFERTEC and Imagine structures as well as the Fachgebiet Fertigungstechnik at the TU Ilmenau as part of the research project "16KN0176127: Additives Bauen - Stahlbauknoten".

## REFERENCES

- [1] C. Buchanan and L. Gardner, "Metal 3D printing in construction: A review of methods, research, applications, opportunities and challenges," *Engineering Structures*, vol. 180, pp. 332-348, 2019, DOI: 10.1016/j.engstruct.2018.11.045.
- [2] J. P. Bergmann, J. Lange, J. Hildebrand, et al., "Herstellung von 3D-gedruckten Stahlknoten," *Stahlbau*, vol. 89, no. 12, pp. 956-969, 2020, DOI: 10.1002/stab.202000080.
- [3] V.-A. Silvestru, I. Ariza, J. Vienne, et al., "Performance under tensile loading of point-by-point wire and arc additively manufactured steel bars for structural components," *Materials & Design*, vol. 205, p. 109740, 2021, DOI: 10.1016/j.matdes.2021.109740.
- [4] C. Huang, P. Kyvelou, R. Zhang, et al., "Mechanical testing and microstructural analysis of wire arc additively manufactured steels," *Materials & Design*, vol. 216, p. 110544, 2022, DOI: 10.1016/j.matdes.2022.110544.
- [5] M. Erven and J. Lange, "Design of optimized 3D-printed steel nodes," in *Structures and Architecture A Viable Urban Perspective?*, CRC Press, London, 2022, pp. 229-236.
- [6] M. Erven, T. Feucht, J. Lange, et al., "Numerische und experimentelle Untersuchungen von Knoten im konstruktiven Stahlbau," in *DVS Congress 2019 - Große Schweißtechnische Tagung*, DVS-BerichteBand 355, DVS Media GmbH, Düsseldorf, 2019, pp. 287-294.
- [7] G. Kotteman, "Steel 3D printing for structures: An explorative study on the tear-out strength of a pin or bolt in a Wire and Arc Additively Manufactured carbon steel plate," 2020.
- [8] X. Guo, P. Kyvelou, J. Ye, et al., "Experimental investigation of wire arc additively manufactured steel single-lap shear bolted connections," *Thin-Walled Structures*, vol. 181, p. 110029, 2022, DOI: 10.1016/j.tws.2022.110029.
- [9] M. Erven and J. Lange, "Material efficient 3D printed Steel Construction Details," in *IABSE Congress New Delhi 2023*, to be announced.
- [10] M. Hartke, K. Günther, and J. P. Bergmann, "Untersuchung zur geregelten, energiereduzierten Kurzlichtbogentechnik als generatives Fertigungsverfahren," in *DVS Congress 2014*, DVS Media GmbH, Düsseldorf, 2014, pp. 98-102.
- [11] D. Ding, Z. Pan, D. Cuiuri, et al., "A multi-bead overlapping model for robotic wire and arc additive manufacturing (WAAM)," *Robotics and Computer-Integrated Manufacturing*, vol. 31, pp. 101-110, 2015, DOI: 10.1016/j.rcim.2014.08.008.
- [12] Y. Li, Q. Han, G. Zhang, et al., "A layers-overlapping strategy for robotic wire and arc additive manufacturing of multi-layer multi-bead components with homogeneous layers," *The International Journal of Advanced Manufacturing Technology*, vol. 96, nos. 9-12, pp. 3331-3344, 2018, DOI: 10.1007/s00170-018-1786-3.
- [13] J. Xiong, G. Zhang, H. Gao, et al., "Modeling of bead section profile and overlapping beads with experimental validation for robotic GMAW-based rapid manufacturing," *Robotics and Computer-Integrated Manufacturing*, vol. 29, no. 2, pp. 417-423, 2013, DOI: 10.1016/j.rcim.2012.09.011.
- [14] J. Reimann, P. Henckell, Y. Ali, et al., "Production of Topology-optimised Structural Nodes Using Arc-based, Additive Manufacturing with GMAW Welding Process," *Journal of Civil Engineering and Construction*, vol. 10, no. 2, pp. 101-107, 2021, DOI: 10.32732/jcec.2021.10.2.101.
- [15] P. Grebner, "Auswirkungen von Slicingstrategien auf die Materialeigenschaften von additiv gefertigten Strukturen," Darmstadt, TU Darmstadt, Master's thesis, 2022.
- [16] M. Erven and J. Lange, "Influence of process irregularities in additively manufactured structures," in *Current Perspectives and New Directions in Mechanics, Modelling and Design of Structural Systems*, CRC Press, London, 2022, pp. 374-379.



# WIRE ARC ADDITIVE MANUFACTURING OF STEEL COLUMNS

Benedikt Waldschmitt

Jörg Lange, Christopher Borg Costanzi

Wire Arc Additive Manufacturing (WAAM) is a robot-controlled welding process used to build up three-dimensional structures in steel, which may be unfeasible to manufacture using conventional methods. This article focuses on the wire arc additive manufacturing of several steel column elements and a cross-section-changing steel node. The steel column segments are divided into varying cross sections while the steel node demonstrates high geometric complexity combining different cross sections. Following a previously developed design-to-manufacturing process, the single process steps highlight the approach to implement WAAM into the steel construction industry. (Partial) parametric robot programming and multiple process-control checks were used to manufacture each structure and to achieve the desired geometries and a structure with a high level of dimensional accuracy. In addition, the printed structures should undergo post-processing by means of machining, which will be described as a following step.

## INTRODUCTION

Today, many buildings not only have to serve functional requirements but also have representative purposes. Their construction and design calls for a non-standardized approach, making use of highly individualized structures in addition to standard elements. To connect standard elements with each other, steel connections (e.g., flag plate connections or head plates) have been optimized for the conventional manufacturing processes. Although today's steel fabricators are already capable of producing rather individualized structures and connections (Figure 2), the manufacturing process is still very elaborate and so expensive

and time-consuming (Fischer). In addition, an increased shortage of skilled workers argues for greater automation (Statistische Ämter des Bundes und der Länder). In a first approach, fully automated I-beam production lines were implemented, which are only used by specialized steel fabrication companies worldwide (Voortman Steel Machinery B.V.) (Zeman Bauelemente Produktionsgesellschaft mbH). In these systems, handling robots hold plates (stiffeners, base and head plates, etc.), while welding robots weld the seams (Figure 1).

This is not feasible for complex geometries, such as Y-shaped columns. Figure 2 visualizes a three-dimensional model of a complex, branching steel structure, multiple

times manufactured by spanverbund GmbH. It combines straight and twisted column segments by individualized nodes [1]. Although Additive Manufacturing (AM) has not yet been established in the steel construction industry, it shows the potential in terms of individualization and automation for different applications [2]. It provides a high variety of utilizations which could improve constructions as seen below. This work presents first approaches to achieve a fully additively manufactured steel column and the potential of its design-to-manufacturing workflow.

## WIRE ARC ADDITIVE MANUFACTURING

Within the steel construction industry, the research in Wire Arc Additive Manufacturing (WAAM) has raised attention. WAAM is an additive manufacturing process based on gas shielded metal arc welding (GMAW). The electric arc (mostly short arc and spray arc) melts the welding wire which serves as the printing material. The liquid molten pool solidifies in lines or spots and forms three-dimensional structures. The shielding gas protects the material deposition from atmospheric influences and impurities (Figure 3). At the same time, it stabilizes the heat input of the welding process and influences the molten pool [3]. The degree of viscosity, the cooling rate and thus the solidification process are decisive for the geometric shape of the seam and the target geometry. The selection of the wire electrode significantly determines the material characteristics of the manufactured structure. Compared to other metallic additive manufacturing processes, WAAM is characterized by a 30 to 40-fold higher deposition rate [4]. At the same time, investment costs for system technology and supplies are significantly lower [5]. Six-axis robotic systems, like the one at the laboratory of IfSW and ISM+D at TU Darmstadt, given in Figure 4, for guiding the welding torch offer great flexibility in the manufacturing of components and are used to ensure production in large installation spaces. With increasing size, accuracy decreases as the distance to the machine origin extends [6]. To avoid inaccuracies large structures might be divided in segments to be manufactured simultaneously. These aspects make the process attractive for the fabrication of large structural components like free form columns and its single components.

### WAAM as a versatile tool in steel construction

Through the widespread availability of digital design tools, architects have been enabled to design ever more unusual structures. This is particularly evident in the context of additive manufacturing. Standardized load-bearing elements

such as walls [7] and beams [8, 9] are redesigned into geometrically complex and structurally efficient elements as well as column structures. Researchers at the University of Bologna worked with MX3D to illustrate the possibilities of combining digital design tools with additive manufacturing by producing large-scale, lattice-like columns [10]. Similarly, researchers at ETH Zurich used the possibilities offered by AM to incorporate them into the design of columns. Smart Dynamic Casting (SDC) used an adaptable sliding formwork to build reinforced concrete columns with different cross-sections step by step [11]. In addition, the AM of direct connections between beam elements [12] and nodal elements [13-15] shows great potential for the steel construction industry.

## COLUMN STRUCTURES

The research presented in this paper focuses on the combination of digital design tools and WAAM to manufacture performative and expressive column elements, which might be cost-intensive or impossible to produce using conventional manufacturing processes.

First, column structures are shown as scale models in Figure 5 (Column a) to d)). While the transfer to large column structures spanning several meters and adapted wall thicknesses is possible, it is simultaneously limited by the radius of action of the welding robot. In these cases, the entire structure must be manufactured in segments. The individual components are then welded together either in the factory or on the construction site. Figure 5 model a) is a column whose quadrangular cross-section expands or tapers uniformly with increasing height. Model b) represents an octagonal cross-section that twists constantly over the element height, revealing some possibilities for expressive architectural forms. Model c) and d) are columns with ellipsoidal cross-sections. In model c), both axes have been modified according to the moment load of a column hinged on both sides, with a corresponding progression of imperfection. In this case, the structure obtains a smaller cross-section at the base, where lower bending moments are expected, and a larger cross-section near the center. Model d) was used to investigate the feasibility of column c) for more significant cross-section changes-in particular, the manufacturability of the cantilevered shape at the top.

Although the designs are relatively simple in terms of geometry, they are intended to serve as initial iterations toward more geometrically complex columns defined by material application limits such as maximum cantilevers, minimum cross-sectional areas, and wall thicknesses. This manufacturing approach could be combined with other design factors such as shape optimization to maximize

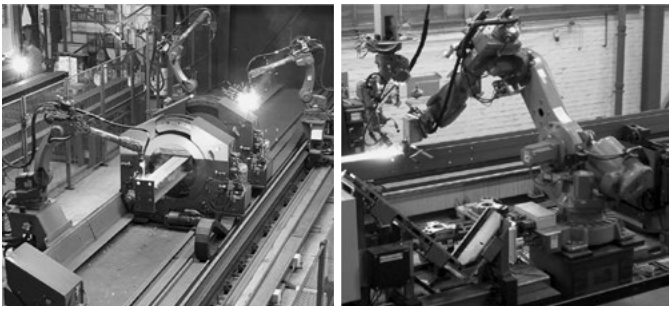


Figure 1: Automated production line with three welding robots a) and one welding- and one handling robot b).

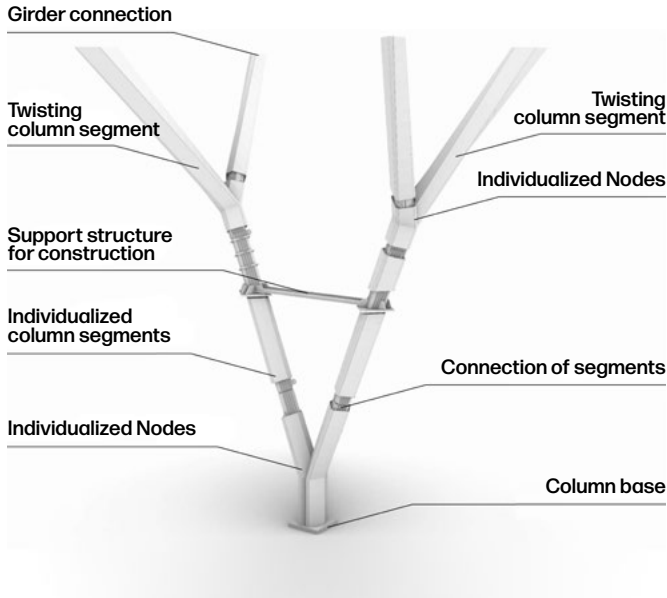


Figure 2: Y-shaped steel structure of combining individualized steel nodes and column segments.

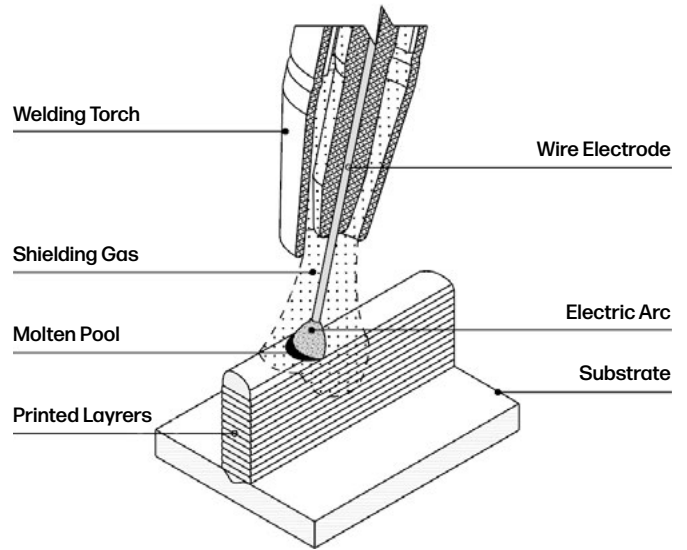


Figure 3: Schematic illustration of the material deposition by WAAM.

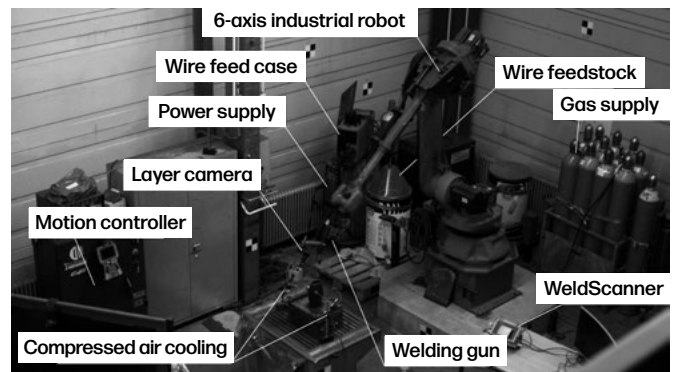


Figure 4: Six-axis robotic system for Wire Arc Additive Manufacturing at the laboratory of the IfSW and ISM+D at TU Darmstadt, manufacturing a column structure.

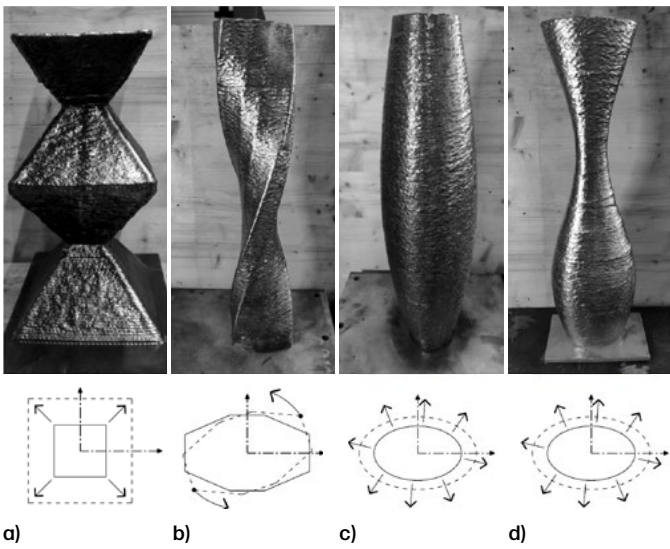


Figure 5: Investigated columns with a changing square cross-section (a); a twisted octagon cross-section (b); and two non-uniformly changing ellipse cross-sections (c) and (d).

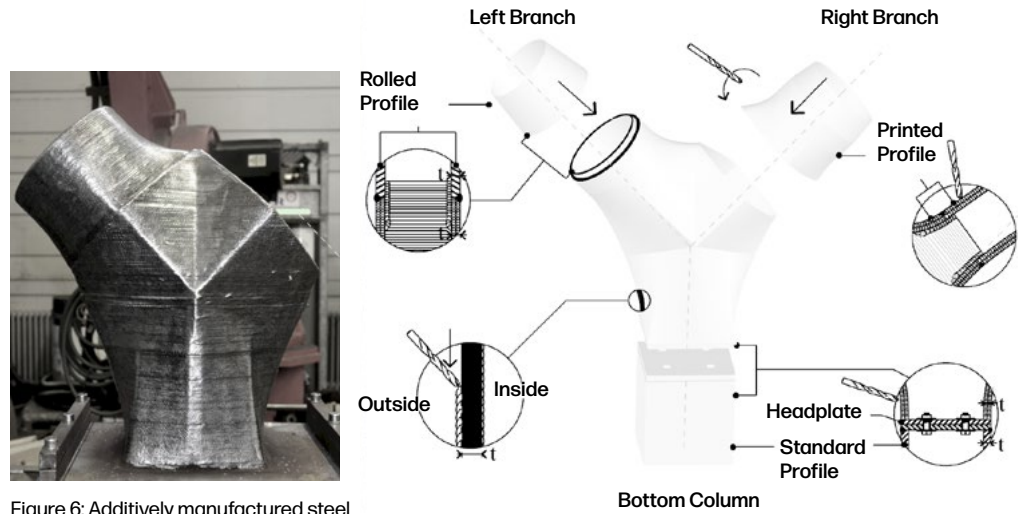


Figure 6: Additively manufactured steel node (left); Connecting methods to join elements of different shape and manufacturing (right).



Figure 7. Steel node while manufacturing and in a manufactured state.

load carrying capacity. In the following, we focus on the “design-to-manufacturing” workflow of the model shown in Figure 5 (Column d)).

According to the Y-shaped structure illustrated in Figure 2, the second focus of this article lies in the context of presenting a steel node (Figure 6 left and Figure 7) to join different standard profiles of closed cross-section or additively manufactured elements. To accomplish this target, the nodal structure illustrated in Figure 6 (right) aims to connect column elements with simple cross-sections by different connection methods. A rolled rectangular hollow section RHS (bottom), a rolled circular hollow section CHS (top left), and an additively manufactured ellipsoid branch (top right), which cantilever at a 45° angle are connected by an also additively manufactured node of continuous changing cross-section (center). Thereby, cross-sectional profiles of different dimensions or geometric shapes can be joined together using various connection techniques. The required substrate plate (bottom) can be used for a bolted head plate connection. Therefore, a bolted connection through the head plate of the RHS or a thread in the plate itself can be used to connect the elements. A second method can be seen for the left branch, where a CHS is connected by means of a fully welded plug joint (left). Hereby, the thicker printed upper end of the cantilevered node is milled on the outside so that the standard profile can be slipped over it. After being centered, it gets fully welded to the steel node. Also conceivable as an alternative is a fully welded connection of a freely formed, separately additively manufactured steel profile according to a similar scheme (right). A special characteristic of the knot is its wall thickness, which is the result of two overlapping welds.

## DESIGN-TO-MANUFACTURING WORKFLOW

### Approach and Rudimentary Digital Twin

For conventional 3D-printing a three-dimensional model is divided into predefined layers (slicing), which are then converted into motion instructions or G-code. Since WAAM is dependent on a high variation of parameters, during the printing process there are often discrepancies between the designed model geometry and the actual printed structure. These can result from differences from the preset layer height or from distortion of the printed structure while being manufactured. Therefore, the feasibility of adjusting robot motion paths, layer heights and welding parameters is critical to ensure a stable printing process. Figure 8 illustrates the workflow from design to manufacturing for the manufactured node, that was applied to all structures until

evaluation. Like shown above, the structures differ in particular in their geometric complexity.

The digital model contains information about process and input parameters, weld-seam geometries, and material properties. The weld trajectories are generated using (partial) parametric robot programming (PRP), a coordinate determination method based on mathematical functions. Therefore, current heights among other factors were checked regularly with a tactile measuring method called TouchSense [16]. The results were then compared to the digital model by the robot controller leading to adaptively updated welding path coordinates. The final evaluation of the recorded data, supplemented by 3D-scanning for a target/actual-comparison, could be used to generate milling trajectories for an outer surface finish. Furthermore, data such as welding, cooling, measuring and robot movement times are used to determine optimized motion sequences or cooling and measuring processes. The measured layer heights of the manufactured structure are recorded for reproduction and so proof of concept. All stored information of each layer results in a rudimentary digital twin. This is essential for process control, as it allows partial real-time feedback of information between the original 3D-geometry and the data generated during the printing process.

### Process and input parameters

The material deposition under a stable welding process depends significantly on the selected welding and input parameters, which influence both the geometric dimensions of a weld seam and the subsequent material properties [17]. It is decisively controlled by the defined travel speed (TS) of the robot, the wire feed speed (WFS) and the CMT process regulation, which is an energy reduced welding process (Cold Metal Transfer) provided by Fronius [18]. They offer “CMT Cycle Step”, a welding process variant in which the ratio of the number of droplets (CMT cycles) to the pre-defined pause interval for the solidification of the melt can be selectively controlled. This targeted control is essential for the additive manufacturing of free-formed geometries especially for overhanging material deposition, for which dripping of the molten material must be prevented.

Table 1: Process and input parameters.

Process and input parameter	Node	Column elements	Unit
Number of CMT-Cycles	15 - 25		
Pause time	80 - 120		ms
Wire-Feed Speed (set)	6.0		m/min
Travel-Speed	0.6		m/min
Shield gas	Ferroline C6X1 (93 % Argon, 6 % CO <sub>2</sub> , 1 % O <sub>2</sub> )		
Gas-flow rate	15		l/min
Wire electrode	Weko 2 G3Si1 (ER70S-6) Ø 1.2 mm		
Welding torch orientation	90° and 45° to the horizontal	90° to the horizontal	
Cooling time (set)	25 - 60	25 - 45	s

Table 1 lists the welding parameters for a Fronius CMT Advanced 4000 R welding source with a CMT Cycle Step characteristic and relevant process parameters. To prevent the weld metal from dripping, a cooling period is set after each layer so the structures can cool down.

### (PARTIAL) PARAMETRIC ROBOT PROGRAMMING

Manufactured objects that are created using AM are simultaneously digitally visualized as simplified layers and coordinates which form a three-dimensional object. The generation of this collection of coordinates often results in excessive amounts of data. Parametric Robot Programming (PRP) uses mathematical functions to define motion paths to generate coordinates (Figure 9 left). This reduces the amount of data generated and allows for real-time determination of the structure development to be incorporated into the manufacturing process. When layers do not consist of geometries for which mathematical equations are already known, like for the node, (Partial) PRP is used to determine coordinates for single sections (vertical base and cantilevered branch of the node). All structures were divided into segments of 10 layers and sliced using conventional methods (Figure 9 middle). Each layer was analyzed for its curvature and the coordinates were distributed accordingly. Tactile measuring was used to systematically record the height of all structures during the printing process. This information was used to parametrically adjust the z-coordinates of the print path once each segment was printed. It allowed for a very stable printing process. For a full PRP with non-standard geometries like the presented column elements, an alternative strategy is needed. In 2019 the au-

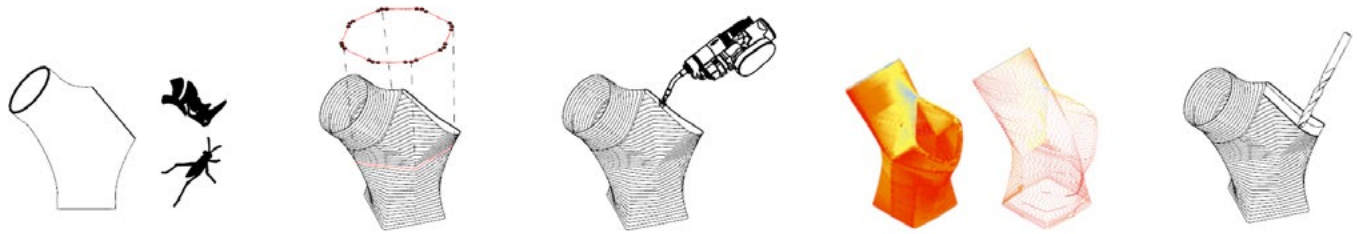
thors used polynomial regression to obtain the best-fitting polynomial function of an arbitrary open curve [19]. PRP may be possible by generating the iso-parametric (iso) curves of the surface (Figure 9 right) using polynomial regression to determine the polynomial function for each curve. However, this method was not carried out during this process and remains a topic still to be solved.

### PROCESS SEQUENCE PARAMETERS

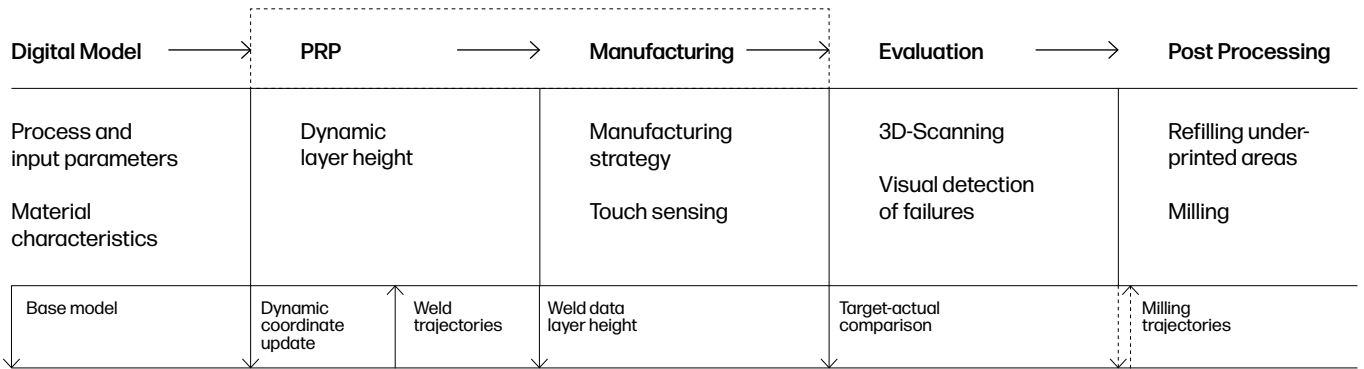
WAAM offers various possibilities to additively manufacture large structures. Each individual layer is determined by the process sequence parameters. These are shown in Figure 10. First, the x and y coordinates of each point of the weld path are calculated as a mathematical function of the current structure height with (Patrial) Parametric Robot Programming. It includes a slight change of the starting welding point of each layer. Since welding has its origin as a joining process, the energy starting the process is significantly higher to heat the basic workpieces. It leads to a shortly higher deposition rate at the beginning while moving at a constant speed. Therefore, the height of the end-point of each seam is slightly lower compared to the continuous welding [20]. In addition, the welding seam thickness at the start point is increased. To prevent a punctual error propagation of the layer height, the starting point of each layer was changed. Each layer then can be welded with the pre-set welding and input parameters given above.

To ensure a stable manufacturing process an inter-layer temperature of less than 150 °C and a reduction of cooling time is targeted. The structures are cooled for at least 13 s (apex of the node) and 25 s (tapered area of column d). A converted minimum quantity lubrication system with water was used as an automated compressed air-cooling system for the purpose of cooling. The water evaporates on the heated surface of the structure, extracting the thermal energy from the body faster than it would for pure compressed air. In preliminary investigations no negative influences on the metallurgical properties and microstructures were detected for this cooling method [21]. The control of the interlayer temperature was carried out with a pyrometer at the last applied welding layers.

The TouchSense method - a tactile measuring method - is used to detect the current z-height of the structure. For this process the filler wire is automatically cut by a wire cutting station to a defined length and a small sensor voltage is applied. While slowly moving the wire vertically onto the workpiece the signal contained in the short circuit at the moment the wire touches the surface is recorded by the robot. It serves to calculate the next coordinates corresponding to the current layer height. This is executed automatically



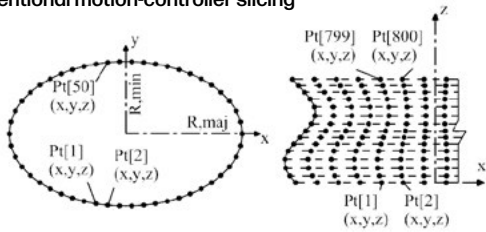
Interlayer update every 10 layers



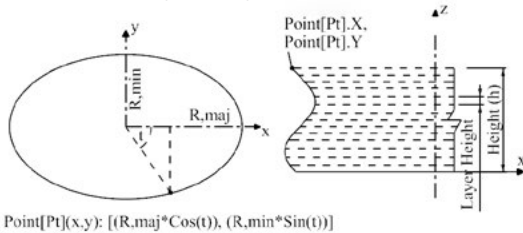
### Rudimentary Digital Twin

Figure 8: Design-to-manufacturing workflow schematically shown for the manufactured steel node.

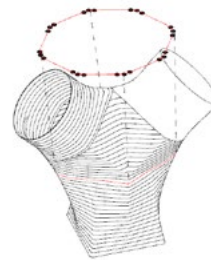
#### a) Conventional motion-controller slicing



#### b) Parametric Robotic Programming

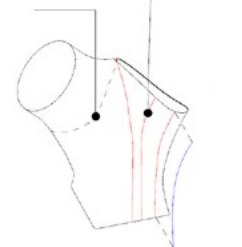


by curvature



c)

Border function  
Iso-Curve



d)

Figure 9: Welding path determination conventionally a) and by Parametric Robot Programming b); Distribution of points on welding layers c) and coordinates defined by iso-curves of the two segments of the node d).

by the program code so the CTWD stays on a constant value. Like the welding parameters, characteristics influencing the measurement were examined in preliminary investigations to enable a precision of 0.2 mm accuracy. These included the CTWD, the motion and acceleration profile of the robot, the orientation of the welding torch to the target surface and the distance at the start of the tactile measurement.

The whole process sequence was first executed for column d). The results of 18 coordinate points were measured for each 10<sup>th</sup> layer of the changing ellipsoid cross-section. The results were used to determine a layer height by section. Erroneous measurements outside of a tolerance range of  $\pm 1.5$  mm to the expected layer height of 1.3 mm (caused by welding slags for example) are firstly remeasured and then not considered in case they still exist.

During the complete manufacturing processes, welding data and time consumption are stored in the rudimentary digital twin. They are supplemented by layer images for further processing and the frequent tactile measurement of the structure height and a final three-dimensional scan.

## MANUFACTURING

The first element manufactured was column d). The welding path planning was based on 181 coordinates. The weld width of approx. 4.5 mm was achieved by depositing a single weld seam per layer - with rotating start and end point of the seam and a neutral welding torch orientation. After each layer, a layer image was taken while automated cooling was in progress to allow visual inspection of the weld seam quality. After up to 45 s, the material for the next layer was usually welded. The cantilevered shape of the column results from an offset in the transverse direction of the layers printed. The nonlinear progression of the structure leads to a variable layer height, which is detected by the tactile measurement and taken into account by the PRP. During manufacturing, failures occurred at random intervals during welding, e.g., due to arc-start failures of the welding device or wire stick burns at the end of a welding process. Visual inspection was carried out each time to ensure that the structure was not weakened by pores. In the rare case of pores appearing, these were removed, and the resulting gap filled manually. Figure 11 presents the growth of the column manufactured.

The node was manufactured based on the experience gained through the process of the several column elements. To create a higher wall-thickness the layer consists of two weld seams with a center distance of 4 mm from each other. In addition, the welding direction alternates frequently. The manufacturing is visualized in a series of images in Figure 12. The first segment was printed with a vertical orientation of the welding torch up to the apex, forming a

base inclined by 45° for the branches (also shown in Figure 6 and Figure 7). The figure illustrates the shape-changing cross-section of the node over its height. This geometry requires a more complex coordinate generation by partial parametric robot programming. Around layer 183, the hollow cross-section changed to the inwardly cantilevering “triangular elements”, which meet at the apex. The slightly uneven surface - created by the non-uniform seam geometry of the start and end points - was smoothed out by the deposition of the first layer and the manufacturing process could be continued without any problems. The cantilevered area for connecting a circular rolled section was manufactured at an orientation of 45° of the welding torch to the horizontal base plate (Figure 7). In the uppermost 3 cm of the cantilevered circular hollow cross-section, a third weld seam was applied to the inside of the wall thickness. This allows the planned plug connection to be achieved form fitting without a cross-sectional offset by subsequent milling.

## EVALUATION

The results of the evaluation of both in detail presented structures are stored in rudimentary digital twins. First a description of the digital model is given followed by detailed information about the physical models. It is supplemented by the target/actual comparison done with two different methods. At the end, a statement regarding the time consumption of the process and the potential for optimization is given.

### Digital Model and Tactile Measured Coordinates

Figure 13a) (left) shows the progression of single coordinate points and their changing horizontal distance,  $\Delta d$ , for each layer. In the area of the tapered cross-section between layers 200 to 300, the distance decreases below the limit value to be processed by the robot controller. There, only every fifth weld path coordinate must be approached due to the weld path density. The geometry of the column is not unexpectedly affected by this.

Illustrated in Figure 13a) (right) the evaluation of the tactile height measuring, carried out with the TouchSense, for every 10<sup>th</sup> layer over one half of the column is given. The vertically significantly deviating measurement shown in the enlargement - the measured height is in the existing structure - is erroneous and was not taken into account in the averaged height determination consisting of 18 recorded values. The small number of faulty deflections illustrates the reliability of the information generated by the touch-sensing method for the rudimentary digital twin.



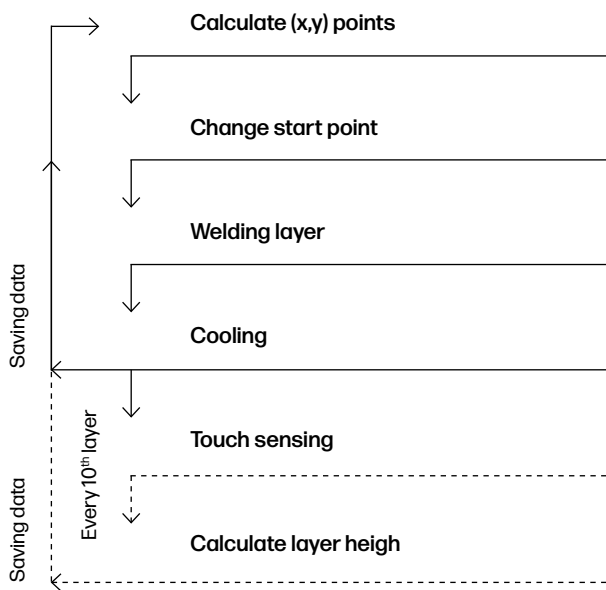


Figure 10: Schematic chart of the process sequence of each layer.



Figure 11: Manufacturing process of one column element.



Figure 12: Manufacturing process of the steel node.

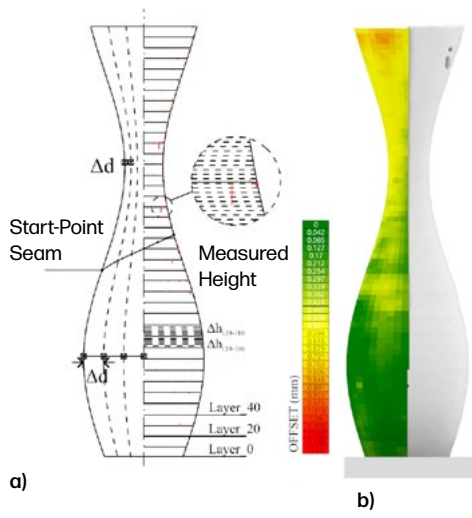


Figure 13. Coordinate determination and tactile measurement results a) and visualization of the target/actual comparison (b)) of column d).

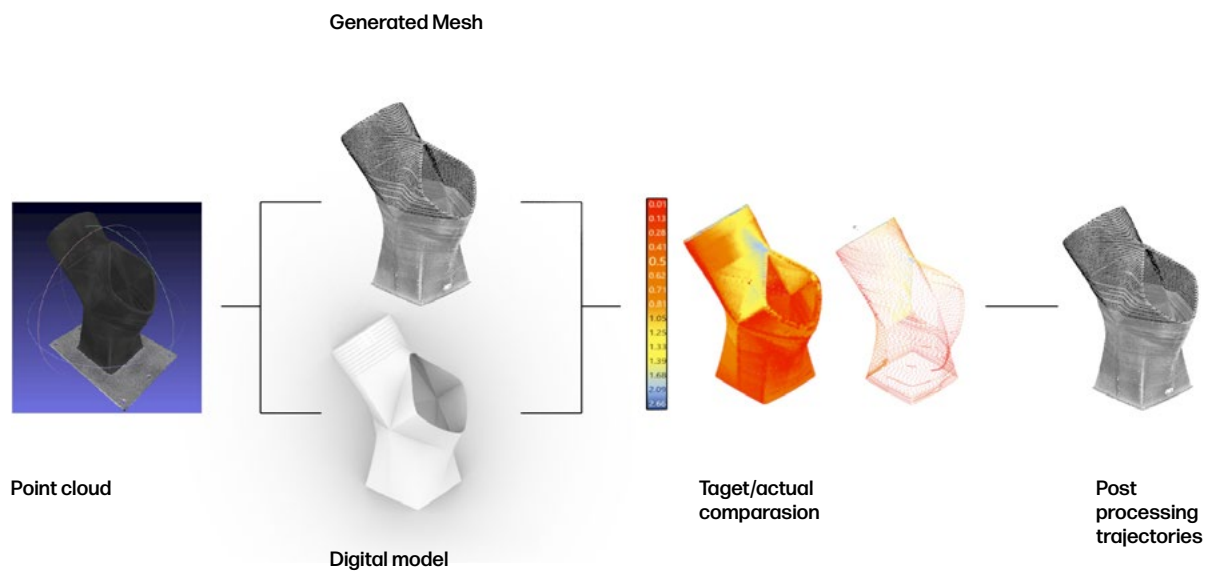


Figure 14. Target-actual comparison node.

## Physical Models

For the 52.2 cm high scaled column model, shown in Figure 13, 400 welding layers were applied. This corresponds to an average layer height of 1.304 mm. The ellipse had maximum major and minor radii of 150 mm and 100 mm respectively and a minimum cross-sectional dimension of 32 mm in the tapered area. The applied mass of 5.12 kg was deposited within 3.35 hours of pure welding time, which corresponds to a deposition rate of 1.52 kg/h. The node was fabricated in 379 layers (297 vertical; 82 cantilevered). While the square cross-section of the bottom measures almost 18.5 cm in diameter it changes slightly over height to measure 18.5 cm for the circular shape. The node measures 40.8 cm in height at the apex, up to 45.5 cm while in total spanning about 42 cm in longitudinal direction. The wall thickness amounts 9 mm targeting an overprinted width of 3 mm for further machining. The upper edge of the circular section printed with a third seam result in 12.15 mm wall thickness. The node has a total weight of 20.12 kg of deposited material. The deposition rate related to the welding time results in 1.65 kg/h, which is slightly higher than for the column.

### Target/Actual comparison

For the target/actual comparison of the steel column element the mesh is directly generated by means of a FARO Freestyle 2 handheld scanner. The deviations are homogeneous, and range between 0.0 to 0.3 mm from the lower to the upper part, with a maximum of 0.8 mm at the upper edge of the column. At this point, the scan result shows a lower accuracy (Figure 13b)). Information explained in detail can be found in [22].

For the target/actual-comparison of the node, a 3D-scan model was also needed. This time a different scanning method was carried out. A point cloud was generated by the Department of Geodetic Measuring Systems and Sensors, TU Darmstadt, using a terrestrial laser scanner. Meshlab, an open-source mesh editing software, was used to convert the point cloud into a mesh geometry (Figure 14), which is necessary for performing the target/actual comparison between the planned and manufactured object as well as generating trajectories for further machining. The mesh, which had  $\approx 166,000$  vertices, an average edge length of 0.16 mm and so a higher resolution compared to the column, was imported into Rhinoceros 3D for analysis. It contains a large degree of surface noise which needs to be removed manually. Inaccuracies between the planned and scanned 3D-model, due to numerous errors show deviations above 2 mm especially at the area of the apex. Moreover, they were produced during the printing process, particularly when the overhang angle approached over  $26^\circ$ . In total the effort for manual post-processing of the scan data was significantly higher for the second method which also impedes a fully automated process.

## Time Consumption

Figure 15 visualizes the time spent for the manufacturing of the column (left) and the node (right). The diagram is divided into welding time (red), cooling time (blue) and measuring time (black) for the tactile detection of the layer heights.

The column diagram shows 10 fluctuations of the red welding curve, especially up to layer 100. These indicate interruptions in the welding process, e.g. due to wire stuck, which led to an interruption of the material deposition. Beside the deflections of the lower part, the welding curve displays the shape of the column structure following the minor and larger cross-section diameters. The blue curve shows a variation in the course of the cooling time. The different lengths of the tactile measurement processes (squares) are the result of faulty measurements, which meant that measurements had to be repeated.

To manufacture the node only 43.5 % of the manufacturing time was spent on welding directly while 31.9 % were needed for tactile measurement, and 20.3 % on cooling the structure. The total manufacturing time was 28.51 h.

Time required for adjusting the coordinates by means of partial PRP is not taken into account here. Significant fluctuations in the welding and cooling times, particularly in the area of layer 150, reflect the difficulties encountered in manufacturing the sections with large overhangs, which interrupted the process. For welding, some records got lost around layer 150 which led to the deflection of the welding results. In some cases, manual reworking was necessary or defects had to be removed and reworked. The time for tactile measuring also varies, caused by some repeated measurements.

In total the printing of the column elements was more time efficient since the time to readjust the coordinates and solve the appearing difficulties while printing the node are not fully recorded. There is a necessity to improve the recorded data.

All evaluated data is stored in the rudimentary digital twins (see Figure 8). They can serve as reference values for a reproduction and the manufacture of upscaled structures and be supplemented by additional information for post-processing like milling trajectories or monitored lifetime data.

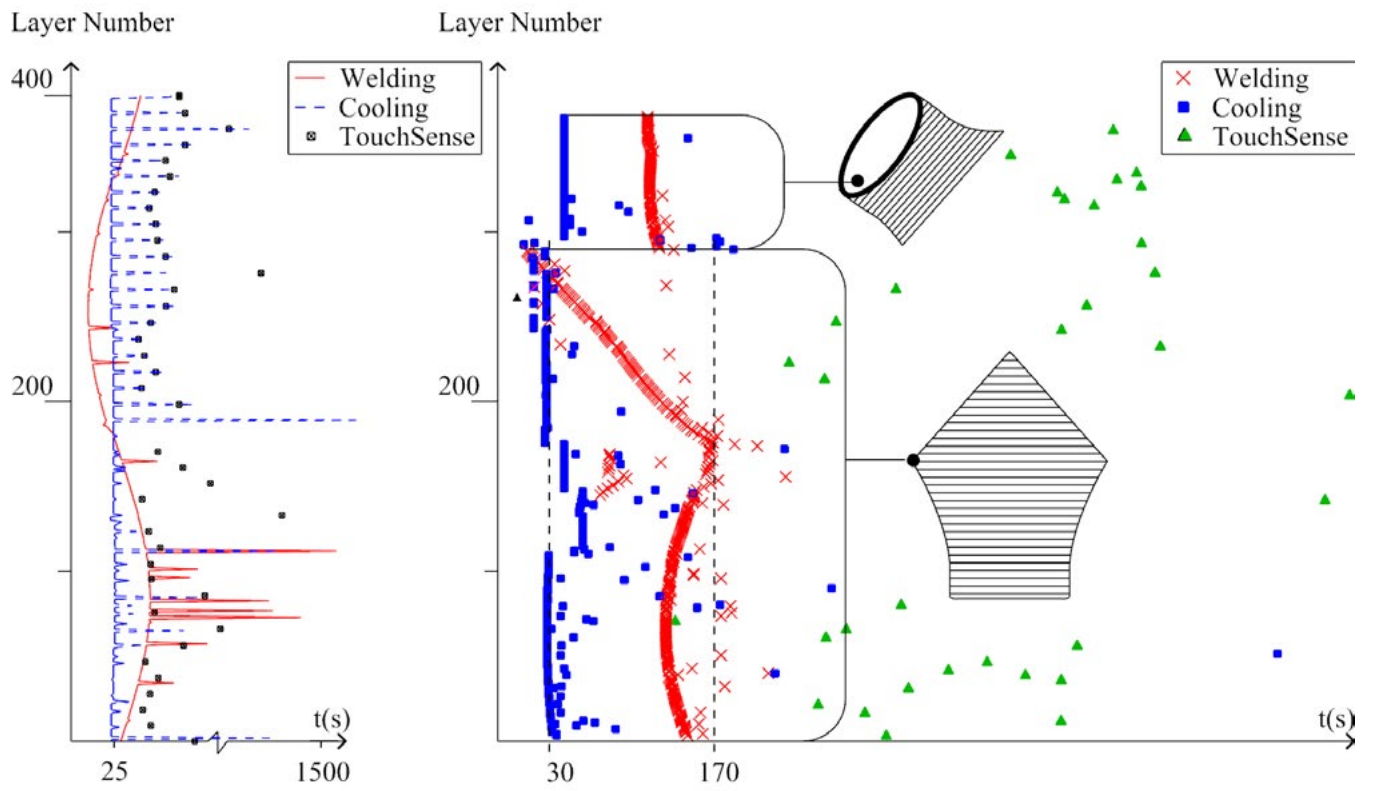


Figure 15. Time consumption of the column (left) and the node (right).

## CONCLUSION

The robot supported Wire Arc Additive Manufacturing (WAAM) of steel column elements and a steel node was presented. As parts of larger structures, the AM of geometrically complex steel columns is another implementation option of WAAM for the steel industry and already under investigation at different research groups. Four different column cross-section types and one unique node were manufactured using the presented design-to-manufacturing workflow. It illustrates a reasonable manufacturing flow.

The selected process parameters, in conjunction with the determination of weld path coordinates using PRP for the column elements guarantee a stable manufacturing process with simultaneous high geometric correspondence between the digital and physical model. The necessary (Partial) PRP to generate the welding path coordinates of both nodal segments showed the potential for more complex structures. Failures and deviations appearing in the target/actual-comparison caused by critical overhang angles need further improvement to reduce manual adjustment during printing. The recorded data also indicate the difficulties in manufacturing very complex free forms with overhang.

An evaluation of the recorded measuring data, stored in the rudimentary digital twin, provides the basis for a post-processing of the surfaces and the economic improvement of the manufacturing process and serves as base for reproduction. To supplement the rudimentary digital twin the current data could be combined with a shape optimization to maximize the load-carrying capacity. Therefore load-bearing capacity tests have to be carried out to confirm the structural behavior of the column elements based on preliminary investigation on the material properties.

## ACKNOWLEDGMENTS

We like to thank the companies Fronius Deutschland GmbH, Messer SE & Co. KGaA, Westfälische Drahtindustrie GmbH, spanverbund GmbH, and the GMSS at TU Darmstadt for their support. Our special gratitude goes to Ulrich Knaack of ISM+D at TU Darmstadt. This research was funded by the German Federal Ministry for Economic Affairs and Energy (grant number: 16KN076133).

## REFERENCES

- [1] Fischer, Rigbert. *Eine Untersuchung zur roboterbasierten Baugruppenfertigung im Stahlbau*. vol. Schriftenreihe des Instituts für Baubetrieb, Darmstadt, Techn. Univ., Inst. für Baubetrieb, 2014. D 71 vols.
- [2] Statistische Ämter des Bundes und der Länder. "Bauhauptgewerbe, Ausbaugewerbe / Lange Reihen." *Statistische Bibliothek*, Statistische Ämter des Bundes und der Länder, [https://www.statistischebibliothek.de/mir/receive/DESerie\\_mods\\_00000675](https://www.statistischebibliothek.de/mir/receive/DESerie_mods_00000675). Accessed 19 July 2023.
- [3] Voortman Steel Machinery B.V. "Introducing The Voortman Fabricator." *automated fitting and full-welding machine for the steel fabricating industry*, Voortman Steel Machinery B.V., <https://www.voortman.net/de/produkte/voortman-fabricator-automatisches-schweissen-montage>. Accessed 19 July 2023.
- [4] Zeman Bauelemente Produktionsgesellschaft mbH. "Zeman - Steel Beam Assembler." SBA Steel Fabrication Automation, Zeman Bauelemente Produktionsgesellschaft mbH, <https://zebau.com/machines/sba>. Accessed 19 July 2023.
- [5] spanverbund GmbH, booking.com headquarter, Amsterdam, <https://www.spanverbund.com/booking-com-headquarter-amsterdam/#more>. Accessed 5 February 2023
- [6] C. Buchanan, L. Gardner, *Engineering Structures* (2019) doi:10.1016/j.engstruct.2018.11.045
- [7] D. Kampffmeyer, M. Wolters, in *DVS Congress 2015*. DVS Congress 2015, Nürnberg, 15. u. 17.09.2019 (DVS Media, Düsseldorf, 2015), p. 249
- [8] J.P. Bergmann, P. Henckell, J. Reimann, Y. Ali, J. Hildebrand, *Grundlegende wissenschaftliche Konzepterstellung zu bestehenden Herausforderungen und Perspektiven für die Additive Fertigung mit Lichtbogen* (DVS Media GmbH, Düsseldorf, 2018)
- [9] F. Martina, S. Williams, *Wire+arc additive manufacturing vs. traditional machining from solid: a cost comparison* (Cranfield University, Cranfield, 2015)
- [10] Y. Bandari, S. Williams, J. Ding, F. Martina, in *Proceedings: 26th annual international solid freeform fabrication symposium. 26th international solid freeform fabrication symposium*, Austin, Texas, 10 - 12 August (2015)
- [11] N. Hack, H. Kloft, in *Second RILEM International Conference on Concrete and Digital Fabrication*, ed. by F.P. Bos, S.S. Lucas, R.J. Wolfs, T.A. Salet (Springer International Publishing, Cham, 2020), p. 1128
- [12] Francesca Moretti, *3d printed concrete beam* (2015), <https://www.3dwasp.com/en/concrete-beam-created-with-3d-printing/>. Accessed 29 November 2021
- [13] V. Laghi, M. Palermo, M. Bruggi, G. Gasparini, T. Trombetti, *Prog Addit Manuf* (2022) doi:10.1007/s40964-022-00335-1
- [14] V. Laghi, M. Palermo, G. Gasparini, T. Trombetti, *Additive Manufacturing* (2020) doi:10.1016/j.addma.2020.101505
- [15] E. Lloret-Fritschi, L. Reiter, T. Wangler, F. Gramazio, M. Kohler, R.J. Flatt, in *HPC/CIC Tromsø 2017. Eleventh High Performance Concrete (11th HPC) and the Second Concrete Innovation Conference (2nd CIC)*, Tromsø, Norwegen, 6 - 8 März (Norwegian Concrete Association, Oslo, 2017)
- [16] I. Ariza, A. Mirjan, A. Gandia, G. Casas, S. Cros, F. Gramazio, M. Kohler, in *Recalibration: On Imprecision and Infidelity*. ACADIA 2018, Mexico City, 18. - 20. Oktober (Association for Computer Aided Design in Architecture (ACADIA)2018), p. 312
- [17] S. Galjaard, S. Hofman, S. Ren, in *Advances in Architectural Geometry 2014*, ed. by P. Block, J. Knippers, N.J. Mitra, W. Wang (Springer International Publishing, Cham, 2015), p. 79

- [18] MX3D, Connector for Takenaka | MX3D (2022), <https://mx3d.com/industries/construction/connector-for-takenaka/>. Accessed 5 April 2022
- [19] J. Bergmann, J. Lange, J. Hildebrand, M. Eiber, M. Erven, C. Gaßmann, C.-H. Chiang, C. Lenz, T. Röder, W. Bashariar, *Stahlbau* (2020) doi:10.1002/stab.202000080
- [20] Fronius International GmbH, Assistance systems for robotic welding: Support for automated series production (2023), <https://www.fronius.com/en/welding-technology/info-centre/press/robotic-welding-assistance-systems>
- [21] P.M.S. Almeida, PHD Thesis, Cranfield University, April 2012
- [22] Fronius International GmbH, J. Bruckner, S. Egerland, K. Himmelbauer, A. Millinger, M. Schörghuber, D. Söllinger, A. Waldhör, *Schweißpraxis aktuell: CMT-Technologie : Cold Metal Transfer - ein neuer Metall-Schutzgas-Schweißprozess*, 1st edn. (WEKA MEDIA GmbH & Co. KG., Kissing, 2013)
- [23] T. Feucht, J. Lange, M. Erven, C.B. Costanzi, U. Knaack, B. Waldschmitt, *Construction Robotics* (2020) doi:10.1007/s41693-020-00033-w
- [24] Y. Zhang, P. Li, Y. Chen, A.T. Male, *Mechatronics* (2002) doi:10.1016/S0957-4158(00)00064-7
- [25] T. Feucht, J. Lange, B. Waldschmitt, A.-K. Schudlich, M. Klein, M. Oechsner, in *Advanced Joining Processes*, ed. by L.F.M. Da Silva, P.A.F. Martins, M.S. El-Zein (Springer Singapore, Singapore, 2020), p. 67
- [26] B. Waldschmitt, C.B. Costanzi, U. Knaack, J. Lange, *Archit. Struct. Constr.* (2022) doi:10.1007/s44150-022-00050-z

# AM STRUCTURAL NODES FOR FREEFORM STEEL & GLASS FACADES

Lia Tramontini

Sebastian Thieme, Manuel Mueller, Radenko Zoric,

Laurent Giampellegrini, Matthias Oppe

Additive Manufacturing (AM) is explored as a means of producing structural nodes for freeform steel and glass façade construction. Three AM methods are explored: PBF-L; DED-GMA; and DED-L. An overview of the respective fabricated node designs is provided. The novel AM methods are demonstrated in a mock-up and a large feature freeform façade. The mock-up and the feature façade are designed and constructed using a parametric digital workflow. The work presented in this paper is part of the exploratory phase of an on-going product development - a collaboration between Jansen AG, TU Delft, and knippershelbig GmbH.

## INTRODUCTION

Freeform steel and glass façades are an increasingly popular feature in modern construction. The use of glass is an obvious choice as a means of providing spaces with natural daylight, and the use of steel as a substructure, which has high stiffness and strength, enables large spans and the use of slim members for maximum transparency and elegant façade constructions. Steel and glass facades are typically constructed using multi-layered systems (Figure 1) where each layer has specific functions. In freeform applications, using straight profiles and planar glass is a common strategy for cost and fabrication efficiency. In these cases

the complexity of the system is concentrated at the nodes. Node conditions are particularly challenging because the geometry required to effectively bridge each layer of the assembly without compromising their respective functions is complex, and also because each individual node condition is usually unique. The structural node, which is responsible for the transfer of forces, is the focus of this study.

The current practice for the fabrication of structural nodes for freeform applications relies heavily on Computer-Aided Manufacturing (CAM). CAM technologies such as numerically controlled plate cutting [1,2], and Computer Numerical Control (CNC) milling [3-5] have all been used to create different structural nodes. Existing node solutions

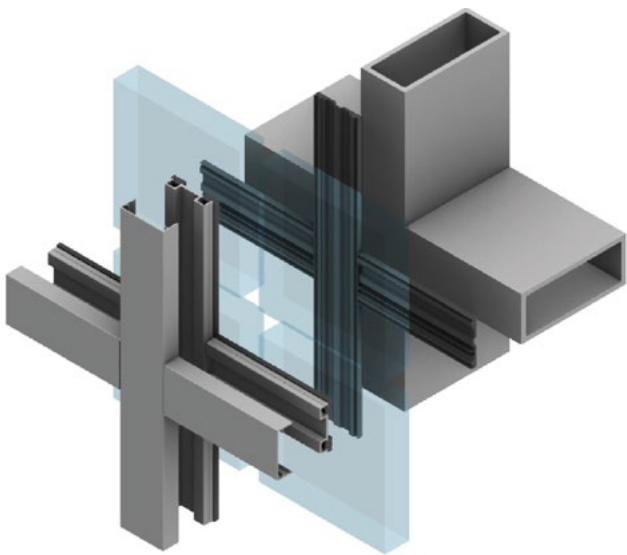


Figure 1: Multi-layer steel-glass construction.

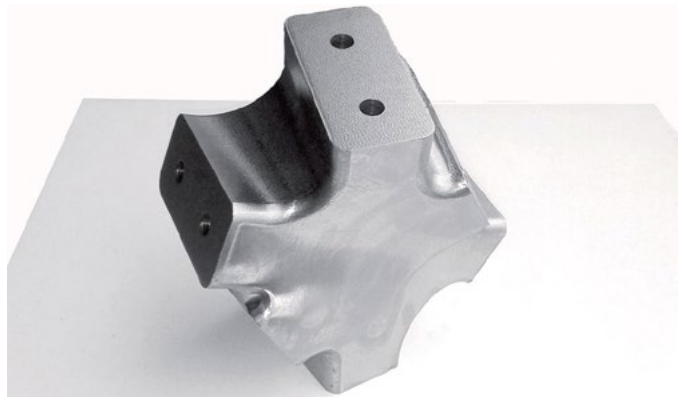


Figure 2: Solid CNC-milled Node for Bratislava Shopping Centre (Source: Metal Yapi).



Figure 3: Hand samples of DED-L (left) and PBF-L node design exterior face (right).



Figure 4: Hand samples of DED-L (right) and PBF-L node design interior face (left).



Figure 5: DED-GMA node.



Figure 6: DED-GMA node interior structure, during printing. (Source: MX3D).



Figure 7: Test print for DED-GMA node during CNC-milling.



generally have key challenges related to fabrication efficiency, material efficiency, and/or performance. The solid CNC-milled node (Figure 2) is perhaps the most popular contemporary typology of freeform structural node, which enables elegant seemingly continuous grid-shells through the form-freedom afforded by multi-axis CNC milling. This type of component, however, is often underutilized and materially inefficient. Especially in larger nodes this can add significant loads to the structure.

Additive Manufacturing (AM) enables an unprecedented level of geometrical freedom which allows designers to not only address the aforementioned challenges, but also allows for more design flexibility. This study explores the potential of AM as means of improving freeform steel/glass construction, and to expand the use of a commercial high-performance steel-glass façade system for freeform applications using AM node components. Three different metal AM methods are explored for the development of structural nodes. A full-scale mock-up and feature wall are constructed using the AM components.

### **A SYSTEM-APPROACH TO FREEFORM CONSTRUCTION**

A “system approach” in reference to façade construction refers to the development of series of parts within a façade system which can be interchanged and/or adjusted based on the specific requirements of a given project without modifying the technical core of the system. Such an approach allows façade system providers to supply designers with a range of design possibilities for their buildings with a high level of engineering and manufacturing efficiency. The idea of a “system approach” is a key requirement for the development of the AM parts for this study. Standard interfaces are developed for the structural nodes to connect to the Jansen VISS façade system. The node designs should also have a parametrically-driven geometry with set design variables that can be sized based on the specific applied forces of a given application. In this way, the general shape, consistent with the printing strategy, remains the same within each node type. This comes with a number of key advantages: the fabrication operations and path planning can remain consistent; printing parameters, which can take significant effort to fine-tune for high-quality prints and reduced failed prints, can quite reasonably be standardized; and the engineering process can be made more efficient.

## **STRUCTURAL NODE DEVELOPMENT**

### **PBF-L Node design**

The first AM method explored is Laser-based powder bed fusion (PBF-L). The PBF-L node (Figures 3,4) was printed in 316L Stainless Steel. The main geometry of the node consists of a network of walls aligned roughly with the node axis and z-axis of the printer, such their overhangs are well within printing limitations. End faces and side walls make up the main volume of the node, an interior structure of concentric cylindrical walls with varying radii are at the centre, and plates running from each arm end face along the normal force direction of each arm connect the network of walls. Additionally, volumes of solid printed steel are printed around the main features of the end connections. The thus created radially oriented webs of the node arms provide a direct load path for the normal and shear forces as well as bending moments onto the cylinder at the centre of the node. Compression forces are introduced through contact, while tension forces are introduced via the four bolts anchored via the metric threaded blind hole in the thick end plates (not included in picture below). The central cylinder efficiently redistributes these loads predominantly via membrane action through the curved walls to the neighbouring arms and back into the adjacent structural profiles.

### **DED-GMA Node design**

The second AM method explored is Gas Metal Arc Directed Energy Deposition (DED-GMA). The DED-GMA node (Figure 5-7) was printed in 308LSi Stainless Steel. The print sequence and overhang implications of DED-GMA influenced the node design. The node consists of a primary arm that runs through the centre along the main load bearing artery of the node, and secondary and tertiary arms that connect to that one. The hierarchy of arms corresponds to the sequence in which they are printed. Each arm consists of outer plates at the outer-faces of the node, and interior plates running at around 45 degrees from the edges of the outer plates and joining at the centre of the node, gradually decreasing in width. For the end conditions, the plates gradually increase in thickness merging together at the end to form a flat end plate which allows for the standard end conditions. It should be noted that it is possible with more intricate path-planning to achieve flat end faces using less material without the gradual increase in thickness; however, the decision was made to print end conditions in a single plane to contain costs. The end faces and specific end conditions are subsequently CNC-milled to overcome the larger tolerances of the DED-GMA printing process.

The structural logic behind the node geometry is based on the principle of intersecting castellated beams.

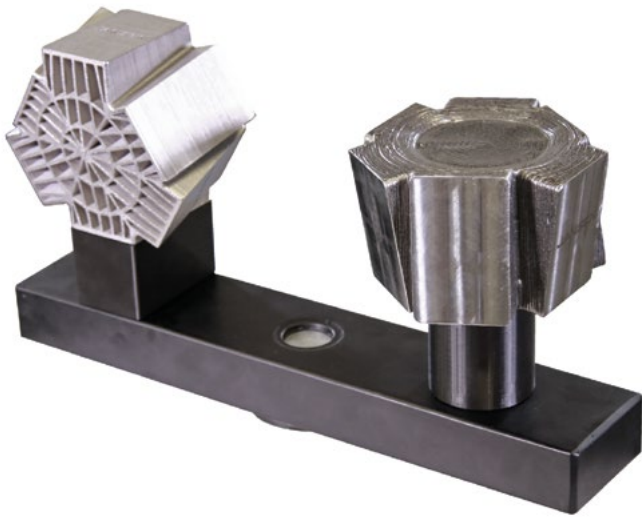


Figure 8: DED-L node design.

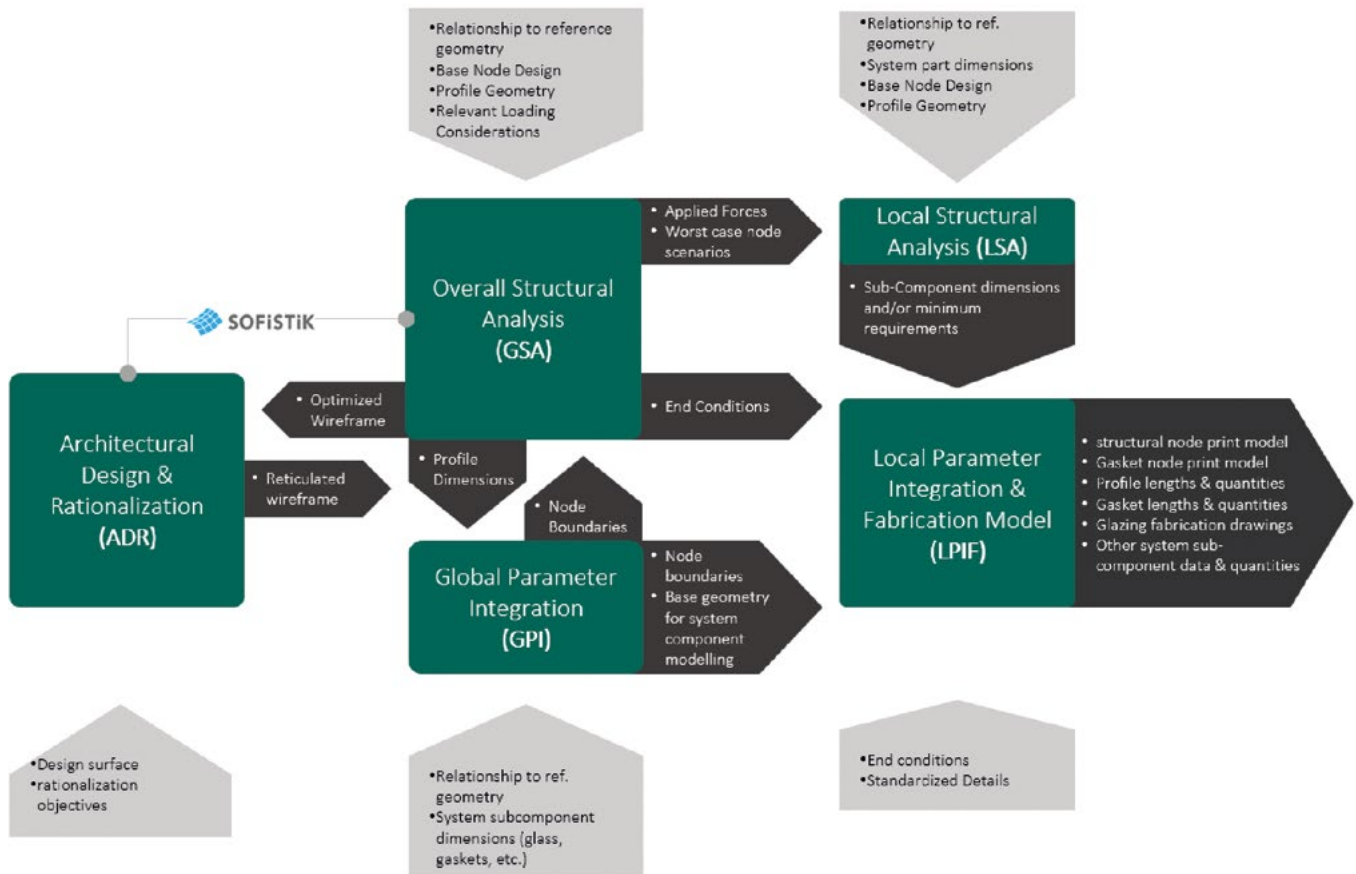


Figure 9: Parametric workflow for mock-up and feature wall development.

The continuous flanges allow a smooth transfer of in-plane forces from bending and axial forces across the node, while the thick webs connected at the centre transfer shear forces between members. The arm hierarchy is clearly visible in the surface pattern of the printed node. While the other two designs were designed to be as small as possible, the DED-GMA node was allowed to have longer arms so that the interior structure could be clearly visible, a design decision which negatively impacted the fabrication-intensity of the design.

It is also worth noting that while DED-GMA is able to produce objects at this scale, it is at the edge of what is appropriate for this technology. Upon reflection, this design would be more suitable for a larger node, or alternatively, at this scale, a better design would avoid such constricted printing space in the center of the node in order to fully take advantage of the strengths of this technology.

### DED-L Node design

The third AM method explored is Laser-based Directed Energy Deposition (DED-L). The DED-L Node (Figure 8) was printed in 316L Stainless Steel. The machine a hybrid 5-axis DED-L/ NC-mill. The node is printed radially in a solid volume so there are limited overhang conditions. The end faces and end conditions are subsequently milled to achieve the high required tolerances.

The structural principles for the node build-up and load transfer follow those described for the PBF-L node. The material displays orthotropic behaviour as a result of the directional printing. The latter was assessed by means of physical tests on small samples: the tensile capacity of the material perpendicular to the direction of printing is lower than in the longitudinal direction but still exhibits sufficient strength compared to the base material so that in combination with the force-optimised node geometry, this provides a robust and efficient solution.

## FULL-SCALE FAÇADE DEVELOPMENT

### Parametric workflow

The realisation of the AM facade is rooted in a parametric workflow from the design of the overall geometry to the generation of the CAM models. This parametric workflow takes place in five phases summarised in Figure 9. The purpose of compartmentalizing the parametric workflow in this arrangement is to complement the system-approach to the node design, which allows generous flexibility over the course of design exploration through fabrication. This strategy also allows for different ownership of the different models for interdisciplinary collaboration.

### First mock-up

In order to demonstrate the novel AM façade system, two full-sized mock-ups were designed, fabricated and assembled at the Jansen HQ in Oberriet. Both use as a base system the VISS façade system, a commercial façade system by Jansen AG, with the AM interventions at the complex connection points - i.e. the nodes.

The first mock-up (Figure 10) incorporated the three nodes produced with the three AM methods during the exploratory phase of the project in a 1.5m x 3m wall section. This phase also included material testing to verify the durability and strength of the materials.

After the first round of node exploration for the mock-up, the decision was made to produce the structural nodes for the feature wall with DED-L technology. The feature wall (Figures 12-14) is an approximately 25m<sup>2</sup> facade with an S-shaped plan and constantly variable double curvature. The design aims to showcase as many application cases as possible, incorporating concave, convex and anticlastic conditions across the facade.

The mock-up and feature wall were subjected to a range of global and local structural calculations and simulations to ensure structural stability and the structural capacity of the facade system (Figure 11). During the design and engineering process, a lot of attention was also paid to the development of the connection detail between the structural nodes and the profiles. Several concepts were examined and tested by means of prototypes.

## CONCLUSION

In this study, three different AM methods and three respective node designs were explored as a means of producing structural nodes for freeform steel-glass façade applications. It should be noted that the node selected for the final construction is not a conclusive assessment of which printing method is more suitable for this type of application. This is because, as mentioned, "this type of application" in itself varies quite significantly and the most suitable printing method for one project may not be the same for another depending on a number of design variables such as size, structural requirements, desired shape and surface quality.

The development of the mock-up and feature wall have highlighted many of the strengths but also the challenges of working with AM. On one hand, each node design brings something to the table that the more traditional designs do not. The DED-GMA node has an organic interior geometry that would be near-impossible to produce using other manufacturing methods. The SLM node also has a unique character as it is approximately 40% lighter than a solid CNC node. The DED-L Node is also 20% lighter than a solid CNC



Figure 10: Mock-up wall with 3 trial nodes: DED-GMA (top); PBF-L (middle); and DED-L (bottom).

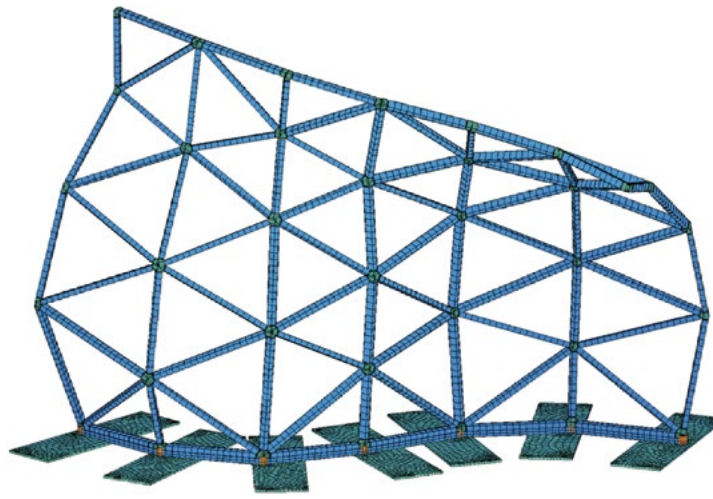


Figure 11: Finite Element Analysis model of feature wall (Source: knippershelbig GmbH).



Figure 12: Detailed view of DED-L node in feature wall construction.



Figure 13: Interior view of freeform feature wall with AM nodes.

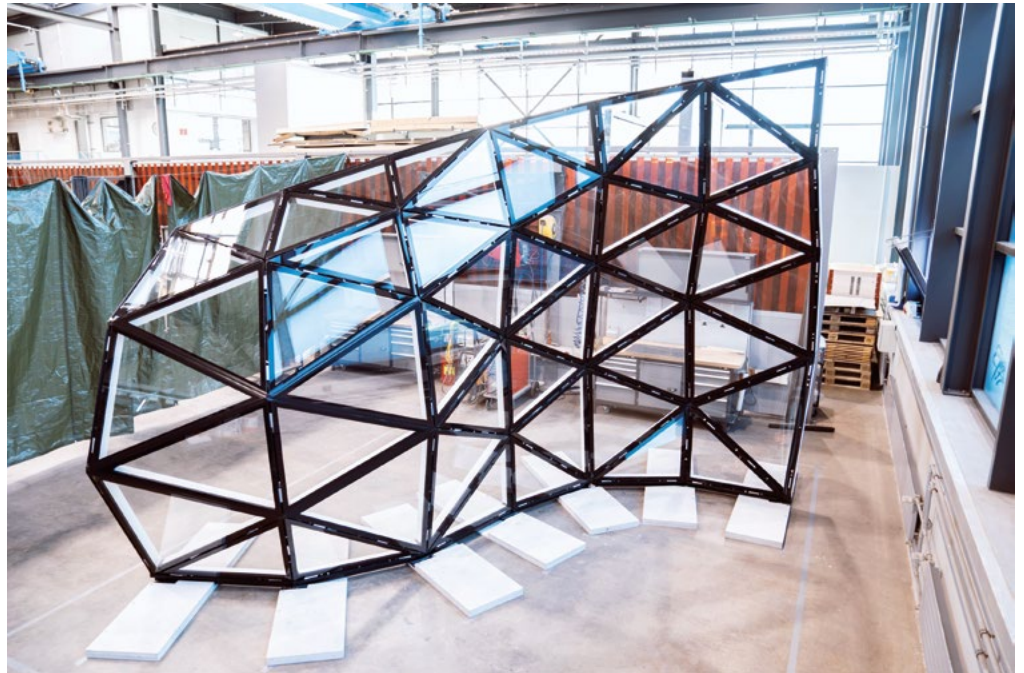


Figure 14: Exterior view of freeform feature wall with AM nodes.

node and has an intriguing surface finish. The designs were conservatively engineered for this study and there is plenty of room for further material optimization in future development. In addition, the AM nodes have an almost insignificant amount of waste material when compared to that from the solid CNC-milled node, which can have high buy-to-fly ratios. The system-approach to design also provides the groundwork for standardized engineering processes for freeform structures that enables to minimize risks in planning and cost. On the other hand, the integration of CNC milling was necessary to varying degrees for each of the printing methods. This is unlikely to change when high-tolerance, concealed mechanical connections are desired. Also, particularly in cases of DED technology, proper path-planning is an integral part of the process and a big factor in the efficiency of the printing process.

Regardless of the AM method in question, the development of AM structural nodes benefits from multi-disciplinary collaboration. The overall geometry of the freeform façade and its discretization dictates the structural requirements of the assembly and the minimum size of the AM intervention. Further, the geometry of the nodes and manufacturing method selected to fabricate them is inextricably linked to their appearance, their structural performance, and their manufacturability. Each AM method also has its own strengths and limitations which need to be navigated in order to achieve time- and cost-effective AM products. The effective use of AM thus benefits from communication between designers, façade system experts, structural engineers, and experts in the field of AM. This on-going project is a multidisciplinary effort between Jansen, TU Delft and knippershelbig GmbH.

## REFERENCES

- [1] J. Sischka et al., "Die Überdachung des Great Court im British Museum in London," *Stahlbau*, vol. 70, no. 7, pp. 492-502, 2001.
- [2] J. Knippers and T. Helbig, "The Frankfurt Zeil Grid Shell," in *Symposium of the International Association for Shell and Spatial Structures*, A. Domingo Cabo and C. M. Lázaro Fernández, Eds., Valencia, 2009.
- [3] H. Barf, "Innovative design + construction: Manufacturing and design synergies in the building process," Institut für internationale, Munich, 2010.
- [4] H. Schober, "Transparent Shells," Wiley, 2015.
- [5] T. Helbig et al., "Free-form on every scale: 'Tornado' roof structure for Bory Mall, Bratislava, Slovakia," *Steel Construction*, vol. 9, no. 3, pp. 249-254, 2016.

## CONTRIBUTORS

### **Adam Pajonk**

Research Assistant, Department of Digital Design and Construction, Faculty of Architecture, Muenster University of Applied Sciences. Researcher, Department of Architectural Engineering + Technology, Architectural Facades & Products Research Group, Faculty of Architecture and the Built Environment, Delft University of Technology.

### **Alexander Wolf**

PhD Candidate, Institute of Structural Mechanics and Design (ISM+D), Technical University of Darmstadt.

### **Alexsander Alberts Coelho**

Researcher, Department of Architectural Engineering and Technology, Delft University of Technology. Lead Alternative Materials Specialist, 14Trees.

### **Benedikt Waldschmitt**

PhD Candidate, Institute for Steel Construction and Materials Mechanics, Technical University of Darmstadt.

### **Christopher Bierach**

Junior Researcher, Department of Architectural Engineering and Technology, Delft University of Technology. Project Manager, Vertico.

### **Christin Lippold**

Assembly Engineer, Donges SteelTec GmbH.

### **Christopher Borg Costanzi**

Design for Additive Manufacturing, BMW Group.

### **David Correa**

Associate Professor, University of Waterloo. Design Partner at LLLab Architects.

### **Dunia A. Abdullah Agha**

PhD Candidate & Research Assistant, Institute of Structural Mechanics and Design (ISM+D), Technical University of Darmstadt.

### **Erno Langenberg**

Architect and researcher at Elstudio, Amsterdam.

### **Georg Vrachilotis**

Full Professor and Head of the Design, Data, and Society Group (DDS), Faculty of Architecture and the Built Environment, Delft University of Technology.

### **Ingrid Paoletti**

Full Professor, Department of Architecture Built Environment and Construction Engineering, Politecnico di Milano.

### **Isabel Ochoa**

Lecturer, School of Architecture, University of Waterloo. OCH Works.

### **James Clarke-Hicks**

Lecturer, School of Architecture, University of Waterloo. OCH Works.

### **Jasmine Wong**

Alumni of the Faculty of Architecture and the Built Environment, Delft University of Technology.

### **Jens Schneider**

Professor, Technical University of Wien.

### **João Carvalho**

PhD Candidate, ACTech Hub, School of Architecture, Art and Design, University of Minho.

### **João Ribeiro**

PhD Candidate, ACTech Hub, School of Architecture, Art and Design, University of Minho.

### **Jörg Lange**

Professor, Institute for Steel Construction and Materials Mechanics, Technical University of Darmstadt.

### **Juan Ojeda**

Research Assistant, Institute of Structural Mechanics and Design (ISM+D), Technical University of Darmstadt.

### **Katia Zolotovskiy**

Assistant Professor, Departments of Art+Design and Chemistry and Chemical Biology, Northeastern University.

### **Kerstin Thiele**

PhD Candidate & Research Assistant, Glass Competence Center (GCC), Institute of Structural Mechanics and Design (ISM+D), Technical University of Darmstadt.

### **Laia Mogas-Soldevila**

Assistant Professor, Director DumoLab Research, Department of Graduate Architecture, Stuart Weitzman School of Design, University of Pennsylvania.

### **Laurent Giampellegrini**

Project Management of Structural Engineering, knippershelbig GmbH.

### **Lia Tramontini**

PhD candidate, Architectural Facades and Products Research Group, Delft University of Technology. Project Manager, Jansen AG.

### **Luca Breseghello**

PhD Fellow, SDU CREATE, University of Southern Denmark.

### **Manuel Mueller**

Head of Project Management, Jansen AG.

### **Maren Dietrich**

Structural Engineer, knippershelbig.

**Maren Erven**

PhD Candidate, Institute for Steel Construction and Materials Mechanics, Technical University of Darmstadt.

**Maria Anishchenkoa**

PhD Candidate, Department of Architecture Built Environment and Construction Engineering, Politecnico di Milano.

**Marvin Kehl**

PhD Candidate & Research Assistant, Glass Competence Center (GCC), Institute of Structural Mechanics and Design (ISM+D), Technical University of Darmstadt.

**Matthias Martin Seel**

Head of Research, Glass Competence Center (GCC), Technical University of Darmstadt.

**Matthias Oppe**

Managing Director, knippershelbig GmbH.

**Max Benjamin Eschenbach**

PhD Candidate & Research Associate, Digital Design Unit (DDU), Faculty of Architecture, Technical University Darmstadt.

**Mohamad Fouad**

PhD Candidate, ACTech Hub, School of Architecture, Art and Design, University of Minho.

**Nadja Gaudillière-Jami**

Postdoctoral Researcher, Digital Design Unit (DDU), Faculty of Architecture, Technical University Darmstadt.

**Olga Beatrice Carcassia**

Associate Research Scientist, Natural Materials Lab - Columbia GSAPP.

**Oliver Tessmann**

Professor, Digital Design Unit (DDU), Faculty of Architecture, Technical University Darmstadt.

**Radenko Zoric**

Project Manager Pre-Development, Jansen AG.

**Roberto Naboni**

Associate Professor, SDU CREATE, University of Southern Denmark.

**Paulo Mendonça**

Associate Professor, School of Architecture, Art and Design, University of Minho.

**Philipp Amir Chhaden**

PhD Candidate & Research Assistant, Glass Competence Center (GCC), Institute of Structural Mechanics and Design (ISM+D), Technical University of Darmstadt.

**Sandra S. Lucas**

Assistant Professor, Department of the Built Environment, Eindhoven University of Technology.

**Sebastian Thieme**

Head of Development, Jansen AG.

**Serdar Aşut**

Senior Lecturer, Department of Architectural Engineering and Technology, Faculty of Architecture and the Built Environment, Delft University of Technology.

**Stijn Brancart**

Assistant Professor, Department of Architectural Engineering and Technology, Faculty of Architecture and the Built Environment, Delft University of Technology.

**Tatiana Campos**

PhD Candidate, ACTech Hub, School of Architecture, Art and Design, University of Minho.

**Tom Finger**

Structural Engineer, Arup.



### **Philipp L. Rosendahl**

Studied mechanical engineering at the Technical University of Darmstadt, the University of Illinois at Urbana-Champaign and the Royal Institute of Technology in Stockholm. The work of his doctoral thesis on the fracture mechanics of thin layers is applicable problems of structural engineering such as adhesive bonding and to geophysical problems such as skier-triggered snow slab avalanche release. The author is currently working as the head of the Generative Design Lab at the Technical University of Darmstadt and co-founded the startup company 2phi, which aims at improving skier safety in the backcountry by transferring scientific advances into practice.

### **Bruno Figueiredo**

Associate Professor at the School of Architecture, Art and Design of the University of Minho (EAAD-UM), being dedicated to teaching Computer Design, Computational Modelling and Digital Fabrication courses. PhD in Construction and Technology by EAAD-UM (2016) with the thesis "Decoding the De re aedificatoria of Alberti: a computational approach to the analysis and generation of classical architecture". Member of the Landscapes, Heritage and Territory Laboratory R&D unit. Co-coordinator of the Architecture, Construction and Technology Hub – ACTech Hub, Guimarães. Visiting student of Design and Computation Group, MIT (2012). Master in Modern and Contemporary Architectural Culture by the University of Lisbon (2009), with the dissertation "Project, Computation and Manufacturing: for the integration of digital technologies in Architecture". Graduated in Architecture by the University of Porto (2000). His research is centred on the use of digital tools in architecture, encompassing the development of generative and analytical computational models, and digital/robotic fabrication in architectural design processes, namely the implementation and control of additive manufacturing techniques.

### **Michela Turrin**

Associate Professor at the Faculty of Architecture and the Built Environment, Delft University of Technology. Expert in Computational Design at the intersection of Architectural Design and Building Technology. Turrin put forward Computational Design to integrate engineering aspects into the architectural design conception, toward architectural design innovation with sound fulfillment of performance-criteria. Pursuits the development of methods for form generation, performance assessment and optimisation by means of new computational methods integrating computational engineering optimisation in architectural design. Turrin harnesses 3D printing for customised and high-performing components for buildings. Project leader and participant in research projects and international collaborations with practice and industry.

### **Ulrich Knaack**

Professor Dr. Ing. Ulrich Knaack (1964) was trained as an architect at the RWTH Aachen / Germany. After earning his degree he worked at the university as researcher in the field of structural use of glass and completed his studies with a PhD. In his professional career Knaack worked as architect and general planner in Düsseldorf / Germany, succeeding in national and international competitions. His projects include high-rise and offices buildings, commercial buildings and stadiums. In his academic career Knaack was professor for Design and Construction at the Hochschule OWL / Germany. He also was and still is appointed professor for Design of Construction at the Delft University of Technology / Faculty of Architecture, Netherlands where he developed the Façade Research Group. In parallel he is professor for Façade Technology at the TU Darmstadt / Faculty of Civil engineering/ Germany where he participates in the Institute of Structural Mechanics + Design. He organizes interdisciplinary design workshops and symposiums in the field of facades and is author of several well-known reference books, articles and lectures.

### **Paulo J. S. Cruz**

Full Professor of Construction and Technology at the School of Architecture, Art and Design of the University of Minho (EAAD-UM) and Researcher at the Laboratory of Landscapes, Heritage and Territory (Lab2PT). He teaches and researches in the field of Structures, focusing on the articulation between Structures and Architecture. Co-coordinator of the Architecture, Construction and Technology Hub (ACTech Hub). President of the EAAD-UM (2021-2023 and 2004-2011). Pro-Rector of the University of Minho for Quality of Life and Infrastructure (2017-2021). Director of Lab2PT (2015-2017). President of the Design Institute of Guimarães (2015-...). Director of the Department of Civil Engineering at the University of Minho (2003-2004). PhD in Civil Engineering from the Technical University of Catalonia, Barcelona, Spain (1995). Master in Structural Engineering from the University of Porto, Portugal (1991). Degree in Civil Engineering from the University of Porto, Portugal (1987). Founder and President of the "International Association of Structures and Architecture" (2016-2022). Coordinator of the organization of international congresses on this theme (ICSA2010, ICSA2013, ICSA2016, ICSA2019 and ICSA2022). Editor-in-Chief of the Journal "Architecture, Structures and Construction", Springer, since 2021.







*Research in additive  
manufacturing*  
for architecture  
and construction

Laboratory of Landscapes,  
Heritage and territory

Institute of Structural  
Mechanics and Design

SOAP | Stichting  
OpenAccess Platforms